Springer Natural Hazards

Sujit Mandal
Ramkrishna Maiti

Semi-quantitative Approaches for Landslide Assessment and Prediction

Springer

Springer Natural Hazards

More information about this series at http://www.springer.com/series/10179

Sujit Mandal · Ramkrishna Maiti

Semi-quantitative Approaches for Landslide Assessment and Prediction

Springer

Sujit Mandal
Department of Geography
Raja N.L. Khan Women's College
Paschim Medinipur, West Bengal
India

Ramkrishna Maiti
Department of Geography and Environment Management
Vidyasagar University
Paschim Medinipur, West Bengal
India

ISBN 978-981-287-145-9 ISBN 978-981-287-146-6 (eBook)
DOI 10.1007/978-981-287-146-6

Library of Congress Control Number: 2014951664

Springer Singapore Heidelberg New York Dordrecht London

Printed on acid-free paper

Springer is part of Springer Science+Business Media (www.springer.com)

Preface

In the present time, our natural environment is frequently associated with a number of destructive hazards such as flood, earthquake, storm surge, drought, landslide, volcanic eruption, etc., worldwide. All these environmental problems may bring about a tremendous change in the geomorphic system over the land surface and may also divide a system into a number of subsystems. It is the task of Physical Geographers to study natural hazards and their destructive impacts over the earth's surface in a scientific way. Here, we studied in detail geologic, geomorphic, and hydrologic processes responsible for landslides in a representative mountain watershed, Shivkhola of Darjiling Himalaya, where landslides are very much active and have destroyed communication lines, settlements, and tea estates. A quantitative understanding of all the triggering landslide inducing parameters can provide a clear vision of the changes and evolution of landforms. The aim of this book is to provide an integrated knowledge and understanding of the application of semi-quantitative approaches in evaluating various landslide triggering factors and assessment of landslide susceptibility as well as landslide risk, which can help planners and policymakers to check the magnitude of landsliding in mountain terrains.

The concerned area, Shivkhola, is badly affected by slope instability jeopardizing the economy and social systems; taking a toll of lives, lands, and properties; promoting road blockage and hampering flow of tourists; destroying pipelines of water; and causing subsidence of road and rail cut benches. The effects are conveyed over a long distance, both upslope and downslope, by disruption of transport and hydrological systems and thus invites instability into both physical and social systems. Most landslides of this trouble-torn district of Darjiling are concentrated in this area where most of the torrential jhoras (Hill Streams) at their upper catchments develop a potential sinking zone, and the Hill Cart Road and Narrow gauge Rail when traversing through these zones invite catastrophic slides. The present work tries to identify the zones of potential slides by investigating into the systematic interaction among the number of prominent physical and human triggering factors.

The geotechnical attributes, viz., major principal stress, minor principal stress, normal stress, shear stress, angle of internal friction, angle of rupture, cohesion,

shear strength, and safety factor of the Shivkhola watershed have been determined using the Tri-axial Compression Test from the geotechnical laboratory, Geological Survey of India (Kolkata). There is every possibility for the generation of geomorphic thresholds for initiation of slides due to hydrologic factors. Thus debris slide occurs and the slope on scar face is reduced to that of repose angle to attain temporary stability through internal feed back in a process of homeostatic adjustment. Remote Sensing and GIS-based Landslide Susceptibility Zone Map reveals that Paglajhora, Shiviter, Gayabaria, and Tindharia are more susceptible in terms of slope instability. The prepared Landslide Hazard Risk Map also states that Tindharia, Gayabari, Shiviter, and Paglajhora are prone to landslide risk because of prevalence of risk elements such as road network and settlements. As most landslides occur along Hill Cart Road (NH-55), and a huge amount is spent on Post Slide Management, an attempt toward pre-slide management of the susceptible areas has to be introduced with immediate effects with less efforts and investment. A sector-wise job assignment has to be made for regular supervision of the slope stability and a serious drive for pre-slide management of potential slope failure zones should be introduced; these should be considered as emergency as in post-slide condition. In such a highly instable region the protection of slope and soil is a great challenge through rational use of these resources for harnessing greater utility over a long time.

Midnapore, India, August 2014

Sujit Mandal
Ramkrishna Maiti

Acknowledgments

It is a moment of jubilance and euphoria to me because of the candid endeavor so far made, be it small or large in this book, in illuminating the unexplored domain of knowledge in "Semi-quantitative Approaches for Landslide Assessment and Prediction". We would like to pay our humble regards, indebtedness, and immense sense of gratitude to our respected Teacher, Professor Late Subhas Ranjan Basu, Ex-Head of the Department Geography, University of Calcutta, who had shared with us a lot of his experiences, suggestions, and encouragement till his last breath so that we always bear his fragrance of affection and bliss showered on us. His prudent direction, all sorts of support, and sleepless effort for preparation of this book can never be forgotten.

We also acknowledge the financial support of University Grant Commission, New Delhi, through granting a research project that helped in data collection and subsequent analysis involved in this research work. We would like to express our appreciation and thanks to Mr. Manik Das Adhikari, Project Fellow, IIT, Kharagpur for his immense support throughout the work.

We wish to record our sincere gratitude to all the officials of all Departments, including Geological Survey of India (GSI), Kolkata, Tea Research Centre, Department of Agriculture, Department of Forest of Kurseong, Government of West Bengal who had provided valuable information in the study area. Thanks are due to Department of Geography and Environment Management, Vidyasagar University, Paschim Medinipur, West Bengal, India, and the authority of Raja N.L. Khan Women's College, Paschim Medinipur, W.B., India and especially the department of Geography and Zoology for offering logistic support and fulfilling all sorts of lack occurred in that institution for involvement in this research work.

It is difficult for us to fully express our gratitude to our families, parents, brothers, sisters, relatives, and students for their sacrifice, constant love, cordial affection, and inspiration throughout the work.

Midnapore, India, August 2014

Sujit Mandal
Ramkrishna Maiti

Contents

Abbreviations

AHP	Analytical hierarchy process
AMC	Antecedent moisture condition
CI	Consistency index
CR	Consistency ratio
CRV	Class rating value
DEM	Digital elevation model
D_w	Height of water
F_i	Fraction of flow
FR	Frequency ratio
FS	Factor of safety
GANN	Geomorphology-based artificial neural networks
GPS	Global positioning system
GSI	Geological Survey of India
HHCS	Higher Himalayan Crystalline Sequence
HI	Hypsometric Integral
Ia	Initial abstraction
ICAR	Indian Council of Agricultural Research
IRS	Indian Remote Sensing
IS	Indian Standard
ITSZ	Indo-Tsangpo Suture Zone
L	Effective contour length
LF	Landslide frequency
LHEF	Landslide hazard evaluation factor
LHRA	Landslide hazard and risk assessment
LHS	Lesser Himalayan Sequence
LISS	Linear imaging self-scanning sensor
LPIV	Landslide potentiality index value
LSC	Landslide Susceptibility Coefficient
LULC	Land use and land cover
MATLAB	Matrix laboratory

MBF	Main boundary fault
MBT	Main boundary thrust
MCT	Main central thrust
NRSA	National Remote Sensing Agency
PCRV	Prioritized class rating value
PFRV	Prioritized factor rating value
Pt	Depth of rainfall
Qt	The depth of runoff
RCA	Road contributing area
RCL	Road contributing length
RCW	Road contributing width
RCN	Run-off curve cumber
RI	Random index
S	The potential maximum retention of water by the soil
S	Directional slope
SCS	Soil Conservation Service
SINMAP	Stability index mapping
SOI	Survey of India
SPOT PAN	French: Satellite Pour l'Observation de la Terre
SRTM	Satellite Radar Topographic Mission
SVL	Soil-vegetation-land
TOPMODEL	Topographic index model
TT	Tethyan thrust
UCA	Upslope contributing area
USDA	United State Department of Agriculture
USGS	United State Geological Society
c_r	Critical rainfall
c_s	Critical slope angle
c_h	Critical height
φ	Angle of internal friction or angle of repose
Θ	Slope angle
α	Threshold angle of Failure
u	Pore water pressure on potential sliding surface
γ	Bulk unit weight of the sliding materials
γ_s	Soil density
γ_w	Density of water
σ_1	Major principal stress
σ_3	Minor principal stress
σ_n	Normal stress
T	Transmissivity
p_s	Wet soil density
p_w	Density of water
c	Cohesion
h	Thickness of total soil
z	Thickness of saturated soil

Sc	Compressive strength of the rocks
W	Unit weight of the rocks
λ	Average rate of landslide occurrence
$\boldsymbol{\mu}$	Mean recurrence interval between successive landslide events
m	Soil saturation index
τ	Shearing stress along plane
μ	Coefficient of internal friction
β	The terrain surface inclination
λ	Shearing strength
α	Rupture angle
1D	One dimensional
2D	Two dimensional

Chapter 1
Introduction

1.1 Key Concepts on Landslide

Landslides are simply defined as the movement of mass of dislodged rock, debris or earth materials down a slope including a broad range of motions whereby falling, sliding and flowing under the influence of gravity. A landslide is a type of 'mass wasting' or down slope movement of soil and/or rock under the influence of gravity (USGS). The word 'landslide' is actually a general term for several kinds of slope movements and they can be classified in several ways. They can be classified by rate of movement, type of materials and nature of movement and presence of lubricating agent (slide, slump, flow or fall, Chorley et al. 1985). In Australia, landslide is defined as the movement of rock, debris or earth down slope. They result from the failure of the materials which make up the hill slope and are driven by the force of gravity. Landslides are known also as landslips, slumps or slope failure. The most common types of landslide in Australia are earth slides, rock falls and debris flows. The movement of landslide materials can vary from abrupt collapses to slow gradual slides and at rates which range from almost undetectable to extremely rapid. Sudden and rapid events are the most dangerous because of a lack of warning and the speed at which material can travel down the slope as well as the force of its resulting impact. Extremely slow landslides might move only millimetres or centimetres a year and can be active over many years (creep).

Landslide can also be termed as 'mass movement'. According to Chorley et al. (1985) 'Mass movement' is the detachment and down slope movement of soil and rock materials under the influence of gravity. The sliding or flowing of the materials are caused due to their position and to gravitational forces. But this type of movement is accelerated by the presence of water, ice and air. Basically, all kind of rock-waste movements including soil and ice are collectively termed as landslide. The moving distance covered by the earth materials involved in landsliding from the place of origin to the place of destination, called as '*run-out distance*'. To define landslides, we must define fall, slide, flow, lateral spreads and topple as all these are the major

S. Mandal and R. Maiti, *Semi-quantitative Approaches for Landslide Assessment and Prediction*, Springer Natural Hazards, DOI 10.1007/978-981-287-146-6_1

slope movement types. The continuous downward movement of weathered rock materials involving large blocks, earthen materials from steep slopes or cliffed valley sides of streams under the impact of gravity, termed as *fall*. According to Selby (1982) rocks falls are relatively small landslide caused by the removal of individual and superficial blocks from cliff base and are promoted by hydrofracturing, stress release, the wedging action of tree roots and other weathering process. Bloom (1978) treated fall as one of "the distinct landslide process but it is rarely independent of subsequent events". This type of landslide is common in humid region. *Slide* is one of the most common forms of failure and can be subdivided into translational and rotational slides. *Rotational slides* are sometimes called slumps because they move with rotation. *Translational slides* have a planar, or two dimensional surface of rupture. Slides are most common when the toe of the slope is undercut. They have a moderate rate of movement and the coherence of material is retained, moving largely intact or in broken pieces. The accounts of various translational slides in the Appalachians are cited by Jacobson et al. (1989), in Puerto Rico by Simon et al. (1990), in New Zealand by Salter et al. (1981), and in California by Ellen and Wieczorek (1988). *Flow* is the most destructive and turbulent form of landslide. Flows have a high water content which causes the slope material to lose cohesion, turning it into *slurry*. They are channeled by the landscape and move rapidly. Hutchinson and Bhandari (1971) studied this type of landslide and suggested that flows may be promoted by the collapse of soil from the surrounding cliffs, steep slopes on to the upper part of the concave moving mass and raising pore-water pressure in the debris. *Spread* is characterized by the gradual lateral displacement of large volumes of distributed material over very gentle or flat terrain. Failure is caused by liquefaction which is the process when saturated loose sediment with little or no cohesion such as sands or silts are transformed into a liquid-like state. This process is triggered by rapid ground motion most commonly during earthquakes. Nearly all known examples come from southern Norway, the St. Lawrence lowlands of eastern Canada and the Alaska Coast. *Topple* is characterized by the tilting of rock without collapse, or by the forward rotation of rocks about a pivot point. Topples have a rapid rate of movement and failure is generally influenced by the fracture pattern in rock. Material descends by abrupt falling, sliding, bouncing and rolling. Varnes (1978) observed various states of activities of landslide with time such as active, dormant, reactivated, suspended, abandoned, stabilized and relict. All these characteristics of landslide vary from one place to other with varying geological, morphological and physical attribute of topography. A landslide should have some nomenclatures such as crown, main scarp, top, head, main body, foot, toe, failure surface, toe of failure surface, surface of separation, displaced mass, zone of depletion, zone of accumulation, depletion, accumulation, flank and pre-failure topography. But the entire landslide does not possess all of these nomenclatures. The failure of the slope happens when gravity exceeds the strength of the earth materials. Although the action of gravity is the primary driving force for a landslide to occur, there are other contributing factors affecting the original slope stability. Typically, pre-conditional factors build up specific sub-surface conditions that make the area/slope prone to failure, whereas the actual landslide often requires a trigger before being released.

1.2 A Brief Account of Some Destructive Landslides Occurrences

The large scale landslides in populated areas made a disastrous effect on natural environment and human structure. The scale of damage caused by earth-quake triggered landslide is more destructive than any other type of causative factors. The destructive slope movements may threaten single structure, villages or towns; agricultural and forest land; communication lines and tunnel in use or under construction; reservoirs and lakes. In 1584, a large scale landslide on the Rhone valley side slopes wrecked the community of Yvorne and more than 300 lives were lost (Heim 1932). A catastrophic slope failure (rock slide) took place in North America which destroyed part of the town of Frank in Canada in 1903 and only within 2 min about 30 million m^3 of Carboniferous limestone wiped out from the mountain face and buried long railway track and took 70 lives (McConnel and Brock 1904). The disastrous landslide occurred near Vaerdalen, north of Trondheim in Norway in 1893 (Holmsen 1954) and that destroyed 22 farms and 11 persons were killed. In 1920, the Kansu Province of China got affected by great magnitude earthquake and caused the sliding of thick loess deposits covering an area of 160 × 480 km and killed about 200,000 people (Close and McCormick 1922). In 1935 a noteworthy tunnel failure took place due to landslide in New Zealand (Benson 1940). In 1936 a rock fall, 10^6 m^3 in volume occurred near Loen and produced a 74 m swell in the Nordfjord that resulted a loss of 73 lives (Bjerrum and Jorstad 1966). Sometimes major landslides are indirectly responsible for catastrophic events that occur when the slipped material blocks a river and hold back the water. One of the biggest catastrophy of this kind occurred in the Southern Alps in the Sixteenth Century. Extensive landslides of this kind were recorded in the Himalayan region and in this way in 1893 a temporary 320 m high dam was created on the upper Ganges. One of the largest slope failure of this type occurred on April 25, 1974 in the Mantaro river valley in Peru. Kojan and Hutschinson (1978) treated the high rate of river erosion as a significant contributing factor of landslip which resulted in a very deep valley with steep slopes. Recently (2013), the Himalayan region faced destructive slope failure events and that have taken unexpected causalities. Statistical records prove that landslide is one of the most destructive natural hazards all over the World (Tables 1.1 and 1.2).

1.3 Relevance of the Landslide Study

In the hilly terrains of India, landslides have been a major and widely spread natural disaster that often strike life and property and occupy a position of major concern. In India, two regions are most vulnerable to landslides i.e. the Himalayas and the Western Ghats (Fig. 1.2). The Western Ghats and Nilgiris are geologically stable

Table 1.1 Some destructive landslide events

Date	Place	Casualties	Remark
25th November, 1248	Mont Granier, France	1,000+	Destroyed five villages
2nd September, 1806	Canton of Schwyz, Switzerland	457	Destroyed four villages
1843	Mt Ida, Troy, New York	15	Sediment slump and flow
1881	Elm, Switzerland	115	Rock avalanche demolished 83 houses
1893	Trondheim, Norway	111	Liquifaction flow in marine clays
1903	Frank, Canada	70	Rock avalanche demolished most of the town
18th February, 1911	Usoy, Tajikistan	54	Triggered by M 7.4 earthquake
19th May, 1919	Kelud, East Java	5110	Lahars caused 5,110 deaths and destroyed 104 villages
16th December, 1920	Haiyuan County, Ningxia, China	>100,000	Loess flows and landslides over an area of 50,000 km^2
25th August, 1933	Diexi, Mao County, Sichuan, China	~3,100	The largest landslide formed a 255 m high dam on the river Min
5 July, 1938	Kwansai, Japan	~1,000	1,30,000 homes damaged or destroyed
1953	Minamiyamashiro, Kyoto, Japan	336 dead or missing	5,122 homes destroyed
13 December, 1941	Huaraz, Peru	4,000–6,000	Caused by rupture of a moraine dam
10 January, 1962	Ranrahirca, Peru	4,000–5,000	An avalanche of ice and rock triggered by collapse of part of a hanging glacier
9 July, 1967	Kure, Hiroshima Prefecture, Japan	159	Landslide destroyed 352 buildings
3–5 October, 1968	Darjiling, India	'Thousands'	Landslide destroyed 60 km long highway
31 May, 1970	Yungay, Peru	>22,000	Combined rock avalanches and debris-flow buried two cities
4 May, 1971	St Jean Vianney, Cannada	31	Slab flows buried people and houses
April, 1974	Junin Region, Peru	450	218 mm rain in 5 h triggered many landslides
13 November, 1985	Armero, Colombia	23,000	Volcanic mudslides, that flowed at speeds of up to 50 km/h down the slopes of the volcano. These lahars moved into valleys, merging to form larger flows, one of which destroyed the town of Armero

(continued)

Table 1.1 (continued)

Date	Place	Casualties	Remark
14–16 December, 1999	Vargas, Venezuela	30,000	Caused by a heavy storm that deposited 911 mm of rain in a few days
9 November, 2001	Amboori, Kerala, India	40	Supposedly worst landslide in Kerala state's history
17 February, 2006	Southern Leyte, Philippines	1,126	Rock-debris avalanche triggered by ten-day period of heavy rain
11 June, 2007	Chittagong, Bangladesh	123	Series of landslides caused by illegal hillside cutting and monsoon rains
6 September, 2008	Cairo, Egypt	119	Rock fall from cliffs, individual boulders up to 70 tonnes
8 August, 2010	Gansu, China	1,287	caused by heavy rainfall and flooding in Gansu Province
16 June, 2013	Kedarnath, Uttarakhand, India	5,700	High intensity rain (cloud burst)
22 March, 2014	Oso, Washington, United States	41 Confirmed missing	the flow of the landslide was extreme because of the extraordinary run-out of mud and debris
2 May, 2014	Ab Barak, Badakhshan, Afganistan	2,000 death confirmed	The landslides were triggered by heavy rains in Badakhshan province bordering Tajikistan, where melting snow and seasonal showers make the region vulnerable to such calamities

Source [Wikipedia, the free encyclopedia (Retrieved from http://en.wikipedia.org/w/index.php) and Coates (1977), Table 2, p. 19]

but have uplifted plateau margins influenced by neo-tectonic activity. The Himalayas mountain belt comprises of tectonically unstable younger geological formations subjected to severe seismic activity. According to Prasad (1986), Rao and Chacko (1986), Thigale and Khandge (1996) that landslide activities are increasing gradually in the Western Ghats, for over 1,200 km, covering parts of Maharashtra, Goa, Karnataka, Tamilnadu and Kerala. Major landslide locations of Western Ghats are Ghatkopar (Mumbai), Morbad (Thane), and Panchmukhi (Thiruananthpuram). Landslide has become an annual phenomenon in the Iddukki and Wynad district of Kerala as a result of deforestation and soil erosion. Compared to Western Ghats region, the slides in the Himalayas region are huge and massive and in most cases the overburden along with the underlying rocks are displaced during sliding particularly due to the seismic factor. Himalaya is the youngest and highest mountain range on Earth, which extends over a length of about 2,400 km. It is one of the most active and fragile mountain chains in the world; it is home to millions of people

Table 1.2 Location and character of the major landslide phenomena in the Shivkhola Watershed

Landslide No.	Location	Specific location of the slides	Elevation and slope angle	Lithology	Area of the slide	Triggering factors	Type of the slide
1	Mahanadi-I	36.5 km. N of Siliguri	57° 1,150 m	Phyllite	390 m^2	Solifluction and gravitational pull	Debris slide
2	Mahanadi-II	36.55 km. N of Siliguri	62° 1,148 m	Quartzite	120 m^2	Solifluction and seeping of water	Debris slide
3	Mahanadi-II	36.6 km. N of Siliguri	65° 1,150 m	Quartzite and phyllite	300 m^2	Supersaturation of the materials	Debris slide
4	Tindharia (Rly. Station)—September 2006	26 km north from Siliguri	57° 927 m	Phyllite, Quartzite-schist	56 m × 31 m	High intensity rainfall and saturation of materials	Earth slide
5	Tindharia downslope	26.5 km north from Siliguri	>65° 925 m	Phyllite, Quartzite-schist	6532.5 m^2	Cohesiveless materials and steep slope	Earth fall
6	Paglajhora sinking zone (lower)	39 km north from Siliguri	>65° 1,136 m	Foliated gneiss and mica schist	Around 2 km (both up and down slope)	Reduction of shearing strength due to supersaturation of slope materials	Subsidence and sinking
7	Lower Paglajhora road subsidence	38.5 km north from Siliguri	68° 1,137 m	Foliated gneiss and mica schist	200 m length of road	Reduction of shearing strength due to supersaturation of slope materials	Subsidence and sinking
8	Lower Paglajhora Road Abandonment	38 km north from Siliguri	70° 1135 m	Foliated gneiss and mica schist	125 m length of road	Reduction of shearing strength due to supersaturation of slope materials	Subsidence and sinking

(continued)

Table 1.2 (continued)

Landslide No.	Location	Specific location of the slides	Elevation and slope angle	Lithology	Area of the slide	Triggering factors	Type of the slide
9	Upper Pag-lajhora road subsidence	15 km donwn from Kurseong	67° 1,220 m	Foliated gneiss and mica schist	85 m of road	Steep slope and saturation of unconsolidated materials	Subsidence and sinking
10	14 miles bustee road abandonment	37.5 km North from Siliguri	>65° 1,130 m	Foliated gneiss and mica schist	68 m length of road	Existence of non-cohesive materials on steep slope	Subsidence and sinking
11	14 miles bustee Slide	37.25 km north from Siliguri	59° 1,118 m	Calc-granulite, Foliated gneiss and mica schist	2,250 m^2	Steep slope, unconsolidated materials, formation of narrow nala	Earth slide
12	Shiviter T.E. (along the road)	2.0 km north from Mahanadi	64° and 950 m	Highly foliated and decom-posed granite	312 m^2	Steep slope, supersaturation of unconsolidated materials	Weathered debris failure
13	Shiviter tea garden slide	3.0 km north from Mahanadi	>65° and 1,050 m	Highly foliated and decom-posed granite	3 acres of tea area	Steep slope, supersatu-ration of unconsolidated materials	Debris fall and earth fall
14	Jogamaya T.E.	Downslope between Tindharia and Gayabari	50°–65° 900–1,050 m	Phyllite, Quartzite-schist	Large tea area affected by slide		Soil-slip and debris slide
15	Sepoydhura T.E.-I	2.00 km north from Chunabhati Rail Station (Hill Cart Road)	>65° 295 m	Soft yellowish mudstone, shale and conglomerate	66.6 m^2	Steepening of slope by road cutting and less cohesive materials	Debris slide and earth slide

(continued)

Table 1.2 (continued)

Landslide No.	Location	Specific location of the slides	Elevation and slope angle	Lithology	Area of the slide	Triggering factors	Type of the slide
16	Sepoydhura T.E.-II	2.5 km north from Chunabhati Rail Station (Hill Cart Road)	45° 295 m	Soft yellowish mudstone, shale and conglomerate	77 m^2	Steepening of slope by road cutting and less cohesive materials	Debris slide and earth slide
17	Sepoydhura T.E.-III	1.5 km. north from Chunabhati Rail Station (Hill Cart Road)	>65° 300 m	Soft yellowish mudstone, shale and conglomerate	102.6 m^2	Steepening of slope by road cutting and less cohesive materials	Debris slide and earth slide
18	Nurbong T.E.	4.5 km. north from Chunabhati Rail Station (Hill Cart Road)	>65° 375 m	Soft yellowish mudstone, shale and conglomerate	1,425 m^2	Steep slope, loss of basal support by toe erosion, unconsolidated materials	Subsidence and sinking
19	Gitange T.E.	5.00 km north from Chunabhati Rail Station (Hill Cart Road)	>45° 300 m	Soft yellowish mudstone, shale and conglomerate	Lower section is affected by failure	Bared slope surface, saturation and Steep slope	Rock-soil creep

living in northern India, northern Pakistan, Nepal, Bhutan, Tibet and parts of other Asian nations. Owing to the rugged topography, the complex geological structures, the fragile soil cover, occurrences of unconsolidated Quaternary sediments along hill slopes, the high physical weathering, the high intensity monsoon rainfall, the large temperature variations, and the occurrence of very large magnitude earthquake events, landslides, debris flows, soil erosion, and other mass wasting processes are very frequent in this region, which in fact are the primary cause of environmental degradation in the region. Most of the landslides in the Himalayan region occur along or very close to major thrust and fault like the Main Boundary Fault (MBF), the Main Central Thrust (MCT), the Tethyan Thrust (TT), and the Indo-Tsangpo Suture Zone (ITSZ) where rocks are heavily crushed due to regular tectonic activity (Fig. 1.1). The region comprises lithological groups of Quaternary sediments, Siwaliks, Lesser Himalayan Sequence, Greater Himalayan Sequence, Leucogranites, Chekha Formation and Tethyan Sediments from south to north. There are six thrust planes passing parallel to Himalayan range that have made the region most vulnerable to landslips.

Himalayan Region can be grouped into four major sections with respect to the distribution of landslides: i. Jammu and Kashmir Region ii. Himachal Pradesh Region iii. Uttaranchal Region and iv. North-Eastern Region (Fig. 1.2). Major landslide of Jammu and Kashmir region are Khuni Nala Slide (Before 1947), Nashri Slide (1953) and Sansara Slide (1972). In Himachal Pradesh region, Malling slide (1980, 1990), Ropagad Slide (1990), Thangi Slide (1985), Telangi Slide (1975), Sapni Slide (1989) and Urni Rock Fall (1992) are well known landslide sectors. Kaliasaur Slide (1969), Nandprayag Slide (1970), Patalganga Slide (1970), Debidhar Slide (1979), Banswara Slide (1998), Bhiri Slide (1982), Guptkashi Slide (1984), Barua-Bhenti Slide (1998) are the major landslide locations of Uttranchal Region in Alakananda Valley (Fig. 1.3). In Uttaranchal, steep mountain slope, passing of major thrust plane and existence of weak lithology promotes landslide activities.

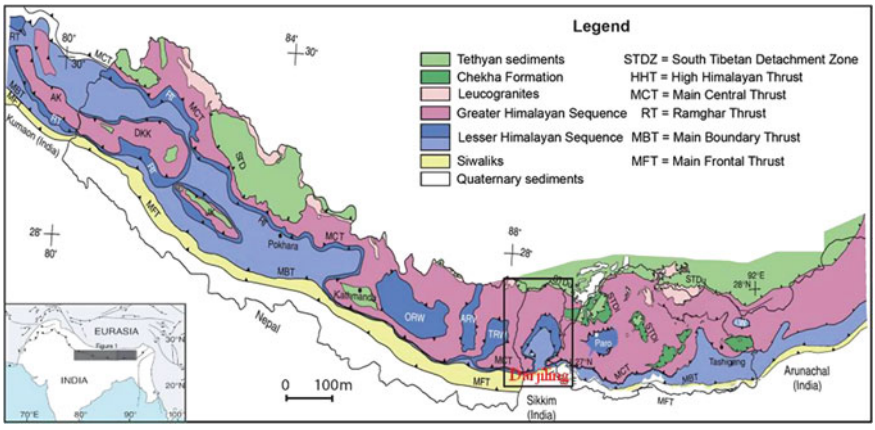

Fig. 1.1 Lithology and various thrust plane passing through himalayan range (*Source* www.iisc.ernet.in)

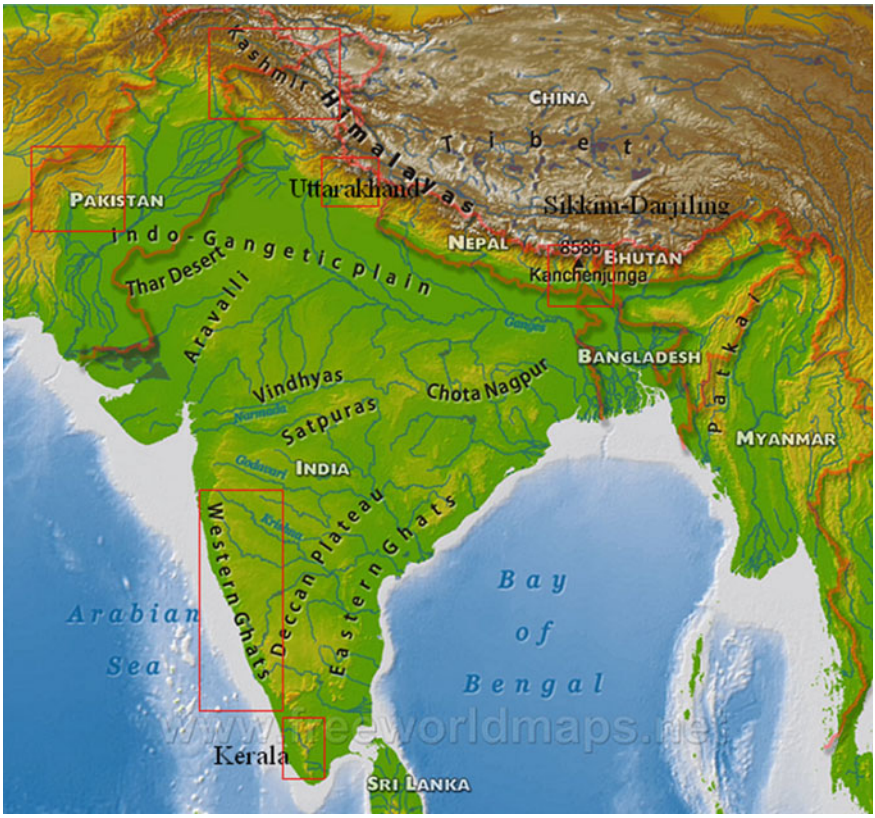

Fig. 1.2 Location of major landslide prone area in India

Major landslides in North Eastern Region are Padamchen Slide (1968, 1971), Rishi Slide (1964), Lepchajhora Slide (1968), Barrik Slide (1968), Rangpo Slide (1968, 1971), 9th Mile Slide (1968), Labha Slide (1968), Manul II Slide (1966), Myang Slide (1967, 1973), Richu Slide (1966), Vong Slide (1962), Shivakhola Slide (1968, 1998, 2006, 2011), Keukhola Slide (1965, 1968) and Likibur Slide (1998, 2006) (Source: Chandra 1975; Sinha et al. 1975; Sinha 1975; Engineer 1975; Krishnaswamy and Jain 1975; Didwal 1988; Bartaya et al. 1996; Sah et al. 1996; Sah and Bartaya 2002; Mandal and Maiti 2012, 2013).

Alakanand river valley of Uttaranchal region is one of the most important landmarks with regard to landslide events at present. All the major thrust planes (weaknesses planes) crossed the river valley region and made lthologically more fragile segment of the Himalayan Range (Fig. 1.3a). In this region, Main River and its tributaries are always engaged in down cutting processes. The active erosion process over weak lithology has aggravated the mountain slope more susceptible to landslide by steepening the valley side slope (Fig. 1.3b).

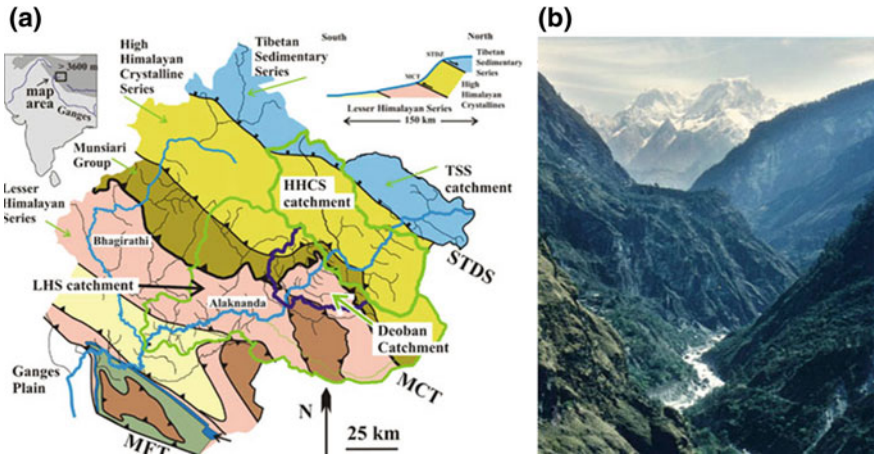

Fig. 1.3 Alakananda River Valley with various thrust planes and lithology (*Source* www.esc.cam.ac.uk)

Every year, especially during the summer monsoon period, landslide and related natural disaster events claim many lives and destroy property, infrastructure, and the environment of the Himalayas. The economic loss in landslide alone in this region is estimated at $1 billion per year. It is estimated that the loss of life due to landslides and related earth flow phenomena in the Himalayan Region constitutes about 30 % of the world's total landslide-related damage value. The earthquake induced landslide in Himalayan terrain is quite common phenomena. A large number of landslips took place after Uttarkashi Erathquake in 1991 (SOI, Publication 30). The Durham Landslide Fatality Database suggests that over 1,000 people were killed in landslide events in the Himalayas in 2007 alone, which represents almost 35 % of the global total. It was estimated that over 20,000 people were killed by landslides during the 2005 Kashmir Earthquake in Pakistan and India. These people generally live in widely-spread settlements in the fragile Himalayan terrains, and suffer more from the landslides than any other types of natural disaster. A large number of human settlements on the Himalayas are situated either on old landslide masses or in landslide-prone areas. As a result, a great number of people are affected by large- and small- scale landslides throughout the Himalayas, especially during rainy seasons. In 1988, a huge landslide at Darbang, about 200 km west of Kathmandu in Nepal, killed 109 people and temporarily blocked Myagdi River. About 62 years before this incident, the same landslide had buried Darbang area killing about 500 people. Likewise, one of the worst landslide tragedies took place at Malpa Uttarkhand, India on 11 and 17 August 1998 resulting in death of 380 people when massive landslides washed away the entire village (www.hils.org.np/publication.hils.org.np).

Due to the 18th September 2011 Sikkim earthquake (M: 6.8), several "new" and a few "reactivated" landslides occurred right from the Himalayan foot-hill region (e.g. Dudhia in Kurseong Sub-division, Darjeeling District, West Bengal) up to the

higher Himalayan range in the higher reaches of Sikkim-Darjeeling Himalayas (Chakraborty et al. 2011). This earthquake invited cracks and subsidence of roads along Nathula-Gangtok Highway (Fig. 1.4). The new landslides that occurred in the lower elevations are mostly concentrated within the terrace deposits of trunk streams such as Tista, Rangit and Balason etc. (Fig. 1.5) and within the old colluvial deposits on the lower reaches of slope adjacent to trunk streams (e.g. Jorethang-Rishi-Legship section along the right bank of Rangit river). In the slopes having steep relief, the frequencies of rock/debris fall are more than to slides, whereas field observation clearly indicated that proximal to epicentral region, frequencies of both rock fall and rock slides are much higher than the debris/soil slides and the same are more concentrated towards the crest of steep ridges. Recent field observation of the

Fig. 1.4 Cracks and subsidence, Nathula-Gangtok Road, Sikkim-Darjiling Himalaya (*Source* GSI, Engineering Division, Gangtok, Sikkim)

Fig. 1.5 Some fresh landslips after Sikkim Earthquake, 2011 (*Source* GSI, Engineering Division, Gangtok)

landslide-related damages further indicated that lithology and geomorphology also played a significant role in causing these earthquake induced landslides. The debris-laden slope which is made of loose unconsolidated material and the slope covered by thin unconsolidated scree deposits have been more prone to failure by this earthquake. Frequency of rock fall and rockslides are more in areas which are generally vulnerable due to steep slope, weathered and fractured lithology and unfavourably jointed and kinematically-unstable slopes (GSI Report October 19, 2011, Engineering Geology Division, Eastern Region, Kolkata).

From 14 to 17 June 2013, the Indian state of Uttarakhand and adjoining areas received heavy rainfall, which was about 375 % more than the benchmark rainfall during a normal monsoon. The upper Himalayan territories of Himachal Pradesh and Uttarakhand are home to several major and historic Hindu and Sikh pilgrimage sites besides several tourist spots and trekking trails. Heavy rainfall for four consecutive days as well as melting snow aggravated the floods. Torrential and unrelenting downpour, landslides and floods saw the raging waters sweep away more than 180 people and hundreds of livestock to death. More than 70,000 pilgrims have been stranded even as the Army and Air Force try to rescue them in a hostile terrain. Of all the affected areas, Kedarnath was the worst hit. Extreme rains have wreaked havoc in the region, with the tenuousness of the Himalayan soil stability resulting in killer landslides. But environmentalists claim that widespread and almost unregulated expansion of giant hydro-electric projects in the region, the incessant construction of roads to serve the burgeoning tourist population, and the adverse effect on the fragile ecosystem in the region due to growing human presence and pollution are the major causes for the devastation that Uttarakhand has been subjected to.

However, according to eyewitnesses huge rocks broke away from Kedar Dome after the flash floods caused by the cloudburst (Fig. 1.6a, b). Reports say that the temple's courtyard has been washed away and Nandi, Shiva's mount at the gateway to the temple, too was buried under over 6 feet of mud and rocks, like most of Kedarnath. It however survived the onslaught of the mudslide. Even the 14-km stretch of roadway from Gaurikund to Kedarnath has been totally submerged, making entry or exit impossible. This is what led to pilgrims being stranded (Fig. 1.10). Even Ram Bada, between Gaurikund and Kedarnath, is totally invisible from the rescue helicopters. So while the two sides—the environmentalists and the government—squabble over the root causes of the disaster, thousands of lives hang by a thin thread. The massive slope failure destroyed human settlements (Figs. 1.7 and 1.8) and eliminated Ram Baba Road (Fig. 1.19) at Kedarnath and its adjoining areas. Some fresh slope failure completely damaged mountain slope vegetation cover (Figs. 1.9, 1.11 and 1.12) [Source: Disaster Mitigation and Management Centre, Govt. of Uttarakhand, 2014].

Apart from such catastrophic landslides, many small-scale slope failures go unreported, especially when they occur in remote areas of the Himalaya. Furthermore, the loss of productive lands in the hills due to landslides and related mass erosion phenomena during every rainy season, which are seldom reported unless they involve the loss of life, is so great that a quantified economic loss would

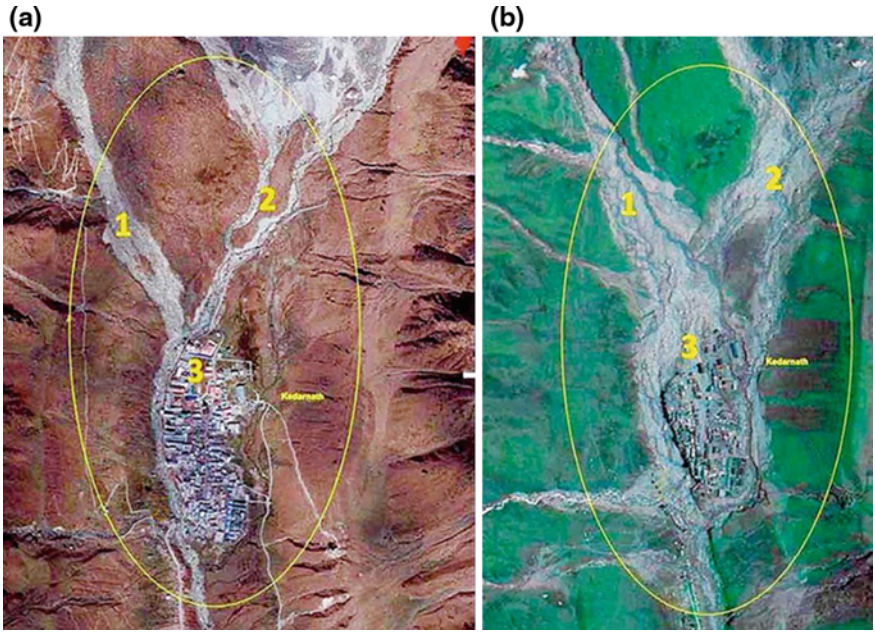

Fig. 1.6 **a**, **b** Previous satellite image and settlement around Kedarnath Temple (**a**); and Post-disaster satellite image and complete destruction of the town Kedarnath (**b**) (2013) (*Source* www.dailymail.co.uk)

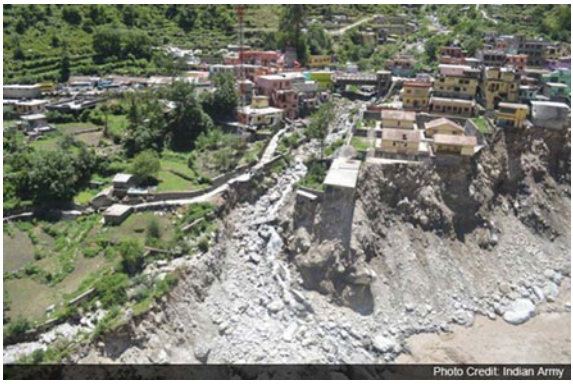

Fig. 1.7 Slope failure and destruction of settlement at Kedarnath (*Source* www.dailymail.co.uk)

probably be in the same range as for a one-off natural disaster. National infrastructures like roads, bridges, dams, hydropower stations, canals, buildings are also repeatedly damaged by landslides in this region. A rapid rise in construction of national infrastructures including roads, hydropower stations and dams, etc. with inadequate or little consideration for the natural hazards has considerably contributed to triggering of landslides in the mountains of the Himalayas (*Himalayan*

Fig. 1.8 Slope failure and destruction of settlement at Kedarnath (www.dailymail.co.uk)

Fig. 1.9 Elimination of road by landslide, Kedarnath (*Source* www.srinistuff.com)

Fig. 1.10 Trapped people by landslide along the road, Gourikund to Kedarnat (*Source* www.theaustralian.com.au)

Fig. 1.11 Down ward movement of fragile slope materials (*Source* www.dailymail.co.uk)

Landslide Society, www.hils.org.np/publication.hils.org.np). Similarly, due to a rapid increase in population over the Himalayan hills in the last three decades, the trend of settling in comparatively hazardous areas is increasing. Thus, the rising levels of risk from the landslides triggered by hydro-meteorological variability invariably entail considerable loss of life and property losses and inflict significant damage on the vital economic system of the Himalayan nations (Dahal 2009). A further key issue is the deterioration of the ecological balance and environment of the Himalayas, most notably through excessive deforestation, soil erosion and river sedimentation. This is likely to be exacerbated by global warming, which is likely to cause increased levels of extreme climatic events. Warming is also putting many Himalayan glacial lakes in great danger of bursting, which may lead to complete destruction of downstream human settlements and the habitat to world's rare flora and fauna. Unfortunately, however, despite the rapid climatic, geomorphological, environmental and ecological changes taking place in the Himalayas, all of which can be linked to landslide occurrences, systematic research on landslide processes and environmental changes in the Himalayas is at best in its infancy. Although some efforts have been made by the professionals and researchers from government agencies in, for example, India, Nepal, Pakistan, and Bhutan as well as from nongovernmental organizations, international agencies, and academic institutions, the areas of investigation, the methodologies adopted, and the classification criteria considered in the study differ considerably. Furthermore, there is a serious lack of knowledge transfer and research output dissemination among the researchers. Partly, this is because there are very few scientific gatherings among the geoscientists, environmentalists, and engineers who are involved in Himalayan landslide and environmental research. To deal with all these issues in the Himalayan Region and to foster investigations, collaborations, discussions, and integration among the stakeholders in Himalayan landslide and environmental issues, a common forum of

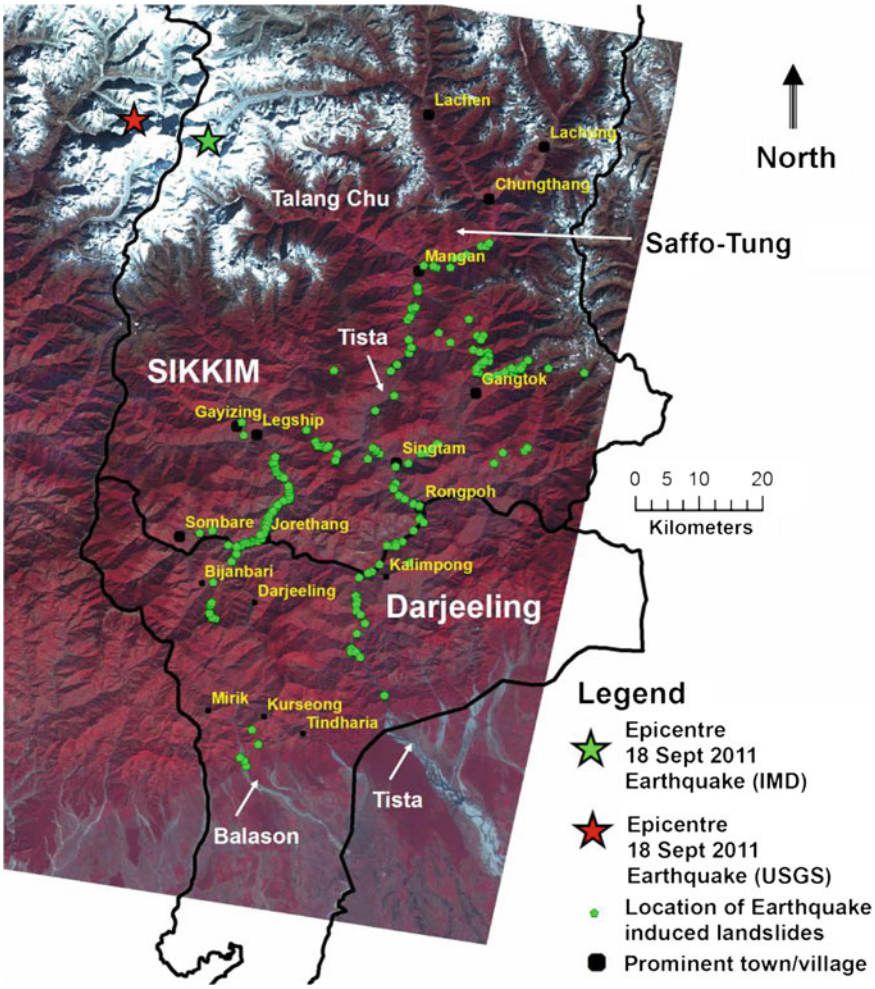

Fig. 1.12 Location of earthquake induced landslide (2011) in Sikkim-Darjiling Himalaya (*Source* Geological Survey of India, Eastern Region (Kolkata), darjeelingnew1blog)

geoscientists, environmentalists, engineers, and stakeholders needs to be established immediately (Bhandary et al. 2012, 2013; Dahal and Bhandary 2013).

1.4 Landsliding in Darjiling Himalaya

The appalling landslip of 23rd September, 1899 which occurred in the eastern side of Darjiling Town and confined to the soil-cap covering the gneisses that form the Darjiling ridge. This landslip took away 72 lives and the damage to property was

extensive. The widespread landslides occurred throughout the Darjiling District in 1950 as a result of heavy spell of rain for 3 days. The loss of life reported from the district was 127 and out of which 100 was in Darjiling Sadar Sub-division alone. The town Darjiling was cut-off for about 5 days and the Siliguri-Kalimpong Railway line was washed away. Large sections of the Kurseong-Darjiling Railway track were washed away. In 1950, K.K. Dutta, a Geologist, carried out a detailed investigation and opined that while the pore-water pressure was the immediate causes of slope instability, the stability of a slope depended primarily upon its inclination and the nature of the structure of material adjoining it. During rains the pore spaces and the voids are completely get filled with water and cause a rise of piezometric surface, which, in turn increases the pore pressure and decrease the shearing resistance of the materials and create slope failure. Due to incessant and heavy rain of 809 mm for 3 days between 3rd and 5th October 1968, there were numerous landslides in Darjiling Himalaya. On October 5, the rainfall was 499 millimetres. The number of deaths were estimated officially 677 on 12 October. The Rangpo Bridge on the Sikkim border along the Tista-Gangtok Highway, the magnificent, one-span concrete bridge on the Tists River near Tista Bazar and several other bridges at strategic points were badly damaged. The Hill-Cart Road, the arterial route between Siliguri and Darjiling was breached at 18 different places. The Indian Tea Association in a statement claimed that between ten and fifteen percent of the total tea area in Darjiling Himalaya has been destroyed. It also claimed that over 100 lives had been lost in the tea estates and there had been widespread damage to factories buildings and other installations. It is assumed that the problems of landslide cannot be prevented entirely but they can be checked by proper preventive measures. Turfing and afforestation of bare slopes, well-directed and efficient drainage, reduction of the steepness of hill slopes by terracing, outward protection of the soil cap by means of revetments and buttresses, protection of the harder rock outcrops, systematic quarrying in hillsides and control of the erosive action of streams and waterfalls are some of the preventive measures which may check landslides (Figs. 1.13, 1.14, 1.15, 1.16 and 1.17).

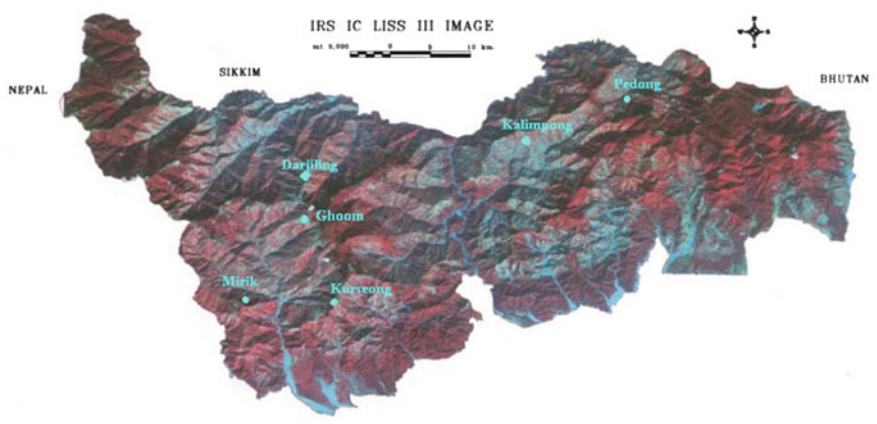

Fig. 1.13 IRS IC LISS III satellite image of Darjiling district (*Source* www.darjeeling.gov.in)

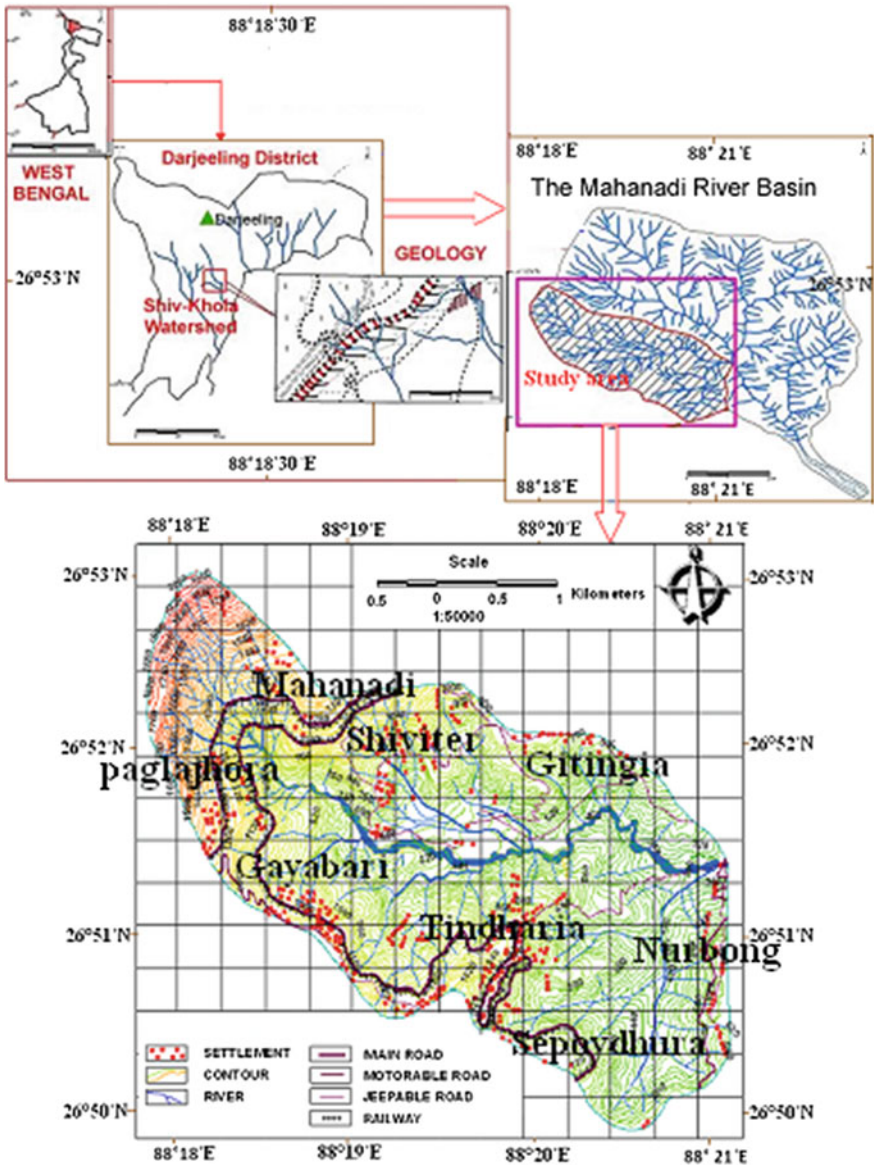

Fig. 1.14 Location of concerned study area, the Shivkhola Watershed, Darjiling Himalaya

The concerned study area, the Shivkhola Watershed is badly affected from slope instability jeopardizing the economy and social systems taking the toll of lives, lands and properties. The effects are conveyed to a long distance propagating both in upslope and down slope direction by the disruption of transport, hydrological systems. Most of the landslides of this trouble torn district of Darjiling are

Fig. 1.15 Road damage at Tindharia

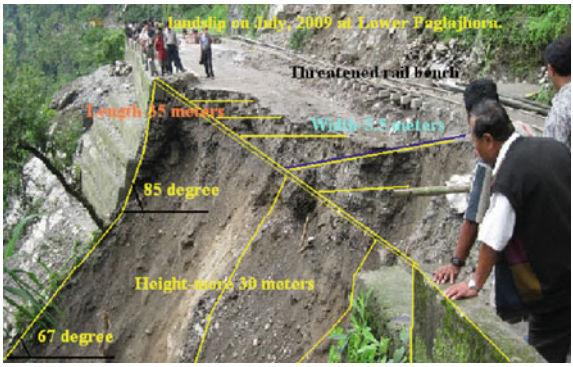

Fig. 1.16 Elimination of Hill Cart Road

Fig. 1.17 Destruction of toy train line

concentrated to this area where most of the torrential jhoras (Hill Streams) at their upper catchments develop a potential sinking zone and the Hill Cart Road and Narrow gauge Rail, when traverse through these zones, invite catastrophic slide. The present work tried to identify the zones of potential slides by investigating into the systematic interaction among the numbers of prominent triggering factors.

The Shivkhola watershed, a landslide prone spatial unit in Darjiling Himalaya, dominated by a large number of destructive landslide events. Most of the landslides took place at Tindharia, Lower Paglajhora, Gayabari, Shiviter and Nurbong. Since the first half of 20th century, the Watershed experienced following major landslip events.

- The landslip in Tindharia on 15th Januay, 1934 due to Bihar-Nepal earthquake.
- Between the 11th and 13th June, 1950 a series of devastating landslide after a spell of 834.10 mm rainfall around Kurseong, Darjiling Himalaya (Basu et al. 2003).
- Landslide at Giddapahar near Kurseong damaged over 175 m of road and railway track and demolished many bustee hamlets between 3rd and 5th October, 1968 due to heavy rainfall of 1121.40 mm (Basu et al. 2003).
- During 3rd and 4th September, 1980 again Tindharia was affected by severe landslide due to heavy and concentrated rain of 299.1 mm (Basu et al. 2003).
- During 15th and 16th September, 1991 numerous landslide phenomena at Paglajhora and Chunabhati (Basu et al. 2003) due to 462.5 mm heavy rain.
- During 11th and 13th July, 1993 innumerable landslide devastated Mahanadi, Gayabari and Tindharia due to concentrated rainfall of 211.3 mm.
- The year of 1995, 1998, 2001, 2002, 2003, 2006 and 2007 are major cases of landslips along the Hill Cart Road mainly at Paglajhora, Giddapahar, Tindharia and Gayabari.
- A devastating landslide at Shiviter Tea Estate in 2005 (Fig. 1.18), which destroyed a tea garden area of 1.5 acres (Field study by author, Tea Garden Manager, 2006).
- On 10th September, 2006 a devastating landslide took place along the Hill Cart Road (Fig. 1.17) at 14 miles Bustee and blocked the railway line for few days due to sudden and catastrophic rainfall (Opinion Survey, 2007).

Fig. 1.18 Massive damage of tea estate, Shiviter

- A road crack was formed along NH-55, the road to Darjiling from Siliguri, at Tindharia following heavy rain in the past few days on 4th August, 2007. Another landslide incident happened in the same year on 16th July along the Hill Cart Road and completely broken down the guard wall nearby Kurseong town (Field Survey, 2008) (Fig. 1.15).
- A major landslides at 14 mile near Paglajhora disrupted traffic along the National Highway-55 (Fig. 1.16) and toy train services between New Jalpaiguri and Kurseong on 16th June, 2010 morning (Field Survey, August, 2010).
- Heavy showers and the vibration caused by Sikkim Earthquake invited destructive landslide events at Tindharia (Fig. 1.12) and Lower Paglajhora on 10th May, 2011.

Recently, landslide risk analysis, like many other forms of management of either natural or civil engineering hazards, is a relatively new discipline. Earlier attempts to reduce landslide risk were largely the history of management of landslide terrain, construction of protective structures or monitoring and warning systems, or the ever-increasing sophisticated methods for mapping and delineating areas prone to landslide (Dai et al. 2002). Risk of landslide is normally defined as the expected number of lives lost, persons injured, property damaged and disrupted economic activities due to particular landslide hazard for a given area and reference period (Varnes 1984). To reduce the risk from the landslide events, the knowledge about potentiality to landslide activity is crucially needed. But the information of landslide events is described in the form of landslide susceptibility map of the concerned region and the preparation of this map depends on the complex sets of knowledge of slope movement factors. The process of creating the maps involves several qualitative or quantitative approaches (Soeters and Van Westen 1996; Guzzetti et al. 1999a, b, c).

The Shivkhola, the Right Hand Tributary of the mighty Mahanadi is located at the southern flanks of Darjiling Himalayan Range of Kurseong division of Darjiling District in West Bengal between Kurseong to the north and Tindhria to the south within 88°17′30″ E to 88°23′45″ E and 26°50′15″ N to 26°53′35″ N covering an area of about 22.05 km^2. It is famously known as Paglajhora, the most destructive and torrential hill stream at its upper catchment (Fig. 1.14). The presence of a weak and young set of rocks, a monsoonal climate with high intensity and long duration rainfall and steep mountain escarpment slope are supposed to be the major problems associated with landslide in the study area become clear. Landslide in the Himalayan region has been emerged as the dominant hill slope process. In the Shivkhola Watershed, landslides at Jogmaya Tea Garden (Fig. 1.19), Tindharia Tea Garden, and Paglajhora are destroying roads and others infrastructure, eliminating the tea garden area and also disrupting transport and communication. This has brought a serious attention of the local people and respective authorities to take care the vulnerable communities living with hazards.

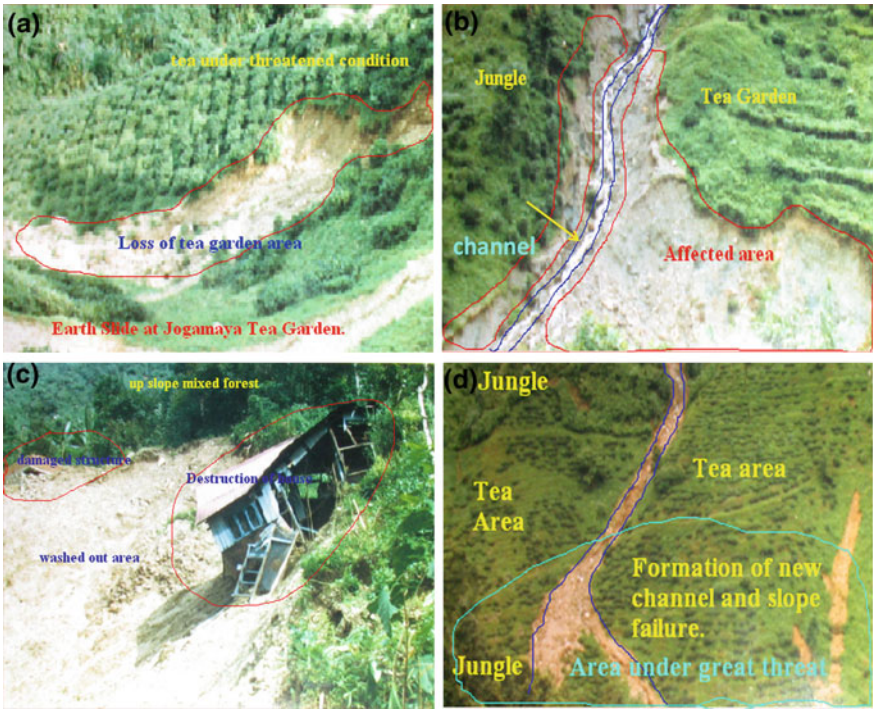

Fig. 1.19 **a–d** Destruction in Jogmaya Tea Garden Area

1.5 Mechanism and Causes of Landslides

Recently the process studies are getting increasing importance in the field of hill slope evolution though the obsession to trace cyclic landform elements and to fit them in a global model of geomorphic cycle has ultimately retarded rather than activated the development of empirical process research (Poesen and Poley 1987). Slope failures are considered as the most active agent of soil erosion in steep mountains. Proper understanding of the geomorphic evolution of mountain landscapes requires that they be given increased attention (Brardinoni and Church 2004). The evolution of hill slope is described as a complex and systematic interaction between sets of physical and manmade factors governed by geologic, hydrologic, climatic, geomorphic and land use attributes. Those factors in their interactive combination yield more than the sum of individual factors (Wilson 1981). The geomorphic processes and elements, in their systematic relationship show short-term equilibrium manifested by low rate of mass transfer and maintenance of form characterized by slope and height. Although 'true' or absolute equilibrium is a rare theoretical state towards which the system behaviour is tending with greater rapidity by attempting to absorb the successive effects of a sequence of process inputs of lower magnitude and frequency (Chorley et al. 1985). The

geotectonic factors like angle of repose, static and dynamic friction of particles, interlocking and sorting of grains (Brudsen 1979; Jumikis 1967; Carson 1977), thickness of total soil and that of saturated soil (Borga et al. 1998) are considered as important in the analysis of slope failure.

The hydrologic factors like daily rainfall threshold in connection with slope angle and regolith thickness (Gabet et al. 2004), rainfall intensity, infiltration etc. are practiced in the analysis of slope instability. The geographical factors including the anthropogenic actions for slope instability in Himalayan slopes are widely studied by Basu and Sarkar (1985, 1988), Basu and Ghatowar (1988). The slope failure in the upper catchments and its subsequent effects on fluvial dynamics are discussed considering hill and foot hill as an interactive whole and the operating geomorphic processes being interconnected (Basu and Ghatowar 1986, 1988, 1990; Basu 1989; Basu and Ghosh 1993). The anthropogenic processes like unscientific use of slope for agriculture, mining (Basu and Ghatowar 1988; Basu and Maity 2001; Bhattacharya 1999) and deforestation (Bhattacharya 1996) etc. are widely studied in relation to the slope instability. Numerous models in connection to the slope stability, shallow and deep seated landslides are introduced and verified by Hollingworth and Kovacs (1981), Burton and Bathrust (1994), Bradinoni and Church (2004), Young (1963) and Montgomery et al. (1994). The stability of natural slopes are examined and analyzed by Skempton and Hutchinson (1969). The interaction among those processes are not always possible to express in mathematical language and so an attempt is made for the establishment of empirical and verbal models both to express the possible interactions which partially support the governing processes of hill slope evolution following Ahnert (1970), Kirkby (1980), Poesen (1985), and Deploey (1982). The understanding of probable interaction among the major factors helps in the assessment of processes and in their management for the restoration of slope to ensure optimum utility from land and mineral resources.

A body will not move unless a force is applied. In geomorphic processes, gravitational force, water pressure force, expansion force and biological force play a significant role in changing the shearing strength of slope materials and in moving the earth materials down slope. We can say, the forces that drive sediments largely derive from the gravity, the climatic effect and the action of plants and animals. *Gravitational force* acts directly on rock bodies, sediments, water and ice and tending to make them move. It acts world over at a nearly uniform magnitude of 9.81 m/s^2, with slight variation resulting from distance from the Earth's centre and latitude. The presence of water within rock-soil debris produces various forces that can drive them downward. The forces developed by the presence of water are called as *water-pressure force*. Attewell and Farmer (1976) pointed out that when the pore spaces are filled up, a pore-water pressure is generated. This situation can reduce the pressure of contact of the grain. The pore water pressure υ at depth h below the water table is given by $\upsilon = \gamma h$ where γ is the density of water. The pore water pressure acts in all direction and it exerts uplift or buoyancy effect and that can produce slope instability. Sometimes *expansion forces* expand and contract sediment, soil and rock body by changing physical and chemical properties of the minerals and cause slope movement.

Biological force is being generated when plant root system push materials side ward and if this occurs on a slope a down slope movement may take place. Gray (1970), Brown and Sheu (1975), Greenway (1987) and Yim et al. (1988) studied the relationship between slope stability and vegetation.

Earth materials are always subject to stress and strain where a *stress* is a force that tends to move materials down slope. All the mentioned forces produce stress within a body. The stress of a body of soil on slope depends upon the mass of the soil body, m and the slope angle, Θ (theta), expressed as, Stress = m sin Θ. Slope materials possess an inherent resistance against downslope movement of the materials. Friction force acts against gravity and resist movement. The downslope movement of a soil body can happen when the applied stress is large enough to overcome the maximum frictional resistance. Friction is expressed as co-efficient, $\boldsymbol{\mu}$ which is equivalent to the angle at which sliding starts and called as *angle of sliding friction* (Hugget 2007). Frictional resistance is a function of both the inherent frictional properties of slope materials and the normal stress acting upon them. As the shear plane angle becomes steeper, the shear stress becomes larger and the normal stress smaller. The slope angle attained after the slope failure is known as the *threshold angle of stability*.

Cohesion is one of the most important factors of mass movement that affects the internal strength of the slope materials. It includes the chemical bonding of rocks and soil particles. The chemical bonding of rocks and soils occur with the presence of cements composed of silica, carbonates or iron oxides. Cohesion also rises through capillary suction of water in pores, compaction, and plant root systems. Soil particles affect cohesion of a soil body and generate friction between one another, called as the *internal friction* or *shearing resistance* which is determined by particle size and shape and the degree to particles touch to each other. *Mohr-Coulomb equation* defines the shear stress that a body of soil on a slope can withstand before it moves. This equation shows the shear strength as effective normal stress and cohesion, referred to as the *Coulomb-Terzaghi shear strength* equation (Summerfield 1991). The total shear strength of slope materials (s) is given as,

$$s = c + \sigma \cdot \tan\varphi, \tag{1.1}$$

where c is cohesion, σ is the effective normal stress and tan φ represents the coefficient of plane sliding friction.

The slope stability of the hill slope can be expressed in terms of the relationship between the forces tending to drive the slope materials and the forces tending to resist driving stresses. It is clear that the movement will starts when driving force exceeds the resisting force and this relationship is represented as the safety factor (FS). The slope can exist in three states: i. where shear strength is larger than shear stress, the slope is described as stable slope (FS > 1.3), ii. Where shear stress exceeds the shear strength (FS < 1.00), the slope is described as actively unstable slope. Sometimes the shear strength can vary over time with the interaction of climatic phenomena and where the third stability category becomes prominent such

as conditionally stable slope (FS = 1.00–1.30). Basically the triggering factors transform the slope from a conditionally stable to an actively unstable slope.

The safety factor (FS) is defined as:

$$FS = \frac{s}{\tau} \tag{1.2}$$

where s is the total shear strength along a specific shear plane, and τ is the total amount of shear stress developed along this plane.

For the shallow translational slide FS is described as:

$$FS = c + \frac{(\gamma z \cos^2 \beta - u) \tan \varphi}{\gamma z \sin \beta \cos \beta} \tag{1.3}$$

where c is cohesion, γ is the unit weight of regolith, z is the vertical depth to the shear plane, β is the angle of the shear plane, u is pore-water pressure and φ is the angle of internal friction.

The stability condition of the hillslope varies from place to place as a result of the variation in prevalence of landslide triggering factors. It is inferred that some factors are responsible for increasing shearing stress and some factors for reducing shearing strength. The changes of both shear stress and shear strength are major contributing factors against slope instability. Varnes (1978), introduced several factors contributing the increase in shear stress and the reduction of shear strength that is stated below.

A. Factors contributing the increase in shear stress:

1. Removal of lateral support: erosion by rivers and glaciers, wave action, faulting, previous rock fall or slide.
2. Removal of underlying support: undercutting by rivers, waves, sub-surface solution, and loss of strength by extrusion of underlying sediments.
3. Loading of slope: weight of water, vegetation and accumulation of debris.
4. Lateral pressure: water in cracks, freezing in cracks, swelling and pressure release.
5. Transient stress: earthquake and movement of tress.

B. Factors contributing the reduction of shear strength:

1. Weathering: disintegration and decomposition of granular rocks, hydration of clay minerals, dissolution of cementing materials in rocks or soils.
2. Changes in pore-water pressure: saturation and softening of weathered materials.
3. Changes of structure: creation of fissures in shales and clays, remoulding of sands and sensitive clays.
4. Organic impact: burrowing of animals and decay of tree roots.

The *causes of landslides* are usually related to instabilities in slopes. It is necessary to identify one or more causes for landslide and most important landslide trigger. The difference between these two concepts is subtle but important. The landslide causes are the reasons behind a landslide occurrence in a location and at a time. Causes may be considered to be factors that make the slope vulnerable to failure, that predispose the slope to becoming unstable. The trigger is the single event that finally initiates the landslide. Thus, causes combine to make a slope vulnerable to failure, and the trigger finally initiates the movement. The trigger is in fact a slow but steady decrease in material strength associated with the weathering of the rock—at some point the material becomes so weak that failure must occur. Hence the trigger is the weathering process, but this is not detectable externally. In most cases we think of a trigger as an external stimulus that induces an immediate or near-immediate response in the slope and in this case in the form of the movement of the landslide. Generally this movement is induced either because the stresses in the slope are altered, perhaps by increasing shear stress or decreasing the effective normal stress, or by reducing the resistance to the movement perhaps by decreasing the shear strength of the slope materials forming.

In the majority of cases the main trigger of landslides is *heavy* or *prolonged rainfall* (Caine 1980). Generally this takes the form of either an exceptional short lived event, such as the passage of a tropical cyclone or even the rainfall associated with a particularly intense thunderstorm or of a long duration rainfall event with lower intensity, such as the cumulative effect of monsoon rainfall in South Asia. In the former case it is usually necessary to have very high rainfall intensities, whereas in the latter the intensity of rainfall may be only moderate—it is the duration and existing pore water pressure conditions that are important. The importance of rainfall as a trigger for landslides cannot be underestimated. A global survey of landslide occurrence in the 12 months to the end of September 2003 revealed that there were 210 damaging landslide events worldwide. Of these, over 90 % were triggered by heavy rainfall. One rainfall event for example in Sri Lanka in May 2003 triggered hundreds of landslides, killing 266 people and rendering over 300,000 people temporarily homeless. In July 2003 an intense rain band associated with the annual Asian monsoon tracked across central Nepal, triggering 14 fatal landslides that killed 85 people. The reinsurance company Swiss Re estimated that rainfall induced landslides associated with the 1997–1998 El Nino event triggered landslides along the west coast of North, Central and South America that resulted in over $5 billion in losses. Finally, landslides triggered by Hurricane Mitch in 1998 killed an estimated 18,000 people in Honduras, Nicaragua, Guatemala and El Salvador. This is because the rainfall drives an increase in pore water pressures within the soil. Movement is driven by shear stress, which is generated by the mass of the block acting under gravity down the slope. Resistance to movement is the result of the normal load. When the slope fills with water, the fluid pressure provides the block with buoyancy, reducing the resistance to movement. In addition, in some cases fluid pressures can act down the slope as a result of groundwater flow to provide a hydraulic push to the landslide that further decreases the stability.

Considerable efforts have been made to understand the triggers for landsliding in natural systems, with quite variable results. Simon et al. (1990) found that storms with a total precipitation of 100–200 mm, about 14 mm of rain per hour for several hours, or 2–3 mm of rain per hour for about 100 h can trigger landslides in that environment. Corominas and Moya (1999) investigated the upper basin of the Llobregat River, Eastern Pyrenees area and found that without antecedent rainfall, high intensity and short duration rains triggered debris flows and shallow slides developed in colluvium and weathered rocks. A rainfall threshold of around 190 mm in 24 h initiated failures whereas more than 300 mm in 24–48 h were needed to cause widespread shallow landsliding. With antecedent rain, moderate intensity precipitation of at least 40 mm in 24 h reactivated mudslides and both rotational and translational slides affecting clayey and silty-clayey formations. In this case, several weeks and 200 mm of precipitation were needed to cause landslide reactivation.

Rapid *changes in the groundwater level* along a slope can also trigger landslides. This is often the case where a slope is adjacent to a water body or a river. When the water level adjacent to the slope falls rapidly the groundwater level frequently cannot dissipate quickly enough, leaving an artificially high water table. This subjects the slope to higher than normal shear stresses, leading to potential instability. In some cases, failures are triggered as a result of undercutting of the slope by a river, especially during a flood. This undercutting serves both to increase the gradient of the slope, reducing stability, and to remove toe weighting, which also decreases stability. For example, in Nepal this process is often seen after a glacial lake outburst flood, when toe erosion occurs along the channel. Immediately after the passage of flood waves extensive landsliding often occurs. This instability can continue to occur for a long time afterwards, especially during subsequent periods of heavy rain and flood events.

The second major factor in the triggering of landslides is *seismicity*. The passage of the earthquake waves through the rock and soil produces a complex set of accelerations that effectively act to change the gravitational load on the slope. So, for example, vertical accelerations successively increase and decrease the normal load acting on the slope. Similarly, horizontal accelerations induce a shearing force due to the inertia of the landslide mass during the accelerations. These processes are complex, but can be sufficient to induce failure of the slope. These processes can be much more serious in mountainous areas in which the seismic waves interact with the terrain to produce increases in the magnitude of the ground accelerations.

Some of the largest and most destructive landslides known have been associated with *volcanoes*. There are two main types of volcanic landslide: lahars and debris avalanches, the largest of which are sometimes termed as *flank collapses*. An example of a lahar was seen at Mount St Helens during its catastrophic eruption on May 18, 1980. The lahar killed more than 2,000 people as it swept over the towns of El Porvenir and Rolando Rodriguez at the base of the mountain. Debris avalanches commonly occur at the same time as an eruption, but occasionally they may be triggered by other factors such as a seismic shock or heavy rainfall. They are particularly common on strato volcanoes, which can be massively destructive

due to their large size. The most famous debris avalanche occurred at Mount St Helens during the massive eruption in 1980. The debris avalanche had a volume of about 1 km^3 (0.24 cu mi), traveled at 50–80 m/s (110–180 mph), and covered an area of 62 km^2 (24 sq mi), killing 57 people (Table 1.3).

The major causes of the landslides that may induce the slope materials to move downward in the representative mountain watershed of the Shivkhola Watershed of Darjiling Himalaya are:

- Average inclination of rocks is generally steep towards the roadside (60–70°).
- Weathering due to diurnal and seasonal ranges of temperature causes rapid disintegration and decomposition of the rock body.
- Due to intensity of local rainfall, the feldspar present in quartzite, decompose to form kaolin which helps rock particle to slide down.
- Continuous and heavy rain during monsoon period reduces cohesion of slope materials.
- Percolation of high intensity rain water through joints and cracks increases the hydrostatic pressure within the soils and bring a change in the consistency of the soil.

Table 1.3 Basic causes of landslide

Geological causes	Morphological cause	Physical causes of landslide	Human intervention
Weathered materials e.g. heavy rainfall	Slope angle	Intense rainfall	Excavation
Sheared materials	Uplift	Rapid snow melt	Loading
Jointed or fissured materials	Rebound	Prolonged precipitation	Draw-down
Adversely orientated discontinuities	Fluvial erosion	Rapid drawdown	Land use (e.g. construction of roads, houses etc.)
Permeability contrasts	Wave erosion	Earthquake	Water management
Material contrasts	Glacial erosion	Volcanic eruption	Mining
Rainfall and snow fall	Erosion of lateral margins	Thawing	Quarrying
Earthquakes	Subterranean erosion	Freeze-thaw	Vibration
Working of machinery	Slope loading	Ground water changes	Water leakage
	Vegetation change	Soil pore water pressure	Deforestation
	Erosion	Surface runoff	Land use pattern
		Seismic activity	
		Soil erosion	

- Consequently the angle of internal friction is far less than the regional slope (60°) that sets in instability. Cohesion is very less and that cannot bind the soil effectively.
- With the onset of monsoon rill cutting as well as gully erosion starts and the run-off, concentrating through these denuded portions, becomes the dominant agent of soil erosion.
- The geological deformation due to the pushing effects of the Damuda Series of rocks of lower Gondwana period against the Daling Series.
- Existence of very fragile rock-soil composition (rock waste of quartz-mica-schist) over the slope surface.
- Coarse textured soil with very low amount of cohesive substances like salt, calcium, and magnesium with high degree of percolation and leaching of upper soil materials to the bottom leading to disintegration and displacement of soil.
- Unscientific coal dust drills and tunnels leading to rupturing of basal support.
- Depletion of vegetation covers which increases surface run-off and soil erosion.
- Concentration of settlement along the Hill Cart Road (NH-55) and their illegal household activities over steep mountain slope and immense pressure over the fragile slope materials by man-made concrete structure.
- Physiographic configuration (arcuate) of the Paglajhora sinking (major landslide section) area provides favourable condition to produce hydrostatic pressure.
- Proximity to Main Central Thrust (MCT).
- Existence of intensely fractured and sheared nature of the bed rock.
- Toe cutting and headword erosion of debris covered slope by a fast flowing tributaries which losses the basal support.
- Moderate to steep slope gradient which favours the concentration of water and drainage.
- Improper drainage network orientation throughout the region.
- Accumulation of highly anisotrophic materials with a great thickness and low shearing resistance.
- Disintegration of phyllite and its surcharge with water caused by heavy downpour.
- Hill face, composed of phyllite and mica-schist, lost its shearing strength due to saturation and tends to move downward in the name of failure.
- The entire tea garden area is dominated by steep slope (>60°) and toe cutting by narrow channels.

1.6 Types and Classification of Landslide

The movement of the slope materials varies from place to place. Landslide can be classified based on the rate of movement of slope materials, the shape of the slope surface, the materials in the slope movements and other criteria involved in causing slope movement. Considering all these many researchers such as Heim (1882),

Almagia (1910), Terzaghi (1925), Ladd (1935), Sharpe (1938), Savarenski (1939), Emelyanova (1953), Varnes (1958), Hutchinson, developed varied schemes of landslide classification. Terzaghi classified landslide based on the physical properties involved in downward movement of materials. Sharpe (1938) classified slide, on the basis of the materials displaced and the type and rate of movement. Savarenski (1939) divided landslide into asequent, consequent and insequent considering the shape of landslide surface. *Asequent landslides* develop in homogeneous cohesive soils along curved and approximately cylindrical surfaces. *Consequent landslides* move along the bedding planes, joints or plane of schistosity dipping downslope. *Insequent landslides* run transversely to bedding plane and are generally of large dimensions.

Karson and Kirkby (1972) classified mass movement processes into three major types such as, *slide, flow* and *heave* on the basis of type of movement. *Slides* take place along clear-cut shear planes and are ten times longer than they are wide. Two main types are translational slides and rotational slides. *Translational slides* occur along planar shear planes and include debris slides, earth slides, earth block slides, rock slides and rock block slides. *Rotational slides* are called as slumps which occur along concave shear planes. This type of movement includes rock slumps, debris slumps and earth slumps. *Flow* is the gravity induced mass movement (Selby 2005). It is one of the most destructive natural processes, causing hundreds of deaths and losses of millions of dollars worth of property each year (Costa 1984). Flows are generally categorized ad *avalanches*, *debris flows*, *earth flows* or *mud flows* (Varnes 1978). Hsu (1975) suggested the term '*sturzstroms*' to explain high velocity mass movement that shows clear flowage behaviour. The very slowest type of flow is termed as '*solifluction*' which involves the oversaturation of earth materials and their downward movement. *Heave* is caused by alternating phases of expansion and contraction as a result of heating and cooling, wetting and drying and burrowing activities of animals. Heave is classed as soil creep and frost creep.

Varnes (1978) proposed for five principal types of mass movements.

1. Falls: the free fall of loosened rock mass for the greater part of distance of movement.
2. Topples: overturning of rock mass about a point below its centre of gravity.
3. Slides: the rock mass moves about a point above its center of gravity, known as rotational slide. The rock mass when moves along more or less planar or gently undulating surfaces, known as translational slide.
4. Lateral spreads: when the lateral extension movements occur in a fractured rock mass.
5. Flows: it includes continuous deformation of the rocks and gradual downward movement of the materials. In soil it represents flow like viscous fluid.
6. Complex Slides: a combination of two or more of the above stated types.

Zaruba (1969) classified slope movements considering the character of the rocks and the type of movements:

A. Slope movements of superficial deposits (slope detritus, weathering material), produced mainly by subareal agents.

   i. Talus creep that creates the terminal bending of strata
   ii. Sheet Slides
   iii. Earth Flows
   iv. Debris Flows and liquefaction of sand.

B. Slides in Clays, Marls, Claystone, Clayey shales etc.

   i. Along cylindrical surfaces
   ii. Along composite sliding surfaces
   iii. Caused by squeezing out of soft underlying rocks.

C. Slope Movements of solid rocks:

   i. Rockslides on predisposed surfaces (bedding, schistosity, jointing and fault planes)
   ii. Long term deformation of slopes
   iii. Rock falls.

D. Slope Movements include geological phenomena:

   i. Solifluction
   ii. Slides in sensitive clays
   iii. Subaqueous slide.

Chorley et al. (1985) presented a very simplified classification of mass wasting-mass movement phenomena (landslides) based on direction and type of movement:

i. Vertical movement:

   (a) Fall—rock fall, earth fall and topple
   (b) Subsidence—collapse and settlement.

ii. Lateral Movement:

   (a) Slides—block slide
   (b) Spreading—cambering (draping of sedimentary units) and Sackung (lateral spreading away from the anticlinal crest).

iii. Diagonal Movement:

   (a) Creeping—soil creep, rock creep and talus creep
   (b) Slide—rock slide, debris slide, slumping
   (c) Flows—earth flow, debris flow and mud flow.

Hutchinson in 1968 classified mass movements into three major types such as: i. creep, ii. Frozen ground phenomena and iii. Landslides. His classification was based on the rate of movement and the type of materials involved in failure. He divided landslides into translational slide, rotational slips, falls, and subaqueous slides. In 1988 Hutchinson classified landslides in the following manner based on

morphology of the moving mass with consideration of mechanism, material and rate of movement.

1. Confined failures:
   (a) in natural slopes and
   (b) in excavated slopes.
2. Rotational slips:
   (a) Single rotational slips
   (b) Successive rotational slips
   (c) Multiple rotational slips.
3. Compound Slides:
   (a) In slide mass of low to moderate brittleness
   (b) In slide mass of high brittleness.
4. Translational Slides:
   (a) Sheet slides
   (b) Slab slides; flake slides
   (c) Peat slides
   (d) Rock slides:
      i. planar slides; block slides
      ii. Stepped slides
      iii. Wedge failures
   (e) Slides of debris:
      i. Debris-slides: debris avalanches (non-periglacial)
      ii. Active layer slides (periglacial)
   (f) Sudden spreading failures.

On the basis of Soil Fabric and Pore Water Pressure, Hutchinson (1988) also classified landslides.

A. Soil Fabric [effects on c, φ]
   1. First-time Slides in Previously Unsheared Ground: soil fabric tends to be random and shear strength parameters are at peak or between peak and residual values.
   2. Slides of pre-existing shears associated with:
      i. Re-activation of earlier landslides
      ii. Initiation of landsliding on pre-existing shear produced by processes other than earlier landsliding, i.e.:
         (a) Tectonics
         (b) Glacitectonic

(c) Gelifluction of clays
(d) Other periglacial processes
(e) Rebound
(f) Non-uniform swelling.

B. Pore-water Pressure [effects on μ]

1. Short-term (undrained)- no equalization of excess pore water pressure set up by the change in total stress.
2. Intermediate- partial equalization of excess pore-water pressures. Delayed failures of cutting in stiff clays fall in this category.
3. Long-term (drained)- complete equalization of pore-water pressures to steady seepage values.

The several types of landslides are being observed in the Darjiling Himalaya. The *fall of boulders* from the steep slopes is the simplest form of landslide. Such rock body is separated from the bedrock. Second type is the *sliding of rock masses* which is quite frequent in the Tista Valley between Sivok and Kali Jhora, where the hills consist of interbedded sandstones and shales inclined at high angles in the same direction as the hill slopes. The scouring of underlying bands of soft shales by rain-water causes the overlying sandstones to slip and slide down the hillsides. The third type is the *soil slip*, caused by slow downward movement of soil or unconsolidated materials along unprotected hill slopes. This happen frequently in the vicinity of *the Hill Cart Road*, between Mahanadi and Rangdong, where sections of the road sink from a few inches to several feet. In the fourth type, *slow downward movements of soil* sometimes causes violent landslip. In Darjiling Himalaya, the soil slips are of small magnitude in regard to '*length*' and '*affected height*'. But the debris slips are of greater magnitude and are devastating in nature in Darjiling Himalaya. Major rock slips were not observed in Darjiling, where true soil slip and debris slips are common. The shearing resistance in slopes is made up of a combination of internal friction and cohesion. In clay type soil, the angle of internal friction is not more than 2° or 3° and with the internal friction alone, soil cannot be stable. But due to cohesion, for some heights a soil slope is stable at very steep angles. The angle of internal friction in rock debris which is sometimes 30°–40° is known as angle of repose. A slope will safely stand to a great height with an inclination slightly flatter than the angle of repose. In slopes formed of rock, slip occurs along certain planes of weakness like joints, bedding planes etc.

1.7 Objectives of the Present Work

The main objective of the study is to estimate, quantify, and analyze various landslide inducing parameters of land, water and soil and to prepare landslide susceptibility map on a river basin scale which will be very much helpful in planning, designing and implementing the development programmes. Without a

proper knowledge and understanding of the local geological aspects, rainfall and physical and chemical properties of soil, the construction of Hill Cart Road, trunk road between Siliguri and Darjiling by outside planners and designers along the steep escarpment slope has aggravated the problem of slope instability within the Shivkhola watershed. After the completion of the project they leave the place without assurance of sufficient training and maintenance of resources. The responsible local government has also not allocated sufficient resources for regulating land use conversion in the concerned area. Therefore the study on landslides in relation to land, water and soil will be beneficial to the local and national government in planning land use pattern and human construction in a rational manner for the future prospect and well being of the people living in the study area. For the fulfillment of three objectives mentioned above, the present work is carried out under the following heads.

- Quantitative measurement and analysis of geomorphic and hydrologic parameters of slope instability in the Shivkhola Watershed of Darjiling Himalaya.
- Preparation of a landslide susceptible map and landslide risk map for understanding the spatial distribution of slope instability by analyzing all the landslide triggering factors corresponding to the Shivkhola watershed.
- Preparation of a suitable management plan.

1.8 Applied Methodology

The deductive methodology is followed to investigate into the destructive impacts of anthropogenic activities on local environment.

- Repeated and continued field studies for long duration (2006–2011) were made for the proper cognition of the processes and their interaction. The topographic factors mainly slope steepness, slope length, contributing area and concavity of the slope were measured in field in consultation with SOI Topographical map (RF-1:50,000). Slope length and upslope contributing area was measured by locating the divide on the topographical map and measuring distance from it. The concavity was measured by means of ratio between area (a) and contour length (b) following Borga et al. (1998).
- The depth of the slide scar was measured by holding a measuring tape at both the margins of scar and the other tape was allowed to hang, the reading is then taken from the base of the hanging tape. The margin of the scars was surveyed by prismatic compass. The intensive survey of the sliding scar was carried on by Abney's level at 0.5 m interval along radial lines originating from lower most part of the scar. The altitude of the points at 0.5 m interval along the radial lines was then estimated in reference to the central base point of known altitude determined by GPS (Basu and Maiti 2001). The rate of road subsidence (along

Hill Cart Road) was being monitored by Dumpy Level Survey and continuous monitoring through GPS and measuring tape.

- The major hydrological parameter like rainfall data was collected during the field investigation from Selim Hill Tea Estate situated within ½ km crow fly distance from the major landslide location Paglajhora. Rainfall data were also collected from Shiviter Tea Estate.
- The collection of soil samples from different locations of the Shivkhola Watershed were being accomplished with GPS to analyze soil texture, water holding capacity, pore space, cohesion, friction angle and others stress parameters of the soil.
- The total thickness of soil and that of saturated soil during monsoon was measured from slope cutting. The soil here was mainly cohesion less with coarser texture, having greater infiltration capacity and so even during the high intensity rain Hortonian overland flow did not occur.
- The continuous changes in the land use character were studied during field investigations with GPS and SOI (Survey of India Topo-Sheet, 1972 and 1987).
- The sufferings from the landslide phenomena and related perception studies have been made through well structured questionnaire to make a suitable management proposal for the unstable terrain, Shivkhola Watershed.

The analysis and interpretation of collected and measured secondary and primary data were done with full care in order to make synthesis of all the studied parameters in a holistic manner for understanding the process operating in the study area.

- Relief aspects i.e. percentage hypsometric curve, slope, and topographic index of the shivkhola watershed were computed following the methods of Strahler (1952), Wentworth (1930), Smith et al. (1979).
- Basin perimeter, basin shape, stream frequency, and drainage density were measured after Horton (1932), Stoddart (1965), Miller (1953), and Schumm (1956).
- The major hydrological parameter like rainfall data was collected from Selim Hill Tea Estate situated within ½ km crow fly distance. The highly porous media helps in the quick drainage of the subsurface water parallel to the slope and thus the subsurface discharge through the porous media (permeable soil) in relation to the hydraulic gradient and Darcian flow can be measured by the following equation.

$$Q = \frac{h}{z} b\, T \sin\theta \tag{1.4}$$

h = Thickness of the saturated soil
z = Thickness of the total soil
b = contour length
T = wet soil transmissivity
θ = slope

- The hydrological factors mainly runoff depends on the upslope contributing factor. The calculation of contributing area was made considering multiple flow direction where the cumulative flow at a point (surrogated by the upslope area) was distributed among more than one neighbouring down slope pixel (Borga et al. 1998). The topographic irregularities at concave and convex slope are responsible for the convergence and divergence of flow and thus necessitate the implication of topographic index by Quinn et al. (1991). Another concept of specific contributing area (total contributing area divided by the contour length) was computed by distributing flow from a pixel among its entire lower elevation neighbour pixel (Borga et al. 1998). Fraction of Flow (F_i) allocated to each lower neighbour was calculated using Eq. 1.5 (Quinn et al. 1991).

$$F_i = \frac{S_i L_i}{\Sigma S_j L_j} \tag{1.5}$$

  where the summation is for the entire lower neighbour; S is the directional slope, and L is an effective contour length that acts as the weighting factor. The value of L used here is 10 m of the pixel size of the cardinal neighbour and 14.14 m of the pixel diagonal for diagonal neighbour.
- The rain is the important factor for triggering slide by introducing lubrication and increasing weight of wet soil in saturation condition. Once the stability threshold is crossed, the slope remains unstable at greater rainfall rates. Thus it is possible to determine the minimum steady state rainfall predicted to cause instability, called critical rainfall (r_{cr}) (Borga et al. 1998).

$$r_{cr} = T \sin\theta \frac{bp_s}{ap_W}\left[1 - \frac{\tan\theta}{\tan\varphi}\right] \tag{1.6}$$

- The amount of surface runoff from certain rain was calculated using USDA SCS Curve Number Technique (1972) and Ministry Agriculture, Government of India (1972).
- Angle of repose is considered to be the important stability factor (Van Burkalow 1945; Bloom 1991). The cohesion and angle of internal friction were measured by tri-axial compression test following Mohr stress Diagram following (Brudsen 1979; Jumikis 1967; Carson 1977; Borga et al. 1998). Geo-technical parameters of the collected soil and rock samples from different locations were measured at Geotechnical Laboratory, G.S.I., Kolkata through tri-axial soil testing mechanism. Besides, Keen Box Method and Sieve Method were used to measure bulk density and texture. To assess the geotechnical parameters of the soil in the Geological Survey of India (GSI) Laboratory (East Kolkata, Salt Lake) Indian Standard IS: 2131 (1981) were applied. This is the Indian Standard (First Revision), adopted by the Indian Standard Institution on 24th December, 1981, after the draft finalized by the Soil Engineering and Rock Mechanics Sectional Committee approved by the Building Division Council. Finally, using all the

geo-technical parameters *1-D Slope stability model* was used to prepare landslide susceptibility maps under dry, semi-saturated and saturated condition.

- The range of cohesion and friction angle of different soil was adopted from Foundation of Engineering Geology (Waltham 2002) for the analysis of slope stability. Similarly, saturated soil density of rock was adopted from the field experiences done by Deoja et al. (Mountain Risk Engineering Handbook 1991) and Specific Yield from Basic Ground-water Hydrology (Ralph C. Heath).
- The values of the Safety factors were calculated dividing the value of shear stress $\left(\boldsymbol{\tau} = \frac{\boldsymbol{\sigma}_1 - \boldsymbol{\sigma}_3}{2} \mathbf{sin}\, 2\,\boldsymbol{\alpha}\right)$ by the value of Shear strength $(\lambda) = [\boldsymbol{\sigma}_\mathbf{n} \tan \varphi + \mathrm{C}]$.
- The angle that fractures (α) should theoretically make with the greatest principal axis is:

$$\boldsymbol{\alpha} = \pm 45 \pm \varphi/2. \tag{1.7}$$

- Landslide susceptibility map of the Shivkhola watershed was prepared using remotely-sensed data, field surveys and GIS tools applying Analytical Hierarchy Approach (AHA)/Decision Support System after Saaty (1990, 1994), Saaty and Vargas (2001) and Yang et al. (2006). In this method, *landslide susceptibility index* (LSI) value for each pixel was computed by summation of each factor's weight multiplied by class weight (or rating) of each referred factor which is expressed as under:

$$\mathrm{LSI} = \sum_{i=1}^{n} (\mathrm{W_i} \times \mathrm{R_i}) \tag{1.8}$$

where, $\mathrm{R_i}$ and $\mathrm{W_i}$ are class weight (rating value) and factor weight.

- Accuracy assessment of landslide hazard map was being performed after Congalton (1991).
- Landslide hazard risk map of the Shivkhola Watershed was made with the help of following equation.

$$\mathrm{Risk} = \mathrm{Hazard} * \mathrm{Exposure}. \tag{1.9}$$

Risk exposure was calculated as a combination of three data layers i.e. weighted land use/land cover, road contributing area and settlement density.

- Management proposal to mitigate landslide and also to avoid the landslide was constructed following Royster (1979), Collison and Bhandari (1988), Valdiya (1987), Carrara et al. (1995), Pla (1997), Montgomery et al. (1989) and Howell (2001).

1.9 Data Used for Quantitative Study on Landslide

In the present work, atmospheric data was collected for Kurseong Tea Research Centre (Darjiling), day wise rainfall data was collected from the Selim Hill and Shiviter Tea Estate, historical landslide records and others relevant information were obtained from research articles (Starkel 1972; Basu and Starkel 1985; Basu and Ghatwar 1988; Basu and Maiti 2001; Basu and Sarkar 2003; Maiti 2007; Ghosh 2009b), news papers (Ananda Bazar Patrika-10/09/06, 14/06/2007, 16/07/2007 and 18/07/2007, Telegraph-04/08/2007, Statesman-August, 2006) and Geological Survey of India Technical Report, Topographical Map from Survey of India (SOI) and Satellite data from NRSA and District Census of Darjiling for the year 1981, 1991 and 2001 and District Gazetteers' of Darjiling (LSS O'Malley). Mountain Risk Engineering Handbook provided information about population growth, geology, soil, natural vegetation. Dow Hill Reserve Forest Office (Kurseong), Soil Conservation Office and Agricultural Office (Kurseong) provided information relating to land use and land cover and rainfall data. Satellite image (IIRS P6/Sensor-LISS-III, Path-107, Row-052, date 18 March 2010), Modified SRTM (Shuttle Radar Topographic Mission) data with scene size 10 latitude and 10 longitude (date 5 April 2008) and Google Earth Image (1 Sept. 2010) were also used in the study. Various thematic data layers were generated using ERDAS Imagine 8.5, Arc View and Arc GIS Software.

1.10 Existing Literature on Landslide Inducing Parameters

Among numerous literatures on slope stability, the following are of worth mentioning. These are grouped into four subheadings according to their major line of contribution. The balance condition between shear strength and shear stress are completely governed by both natural and man-made circumstances. The elements that affect slope stability and landslides are numerous and varied, and interact in complex and often subtle ways (Varnes 1984). Siddle and Ochiai (2006) summarized and reviewed and divided natural factors influencing landslide into five major groups: seismicity; strength, chemistry and mineralogy of soil; geology; geomorphology and hydrology.

Geological parameters play a pivotal role in landsliding. Siddle (1991) pointed out that there exists an association between slope instability and different types of regolith materials. Weathering alters the mechanical, mineralogic and hydrologic properties of the regolith and hence acts as an important factor of slope instability in many settings. Unstable bedding sequences are another important geological attributes for landslide incidents. This situation occurs when mass movement on bedding planes is triggered by either the increase in pore water pressures at the interface between two different alternative strata, or the weakening of strength of the clay deposit by water infiltration through the overlaying regolith layer.

Landslide often occurs when there is heavy rainfall for a long period. Siddle and Ochiai (2006) identified four common unstable bedding sequences: (1) alternating bedding of hard and soft rocks (2) highly altered and permeable regolith overlaying relatively low permeable sub-strata, (3) thin soils overlaying bedrock or till, and (4) hard caprock overlaying deeply weathered rocks. Besides, faults, lineaments or both are usually recognized as the most important triggering factors of slope instability. The relative strength of the regolith is strongly influenced by past tectonic setting as well as contemporary weathering (Julian and Anthony 1996; El Khattabi and Carlier 2004). According to Ibetsberger (1996), and Pachauri et al. (1998) the neotectonics contribute to slope instability by fracturing, faulting, jointing and deforming foliation structures.

Engineering, chemical and mineralogical properties of soil determine shear stress and shear strength of the soil. Shear strength of the soil is an important engineering property which governs the stability of natural and constructed hill slope. The shear strength is described as the function of normal stress, cohesion and angle of internal friction. The relationship within these properties to other attributes of the soil has been given by Terzaghi and Peck (1976), Wu and Sangrey (1978), and Fredlund and Rahardjo (1993). Clay minerals are another important chemical weathering product of the soil and regolith. Yatsu (1966), Duzgoren-Aydin et al. (2002) studied soil chemical properties and concluded that landslide susceptibility and slide type are closely associated with specific clay minerals. Clay accumulation within relict joints is also associated with landslides. Matsuura (1985), Shuzui (2001), Zheng et al. (2002) and Wen et al. (2004) mentioned that clay mineralogy and chemistry can also provide indicators of potential sliding plane conditions.

Geomorphic Factors of Slope Instability include slope angle, slope aspect, height of slope, slope curvature etc. Slope gradient is sometime treated as an index of slope instability and due to availability of Digital Elevation Model (DEM) it can be numerically evaluated and depicted spatially (O'Neill and Mark 1987; Gao 1993). Siddle and Ochiai (2006) suggested that slope aspect strongly affects the hydrologic processes by influencing the evapotranspiration process and thus affects weathering and vegetation and root development especially in drier environments. Churchill (1982), Gao (1993), Hylland and Lowe (1997) and Lan et al. (2004) studied the increase in slope failure in relation to slope aspect characteristics. Altitude and landslide are intimately related by virtue of other factors such as slope, lithology, weathering, rainfall and land use. The strong statistical relationship between elevation and landslide has been studied by Pachuri and Pant (1992), Linebak Gritzner et al. (2001) and Die and Lee (2002).

Spatial and temporal distribution of rainfall, water recharge into soil, lateral and vertical movement of water within the regolith, evapotranspiration and interception are the important *hydrologic attributes* for the initiation of landslide in hilly area. Spatial distribution of rainfall are closely associated with landslide initiation by means of their influence for the generation of pore water pressure in unstable hill slope and it was studied by Campbell (1966), So (1971), Starkel (1976), Siddle and Swanston (1982), Siddle (1984), Iverson and Major (1987). Generally, researchers consider total amount of rainfall, short-term intensity, antecedent storm

precipitation and rainfall duration for the landslide susceptibility analysis. Some researchers e.g. Siddle and Swanston (1982), Keefer et al. (1987) concluded that short-term rainfall intensity is the most important determinant whereas others e.g. Endo (1969) and Glade (1998) found a correlation of long-term precipitation with landslide phenomena. Slope stability over the hill slope is also governed by the rate of water movement into and through the regolith and the water holding capacity. These two important landslide governing parameters are influenced by the structure, density and orientation of fractures and intensities in bedrock and other substrata that underlie the soil profile. On micro-scale, the rate of water movement in hill slope soils is best understood by the hydraulic conductivity (K) and the sub-surface flux of water per unit hydraulic gradient. Clayey soils and compact silty soils with very small interstitial pores have much lower values of K than coarse textured soils. Siddle et al. (1985) put forwarded that the hydraulic conductivity of a confining layer underlying unstable landforms regulates long-term drainage and thus controls the moisture content of the overlying soil mantle. Hardenbicker and Grunert (2001) and Siddle and Ochiai (2006) studied pore water pressure induced slope failure on steep slope with high porosity in moderately deep soils. Infiltration into the soil increases pore-water pressure and make the slope materials unstable which is controlled by soil physical properties (porosity, hydraulic conductivity, pore size distribution, and preferential flow networks), vegetation cover, cultural practices, freezing phenomena and macro and micro topography. Horton (1993) analyzed all these properties and concluded that there exists an indirect relationship between the rate of water infiltration and slope instability. The preferential flow of water both within the soil and with the underlying bedrock was studied by Tsukamoto et al. (1982), Siddle et al. (2000a, 2001), Montgomery et al. (1997), and Siddle and Chigira (2004). Anderson and Burt (1978), Pierson (1980b), Tsukamoto et al. (1982, 2000) analyzed pore water pressure and revealed that the development of perched water table within the regolith is responsible for the initiation or acceleration of landslide.

After analyzing all the geologic, geomorphic, hydrologic, engineering, chemical and mineralogical factors of slope instability, ten landslide triggering factors have been taken into account in the present work such as slope angle, slope aspect, slope curvature, lithology, drainage, lineaments, upslope contributing area, land use and land cover, road contributing area, and settlement density. Besides, relative relief, ruggedness index, constant of channel maintenance, and drainage confluence were also studied to understand the nature of slope instability.

The landslide mechanism and triggering process are key problems acknowledged by the Ersmann (1979), Sassa (1988), Huang (2004). The study of the processes and the triggering mechanism of landslide from the view point of rainfall and hydro-dynamics is attacting more importance in the present day. The mechanism of landslide is accomplished by sliding plane which results from loss of cohesion and friction before the formation of a boundary during a heavy rainfall. It is very much difficult to identify the potential landslide sites through investigation. But there is a close relationship with rainfall where the landslide can be forecasted and analyzed through statistical analysis of the rainfall data. The landslide is also

controlled by the sliding mass resulting from large potentially weak surface around the boundary of the sliding mass, eventually leading to rapid movement on the plane with loss of cohesion and friction. This kind of landslide is associated with long-term relief fracture, weathering disintegration, erosion and washout. Zaruba et al. (1969) identified three main controlling factors of slope instability: (i) slope gradient, (ii) slope consolidation and (iii) presence of water. There are four different stages of landslides (Coppola et al. 2006; Chowdhury et al. 2000):

(a) *Pre-failure stage*: the soil mass is continuous and is mostly controlled by progressive failure and creep.
(b) *Failure stage*: characterized by the formation of shear surface through the entire rock-soil mass.
(c) *Post-failure stage*: includes the movement of the rock-soil mass involved in landsliding.
(d) *Reactivation stage*: occurs when soil-rock mass slides along one or several pre-existing shear surface.

The landslide in the mountainous slope is being governed by resisting force or shear strength and driving force or shear stress which is explained by means of ratio, i.e. resisting forces/driving forces, a dimensionless value, known as Safety Factor (FS). If the safety factor value is less than or equal to 1, the slope will fail because driving forces will equal or exceed the resisting force. During rainy reason, the driving force becomes maximum and resisting force becomes minimum and so landslides are quite common in this season in the concerned study area as a result of reduction of soil cohesion in response to soil wetting, increase of soil weight resulting from water absorption and decrease in effective stress derived from pore-water pressure.

The character and mechanism of slope failure and the processes responsible for it along with their control mechanism were studied in details by Terzaghi (1950), Skempton and Hutchinson (1969), Eden (1970), Brudsen (1979), Zaruba and Mencl (1982) etc. The mechanism of slope failure and related soil loss as a result of rain as well as gradient was studied by Ghosh (1950), Dutta (1966), Starkel (1972), Onodera et al. (1974), Weichmier and Smith (1978), Morgan (1986), Borga et al. (1998) etc. Triggering mechanism of slope instability is caused due to rise of ground water level that saturates the soil and increase the pore water pressure. Simple models have been developed for estimating the soil saturation of the mountainous region as the wetness index was defined in TOPMODEL by Beven and Kirkby (1979). More acceptable soil saturation model was applied by Montgomery and Dietrich (1994), Borga et al. (1998) and Pack and Tarboton (1998). Such model considers the ground water condition and its flow and rainfall intensity.

In the present study, threshold rainfall and threshold slope angle have been considered as triggering mechanism to illustrate site specific slope instability that is described in detail in Chap. 6. An One Dimensional (1-D) slope stability model has been summarized in Chap. 7 to explain the distribution of instability by estimating the safety factor value (FS) from 50 locations considering cohesion, angle of internal friction, slope angle, saturation index, soil-water density and depth of the

soil. Topographic Index Model is applied after Beven and Kirkby (1979) to understand the soil saturation of the slope. Geo-technical parameters were estimated through *Tri-axial compression test* for determining the safety factor values. The study reveals that weak lithological composition with cumulative rain for few days makes the slope more vulnerable and causes debris slide in the Shivkhola Watershed of Darjiling Himalaya.

1.11 Slope Stability Models

Among the various natural hazards, slope failure is the most widespread and damaging hazard (De Smedt 2005). A sudden failure of the slope is caused by sliding, rolling, falling or slumping. The constant pull of gravity makes all the hill slopes and mountain cliffs susceptible to slope failure. When failure occurs, material is transported down slope until a stable slope condition is reestablished. The high susceptibility to failure in the Darjiling Himalayan terrain is due to a complex geological structure and an interaction among various processes acting upon the steep mountain escarpment slopes. The interaction among the processes leading to hill slope evolution was studied by Ahnert (1987), Kirkby (1980), Poesen (1985), and Deploey (1982). The stability of mountain slope is generally viewed in relative terms. It is apparent, that in analysis of slope, stability is not totally a descriptive term. Perhaps, an appropriate term would be functional stability, which necessarily relates to a specific need and specific governing criteria (Cernica 1995). Soeters and Westen (1996) recommended infinite slope stability analysis but due to complication in establishing vertical depth of failure plane in 3D mechanism Monte Carlo Method, a simplified approach was considered by them reducing 3D depth to 2D equivalent depth based slope stability model. Again it (2D MODEL) was converted to equivalent translational depth of 1D slope stability model by Bhattarai et al. (2005).

Hollingworth and Kovacs (1981), Burton and Bathrust (1994), Bradinoni and Church (2004), Young (1963), Montgomery and Dietrich (1994), Van Westen and Terlien (1996), Burton and Bathurst (1998), Pack et al. (2001), Borga et al. (2002) and Saha et al. (2002) introduced numerous models in connection to the slope stability, shallow and deep seated landslides. The stability equation is applied for a mass of loose, friable cohesion less debris after Jumikis (1967), Melnikov and Chesnokov (1969). The most widely used landslide inventory techniques include (Montgomery and Dietrich 1994): (i) field investigation using a check list to identify landslide susceptibility sites; (ii) projection of future pattern of instability from the landslide inventories; (iii) multivariate analysis of factors; (iv) stability ranking based on criteria such as slope, lithology, landform; and (v) failure probability analysis based on slope stability models with stochastic hydrologic simulations. Recently, the availability of GIS data has provided a lot of advantages to quantify topographic attributes related to slope instability and landsliding. Montgomery and Dietrich (1994) propounded a contour based steady state hydrologic model with the infinite slope stability (simplified for cohesionless soils) to define

stability classes based upon slope and specific catchment area. The infinite slope stability model concept based on soil cohesion and root cohesion with the help of determining the safety factor is put forwarded by De Smedt (2005).

1.11.1 Hydrological Models and Slope Stability

The hydrologic system over the mountainous area is seldom simple and rarely exist in steady state. The hydrologic response of a hill slope to rainfall leads to a water table rise that is very difficult to predict. The amount and duration of rainfall and lag time between the rainfall events, and water table rise may vary widely depending on the hill slope configuration, intensity of rainfall, initial saturation condition and the saturated and un-saturated hydro-geologic properties of the hill slope materials (De Bleeschauwer and De Smedt 2002). The hydrologic factors like daily rainfall threshold, rainfall intensity, infiltration were studied by Guzetti et al. (2007), and Gabet et al. (2004) etc. The critical rainfall for initiating landslide was studied (r_{cr}) by Borga et al. (1998). The recurrence interval of rains of certain intensity above threshold value was analysed using log probability law by Chow (1951, 1954) and Schwab et al. (2002). Hydrological model incorporating the saturation excess run-off were constructed by Beven and Kirkby (1979), O'Loughlin (1986), Moore et al. (1988), Moore and Grayson (1991). A geomorphology based artificial neural networks (GANNs) was put forward for estimating direct runoff over watersheds by Zhang and Govindaraju (2003). Mishra et al. (2003) presented a modified SCS-CN Method. Saragni et al. (2007) evaluated three unit hydrograph models to predict the surface runoff from a Canadian watershed. Recently, an integrated approach for estimating surface run-off using Remote Sensing and GIS in the applied field of hydrological research is applied by Durbude et al. (2001), Ambazhagan et al. (2005), Jasrotia and Singh (2006), Tripathi et al. (2002) and Zade et al. (2005).

SCS Curve Number was used for estimation of runoff by correlating generalized land cover with hydrologic soil groups and data were derived from the SCS table by Chandra et al. (1984), Ragan and Jackson (1980), Tiwari et al. (1991) etc. Sing (1975) has pointed out Antecedent Moisture Condition (AMC) as the water content present in the soil at a given time. The build-up of soil pore water pressure at the contact between the soil mantle or weathered regolith and the underlying lithology during rainstorms and the period of rapid snow melt was well recognized as the triggering mechanism of slope failure and it was studied by Pierson (1977), Swanston (1982), and Megahan (1983).

1.11.2 Landslide Susceptibility Zonation Models Concept

Landslide hazard zonation consists the division of an area into several zones, which indicates progressive levels of landslide hazard. To constitute the zonation map of slope instability it is necessary to understand triggering mechanism of landslides.

Generally the location of the landslide and its behavior is governed by the hydrology of the sub-catchment in which it is located rather by the characteristics of the catchment as a whole. Without a thorough mapping of the sub-catchment and without assigning the weighting accordingly, the match between the inferred hazard rating and the observed hazard rating will remain elusive (Bhandari 1987). Disaster Management Support Group suggested a working scale for a slope instability analysis is determined by the requirements of the user for whom the survey is executed. Planners and engineers use the following examples of scales:

- National scale (<1:1,000,000) provides a general inventory of problem areas for an entire country, which can be used to inform national policy makers and the general public.
- Regional scale (1:100,000–1:500,000) is used in the early phases of regional development projects to evaluate possible constraints, due to instability, in the development of large engineering projects and regional development plans.
- Medium scale (1:25,000–1:50,000) is used for the determination of hazard zones in areas affected by large engineering structures, roads and urbanization plans.
- Large scale (1:5,000–1:15,000) is used at the level of site investigations prior to the design phase of engineering works.

There are some basic principles proposed by Varnes (1984), Carrara et al. (1991), Hutchinson and Chabdler (1991), Hutchinson (1995), Turner and Schuster (1996), Guzzetti et al. (1999a, b, c, 2003) behind the landslide susceptibility zonation, though there are some conflicting views among experts. These are:

1. Firstly, the main controlling factors for initiating landslide phenomena should be identified and mapped. So, slope failure can be recognized, classified and mapped in the field or through remote sensing, chiefly stereoscopeic aerial photographs (Rib and Liang 1978; Varnes 1978; Hansen 1984; Hutchinson 1988; Cruden and Varnes 1996; Dikau et al. 1996; Guzzetti et al. 2003).
2. According to Varnes (1984), Carrara et al. (1991), Hutchinson (1995), for landslides, "the past and present are keys to the future". Under this assumption, landslide in future is likely to occur under the same geologic, geomorphic and hydrologic conditions as those that led to landslide in the past. That is why Varnes (1984), Carrara et al. (1991), (1995), Hutchinson (1995), Guzzetti et al. (1999a, b, c, 2003) expressed that the understanding of the past failure is essential for the assessment of landslide hazard.
3. Researchers like Crozier (1986), Hutchinson (1988), Dietrich et al. (1995), Guzzetti et al. (2003) assured that conditions that initiate landslides, or which are directly or indirectly linked to slope failures, can be collected and used to build predictive models of landslide occurrence, because landslides are controlled by mathematical laws that can be determined empirically, statistically or in deterministic fashion.
4. Landslide occurrence can be inferred from the heuristic investigations, computed through the analysis of environmental information or inferred from

physical models studied after Carrara et al. (1995), Soeters and Van Westen (1996), Guzzetti et al. (1999a, b, c, 2003).

Essentially, the following two broad options are available at the start of the mapping program.

1. *Direct mapping* of landslide hazards, based on geological, geomrophological, and geotechnical investigation, and mapping by a single multidisciplinary team.
2. *State-of-nature* (factor) mapping and integration of factor maps into landslide hazards map.

British geomorphologists have cited some of the best examples of landslide hazard maps by using the direct hazard mapping approach. The second option is, however, normally preferred because Factor Maps are, in themselves, a great value to the users of the project output and provide the best assurance of independent evaluation, easy revision, and constant upgradation and revalidation (Bhandari 1994). Guzzetti et al. (2003) evaluated the requirements of indirect/state-of-nature method as: (i) the recognition and mapping of landslides over a target region which is obtained by preparing a landslide inventory map; (ii) the identification and mapping of the physical factors which are directly or indirectly correlated with slope instability; (iii) an estimate of the relative contribution of the instability factors in initiating slope instability; (iv) the classification of land surface into domains of different levels of susceptibility; and (v) the assessment of the model performance.

Crrara et al. (1992, 1995), Van Westen (1993), Hutchinson (1995), Soeters and Van Westen (1996), Van Westen et al. (1997a), Guzzetti et al. (1999a, b, c) and Committee on the National Landslide Hazards Mitigation Strategy (2004), India suggested the most common approaches in the literature review of landslide susceptibility mapping procedure and which can be grouped into five major categories, namely: (i) direct geomorphological mapping; (ii) analysis of landslide inventories; (iii) heuristic or index based methods; (iv) statistical methods, including neural networks, fuzzy logic and expert systems; and (v) process based conceptual models.

Bureau of Indian Standards (BIS-1998), proposed a guidelines for landslide hazard zonation map on 1:25,000 or 50,000 scale. Bhandari (1987) proposed landslide hazard zonation on the basis of the hazard rating values relating to the responsible factors for landslide. The landslide zonation map at regional scale has been attempted in different parts of the world for past two/three decades (Nilsen and Brabb 1973; De Graf 1978; Varnes 1981, 1985). A landslide hazard map (macro) on 1:25,000 scales has been prepared following the landslide hazard evaluation factor (LHEF) rating scheme proposed by the Indian Bureau of Standards (1998) for the area between Singtam and Ranipool (after S.R. Basu and B. Bera). Data for LHEF have been computed from interpretation of 1:50,000 Survey of India topographical maps, 1:25,000 prints of panchromatic aerial photographs (stereoscopic coverage), 1:50,000 geo-coded LISS III Satellite data, existing geological maps and extensive field work. Bhandari (1987) proposed landslide hazard zonation on the basis of the hazard rating values relating to the responsible factors for landslide.

Vecchia (1978) proposed the terrain index for the stability of hill slope that includes numerical rating for lithology, altitude, slope and friction along the potential failure planes. Pachuri et al. (1998) carried out terrain classification and landslide susceptibility mapping in Yamuna valley region of Garhwal Himalaya based on aerial photographs (1:40,000), Landsat Images (1:2,50,000) and topographic maps (1:50,000). In the Himalaya, landslide zonation map has been attempted by Majumder (1980) Chatterjee (1986), Gupta (1998), Gairola and Shukla (1990), Sharan (1992), Chandra (1992), Sharma et al. (1996). The Landslide Hazard Mapping and Risk Assessment (LHRA) was attempted by Fiener in (1999). He considered nine factors i.e. lithology, degree of weathering, structure, slope condition, hydrology, erosion, physical properties, land use and land cover and slope history for the purpose of hazard assessment. Champati Roy et al. (1997) prepared landslide hazard zonation map on the basis of information value method of an area in Chamoli district near Pipalkota town using aerial photographs and IRS LISS-II data. The SINMAP (Stability Index Mapping) was studied by Hammond et al. (1992), Montgomery and Dietrich (1994). Swanston and Dyrness (1973), Dietrich and Dunne (1978), Sidle et al. (1985) concluded that in the forested steep slope region, shallow landslides are dominant erosional processes. Bergin et al. (1995), Sidle et al. (1985), Royster (1979) suggested the reforestation and improved road drainage as the most important slope stabilization strategies and such strategies received considerable attention from Cruz and Reyes (2000).

The landslide hazard and risk analysis with the help of the geotechnical model, logistic regression model and the safety factor was done by Gokceoglu et al. (2000), Romeo (2000), Carro et al. (2003), Shou and Wang (2003), Zhou et al. (2003), Atkinson and Massari (1998), Dai et al. (2001), Dai and Lee (2002), and Ohlmacher and Davis (2003). Rowbothan and Dudycha (1998), Jibson et al. (2000), Luzi et al. (2000), Praise and Jibson (2000), Rautelal and Lakheraza (2000), Baeza and Corominas (2001), Lee and Min (2001), Temesgen et al. (2001), Clerici et al. (2002), Donati and Turrini (2002), Lee et al. (2002a, b), Rece and Capolongo (2002), Zhou et al. (2002), and Lee and Choi (2003) have applied the probabilistic model for landslide risk and hazard analysis.

Shasko and Keller (1991), Guzzetti et al. (1999a, b, c) discussed the possibility and feasibility of integrating sophisticated slope stability modeling with GIS. Ramakrishnan et al. (2002) has carried out extensive work on landslide analysis using aerial photographs. Gorsevski et al. (2000a) used logistic regression model for spatial prediction of landslide hazard. Recently, landslide hazard evaluation using fuzzy logic, and artificial neural network models have been mentioned in the various literature of Ercanoglu and Gokceoglu (2020), Pistocchi (2000) and Lee et al. (2003a, b, 2004a, b). Rowbothan and Dudycha (1998), Baeza and Corominas (2001), Lee and Min (2001), Temesgen et al. (2001), Clerici et al. (2002), Donati and Turrini (2002), Lee et al. (2002a, b), Rece and Capolongo (2002), Lee and Choi 2003), Chung and Fabrri (2003), Lee and Pradhan (2006, 2007), Youssef et al. (2009), and Pradhan and Lee (2010a, b, c) have studied and applied the probabilistic model for landslide susceptibility and risk evaluation. Joshi et al. (2002) carried out landslide hazard zonation in part of Alakananda valley in collaboration

with Space Application Centre (SAC), Ahmedabad in 1:50,000 scale. They used IRS LISS-II and PAN data and integrated different thematic maps giving weightages and ranks in a GIS environment. Lee and Pradhan (2006) introduced landslide hazard and risk mapping on Penang Island, Malaysia using Geographic Information System and Remote Sensing Data. Barbieri and Cambuli (2009) presented statistical method in landslide susceptibility mapping in 18th World IMACS/MODSIM Congress, Australia. An integrated approach for landslide susceptibility mapping using Remote Sensing and GIS was produced by Sarkar and Kanungo (2004), Sharifikia (2007) Pande et al. (2008), and Nithya and Prasanna (2010). Recently, Remote Sensing and GIS based Analytical Hierarchy Approach is one of the most popular and widely applied decision support system and has been used to synthesize various judgement comparisons to derive priorities among the criteria responsible for landslide and to prepare landslide susceptibility map (Saaty 1990, 1994; Saaty and Vargas 2001; Yang et al. 2006).

1.12 Study on Landslide Management

Given the rapid demographic expansion found in much of the region, it simply won't be possible to set aside all vulnerable slopes for protection; therefore, some strategies of slope stability on steep lands are required. Reforestation and improved road drainage (e.g. Bergin et al. 1995; Siddle et al. 1985; Royster 1979; Cruz and Reyes 2000; IADB 1999), have received considerable attention but there is still a need to identify agricultural practices that reduce vulnerability to slope failure. A soil conservation survey conducted in Honduras, Nicaragua, and Guatemala in the wake of Hurricane Mitch failed to find any beneficial effect of "agro-ecological" farming on landslide resistance during the storm (World Neighbors 2000). Use of agro-forestry, contour cropping, physical and vegetative erosion barriers, or integrated weed management were found to reduce soil degradation and surface erosion on farms affected by Mitch, but these techniques did not correlate with a reduction in landslides. While it is possible that soil conservation farming truly has no effect on slope stability, the experience of geotechnical engineers and landslide modelers indicates that land management targeted to soil or site-specific conditions can reduce the probability of slope failure (Montgomery et al. 2000; Collison et al. 1995; Royster 1979).

The number of variables involved makes it difficult to characterize the influence of land management on landslide susceptibility and even more difficult to predict how changes in management will impact the current state. In recent years, the field of physical landslide modeling has made excellent progress in dealing with the complexities of slope failure. Applications of simplified slope-stability models have proved effective as descriptive and predictive tools in temperate zones, allowing for rapid stability assessment over a wide area (Jibson et al. 2000). Knowledge of a stability index alone may be useful for planning timber harvests (e.g. Montgomery et al. 2000) or for citing infrastructure (e.g. Carrara et al. 1995), but it is not helpful

for steep-land farmers for whom non-use and relocation are not viable options. If physical landslide models are to contribute to slope stabilization in tropical, agricultural watersheds, then a driving *cause* for instability must be identified, along with the *probability* that a slope will fail. Importance of causal information is borne out by physical slope-stability models that do consider the influence of dynamic hydrology and plant growth. These models are computationally intensive and, to our knowledge, have only been applied to engineered or "characteristic" slope formations (Duncan 1996; Collison et al. 1995; Anderson et al. 1990). Nonetheless, results of these modeling exercises are relevant to field-level management. Collison et al. (1995) found that planting trees on an engineered embankment only enhances the embankment's stability if soil hydraulic conductivity is relatively high. For deep-soiled embankments with low hydraulic conductivity, planting trees was, in fact, detrimental to stability. Macro-pore flow along tree roots increased permeability, leading to elevated pore pressures in and below the rooting zone, while roots themselves did not penetrate deeply enough to anchor against deep-seated slope failure. Under such conditions, it is preferable to vegetate the embankment with grass, or some similar shallow-rooted ground cover, that sheds water off the saturated portion of the slope. Water management can be more important than physical reinforcement for weathered and frequently saturated soils. Drainage ditches, or water-shedding ground cover, may offer better slope stabilization than trees. Information on the soils and hydrology of a landslide-prone area is therefore necessary for the development of appropriate management recommendations; simply reporting the probability of failure is not enough (Collison et al. 1995).

Landslide mitigation and control measures depend on detailed investigations, including identifying of the causative factors (Bhandari 1988). The landslide mitigation work can be broadly classified into two categories: control work and restriant work (Valdiya 2006). The control works involve modification of the natural conditions such as topography, geology, ground water, and other conditions, that indirectly promote landslide. Restraint works cover construction of structure such as surface and sub-surface drainage works, removal of earth from the unstable area, and building buttress walls, piles, anchors, and retaining walls. Montgomery (1986) and Valdiya (1987) have suggested four-fold strategy of the control of landslides. This includes—(i) reduction of the slope angle and placement of additional supporting material at the foot of the slope; (ii) reduction of the load on the slope by removing the rock or soil situated high up on the slope; (iii) the utilization of retention structure; and (iv) removal of fluid by various kind of drainage systems. Vegetation is being widely used for erosion control, to achieve slope stabilization along the transportation routes in countries like Japan, Korea and Hong Kong. The new technique for slope stabilization with the help of vegetation has been adopted by the Korean Highway Corporation (Sung-Hwan Kim et al. 1997). A list of shrubs and trees that are useful for slope stabilization is given by Gupta (1979). Vegetation turfing is the most effective and important corrective measures, particularly for the freshly-exposed surfaces produced by road cutting and mining. Planting of grasses, shrubs, trees and bamboos, followed by putting of jute net or vegetated stone

pitching upon the freshly-turfed area would ensure rapid and undisturbed growth of vegetation (Howell 2001).

All the studies, mentioned, are area case specific and highly specialized. Understanding the uniqueness of the present study area was of high priority. Degree of importance of individual landslide triggering factor varies from place to place. Present research work was organized to identify relative importance of the landslide triggering factors for the area under study. Again, within the Shivkhola basin, there is also spatial variation in the contribution of the triggering factors. It is essential to analyze spatial variation in the relative importance of the factors and also site-specific variation in the triggering factors. Geomorphic, hydrologic, land use and anthropogenic attributes and their spatial distribution were studied in details through intensive field work. Runoff models, Digital Elevation Model (DEM), I-D Slope Stability Model, Run-off Model (The United States Department of Agriculture Soil Conservation Service (USDA SCS) Curve Number (CN) technique), Geomorphic Threshold, Topographic Index Model, Land Use Index Model, RS & GIS base Frequency Ratio and Analytical Hierarchy Process (AHP) etc. were used to make a detailed spatial analysis and proper integration of factors for proper synthesis. Rainfall characters were analyzed to determine the critical rain and return period of the critical rain at various recurrence intervals. The cohesion, angle of internal friction, and safety factor were derived applying IS: 2131 (1981) Standards and Codes to realize the spatial distribution of slope instability. To identify the potential landslide susceptible places in the study area, RS & GIS based *Analytical Hierarchy Approach* was applied. Verification is made for accuracy judgment. Most of the data were collected from intensive field study. In the present study slope instability in the Shivkhola Watershed was analyzed considering both physical and human factors taken together as a comprehensive whole in a cognitive approach in an attempt to propose for better management and thus to achieve social relevance as an active device for decision makers.

References

Ahnert F (1970) Functional relationship between denudation, relief and uplift in large mid-latitude basins. Am J Sci 268:248–263

Ahnert F (1987) Process response models of denudation at different spatial scales. Catena Suppl 10:31–50

Anderson RS et al (1990) Interaction of weathering and transport processes in the evolution of arid landscapes. In: Cross T (ed) Quantitative dynamic stratigraphy. Prentice Hall, Englewood Cliffs, pp 349–361

Atkinson PM, Massari R (1998) Generalized linear modeling of susceptibility to landsliding in the central Apennines, Italy. Comput Geosci 24:373–385

Attewell PB, Farmer IW (1976) Principles of engineering geology. Chapman & Hall, London

Barbieri G, Cambuli P (2009) The weight of evidence statistical method in landslide susceptibility mapping of the Rio Pardu Valley (Sardinia, Italy). In: 18th World IMACS/MODSIM congress, Cairns, Australia, 13–17 July 2009

Bartarya SK, Virdi NS, Sah MP (1996) Landslide hazards-some case studies from Sutlej Valley, Himachal Pradesh. Himal Geol 17:193–207

Basu SR, Ghatwar L (1988) Landslide and soil erosion in the Gish basin of the Darjiling Himalayas and their bearing on North Bengal Floods. Studia Geomorpholigica Carpatho-Balcanica, vol 22. Krakow, Poland

Basu SR (1989) A study of the impact of landslides on the fluvial processes of the rivers Lish and Gish of the Darjeeling Himalayas. In: Second international conference on geomorphology, Georka Plus, Frankfurt, p 23

Basu SR, Maiti RK (2001) Unscientific mining and degradation of slopes in the Darjeeling Himalayas. Changing environment. Scenerio of the Indian Subcontinent (Bd), pp 390–399

Benson WN (1940) Landslide and applied features in the Dunedin District in relation to geological structure, topography and engineering. Trans Roy Soc NZ 70:249–263

Bjerrum L, Jordtad F (1966) Stability of rock slopes in Norway, vol 67. Nowegian Geotechechnical Institute, Oslo, pp 50–78

Beven KJ, Kirkby MJ (1979) A physically based variable contributing area model of basin hysrology. Hydrol Sci Bull 24(1):43–69

Bhandari RK (1987) Slope stability in the fragile Himalaya and strategy for development. J IGE 17:1–78

Bhandari RK (1994) Landslide hazard zonation mapping in Sri Lanka—a holistic approach. In: Proceedings of national symposium on landslide in Sri Lanka, vol 1. National Building Research Organisation, Columbo, p 271

Bhandary NP, Dahal RK, Okamura M (2012) Preliminary understanding of the Seti River Debris-Flood in Pokhara, Nepal on May 5th 2012. A report based on a quick field visit program. In: International society of soil mechanics and geotechnical engineering (ISSMGE), vol 6, issue 4. Bulletin, pp 8–18

Bhandary NP, Yatabe R, Dahal RK, Hasegawa S, Inagaki H (2013) Areal distribution of large-scale landslides along highway corridors in central Nepal. Georisk Assess Manage Risk Eng Syst Geohazards doi:10.1080/17499518.2012.743377

Bhattarai P, Aoyama K (2001) Mass movement problems along Prithwi Highway Nepal. Annual report of Research Institute for hazards in Snowy Areas, vol 23. Niigata University, pp 85–92

Bhattarai P et al (2005) Quantitative slope stability mapping with Arc GIS: prioritize high way maintenance

Bergin DO, Kimberley MO, Marden M (1995) Protective values of regenerating tea tree stands on erosion prone hill country. NZ J Foresty Sci 25:3–19

Bhattacharya SK (1999) A constructive approach to landslide through susceptibility zoning case study in the Rakti Basin of Eastern Himalaya. Transaction 20–23:317–333

Bloom AL (1978) Geomorphology. Printice-Hall, New Delhi

Bloom AL (1991) Geomorphology, a systematic analysis of the Cenozoic Landforms. Prentice Hall, New Delhi, pp 76–177

Borga M, Fontag DG, Ros DD, Marchi L (1998) Shallow landslide hazard assessment using a physically based model and digital elevation data. Environ Geol 35(2–3):81–88. Springer

Brardinoni F, Church M (2004). Representing the landslide magnitude frequency relation, Capilano river basin, British Colombia. In: Kirkby JM, Darby ES (eds) Earth surface processes and landforms, vol. 29(1). pp 115–124

Brown CB, Sheu MS (1975) Effects of deforestation on slopes. J Geotech Eng Div Am Soc Civ Eng GT2:147–65

Brudsen D (1979) Mass movement in process in geomorphology. Embelton C, Thornes J (eds) Wiley, New York, pp 130–186

Burton A, Bathurst JC (1998) Physically based modeling of shallow landslide sediment yield at a catchment scale. Environ Geol 35(2–3):89–99

Caine N (1980) The rainfall intensity-duration control of shallow landslides and debris flows. Geogr Ann 62A:23–27

Carrara A et al (1991) GIS technique and statistical models in evaluating landslide hazard. Earth Surf Process Land 16(5):427–445

Carrara A, Cardinali M, Guzzetti F, Reichenbach P (1995) GIS-based techniques for mapping landslide hazard in geographical information system in assessing natural hazards. Academic Publication, Dordrecht

Carson MA (1977) Angles of repose, angles of shearing resistance at angle of talus slopes. Earth Surf Process 2:363–380

Chakraborty I, Ghosh S, Bhattacharya D, Bora A (2011) Earthquake induced landslides in the Sikkim-Darjiling Himalaya—an aftermath of 18th September 2011 earthquake. Engineering Geology Division, Geological Survey of India, Eastern Region, Kolkata

Chandra H (1975) Landslide in Teesta Valley. In: Proceeding on landslide and Toe Erosion problems with special reference to Himalaya. ISEG, Kolkata, pp 147–164

Chowdhury G et al (2000) Numerical simulation of building performance under different low energy cooling technologies. Int J Energy Environ 1(1):28–36

Chorley RJ, Schumm SA, Sugden DE (1985) Geomorphology. Methuen, London, New York

Close U, McCormick E (1922) Where the mountain walked. Nat Geogr Mag 41:445–464

Coppola L et al (2006) Reconstruction of the conditions that initiate landslide movement in Weathered Silty Clay Terrain: effects on the historic and architectural heritage of Pietrapertosa, Basilicata, Italy. Landslides 3(4):349–359

Coates DR (1977) Landslide perspectives. Geol Soc Am Rev Eng Geol 3:3–28

Congalton R (1991) A review of assessing the accuracy of the classification of remotely sensed data. Remote Sens Environ 37:35–46

Crozier MJ (1986) Landslides: causes, consequences and environment. Croom Helm, London, pp 252

Costa JE (1984) Physical geomorphology of debris flows'. In: Costa JE, Fleischer PJ (eds) Developments and application of geomorphology. Springer, Berlin, pp 268–317

Dai FC, Lee CF (2002) Landslide characteristics and slope instability modeling using GIS, Lantau Island, Hong Kong. Geomorphology 42:213–228

Dahal RK (2009) Representative rainfall threshold for landslide in the Nepal Himalaya. Geomorphology 100(3–4):429–443

Dahal RK, Bhandary NP (2013) Geo-disaster and its mitigation in Nepal. In: Wang F et al (eds) Progress of geo-disaster mitigation technology in Asia, environmental science and engineering. Springer, Berlin, pp 123–156. doi:10.1007/978-3-642-29107-4_6

Deoja B et al (1991) Mountain risk engineering handbook. International Centre for Integrated Mountain Development (ICIMOD), Kathmandu, 875 pp

De Vleeschauwer C, De Smedt F (2002) Modeling slope stability using GIS on a regional scale. In: Proceedings of the first geological Belgica international meeting, vol 12. Aardkundige Mededelingen, Leuven, 11–15 Sept 2002, pp 253–256

De Smedt F (2005) Slope stability analysis using GIS on a regional scale: a case study of Narayanghat-Mungling highway section, Nepal. Dissertation of Master Degree, Universiteit Gent, Belgium

Didwal RS (1988) Remedial methods employed in Jammu Province in India to control landslides and their efficacy. In: Bonnard C (ed) Landslides, vol 2. A.A Balkema, Rotterdam, pp 897–902

Donati L, Turrini MC (2002) An objective and method to rank the importance of the factors predisposing to landslides with the GIS methodology, application to an area of the Apennines (Valnerina; Perugia, Italy). Eng Geol 63:277–289

Ellen SD, Wieczorek GF (1988) Landslides, floods, and marine effects of the storm of January 3–5, 1982, in the San Francisco Bay Region, California. US Geol Sur Prof Pap 1434:1–310

Engineer MN (1975) Landslide and erosion problems—a case study on road Kimin-Ziro in Arunachal Pradesh. In: Proceedings landslide and Toe Erosion problems with special reference to Himalaya. ISEG, Kolkata, pp 187–206

Ersmann TH (1979) Mechanisms of large landslides. Rock Mech 12:15–46

Gabet EJ, Burbank DW, Putkonen JK, Pratt-Sitaula BA, Oiha T (2004) Rainfall thresholds for landsliding in the Himalayas of Nepal. Geomorphology 63:131–143

Glade T (1998) Establishing the frequency and magnitude of landslide-triggering rainstorm events in New Zealand. Environ Geol 35:160–174

Gokceoglu C, Sonmez H, Ercanoglu M (2000) Discontinuity controlled probabilistic slope failure risk map of the Altindag (settlement) region in Turkey. Eng Geol 55:277–296
Gray DH (1970) Effects of forest clear-cutting on the stability of natural slope. Bull Assoc Eng Geol 7:45–66
Gupta PK (1979) Plants for environmental conservation. Bishan Singh, Mahendrapal Singh, Dehradun, p 247
Guzzetti F, Carrara A, Cardinali M, Reichenbach P (1999a) Landslide hazard evaluation: a review of current techniques and their application in a multi-scale study, Central Italy. J Geomorphol 31:181–216. Elsevier, London
Guzzetti F, Cardinali M, Reichenbach P, Carrara A (1999b) Comparing landslide maps; a case study in the upper Tiber River Basin, central Italy. Environ Manage 18:623–633
Guzzetti F, Cardinali M, Reichenbach P, Carrara A (1999c) Landslide hazard evaluation: an aid to a sustainable development. Geomorphology 31:181–216
Guzzetti F, Cardinali M, Reichenbach P, Ardizzone F, Galli M (2003) Impact of landslides in the Umbria region, central Italy. Nat Hazards Earth Syst Sci 5:1–17
Guzzetti F, Peruccacci S, Rossi M, Stark CP (2007) Rainfall thresholds for the initiation of landslides in central and southern Europe. Meteorol Atmos Phys. Online first version, doi:10.1007/s00703-007-0262-7. Accessed 7 Aug 2007
Hammond C et al (1992) Level I stability analysis (LISA) documentation for version 2. General technical report INT-285, USDA Forest Service, Intermountain Research Station, 121 pp
Heim A (1932) Bergstruz and Meanschenleben. Naturf Gesell 77:218. Vierteljahrsschrift, Zurich
Holmsen P (1953) Landslip in Norwegian quick-clays. Geotechniques 3:187–194
Horton RE (1932) Drainage basin characteristics. Trans Amer Geophys U 14:350–361
Howell JH (2001) Application of bio-engineering in slope stabilization: Experience from Nepal, landslide hazard mitigation in the Hindukush Himalaya. ICIMOD, Kathmandu, pp 147–161
Hsu KJ (1975) Catastrophic debris stream (sturzstorms) generated by rockfalls. Bull Geol Soc Am 86:129–140
Huang R (2004) Mechanism of large scale landslide in Western China. Adv Earth Sci 19:443–450
Hugget RJ (2007) Fundamentals of geomorphology. Routledge, London
Hutchinson JN, Bhandari RK (1971) Undrained loading, a fundamental mechanism of mudfloes and other mass movements. Geotechnique 21:353–358
Jacobson RB, Cron ED, McGeehin JP (1989) Slope movement triggered by heavy rainfall, November 3–5, 1985, in Virginia and West Virginia, USA. Geol Soc Am 236:1–13 Special Paper
Jibson WR, Edwin LH, John AM (2000) A method for producing digital probabilistic seismic landslide hazard maps. Eng Geol 58:271–289
Kirkby MJ (1980) The stream head as a significant geomorphic threshold. In: Coates DR, Vitek JD (eds) Threshold in Geomorphology. Allen and Unwin, Winchester, pp 53–73
Kojan E, Hutchinson JN (1978) Mayunmarca rockslide and debris flow, Peru. In: Voight B (ed) Rockslides and abalanches, vol 1. Elsevier, Amsterdam. pp 315–361
Krishnaswamy VS, Jain MS (1975) A review of major landslides in north and north-western Himalayas. In: Proceedings landslide and Toe Erosion problems with special reference to Himalaya. ISEG, Kolkata, pp 3–40
Lee S, Choi U (2003) Development of GIS based geological hazard information system and its application for landslide analysis in Korea. Geosci J 7:243–252
Lee S, Pradhan B (2006) Landslide hazard assessment at Cameron Highland Malaysia using frequency ratio and logistic regression models. Geophy Res Abstr 8. SRef-ID: 1607-7962/gra/EGU06-A-03241
Lee S, Pradhan B (2007) Landslide hazard mapping at Selangor, Malaysia using frequency ratio and logistic regression models. Landslides 4(1):33–41
Maiti RK (2007) Critical analysis of slope instability on mining scars at Tindharia Cricket Colony, Darjiling, West Bengal. In: Proceedings of eighteenth convention and national seminar on "quarternary climatic changes and landforms. Organized at Manonmaniam Sundaranar University, Tirunelveli 627012, Tamilnadu, pp 189–205

McConnell RG, Brock RW (1904) Great landslides at Frank, Alberta. Canada Department of interior annaul report, 17 pp
Melnikov M, Chensokov M (1969) Safety in open cast mining. Mir Publications, Moscow
Miller VC (1953) A quantitative geomorphic study of drainage basin characteristics in the Clinch mountain area, Virginia and Tenneses, vol 3. Contract N60NR271-30, Technical Report, Department of Geology, Columbia University, pp 1–30
Montgomery DR, Dietrich WE (1989) Source areas, drainage density and channel initiation. Water Resour Res 25(8):1907–1918
Montgomery DR, Dietrich WE (1994) A physically based model for the topographic control on shallow land sliding. Water Resour Res 30(4):1153–1171
Nithya ES, Prasanna RP (2010) An integrated approach with GIS and remote sensing technique for landslide zonation. Int J Geomat Geosci 1(1):121–132
Pack RT, Tarboton DG, Goodwin CN (1998) Terrain stability mapping with SINMAP. Technical description and users guide for version 1.00. http://www.engineering.usu.edu/dtarb/. Accessed 15 June 2007
Pandey A, Dabral PP, Chowdhary VM, Yadav NK (2008) Landslide hazard zonation using remote sensing and GIS: a case study of Dikrong river basin, Arunachal Pradesh, India. Environ Geol 54:1517–1529
Parise M, Jibson WR (2000) A seismic landslide susceptibility rating of geologic units based on analysis of characteristics of landslides triggered by the 17 January, 1994 Northridge, California earthquake. Eng Geol 58:251–270
Poesen J, De Poley J (1987) Geomorphological models—theoritical and emperical aspects. Catena Suppl 10:67–72
Pradhan B, Lee S (2010a) Delineation of landslide hazard areas on Penang Island, Malaysia, by using frequency ratio, logistic regression, and artificial neural network models. Environ Earth Sci 60:1037–1054
Pradhan B, Lee S (2010b) Landslide susceptibility assessment and factor effect analysis: backpropagation artificial neural networks and their comparison with frequency ratio and bivariate logistic regression modeling. Environ Modell Softw 25(6):747–759
Pradhan B, Lee S (2010c) Regional landslide susceptibility analysis using back-propagation neural network model at Cameron Highland, Malaysia. Landslides 7(1):13–30
Prasad MK (1986) Kerala's Western Ghats in the five year plans. In: Nair KSS, Ganaharan R, Menon ARR, Ramachandran KK (eds) Proceedings of the seminar on Eco development of Western Ghats. Kerala Forest Research Institute, Trivandrum, pp 288–292
Quinn P et al (1991) The prediction of hillslope flow paths for distributed hydrological modeling using digital terrain models. Hydrol Process 5:59–79
Roy P, Chacko T (1986) The causes and control of landslides. In: Nair KSS, Ganaharan R, Menon ARR, Ramachandran KK (eds) Proceedings of the seminar on Eco development of Western Ghats. Kerala Forest Research Institute, Trivandrum, pp 244–246
Rautelal P, Lakhera RC (2000) Landslide risk analysis between Giri and Tons Rivers in Himachal Himalaya (India). Int J Appl Earth Obs Geoinf 2:153–160
Rogan MR, Jackson JT (1980) Run-off synthesis using LANDSAT and SCS models. J Hydraulics Div 106(5):667–678
Rowbotham D, Dudycha DN (1998) GIS Modelling of slope stability in Phewa Tal Watershed, Nepal. Geomorphology 26:151–170
Sah MP, Bartarya SK (2002) The impach of March 29, 1999 Chamoli Earthquake on slope stability and spring discharge in Chamoli and Rudraprayag districts of Garhwal Himalaya. Himal Geol 23:121–133
Sah MP, Virdi NS, Bartarya SK (1996) Slope failure and damaging of river channels: some examples from the Sutlej Valley, Himachal Pradesh. Himal Geol 17:183–191
Saha AK, Gupta RP, Arora MK (2002) GIS based landslide hazard zonation in the Bhagirathi (Ganga) Valley, Himalayas. Int J Remote Sens 23(2):357–369
Sarkar S, Kanungo DP (2004) An integrated approach for landslide susceptibility mapping using remote sensing and GIS. Photogram Eng Remote Sens 70(5):617–625

Saaty TL (1990) The analytical hierarchy process: planning, priority setting, resource allocation, 1st edn. RWS Publication, Pittsburgh, 502 pp
Saaty TL (1994) Fundamentals of decision making and priority theory with analytic hierarchy process, 1st edn. RWS Publication, Pittsburgh, 527 pp
Saaty TL, Vargas LG (2001) Models, methods, concepts and applications of the analytic hierarchy process, 1st edn. Kluwer, Boston, 333 pp
Salter RT, Crippen TF, Noble KE (1981) Storm damage assessment of Thames-Te Aroha area following the storm of April 1981. Final report, Water and Soil Conservation Science Centre, Aokautere, New Zealand. Ministry of Works and Development, Internal report, p 44
Sarangi A, Madramootoo CA, Enright P, Prasher SO (2007) Evaluation of three unit hydrograph models to predict the surface run-off from a Canadian Watershed. Water Resour Manage 21:1127–1143
Sassa K (1988) Geotechnical model for the motion of landslides. In: Proceedings of the 5th international symposium on landslides, vol 1. A.A. Balkema, Rotterdam, pp 37–56
Schumm SA (1956) Evolution of drainage systems and slopes in badlands at Perth Amboy, New Jersy. Bull Geol Soc Am 67:597–646
Schwab GO, Fangmeier DD, Elliot WJ, Frevert RK (2002) Soil and water conservation engineering, 4th edn. Wiley, New York, pp 34–35
Selby MJ (1982) Hillslope materials and processes. Oxford University Press, Oxford
Selby MJ (2005) Hillslope materials and processes, Oxford University Press, Oxford (Reprinted volume)
Sharpe CFS (1938) Landslide and related phenomena. Columbia University Press, New York
Sidle RC (1991) A conceptual model of changes in root cohesion in response to vegetation management. J Environ Qual 20(1):43–52
Simon A, Larsen MC, Hupp CR (1990) The role of soil processes in determining mechanisms of slope failure and hillslope development in a humid tropical forest, eastern Puerto Rico. Geomorphology 3:263–286
Sinha BN (1975) A engineering geologic approach to landslides and slope failure, In: Proceedings landslide and Toe Erosion problems with special reference to Himalaya. ISEG, Kolkata, pp 56–65
Sinha BN, Pradhan SR, Sinha P (1975) Geological analysis of Padamchen Slide, Sikkim. In: Proceedings of landslide and Toe Erosion problems with special reference to Himalaya. ISEG, Kolkata, pp 227–234
Skempton AW (1953) Soil mechanics in relation to geology. Proc Yorkshire Geol Soc 29:33–62
Skempton AW, Hutchinson JN (1969) Stability of natural slope and embankment section. In: Proceedings of 7th international congress on soil mechanics and foundation engineering, Mexicom, pp 291–340
Soeters R, Westen CJ (1996) Slope instability recognition, analysis and zonation. In: Turner AK, Schuster RL (eds) Landslides: investigation and mitigation, vol 247. Transportation Research Board Special Report, National Academy Press, Washington, pp 129–177
Starkel L (1972) The role of catastrophic rainfall in the shaping of the relief of the Lower Himalaya (Darjeeling Hills). Geogr Polonica 21:103–147
Strahler AN (1952) Hypsometric analysis of erosional topography. Geol Soc Amer Bull 63:1117–1142
Summerfield MA (1991) Global geomorphology: an introduction to the study of landforms. Pearson, Prentice Hall, Harlow
Kim S-H et al (1997) Slope stabilization using erosion control methods and its application. In: Proceedings of international symposiun on landslide hazard assessment, Xian, pp 387–399
Terzaghi K (1950) Mechanism of landslides. In: Paige S (ed) Application of geology to engineering practice, Berkey volume. Geological Society of America, Boulder, pp 83–123
Terzaghi K, Peck RB (1976) Soil mechanics in engineering practice, 2nd edn. Willey, New York
Thigale SS, Khandge AS (1996) Lnadslide in Western Ghats of Maharashtra. In: Pathan AM, Thigale SS (eds) Contributions to environmental geoscience. Arvalli Books International, New Delhi, pp 161–174

U.S. Soil Conservation Service (SCS) (1972) Hydrology. In: Natural engineering handbook, section 4. GPO, Washington
Valdiya KS (1987) Environmental geology: Indian context. Tata McGraw Hill, New Delhi, pp 269–315
Van Burkalow A (1945) Angle of repose and angle of sliding friction: an experimental study. Geol Soc Am Bull 56:669–707
Van Westen CJ, Castellanos-Abella E, Sekhar LK (2008) Spatial data for landslide susceptibility, hazards and vulnerability assessment: an overview. Eng Geol 102(3–4):112–131
Varnes DJ (1958) Landslide types and processes. In: Eckel EB (ed) Landslides engineering practice, vol 544. Highway Research Board, Special report 29, NAS-NRC Publication, pp 20–47
Varnes DJ (1978) Slope movement types and processes. In: Schuster RL, Krizek RJ (eds) Landslide analysis and control, vol 176. Special report, National Academy of Sciences, Washington, pp 11–33
Varnes DJ (1984) Lanslide hazard zonation: a review of principles and practice. UNESCO Nat Hazard 3:61
Waltham T (2002) Foundations of engineering geology
Wu TH, Sangery DA (1978) Strength properties and their measurement. In: Schuster RL, Krizek RJ (eds) Landslides, vol 176. Transportation Research Board, Special Report, National Academy of Sciences, pp 139–154
Yatsu E (1966) Rock control in geomorphology. Sozosha, Tokyo
Yim KP, Heung LK, Greenway RD (1988) Effects of root reinforcement on the stability of three fill slopes in Hong Kong. In: Proceedings, 2nd international conference on geomechanics in tropical soils (Singapore), vol 1. pp 293–299
Young A (1963) Deductive models of slope evolution. Rep Int Geogr Un Slopes Comm 3:45–66
Zaruba Q et al (1969) Landslides and their control. Elsevier, Amsterdam, p 205
Zaruba Q, Mencl V (1982) Landslides and control, vol 10017, issue 324. Elesvier, New York, 35 pp
Zhou CH, Lee CF, Li J, Xu ZW (2002) On the spatial relationship between landslide and causative factors on Lantau Island, Hong Kong. Geomorphology 43:197–207

Chapter 2
Geo-spatial Variability of Physiographic Parameters and Landslide Potentiality

Abstract The stability of mountain slope depends upon physical and chemical properties of the soil. In the present work geomorphic properties such as slope angle, slope aspect, slope curvature, lithological composition, and lineament as well as behaviour of slope materials such as texture, cohesion (c), friction angle (φ), water holding capacity, porosity, weight soil density and density of soil water were assessed and found out the relationship with landslip in the Shivkhola Watershed. Slope angle, slope aspect and slope curvature were derived from DEM on GIS platform. Lineament map was prepared using Satellite Image LISS III (2010). Soil samples were collected from 50 different locations and their laboratory test were being carried out to assess cohesion, friction angle, water holding capacity, pore space, and wet soil density. The spatial distribution of the mentioned characteristics of slope forming materials is done using ARC GIS Software. To estimate evolutionary stage through which the Shivkhola Watershed is passing, hypsometric analysis was made. Integration between landslides inventory map and derived thematic geomorphic maps was done to assess the spatial distribution of landslide potentiality.

Keywords Slope instability · Geomorphic parameters · Friction angle (φ) soil texture · Cohesion (c) porosity and water holding capacity · Volumetric expansion · Wet soil density · Remote sensing and GIS

2.1 Introduction

As the form of a slope is the end product of past geological processes, the morphological history of the slope must also be understood. Each and every spatial segment of the earth surface possesses some physiographic aspects and the analysis of all the aspects enables us to predict an interrelationship between physical and cultural phenomena and as a whole. The study area, Shivkhola Watershed comprises a number of diversified physical aspects and there is a great

S. Mandal and R. Maiti, *Semi-quantitative Approaches for Landslide Assessment and Prediction*, Springer Natural Hazards, DOI 10.1007/978-981-287-146-6_2

diversity of forms and the complexity of interrelationships. The practical relevance of landslide can be recognized only by the systematic and thorough study of geomorphic attributes such as relief, geology, and soil. A detailed and integrated investigation of the geological structure of the area, the petrographical and physical properties of the rocks and the local hydro-geological conditions with changing slope of the Shivkhola watershed will help to prepare the corrective and preventive measures in a reasonable scheme. The Shivkhola Watershed provides a wide range of elevation from 2,040 m in north-west to 300 m in south-east. The middle section of both north facing slope and south facing slope is attributed with sudden and abrupt steepness. Geologically, the study area owns seven major lithological units with varying degree of resistance and intensity of landslide phenomena. The development of drainage network in the Shivkhola watershed is the outcome of elevation and slope which are the ubiquitous elements of landscape, the structure and tectonic history of the area, and the existing humid climate. There is continuous branching and headward extension as well as the sharpening of the interfluves area caused by the present drainage network within the basin. The soil up to the depth of 1.5 m is heavily disintegrated and decomposed in the study area. The existence of finer to large size soil-rock composition has aggravated the problem of soil erosion and soil slip in the Shivkhola Watershed. Besides the size of the soil particles, the mineralogical composition of the soil changes all the physical and chemical properties within the soil. The amount of sand, silt and clay; porosity, water holding capacity and bulk density; cohesion; and saturated depth of the soil are some of the significant properties which continuously changing the actual nature of the soil-rock properties of the hill slope causing slope failure.

The study of various geomorphic attributes and their interrelations generally offers a concrete accounts and evidences on the morphological characteristics and landscape evolution. The analysis of relief, lithology, dissection, ruggedness, topographic index, slope, aspect and curvature in relation to slope instability will contribute an impression about the degree of importance and dimension of individual geomorphic attribute. Landslide potentiality was estimated incorporating *landslide inventory map* (Fig. 2.1) for all the geomorphic attributes by determining class/ranges wise *Landslide Potentiality Index Value* (LPIV) of each factor by means of a ratio (Eq. 2.1) between the number of cells/pixels disturbed by landslides and the total number of cells/pixels for that specific class. More details of these procedures were obtained in other studies (Vieira et al. 1998; Guimaraes et al. 1999). Topographic Index (TI) Value was calculated in consultation with slope and upslope contributing area. The effectiveness of all these parameters were being influenced by hydrologic conditions and other atmospheric processes. Anderson and Burt (1978) presented the role of topography in controlling through flow generation and related landslips. GIS tools were applied for the identification of topographic settings conducive to landslide occurrences by Gao (1993). Various geomorphic models were being introduced for understanding slope instability by Beven and Kirkby (1979), Ahnert (1987), Montgomery et al. (1994), and Dietrich et al. (1998). Cruz (2000) studied in detail the role of geomorphic processes on

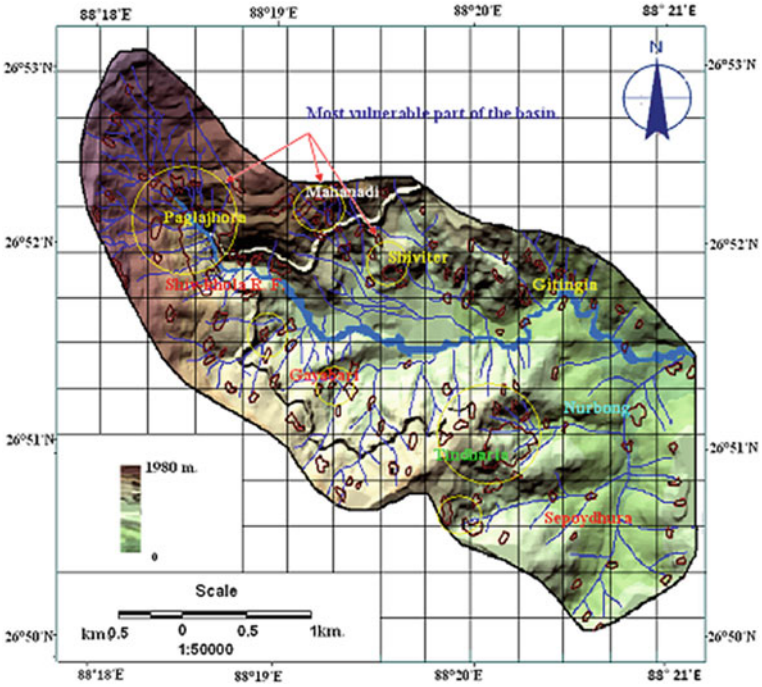

Fig. 2.1 Landslide inventory map

mass movements. Zhou et al. (2002) investigated the spatial relationship between landslides and causative factors.

$$\text{LPIV} = (\text{F2} \div \text{F1}) \times 100 \tag{2.1}$$

where,
F1 number of pixels/cells or grid without landslide
F2 number of pixels/cells or grid with landslide.

2.2 Assessment of Geomorphic Attributes

The success of Geomorphologic research depends mostly on field study. The emphasis has been laid on the field work in the present study, wherever possible. All the problems relating to the study could not be solved because of the great complexity of geomorphologic processes in nature. But the observation of geomorphic features such as the shape of the scarps, roughly the degree of slopes, the development of drainage pattern, shape of the valley and ridges, nature of exposed

surface rock layers, were done by simple instruments, maps and imageries (clinometer, abney's level, GPS, SOI Topographical Map and LISS III Imageries) and their photographs during the field work helped a lot for studying and analyzing the topography and for preparing the various morphometric maps of the Shivkhola Watershed.

2.2.1 Analysis of Contour Orientation

Shiv-khola watershed spreads over a region with varied relief character. Being the hilly drainage system, it possesses a saucer shape having steeper slope almost everywhere except at few localized section at the mid-central and lower part. The contour map prepared in consultation with SOI Topographical Map (No78B/5) and Satellite Imagery (LISS-III, 2003) shows a wide range (1,740 m) of altitude between 2,040 and 300 m. The central middle portion and extreme right part (confluence with the mighty Mahanadi) show the gentle slope. The other parts depict steeper slope through closer contour spacing. The orientation of contours is depicted in the Fig. 2.2. The valleys and the spurs in between those set the remarkable character of the study area. The long profile along the main river, the Shiv-khola, shows a waxing (convex summit) slope at the source region followed down slope by a steep section near Paglajhora area and then by a gentle middle and lower segment. The Hill Cart Road has to cross twice this steep section to harness the facility along-contour extension.

This steeper (almost vertical) slope is more than 500 m high and extends over 2 km length along Hill Cart Road. After this steeper part the Shivakhola river develops the gentle slope along the river and develops cut-and-fill terrace being incapable of clearing all the dislodged material sliding down from steeper upslope. After emerging at this stage river becomes sluggish and shows some spectacular meandering on erosional slope which is quite unusual for a hill stream of such shorter length. The wider valley floor (former) is mainly occupied by the Shivitar Tea Estate and mostly covered with Tea Plants. The newly cut valley under this former one is rather steeper and prone to slide along its entire length. After crossing this, the river has to pass through the constricted valley between Tindharia Tea Garden and Shivitar Tea Garden. Some flat land is again developed at the junction with the mighty Mahanadi due to combined erosional effects of the Mahanadi and the Shiv-khola. The upper catchment of the basin towards the water divide shows gradual steepness and more dissection and efficiency in drainage. More tributaries of lower orders are developed at the upper catchment due to swift drainage. Greater rate of release of kinetic energy from potential is responsible for the dissection of slope at the upper section. The land uses mainly the Hill Cart Road and North Eastern Frontier Rail line (0.61 m gauge) are absolutely guided by the relief. Almost at every part these run parallel to the contour running along the basin boundary. Surprisingly Transport links crosses the main stream through the steepest section of the basin at Upper and Lower Paglajhora section.

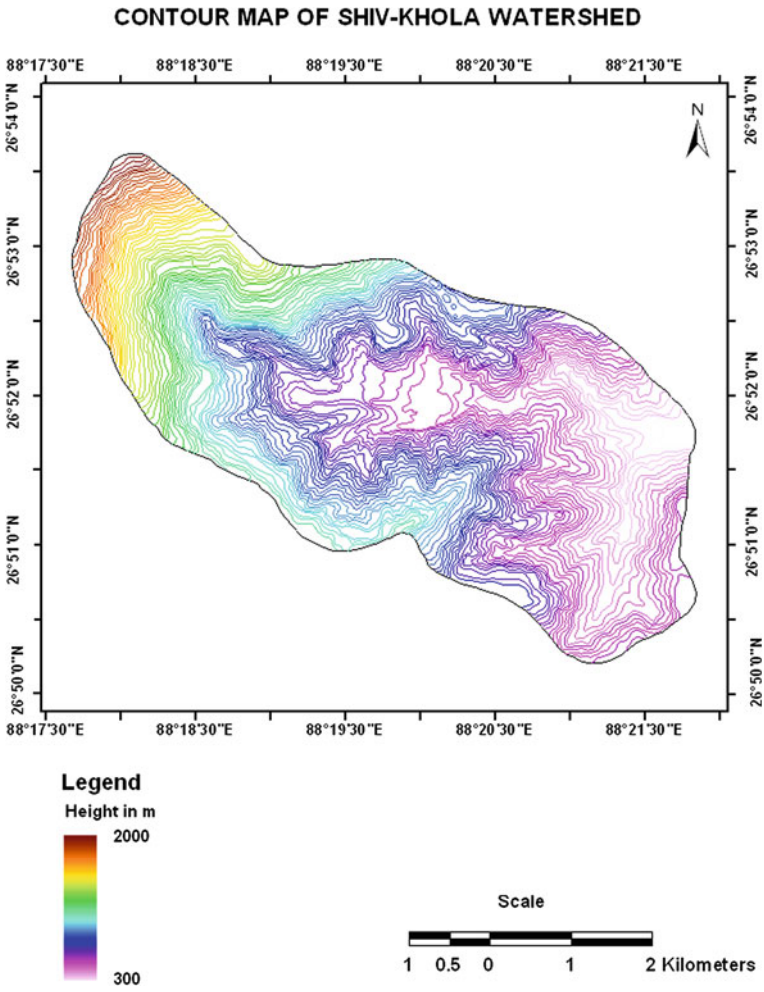

Fig. 2.2 Contour orientation of the Shivkhola watershed

2.2.2 Digital Elevation Model (DEM)

The prepared contour map at 20 m interval from the topographical map of 1987 at the scale of 1:50000 was used for generating the Digital Elevation Model (DEM) by using ARC GIS Software which helped to have an appreciation of the nature of relief and the distribution of slope over the basin area (Fig. 2.3). The relief is mainly guided by the position of the drainage lines and amount of dissection. The graded state, characterized by gentle slope (graded slope) which is established at the confluence at the flag end gradually creeps upward to the upper catchment following the channels. The valley-side slopes are steeper enough showing absolute

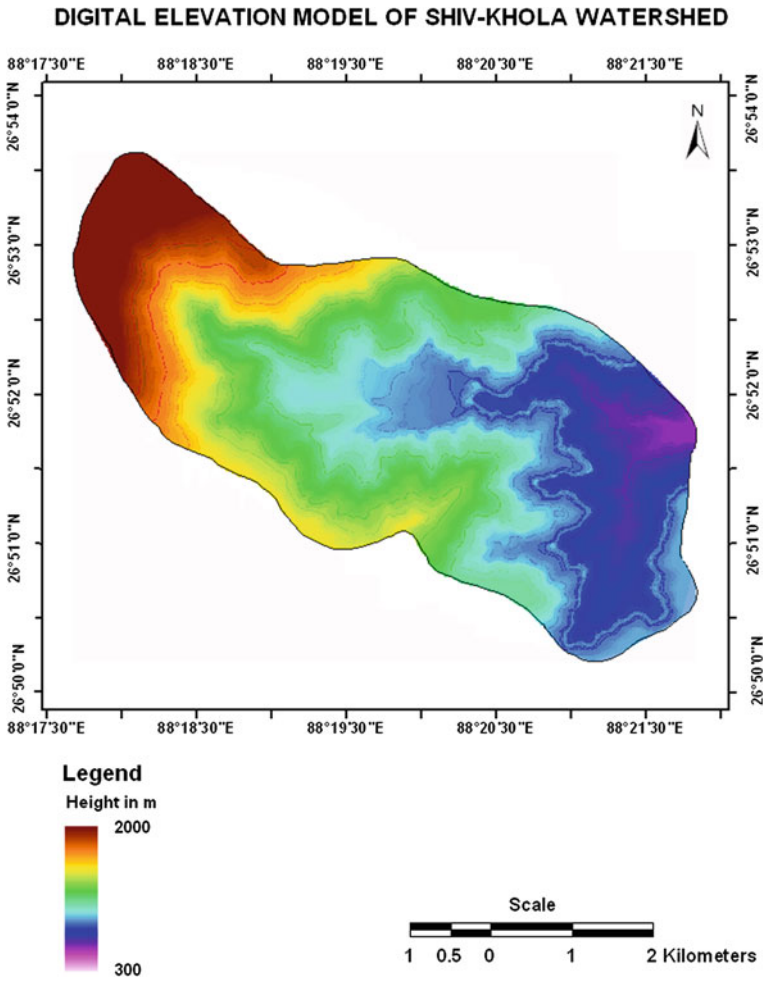

Fig. 2.3 Digital elevation model (DEM)

instability. The steeper part of the slope gets adjustment through slides and thus retreats backward setting a gentle and graded slope at its base which is sufficiently steeper to release kinetic energy sufficient only to transport already eroded materials. Thus the graded condition gradually moves upslope from the confluence point. The deposition at the middle part and erosion at the upper reach and again erosion at the lower section through further down cutting execute the concept of complex response following Chorley et al. (1985).

Table 2.1 Hypsometric analysis

Elevation (m) (h)	Area above the elevation (km^2) (a)	a/A	Cumulative a/A	h/H
300	1.23	0.06	0.06	0.16
400	5.72	0.26	0.32	0.22
600	5.06	0.23	0.55	0.33
800	3.79	0.18	0.73	0.44
1,000	2.34	0.11	0.84	0.55
1,200	1.24	0.06	0.90	0.66
1,400	1.26	0.05	0.95	0.77
1,600	0.81	0.03	0.98	0.88
1,800	0.58	0.02	1.00	1.00

Total area 22.05 km^2 , H maximum elevationfriction angle ranges between$A$ total area

2.2.3 Hypsometric Analysis

In the present study to develop hypsometric curve the ratio between relative height (h/H) and relative area (a/A) were plotted on the ordinate and abscissa respectively to recognize the stages of cycle of erosion in the Shivkhola Watershed after Strahler (1952). The hypsometric analysis of the said basin shows the distribution of area against respective elevation zones (Table 2.1). The study shows that maximum basin area lies within 400–600 m altitude and gradually the area under each successive zone of 100 m is decreasing at a diminishing rate. The area below the curve is waiting for erosion and so the ratio of the two represents the phase of erosion and thus the said basin is approaching to mature stage where maximum of the areas are in sloppy condition and no such flat surface is seen. The ridges are steep enough favouring easy drainage and the absence of flat land is the basic hindrance in the land use and thus the land resource cannot be used with full utility. Any attempt for reduction of slope at one place for effective use increase the slope at other and thus introduces instability of slope which sets instability in the other and the total system becomes instable.

Here, hypsometric integral (H.I.) has been accepted as an important morphometric indicator of the stage of basin development which is the percentage of the total volume of the basin area below the curve and thus it reveals the volume of area unconsumed by the dynamic wheels of erosion (Strahler 1952). The derived hypsometric integral value is 0.46 which depict the area is still passing through the late youthful stage of landform development with moderate to high drainage density which may invite havoc slope failure.

2.2.4 Lithological Composition and Landslide Potentiality

Mallet (1874) stated that in the Darjeeling territory the "Gondwana" rocks are overlain by the metamorphic rocks, which are termed as "Darjeeling" (mainly mica-

gneisses and schists) and "Daling" (mainly slates and phyllites). The "Darjeeling" structurally overlies the "Daling" and Mallet observed that there is a gradual passage from one metamorphic unit into another. Daling consists of garnetiferous biotite schist, biotite schist and kyanite-sillimanite bearing garnetiferous gneiss, indicating higher grade of metamorphism. Garnetiferous biotite-calc-granulite, calc-gneiss, quartzite and muscovite-sillimanite-quartz-schist occur as inclusions in the gneisses and represent the original calcareous, siliceous or other sediments. According to Mallet, "the gneiss should be the older rock and their inverted on to the slates and their turn on to the Damuda or that the boundaries should be faulted one or finally that the relation of these formations to each other should resembles those of the Tertiaries to Damuda". The problem is that the-"Darjeeling"-"Daling"-"Gondwana"-contacts are structural stratigraphic discontinuities.

Roy and Sensharma (1967) suggested that "Darjiling" and "Daling" stratigraphically constitute one continuous unit called "Senchal Series". According to Ray the boundary between Gondwana and overlying Daling near Tindharia cannot be drawn with certainty as there is a possibility that the two constitute one continuous formation in different grades of metamorphism with somewhat different lithology. Folding has not been commonly recorded in "Gondwana" except in a few cases in sandstone and shale. These folds are developed on bedding planes. A few discontinuities fractures occur parallel to the axial planes of the folds, no appreciable recrystalisation or neomineralisation has been observed along this plane. Successive appearance of chlorite, biotite, garnet and kyanite which apparently suggest the occurrence of progressive zones of regional metamorphism of Barrovian type can be recorded from south to north.

Gondwana sandstones and shales are mostly unaltered. Constructive metamorphism has already been observed except for some recrystalisation of small sericitic micas and biotites; these occur along bedding (Laahiri 1973). The lithological map of the concerned study area was collected from Geological Survey of India (GSI), Kolkata (Eastern Region) and then necessary modifications were being incorporated after thorough field investigation. Final lithological map was prepared with seven rock groups and transformed into raster value domain on ARC GIS platform. Each and every lithological group responds differently whenever it exposes to atmospheric processes and also produces varying magnitude of landslide susceptibility/Landslide Potentiality. Darjiling Gneiss (A), Reyang formation (E) and Swialik (G) associated with highly foliated gneiss, mica-schists and occasional bands of flaggy quartzites and granulitic rocks, slates phyllites with occasional quartzite, quartz-schists and greywake schists, soft grayish sandstone, mudstone and shales and conglomerate along with thin bands of marly shales and lignite cover more than 60 % area of the Shivkhola watershed. Chungtung Formation (B) with calc-granulitie, marble, quartz-granulite and mica-schist; Lingtse Granite (C) with foliated granite or mylonitised granite with several close space sub-parallel thrust; Gorubathan Formation (D) with low grade phyllite and silvery mica-chlorite-schist, grey sericite, and Damuda Formation (F) with coarse grained hard sandstones, quartzites, carbonaceous shales and slates, thin seams of crushed and powdery coal share almost same area (around 8 %) each (Fig. 2.4).

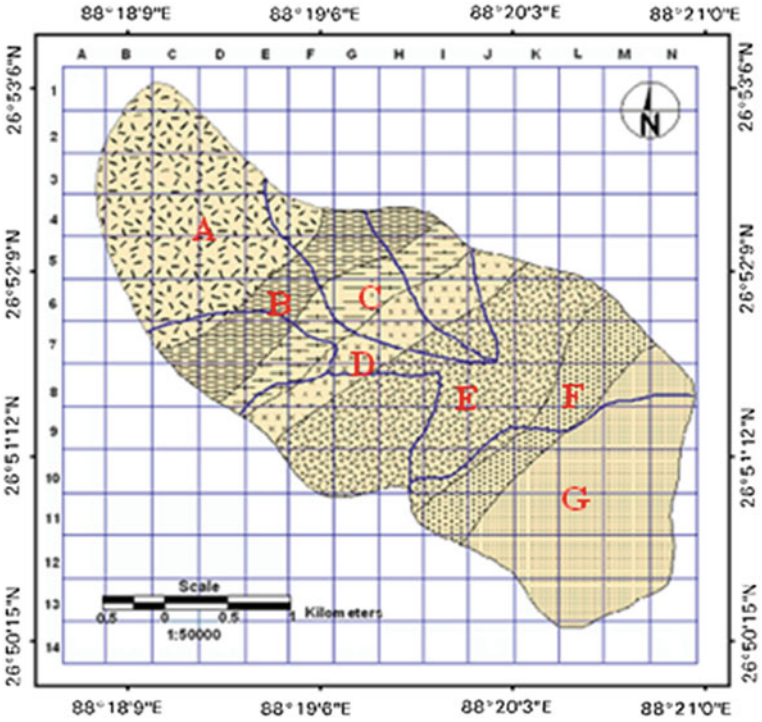

Fig. 2.4 Lithological map of the Shivkhola watershed

Some assessments have been presented for the study area after studying the lithology in detail (Laahiri 1973):

1. The structural-cum stratigraphic succession can be observed in a traverse across Tindharia-Kurseong region.
2. The "Daling"-"Darjiling" metamorphic boundary is gradational and correspond to the passage between silvery mica-schist and garnetiferous mica-schist.
3. The metamorphites (Daling and Darjiling) disclose a well defined sequence of deformation and recrystalisation.
4. The "Gondwana" rocks on the other hand, are mostly unaltered and these show little metamorphism except some local cataclasis.

Landslide occurrences phenomena as well as landslide potentiality index value (Table 2.2) are very high for the lithological composition of gneiss, mica-schist and granulitic rocks (73.07), mylonitised granite with sub-parallel thrust (61.54), phyllite, silvery-mica-chlorite-schist, grey sericite (69.23), and slate phyllite with quartzite, quartz-schist and greywake schist (65.52) at Lower Paglajhora, 14 Miles Bustee, Gayabari, Jogamaya, Tindharia, Shiviter and Mahanadi due to following reasons:

Table 2.2 Lithological composition and landslide potentiality index value (LPIV)

Lithological composition	Number of cells (F_1) (0.25 km^2)	Number of cells (%)	Number of landslide occurrence cells (F_2)	Number of landslide occurrences cell (%)	Landslide occurrence ratio	Landslide potential index (LPI) = $F_2/F_1 \times 100$
Gneiss, mica-schist and granulitic rocks (A)	26	18.57	19	22.09	0.73	73.07
Calc-granulie, marble, quartz-granulite and mica schist (B)	16	11.42	9	10.47	0.56	56.25
Mylonitised granite with sub-parallel thrust (C)	13	9.28	8	9.30	0.61	61.54
Phyllite, silvery-mica-chlorite-schist, grey sericite (D)	13	9.28	9	10.47	0.69	69.23
Slate phyllite with quartzite, quartz-schist and greywake schist (E)	29	20.71	19	22.09	0.65	65.52
Sandstone, quartzites, shales, thin seams of crushed coal (F)	16	11.42	7	8.14	0.43	43.75
Soft sandstone, mudstone, shales, conglomerate and marly shales and lignite (G)	27	19.29	15	17.44	0.55	55.56

- Seepage through heavily disintegrated and decomposed materials and formation of clay minerals, which induces slope instability.
- Rocks are traversed by quartz and quartzo-felspathic veins and the rocks are often highly metamorphosed and jointed.
- Recrystallisation and cataclastic deformation have destroyed the clastic texture with intense granulation along narrow zones of fracture.
- The apexes of the sliding zones are predominated with good amount of organic matter which encourages high water holding capacity and volume expansion.
- The apexes of the sliding zones are deforested and are susceptible to both sheet and gully erosion.
- Both Damuda and Swialik provide intensively deformed sandstone which destroys the clastic texture and promotes slope instability.

Krishnaswamy (1982), Lahiri and Gangopadhyay (1974) studied structure and stratigraphic pattern of rocks and their relation to landslide phenomena with particular reference to Himalayan region. Nautiyal (1951, 1966) presented some

Table 2.3 Rock properties

Rock types	Strength (MN/m^2)			Bulk density (Mg/m^3)	Porosity (%)
	Compressive	Tensile	Shear		
Granite	100–250	7–25	14–40	2.6–2.9	0.15–1.5
Gneiss	50–200	5–20	–	2.8–3.0	0.5–1.5
Slate	100–200	7–20	15–30	2.6–2.7	0.1–0.5
Sandstone	20–170	4–25	8–40	2.0–2.6	5–25
Shale	100–200	7–20	15–30	2.0–2.4	10–30

Source Attewell and Farmer (1976)

geological report on the hill slope stability in and around Darjiling Himalaya. Attewell and Farmer (1976) studied compressive, tensile and shear strength of various rocks and concluded that slate and shale have low range of shear strength (Table 2.3). Sandstone is characterized by high range of shearing strength. The bulk density (Mg/m^3) in most of the rocks varies from 2.00 to 2.9. In the Shivkhola Watershed, Damuda and Swialik rock groups depict high range of shearing strength where porosity ranges from 5 to 25 %.

2.2.5 Analysis of Lineaments and Landslide Potentiality

The lineaments exhibit the zone of weakness surface providing some linear to curvilinear features such as fracture, joint, fault etc. in the geological structure (Fig. 2.5). To extract lineaments of the Shiv-khola watershed PCI-GEOMATICA Software of GIS was used and in the extraction process 3 bands of wavelength were taken into account such as Near Infrared (Band-I; 0.7–1.3 μm), Red (Band-II; 0.6–0.7 μm) and Green (Band-III; 0.5–0.6 μm). The algorithm used to prepare lineament map is 'lineament extraction'. The lineaments at the places of Lower Paglajhora, Gayabari lower, Tindharia, 14 Miles Bustee, Shiviter Lower slope, Sepoydhura, and Norbong T.E. are closely spaced. The lineaments are absent at extreme north, north-east and eastern marginal part of the Shivkhola Watershed. The LPIV of each lineament class exhibits that the greater the distance from the lineaments lesser is the probability of landslide phenomena. The distance of 125 m from lineaments is dominated by high percentage of landslide affected pixels as well as high landslide potentiality index value of more than 17. The distance of more than 600 m from lineaments is less affected by landslide where LPIV ranges from 0 to 10 (Table 2.4).

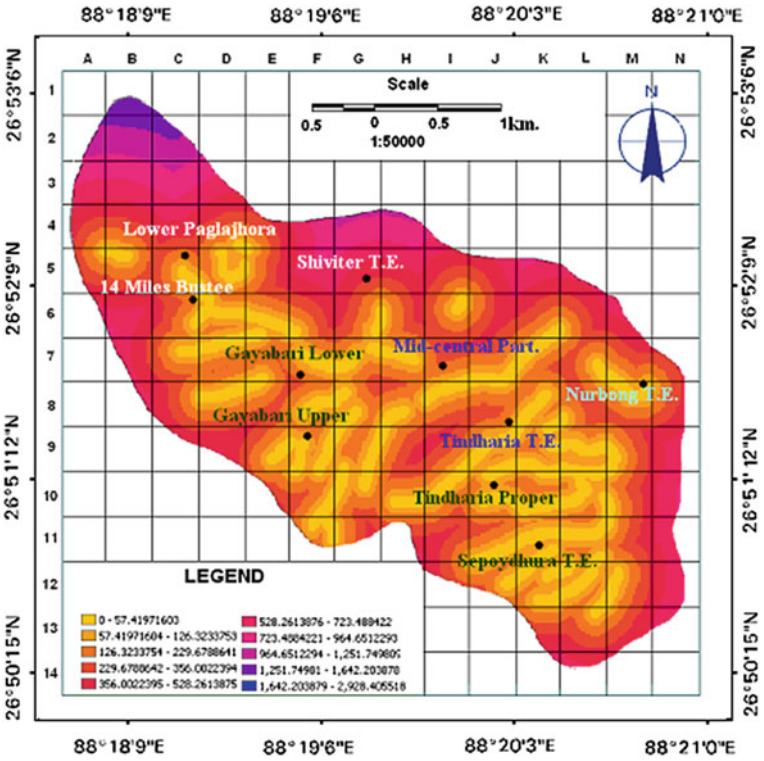

Fig. 2.5 Lineament distribution map of the Shivkhola watershed (distance from lineament in meter)

Table 2.4 Lineament and landslide potentiality index

Class (dist. from lineament in m)	Number of pixels (F1)	Number of landslide affected pixels (F2)	Landslide potentiality index (LPI) = (F2/F1 × 100)
0.00–57.42	3,381	624	18.46
57.42–126.32	3,786	668	17.64
126.32–229.68	3,695	451	11.37
229.68–356.00	3,252	522	16.05
356.00–528.26	4,799	444	9.25
528.26–723.45	4,141	286	6.91
723.45–964.65	3,887	221	5.67
964.65–1251.75	3,921	120	3.06
1251.75–1642.20	1,419	37	2.61
1642.20–2925.40	850	0	0

2.2.6 Slope Angle and Landslide Potentiality

Firstly, the *contour map* at 20 m interval was prepared and digitized from the SOI Topo-sheet (1987, 78B/5) at the scale of 1:50000 and was subsequently used for generating Digital Elevation Model (DEM) using ARC GIS Software. Then *slope gradient*, *slope curvature* and *slope aspect maps* were derived from DEM with 25 m grid cell size and classification was made following the earlier works of Anbalangan (1992) and Dhakal et al. (2000). The slope is maximum near Paglajhora area. Hill Cart Road and North Eastern Frontier Rail line (0.61 m gauge) cross the entire river system twice through this steeper and unstable zone. The slope is least at the central part where the river develops a cut and fill terrace. The slope registers one of the minimum at the crest of water divide and towards the bottom right of the basin. *Slope gradient* of the watershed varies from very gentle gradient (around 10°) in the mid central and mid-lower part to that of high (more than 60°), towards the marginal part/water divide. Most of the landslide phenomena were found in the area of above 35° slope gradient.

In the Shivkhola Watershed high to very high landslide hazard risk is being found at the place with slope angle between 24° and 40°. Low to moderate level of risk is observed in the area pertaining to the slope angle of less than 24°. Small parts

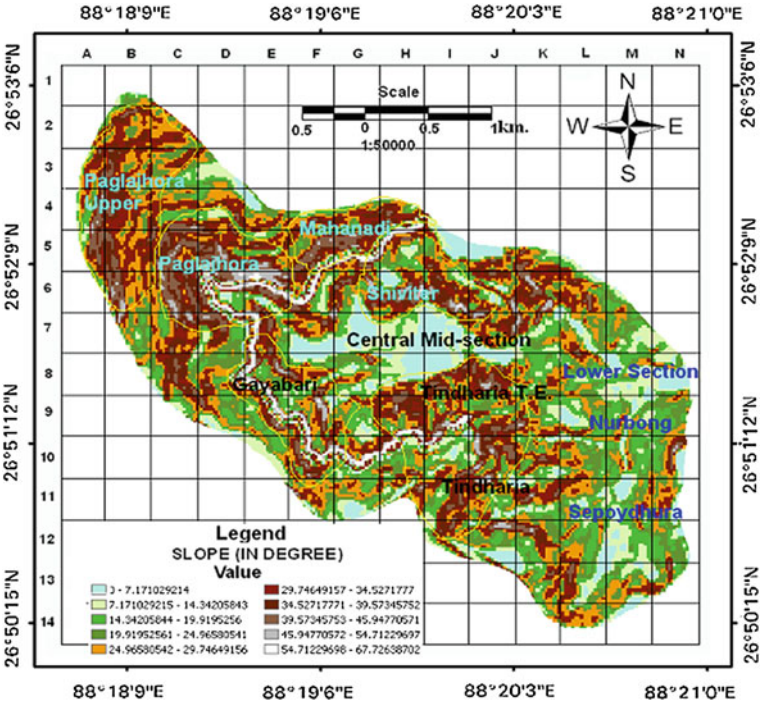

Fig. 2.6 Spatial distribution of slope angle

Table 2.5 Slope angle and landslide potentiality

Classes (slope in degree)	Number of pixels (F1) ($N_{pix(Ni)}$)	% of ($N_{pix(Ni)}$)	Landslide pixels (F2) ($N_{pix(Si)}$)	% of ($N_{pix(Si)}$)	Landslide potentiality index
0–7.17	3,353	10.12	190	5.63	5.67
7.17–14.34	3,238	9.77	202	5.99	6.24
14.34–19.92	3,587	10.83	211	6.26	5.88
19.92–24.97	2,445	7.38	201	5.96	8.22
24.97–29.75	3,555	10.73	311	9.22	8.75
29.75–34.53	2,776	8.38	329	9.75	11.85
34.53–39.57	3,854	11.63	413	12.24	10.72
39.57–45.95	3,276	9.89	427	12.65	13.03
45.95–54.71	3,557	10.74	543	16.09	15.27
54.71–67.73	3,490	10.53	646	19.15	18.51

of the Shivkhola Watershed with slope angle of more than 40° is registered with high to very high landslide hazard risk (Fig. 2.6). It could be demonstrated that 50 % area of the Shivkhola basin is dominated by the high intensity of landslide with 24° and 40°. The landslide potentiality index value increases with increasing slope angle. It is inferred that there is a positive relationship between slope angle and landsliding in the corresponding study area (Table 2.5).

2.2.7 Slope Aspect and Landslide Potentiality

Slope aspect of the Shivkhola Watershed was derived from the developed digital elevation model (DEM) with the help of ARC GIS Software. In general, the watershed shows the south facing slope with some local variation due to the location of ridges, spurs and valleys. The concentrated local erosion and consequent development of valleys, landslide scars and other topographic depressions are responsible for the spatial distribution of slope aspect. This slope aspect is helpful for the identification of slope segments which are required for the analysis of potentiality of slope failure. The Fig. 2.6 shows the slope direction and most of the places show the southward slope with some places of northward slope. The varied direction of flow based on local slope and orientation of ridges, spurs and valleys shows the pattern of concentration of surface water and the places of potential surplus region. The availability of water increases with the increase in the distance from water divide. Thus at the lower reach, of every stream, the availability becomes more than the upper portion.

North, south, east, north east and south east facing slope are registered with the landslide potentiality index value of 17.14, 13.10, 15.53, 11.67 and 12.54

Table 2.6 Slope aspect and landslide potentiality index (LPIV)

Aspect	Number of pixels (F1)	Number of landslide affected pixels (F2)	Landslide potentiality index (LPI) = (F2/F1 × 100)
Flat	784	24	3.06
North	3,879	665	17.14
North east	3,797	443	11.67
East	4,346	675	15.53
South east	6,290	789	12.54
South	4,556	597	13.10
South west	3,332	35	1.05
West	2,870	69	2.40
North west	3,277	76	2.32

respectively (Table 2.6). South west, west, northwest and middle section is attributed as minimum number of landslide occurrences phenomena as well as landslide potentiality index (LPIV). According to the number of pixels affected by slope failure south east facing slope rank first which is followed by east, north, south, north east, north west, west, and south west. Upper halve of the watershed is dominated by south east and south ward facing slope and lower halve is dominated by east and north ward facing slope with LPIV >11 (Table 2.6). Such landslide prone facets are closely associated with maximum slope and relief which is found at upper and lower Paglajhora, Shiviter T.E., Gayabari Lower slope and Tindharia (Fig. 2.7).

2.2.8 The Surface Curvature and Landslide Potentiality

The retention of moisture in the soil depends mainly on the convexity (positive curvature) or concavity (negative curvature) of surface. Slope curvature plays a significant role in changing landform character (Gilbert 1909). The concave surface holds moisture for long where the convex surface drains moisture immediately. The curvature value represents the morphology of the topography. A positive curvature represents the surface is upwardly convex at the pixel and a negative curvature value represents the surface is upwardly concave at that pixel. A value of 0 indicates that the surface is flat. The more positive and negative curvature value indicates the surface is more susceptible to landslide occurrences. The reason for this is that following heavy rainfall, a concave slope contains more water for a longer period and saturates the soil perfectly and also reduces the cohesiveness within soil. On the other hand a convex slope is generally more exposed to frequent expansion and contraction processes which lead to the disintegration and decomposition of rocks. The presence of decomposed or loosened materials along the convex slope allows water particles to move downward, which is the triggering mechanism of landslide phenomena.

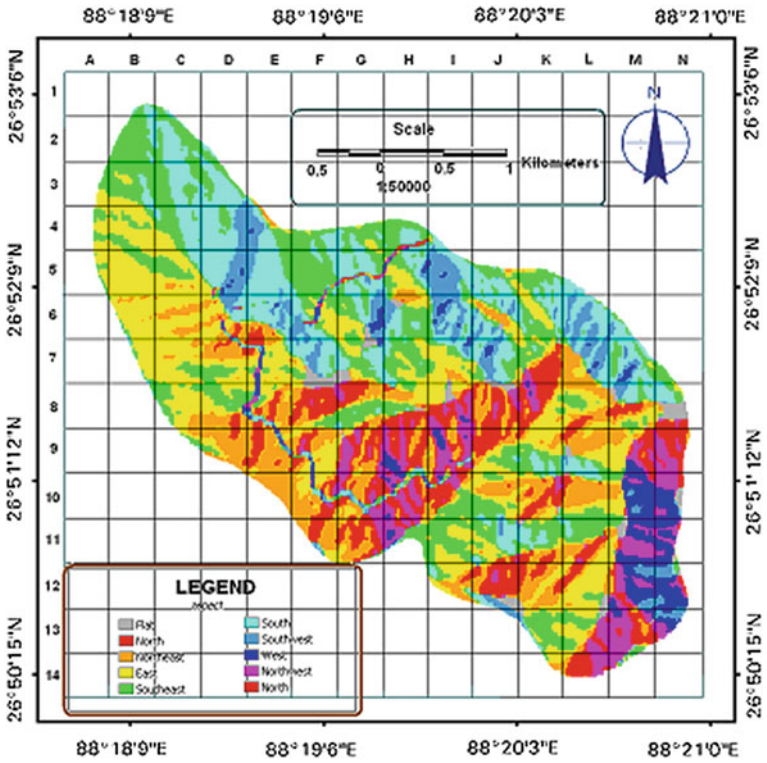

Fig. 2.7 Slope aspect map

The slope curvature map was also extracted from Digital Elevation Model (DEM) on ARC GIS. The map shows (Fig. 2.8) very high negative and positive surface curvature along Hill Cart Road which passes through the steep escarpment slope of the Shivkhola watershed. Paglajhora, Gayabari, Tindharia, and Shiviter are dominated by the moderate to high levels of positive and negative surface curvature with moderate levels of slope surface dissection (Fig. 2.8). Extreme middle and eastern marginal part register minimum curvature value. The study depicts that landslide Potentiality Index Value increases with increasing positive and negative curvature values (Table 2.7). The positive curvature is common and that indicates the tendency of immediate drainage of surface water causing ready washing and so is detrimental to the stability of both soil and slope.

The study on slope angle states that there is rapid flowage of running water along the steep slopes and formation of first order channel with active headward and downward erosion. Such conditions introduce steep valley side slopes and development of drainage network. The continuous development of drainage network yield huge amount of surface water and their confluence at a particular location generate more seepage and reduce cohesive strength of the soil and induce slope

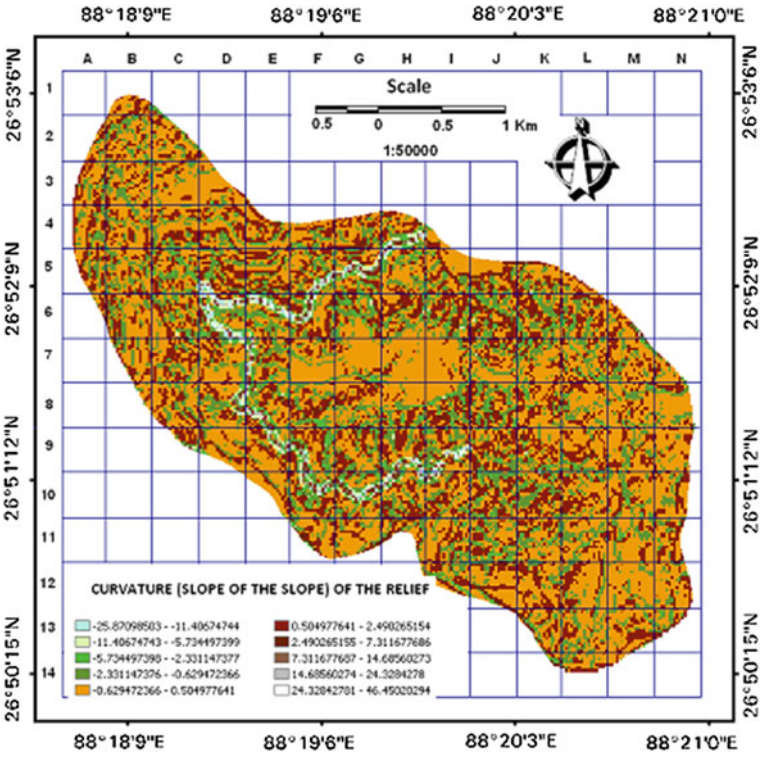

Fig. 2.8 Slope curvature map

Table 2.7 Curvature and landslide potentiality index (LPIV)

Classes (value of slope curvature)	Number of pixels (F_1)	Number of landslide affected pixels (F_2)	Landslide potentiality index (LPI) = ($F_2/F_1 \times 100$)
−25.87 to −11.41	995	221	22.21
−11.41 to −5.73	785	210	26.75
−5.73 to −2.33	2,111	486	23.02
−2.33 to −0.63	2,431	374	15.39
−0.63 to 0.50	1,0045	388	3.84
0.50–2.49	6,302	268	4.25
2.49–7.31	5,438	464	8.53
7.31–14.69	3,343	475	14.21
14.69–24.33	895	222	24.80
24.33–46.45	786	265	33.71

instability. Darjiling Himalaya is situated in the southern flank of Himalayan Mountain Range, which receive frequent orographic rainfall during rainy period. Most of the destructive landslides occur due to high intensity rainfall and it is observed that the south facing slopes of Darjiling Himalaya are dominated by higher amount of rainfall and large number of landslides. In Shivkhola Watershed, concentration of drainage is one of the major causes of landslide. Slope characterized by high positive (slope convexity) and high negative (slope concavity) curvature value allows more concentration of water and drainage which on the other hand decreases mineralogical bonding of soil and invite slope instability. The major landslide prone areas in the Shivkhola Watershed are registered by such feature. The occurrences of landslide phenomena are also aggravated because of the existence of high intensity lineaments at slope convex and slope concave section. Lineaments permit seepage that helps to entrain the particles from vertical section of the soil and introduce slope instability. It is to be concluded that the presence of fragile lithological composition (>60 % area) and the continuous development of drainage network over it, has made the Shivkhola Watershed more vulnerable to landslides.

2.3 The Soil

Officially the soil of the Darjiling Himalaya is divided into two main groups (a) the brown forest soil and (b) the terai soil. The first group of soil is found in the mountainous region whereas the second group is found in the lower elevated zone. The shivkhola watershed is falling under the brown forest soil as it covers hilly area of the Kurseong Division. The inherent fertility of this brown forest soil is very high and has free drainage through their profiles and also have very rich in well-distributed humus. The percentage of organic matter in the top horizon increases with altitude but gradually decreases down the profiles. The principal source of the organic matter present in the top layer of the soil are leaves, stems, branches, roots, barks, fruits, seeds, animals and micro-organism. The maturity of this forest soil depends on the decomposition of the organic matter into humus. Accordingly, the decomposition is slower at higher altitude due to climatic factors, but the decomposition is quicker at lower altitude. Decomposition at higher altitude generally occurs only because of the presence of fungi while at lower elevation it happens by climate, bacteria and animals. In the Shivkhola watershed the major types of humus dominated soil found in the forest soils are ‘Mull’ and ‘Mor’. The former is a porous, loose, crumble and friable mass that develops under deciduous species. The ‘Mor’ is dominated by fungi and mosses and associated to coniferous forest and also display a high degree of saturation of A horizon and little accumulation of sesquioxide in the B horizon (Darjiling District Gazetteers by LSS O’Malley 1999) (Table 2.8). Sarkar (1987a, b) introduced pedo-geomorphic parameters and its impact on soil loss and landslip.

Table 2.8 Percentage of organic matter, nitrogen, and p^H of the A_O horizon under varying altitudinal extent

Altitude (ft)	Mean annual rainfall (in.)	Drainage condition	Vegetation type	p^H content	% of organic matter (A_O layer)	% of N_2 in A_O horizon
6,000	120	Well-drained	Virgin high forest	7–7.5	22.32	1.14
5,000	150	Well-drained	Virgin high forest	6.5	19.23	0.97
4,000	120	Well-drained	Virgin high forest	6.5	18.76	0.77
3,000	150	Well-drained	Virgin high forest	6	24.9	1.05
2,000	150	Well-drained	Virgin high forest	6.5	10.29	0.35
1,000	150	Well-drained	Virgin high forest	6.5	7.05	0.31
500	150	Not well-drained	Virgin high forest	7–7.5	7.57	0.36

Source Darjiling District Gazetteers, O' Malley (1999)

2.3.1 Textural Characteristics of the Soil

Soil texture is defined by size distribution or mass fractions of primary particles in soil (individual grains and particles). Primary mineral particles formed through physical and chemical weathering of parent material and refractory organic substances make up the solid phase. Particle size distribution and shape are the most important characteristics affecting: pore geometry, total pore volume (porosity), and pore size distribution.

The presence of sand, silt and clay within a specific amount of soil are considered as the soil texture. On the basis of the amount of sand, silt and clay present in the soil the porosity, water holding capacity of the soil varies and consequently influence the cohesive nature of the soil. The higher amount of sand present in soil is characterized by the higher rate of permeability and porosity and decreasing tendency of the soil cohesiveness. The finer particles present in soil sometime becomes mobile in presence of seepage water and disturbs the soil cohesiveness. The soil becomes more compact in presence of higher amount of clay particles. All these three attributes of soil texture generally control the seepage, permeability, porosity, cohesiveness, water holding capacity etc. Hence, the stability condition of the slope is governed by the existence of the sand, silt and clay. United State Department of Agriculture (USDA) propounded a soil textural classes which states that particles with <0.002 mm diameter in size is recognized as clay, the size class ≥0.002 and <0.05 mm as silt and Sizes between ≥0.05 and <2 mm and sand and sizes of more ≥2 mm in diameter is treated as gravel. The present work is dealt with USDA System and textural properties are determined applying sieving method.

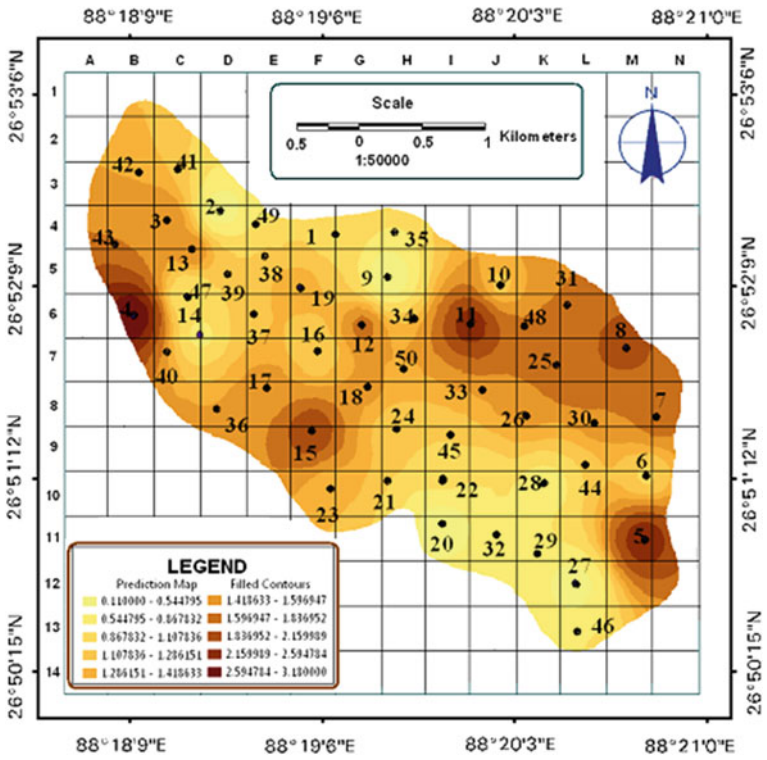

Fig. 2.9 Spatial distribution of clay (%)

Lower part of study area is experiencing very minimum percentage of sand particles whereas extreme south western part, small pockets in the south are characterized by higher percentage of sand particles. Mid-section and most of the marginal area are dominated by moderate to low percentage of sands (Table A.1, Appendix A). Tindharia (26.5 km from Siliguri), Lower Paglajhora, Mahanadi and Nurbong T.E. represents medium percentage of sand particles (Fig. 2.10) and this situation provide numerous micro pore spaces within the sub-soil and consequently increase the water holding capacity and reduce cohesive strength of the soil. In the south eastern part mainly at Tindharia and Sepoydhura, Mahanadi, Upper Paglajhora and Shiviter T.E. percentage of clay particles ranges from moderate to low and so the bonding capacity is low. This leads to soil erosion and slope instability condition. Small pocket in Giddapahar and Gayabari and lower eastern part register with high percentage of clay particles (Fig. 2.9).

Giddapahar, Shiviter and Upper Paglajhora is experiencing fine sand, medium sand, coarse sand and very coarse sand ranging between 10 and 30 % (Appendix A). The percentage of coarse silt and fine silt are very low (below 5 %) and percentage of very fine sand ranges between 5 and 10 %. The study on the distribution of silt particle in the Shivkhola watershed depicts that yet the

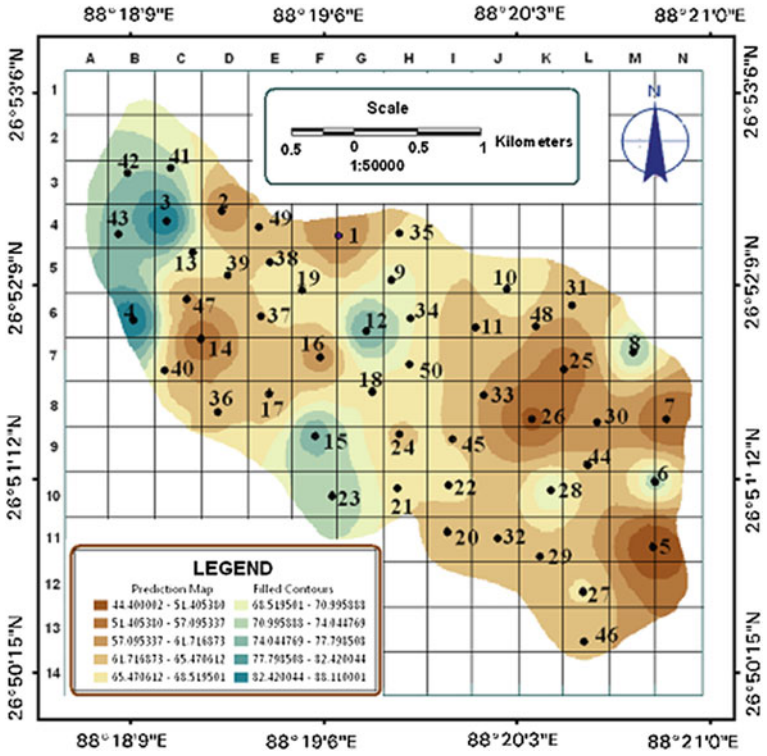

Fig. 2.10 Spatial distribution of sand (%)

percentage of silt is very low in the sub-surface soil, the eastern portions and few other locations at north western part of the basin shows high percentage of silt (Fig. 2.11). Middle section registers moderate to lower percentage of silt particles and this site show moderate level of sands which helps easy percolation and saturation of the soil and promote active soil loss at Tindharia, Gayabari, Lower Paglajhora and Shiviter (Fig. 2.10). The most landslide prone section of the Shivkhola watershed are registered with moderate to high percentage of granule (Fig. 2.12). Such high percentage of granule in the sub-surface part of the mountain slope helps to seepage and percolation of water and increases slope materials saturation level and promote slope failure.

2.3.2 Saturated Soil Depth

Repeated and continued field studies for a period of 7 years were made for the proper cognition of the processes and their interaction. The depth of the failure surface was measured by holding a measuring tape at both the margins of scar and

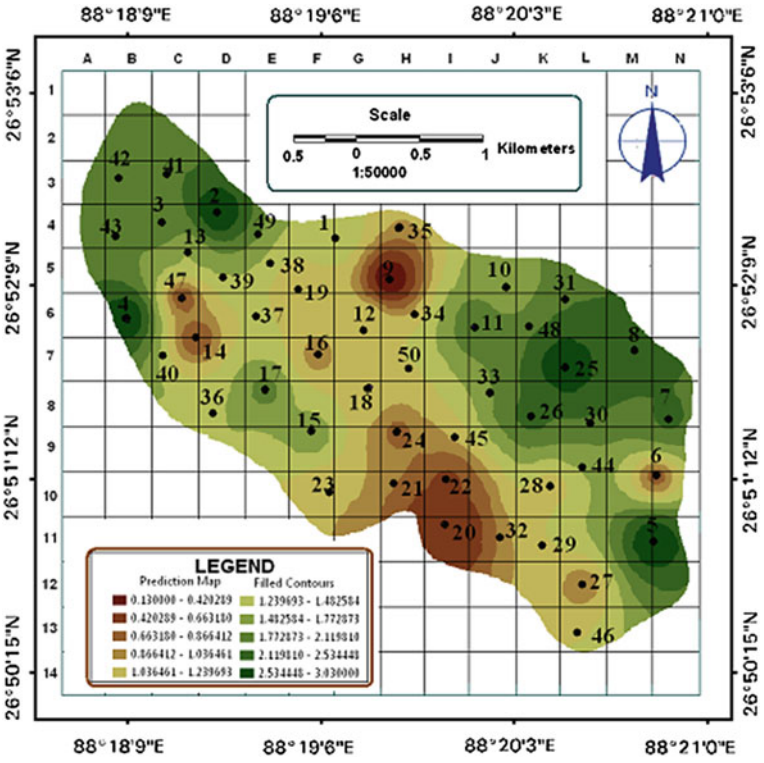

Fig. 2.11 Spatial distribution of silt (%)

the other tape was allowed to hang, the reading was then taken from the base of the hanging tape. The total thickness of soil and that of saturated soil from 50 different locations during monsoon were measured from slope cuttings. After estimating the approximate depth of all known points, a soil depth map (z/D) was made using Arc GIS tool (Fig. 2.13). The maximum depth (>1.75 m) of the saturated soil is found in the middle section (lower segment of Gayabari T.E., lower Paglajhora, Lower segment of Shiviter and Tindharia T.E.) and lower section (mainly Nurbong and Sepoydhura T.E.) of the basin. At marginal parts of the basin basically on the both sides of the Hill Cart Road from Chunabhati to Gayabari, upslope parts from Paglajhora proper, Lezzipur T.E. and Shiviter upslope, the saturated soil depth is less than 1.75 m (Table A.1, Appendix A).

In the present study area, Shivkhola watershed the upper section of the soil at major landslide locations are predominated by large percentage sand particle where the tensile strength in dry and wet situation is low (Table 2.9). This situation promotes shallow landslips. But the area dominated by large percentage of clay and

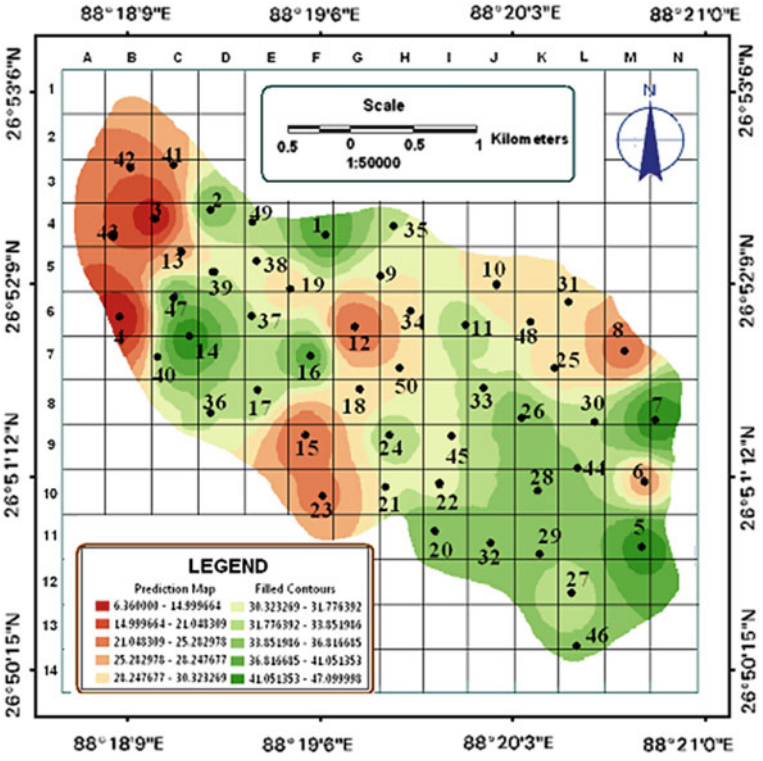

Fig. 2.12 Spatial distribution of granule (%)

silt show the higher plasticity and high to very high tensile strength and low landslide potentiality. We can say that the major size fraction of the soil controls various physical properties of soil such as tensile strength, volumetric expansion, plastic condition, porosity, permeability and water retention capacity as well as the rate of liquefaction of slope materials.

Soil samples from 12 locations of Paglajhora Sinking Zone, one of the major landslide prone areas of Darjiling Himalaya, were being collected and tested in the laboratory (GSI) to understand physical properties of soils related with slope instability. The study envisages that the saturated soil density varies from 2.00 to 2.60 and dry soil density varies from 1.20 to 1.96 (Table 2.10). The variation of saturated soil density is less which helps to liquefy the soils chemical properties and make all the places more conducive to slope failure. Percentage of sand, silt and clay are also distributed in at this place uniformly. The cohesion in the Paglajhora Sinking zone is very less (<0.7) and friction angle ranges from 22° to 37°.

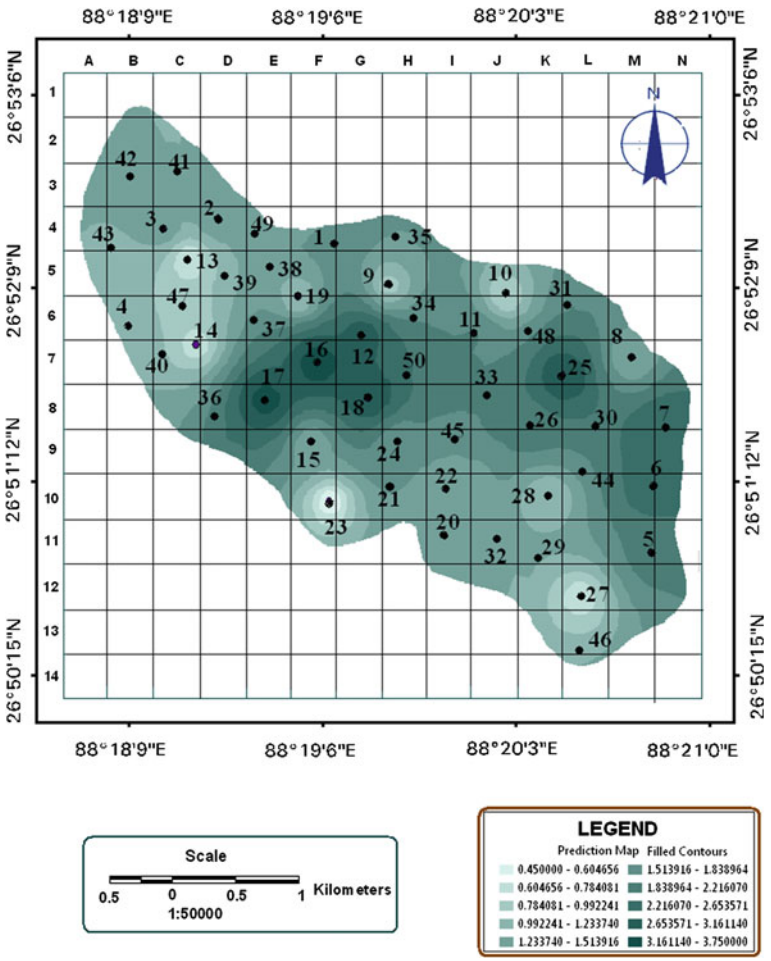

Fig. 2.13 Spatial distribution of soil depth (in meter)

2.3.3 Water Holding Capacity, Pore Space and Volume Expansion of the Soil (in %)

The capacity to contain water particles by a certain volume of soil mass is called Water Holding Capacity. The water holding capacity of soil depends on the presence of impermeable layer below the permeable layer, pore space and solid space of the soil, sources of water supply and shape of the underlying structure, and gravitational force. Pore space in soil consists of that portion of the soil volume not occupied by solids. The volume of a given soil occupied by air is designated by air space, air volume, air space porosity, non-capillary porosity and gaseous phase

Table 2.9 Physical properties of soil according to major size fraction of the particles

Property	Gravel	Sand	Silt	Clay
Volume change	None	None	Slight	Large
Tensile strength (dry condition)	Low	Lower than when wet	Higher than when wet	Very high
Tensile strength (wet condition)	Low	Low	Intermediate	High
Plasticity (wet)	None	Slight	Intermediate	Very high
Plasticity (dry)	None	None	None	None, partial cementation
Porosity	Very high	High	High	Very high
Permeability	Very high	High	Intermediate to low	Very low
Water retention	Very low	Low	High	Very high
Size of voids	Large	Intermediate	Capillary	Subcapillary

Source Dapples (1959), US Department of the Interior, Bureau of Reclamation (1963)

Table 2.10 Study on the geo-technical parameters of soil at Paglajhora sinking zone

Sample no.	Soil density (gm/cc)			Grain size analysis (%)			Direct shear test result	
	Wet	Dry	Saturated	Sand	Silt	Clay	Cohesion (c)	Friction (φ)
1	1.94	1.62	2.12	85	11	4	0.11	30
2	2.18	1.96	2.39	83	12	5	0.22	19
3	2.01	1.52	2.54	90	3	3	0.41	24
4	2.08	1.84	2.27	87	11	2	0.02	35
5	1.98	1.65	2.46	80	14	6	0.04	41
6	1.82	1.45	2.18	79	17	4	0.01	37
7	1.76	1.42	2.38	75	20	5	0.7	13
8	1.99	1.30	2.09	81	16	3	0.23	32
9	1.70	1.36	2.25	73	22	5	0.16	33
10	1.83	1.47	2.06	80	19	1	0.21	30
11	1.66	1.20	2.02	78	15	7	0.06	29
12	1.97	1.36	2.58	82	13	5	0.21	22

Source Mandal and Maiti (2012)

whereas volume of a soil occupied with water is known as liquid phase or capillary porosity. These values are not constant but vary with the soil physical conditions and moisture content. The amount of pore space is determined by the arrangement of solid particles. If they tend to lie close together, the total porosity is low. If they are arranged in porous aggregates, as is often the case in medium textured soils high

Table 2.11 Depth wise distribution of water holding capacity, pore space and volumetric expansion (%)

Location	Parameters	Depth of the soil (cm)						
		0–10	10–20	20–30	30–40	40–60	60–80	80–100
26.5 km from Siliguri near Tindharia (1)	Water holding capacity (%)	83.42	86.50	89.73	89.59	79.75	54.70	40.63
	Pore spaces (%)	43.51	47.29	59.40	52.30	30.75	29.21	21.65
	Volume expansion (%)	31.40	27.10	27.21	28.93	25.23	19.75	13.21
26.5 km from Siliguri near Tindharia (2)	Water holding capacity (%)	73.04	74.06	75.03	71.93	60.51	46.44	34.65
	Pore spaces (%)	45.02	46.51	50.31	46.42	34.73	27.53	24.39
	Volume expansion (%)	21.09	21.09	23.20	24.15	17.46	12.03	9.95
26.5 km from Siliguri near Tindharia (sample-A-3)	Water holding capacity (%)	70.21	71.39	74.45	75.09	62.43	51.03	37.51
	Pore spaces (%)	52.40	59.31	50.43	42.36	37.05	29.00	26.74
	Volume expansion (%)	25.75	23.01	23.04	19.52	15.34	14.31	9.73
26.5 km from Siliguri near Tindharia (sample-A-4)	Water holding capacity (%)	35.73	31.43	26.73	29.72	16.07	13.73	10.93
	Pore spaces (%)	76.72	75.92	71.39	53.03	50.92	56.43	49.02
	Volume expansion (%)	14.71	14.92	13.75	9.78	7.02	5.03	4.01
At Shiviter tea estate	Water holding capacity (%)	45.45	41.25	35.50	32.55	27.30	22.53	10.93
	Pore spaces (%)	69.54	63.75	60.50	49.85	34.75	26.65	22.55
	Volume expansion (%)	34.55	29.45	28.58	19.55	13.25	11.50	9.57
At lower Paglajhora 33.5 km from Siliguri	Water holding capacity (%)	29.22	25.54	22.45	18.50	12.34	9.08	5.45
	Pore spaces (%)	86.75	85.62	81.35	73.93	60.12	46.53	39.82
	Volume expansion (%)	21.11	19.21	15.42	12.22	9.75	6.45	5.40

Source Basu and Sarkar (1985)

in organic matter, the pore space per unit volume will be high. In the present study a comparison has been made between pore space, water holding capacity and volumetric expansion for few major landslide locational sites at different depth of soil (Basu and Sarkar 1985) and their role in slope instability have also been studied (Table 2.11).

2.3.3.1 Volumetric Expansion

Soil Survey Standard Test Method was applied to measure volumetric expansion of the soil. This method outlines the procedure for the determination of the free swell of a disturbed soil on wetting. This test measures the free swelling of a disturbed soil (ground and sieved finer than 0.425 mm) on wetting from air-dry to saturation. The swell is calculated on a volumetric basis using a modification of the Keen-Raczowski Test. The soil samples having at least 150 g of the material passing a no 36 BS Sieve (0.425 mm) were collected from 50 different locations of the Shivkhola watershed and prepared according to the procedure for testing (Keen and Raczowski 1921). To calculate the percentage volumetric expansion (VE), the following equation was applied.

$$VE\,(\%) = \frac{W_3 - W_2}{W_4 - W_1} \times 100 \tag{2.2}$$

where, W_1 = weight of volume expansion box (g); W_2 = weight of the weighing tin (g); W_3 = weight of wet expanded soil + tin (g); and W_4 = wet of wet residual soil + box (g).

2.3.3.2 Water Holding Capacity

Simply defined soil water holding capacity is the amount of water that a given soil can hold for crop use. Soil texture and organic matter are the key components that determine soil water holding capacity. In terms of soil texture, those made up of smaller particle sizes, such as in the case of silt and clay, have larger surface area. The larger the surface area the easier it is for the soil to hold onto water so it has a higher water holding capacity. Sand in contrast has large particle sizes which results in smaller surface area. The water holding capacity for sand is low. Soil organic matter (SOM) is another factor that can help increase water holding capacity. Soil organic matter has a natural magnetism to water. By using Keen-box and oven, water holding capacity of soil was assessed applying the following equation.

$$Water\ holding\ capacity\ of\ soil = \frac{total\ water\ in\ the\ wet\ soil}{oven\ dry\ weight\ of\ the\ total\ soil} \times 100 \tag{2.3}$$

2.3.3.3 Porosity of the Soil

Porosity or *pore space* refers to the volume of soil voids that can be filled by water or air. It is inversely related to bulk density. To calculate porosity, *bulk density* and *particle density* were determined applying Keen-box method. The oven dry weight of a unit volume of soil inclusive of pore spaces, called as *bulk density*. Generally soil with low bulk density provides good physical condition. The bulk density of

sandy soil, loam soil, silt loam, and clay soil are 1.6, 1.4, 1.3 and 1.1 gm/cm^3. On the other hand, the weight per unit volume of the solid portion of the soil is called as *particle density*. The particle density is the true density of soil. The particle density of normal soils is 2.65 gm/cm^3. The particle density of coarse sand, fine sand, silt and clay are 2.655, 2.659, 2.798 and 2.837 gm/cm^3 respectively. The particle density of the soil increases with decreasing the size of particles. The porosity can be calculated by using the following method.

$$\%\, solid\ space = \frac{bulk\ density}{particle\ density} \times 100 \tag{2.4}$$

$$\%\, of\ pore\ space = 100\,\% - \%\, of\ solid\ space \tag{2.5}$$

In the present work, the total porosity in the soil has been derived using the method applied by Brasher (1966).

$$\text{Total porosity}\ (\%) = (\text{particle density-bulk density}) \div \text{particle density} \tag{2.6}$$

Loose, porous soils have lower bulk densities and greater porosities than tightly packed soils. Porosity varies depending on particle size and aggregation. It is greater in clayey and organic soils than in sandy soils. A large number of small particles in a volume of soil produce a large number of soil pores. Compaction decreases porosity as bulk density increases. So, there exists a inverse relationship between bulk density and porosity. If compaction increases bulk density from 1.3 to 1.5 g/cm^3, porosity decreases from 50 to 43 %. Pores of all sizes and shapes combine to make up the total porosity of a soil. Porosity, however, does not tell us anything about the size of pores (http://www.agriinfo.in) (Table 2.12).

The collection and testing of soil samples from different locations and their laboratory results shows that at 14 Miles Basti water holding capacity and volume

Table 2.12 Friction angle (φ) and landslide potentiality index (LPIV)

Classes	Number of pixels (F_1)	Number of landslide affected pixels (F_2)	Landslide potentiality index (LPI) = ($F_2/F_1 \times 100$)
<18.00	3,500	626	17.88
18.00–19.486	3,547	523	14.74
19.486–20.971	3,266	417	12.77
20.971–22.456	3,864	413	10.69
22.456–23.940	2,786	329	10.81
23.940–25.425	3,545	311	8.77
25.425–26.910	2,435	201	8.25
26.910–28.395	3,597	211	5.86
28.395–29.880	3,248	202	6.21
29.880–32.848	3,343	190	5.68

Table 2.13 Result of laboratory analysis (GSI Lab.) of collected soil samples from Tindharia

Sample	Cohesion (C)	Friction angle (φ)	Dry soil density (gm/cm^3)	Wet soil density (gm/cm^3)	Water holding capacity (%)
I	0.64	22°30′	2.20	2.43	35
II	0.25	19°	2.10	2.29	29
II	0.08	24°	1.99	2.21	28

expansion are low than the pore space. The pore space even at the depth of 60–80 cm is prevailing above 35 %. The easy percolation of water through the subsurface soil pore spaces creates the slope more vulnerable to soil erosion and slope instability. On the other hand, near railway station and other places of Tindharia there is higher rate of water holding capacity ranging between 40 and 55 % (Table 2.13) up to the depth of 40 cm. where the percentage of pore space is experiencing 30–50 %. The water holding capacity is reduced with decreasing the pore space beyond the depth of 60 cm. The volumetric expansion takes place in proportion to pore space and water holding capacity and it is high (>10 %) above the depth of 40 cm and shows the gradual decreasing tendency below the depth of 40 cm.

In the Shiviter T.E. the moderate to high percentage of pore space helps soil to hold the moisture content and to expand moderately. The presence of sand, silt and clay at moderate amount within the soil has helped to retain the moisture for a long time without downward movement and has caused slope material more vulnerable to soil loss. In the middle section of the watershed the water holding capacity as well as the pore spaces is very high but there is a uniform rate of decreasing tendency of both the parameters. The volumetric expansion is not as high as the water holding capacity and pore spaces. The water holding capacity and pore space is more than 50 % up to the depth of 40 cm when the volumetric expansion ranges between 10 and 20 %. Beyond 40 cm water holding capacity and pore space are experiencing 45–15 % where 0–10 % volumetric expansion takes place. The decreasing of volume expansion, pore space and water holding capacity are in the same rate at Upper Paglajhora and Tindharia T.E. The percentage of pore space is very high up to the depth of 30 cm and that is why the water holding capacity is reduced sharply and beyond 60 cm depth the pore space is being decreased remarkably which causes easy saturation of surface soil and volumetric expansion also takes place within the sub-surface soil. Such condition reduces the cohesion and internal friction of the slope materials and makes the slope very much prone to shallow soil slip. It is to be concluded from the present study that the average percentage of sand and granules up to the depth of 100 cm are 35 and percentage of silt is around 15 which promotes the soil layer to be saturated very easily and also reduces the cohesion and shearing strength of the soil. Pore spaces, water holding capacity and volumetric expansion decrease with increasing depth everywhere which indicates that the near surface soil layer is saturated easily that reduced its cohesion and shearing strength.

2.3.4 Friction Angle (φ) and Cohesion (c)

The shear strength of the soil is described as the function of normal stress on the slip surface, cohesion, and angle of internal friction. The angle of internal friction (φ) and cohesion are the two important physical properties of the soil which determines angle of rupture, shearing strength, safety factor as well as stability condition of the slope materials. A Mohr Stress Circle was developed to obtain angle of internal friction and angle of rupture through confining pressure (σ_3) and compressive stress (σ_1) with the centre on the horizontal axis; the centre of the circle was obviously ($\sigma_1 + \sigma_3$)/2 and the radius was ($\sigma_1 - \sigma_3$)/2. The values of confining pressure, σ_3, and compressive stress, σ_1 were plotted on horizontal axis where stress difference is $\sigma_1 - \sigma_3$. On a plane parallel to the greatest principal stress axis ($2\alpha = 0$) the normal stress across the plane was σ_3 and the shearing stress was 0. If the plane makes an angle of 45° with the greatest principal stress axis ($2\alpha = 90$), the shearing stress is at a maximum and the normal stress is ($\sigma_1 + \sigma_3$)/2. If the plane makes an angle of 90° with the greatest principal stress axis ($2\sigma = 180°$), the shearing stress is 0 and the normal stress is σ_1.

Cohesion (C) is the attraction of particles to each other which is not directly governed by a friction law but does provide a measure of strength of a material. Thus sands do not exhibit cohesion, while soil which contains clay show cohesion. It can be measured, as in soil mechanics, by the Mohr-Coulomb Equation.

$$C\ (cohesion) = \frac{\sigma_1 - \sigma_3 \tan^2\left(45 + \frac{\varphi}{2}\right)}{2 + \tan\left(45 + \frac{\varphi}{2}\right)} \tag{2.7}$$

The cohesion of the soil varies from place to place due to variation in the presence of cementing materials which helps to combine soil particles tightly. This is the bonding of the particles with each other. The natural bonding of the soil particles are influenced and loosened by the presence of lubricating agent (water and ice particles) and ensure the materials to collapse. The friction angle of sandstone under dry condition varies from 26° to 35° and under wet condition 25°–34°. Fine-grained granite provides the friction angle of 31°–35° and 29°–31° for dry and wet condition respectively. In case of gneiss, friction angle is 26°–29° for dry and 23°–26° for wet condition (Barton and Choubey 1977). The above mentioned lithological compositions are available in the Shivkhola Watershed and laboratory test of 50 soil samples shows that the friction angle ranges between 18° and 32° (Appendix C).

At Lower Paglajhora and 14 Miles Bustee, the geo-technical properties of soil are very much conducive to soil slip (Table 2.13). In the present study the friction angle for the concerned material varies from 18° to 32° (Fig. 2.14). Around Tindharia and Lower Paglajhora friction angle ranges between 18° and 22°. A steep slope will decline by slope failure to an angle of repose slope to attain short term stability. This concept leads to the concept of limiting or Threshold slope angle. It is clearly observed from the figure that middle section, extreme lower most part,

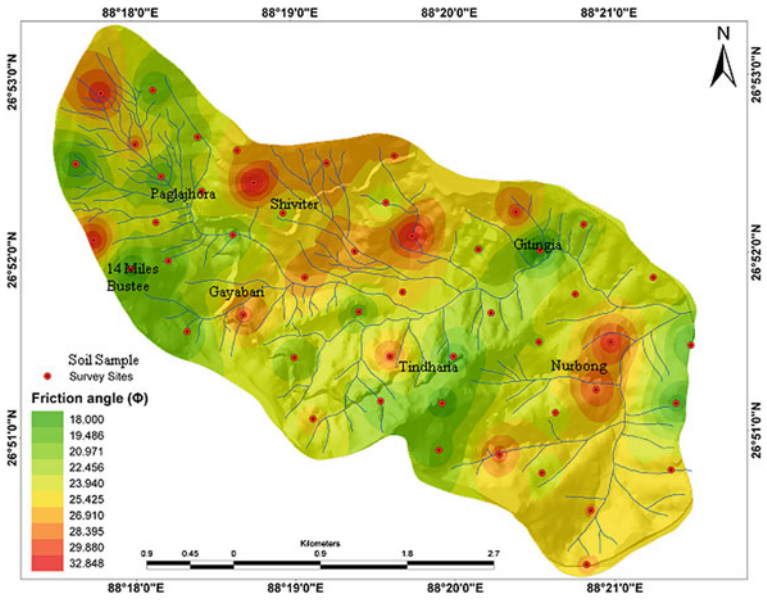

Fig. 2.14 Spatial distribution of friction angle (φ)

Sepoydhura and some northern marginal parts are registering the friction angle of more than 24°. Large parts of Tindharia (Table 2.12), 14 Miles Bustee, and Lower Paglajhora are facing the friction angle of less than 24° and also are considering as the most vulnerable part of the Shivkhola Watershed. The friction angle at Shiviter varies from 21° to 25° (Table 2.15). It is observed that there is an increase in the volume of the landslide area and mass since 1986–2010.

Hill Cart Road is passing through the locations of Tindharia. 14 Miles Bustee and Paglajaora where friction angle is quiet less. Analysis also reveals that more than 50 % area of the Shivkhola watershed is below the friction angle of 24°. The derived landslide potentiality index value reveals that the area having friction angle of less than 20° are registered with high LPIV (Table 2.12). The low LPIV is observed at the places where the friction angle is greater than 25°. The spatial distribution of *cohesion* in the Shivkhola Watershed reveals that Paglajhora, 14 Miles Bustee (Table 2.14), Tindharia (Table 2.12), Shiviter (Table 2.14) are characterized by very low cohesive strength of soil. The range of cohesion is between 0.01 and 0.90 (Fig. 2.15). The places of Gayabari and its adjoining areas, Sepoydhura, middle section of the watershed and extreme north-eastern part are dominated by moderate to high cohesive strength of the soil, varying from 0.35 to 0.90. The estimated cohesion of all the 50 locations shows that the cohesion in the Shivkhola watershed is very less, that is less than 0.90. The study indicates that there is an inverse relationship between cohesion and LPIV. The region of low cohesion of less than 0.29, showed the LPIV of more than 15 (Tables 2.15 and 2.16).

Table 2.14 Result of the laboratory test of soil samples from lower Paglajhora and 14 Miles Bustee

Sample no.	Lithology	Cohesion (kg/cm^2)	Angle of internal friction (φ)	Wet density (gm/cm^3)	Dry density (gm/cm^3)	Water holding capacity (%)
I	Foliated gneiss and mica-schist	0.12	22°30′	2.14	1.86	32
II	Foliated gneiss and mica-schist	0.25	19°	2.08	1.79	28
III	Foliated gneiss and mica-schist	0.18	17°30′	2.02	1.74	23

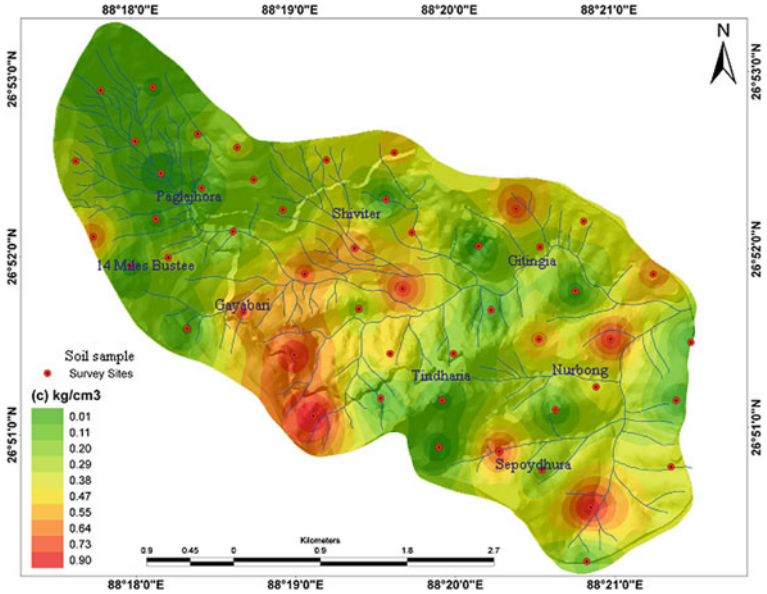

Fig. 2.15 Spatial distribution of cohesion (c)

2.3.5 Wet Soil Density (γ_s)

Specific unit weight of water and unit weight of the soil were estimated by examining the soil samples collected from 50 landslide locations during field investigation from the GSI (Geological Survey of India, East Kolkata) laboratory. The density of soil and water varies from place to place due to in situ geo-hydrologic condition. The saturated soil density of rock was also consulted and

Table 2.15 Volumetric expansion of the landslide with strength properties from Shiviter

Landslide number	Volume (1986) (m^3)	Volume (June, 2006) (m^3)	Volume (August, 2010) (m^3)	Slope angle (Θ) (°)	Cohesion (c)	Friction angle (φ) (°)	Water holding capacity (%)
I	390	450	540	57	0.05	25	24
II	1,200	1,350	1,400	62	0.13	18	33
III	300	500	620	59	0.52	21	35

Source Laboratory test result

Table 2.16 Cohesion (c) and landslide potentiality index (LPIV)

Classes	Number of pixels (F_1)	No. of landslide affected pixels (F_2)	Landslide potentiality index (LPI) = ($F_2/F_1 \times 100$)
<0.01	3,381	691	20.44
0.01–0.11	3,786	668	17.64
0.11–0.20	3,695	451	12.20
0.20–0.29	3,352	522	15.57
0.29–0.38	3,899	344	8.82
0.38–0.47	3,741	286	7.64
0.47–0.55	2,450	110	4.48
0.55–0.64	3,987	221	5.54
0.64–0.73	4,021	120	2.98
0.73–0.90	1,519	60	3.94

adopted from the field experiences done by Deoja (Mountain Risk Engineering Handbook, 1991) and Specific Yield from Basic Ground-water Hydrology. Here, the wet soil density was derived after Brasher (1966). Higher the density, greater is the propensity of landslide occurrences. Wet soils help to liquify the mineralogical properties present in the soil and reduce the cohesive strength.

The wet soil density plays a significant role in changing chemical properties, cohesion (c) and friction angle (φ) of the soil particles. It is proved that greater is the wet soil density, lesser is the cohesive strength of the soil because after wetting the soil, it loses internal bonding capacity and becomes more susceptible to landslide. In Shivkhola watershed, wet soil density is higher (>2.00 KN/m^3) in the areas of Tindharia, 14 Miles Bustee, Paglajhora, Sepoydhura, Gitingia and Upper Paglajhora (Fig. 2.16). All these places are dominated by drainage concentration. Such drainage concentration helped to increase the wet soil density and to reduce the cohesive strength. The study on landslide potentiality shows that soils having high wet soil density are very much prone to landslide phenomena (Table 2.17).

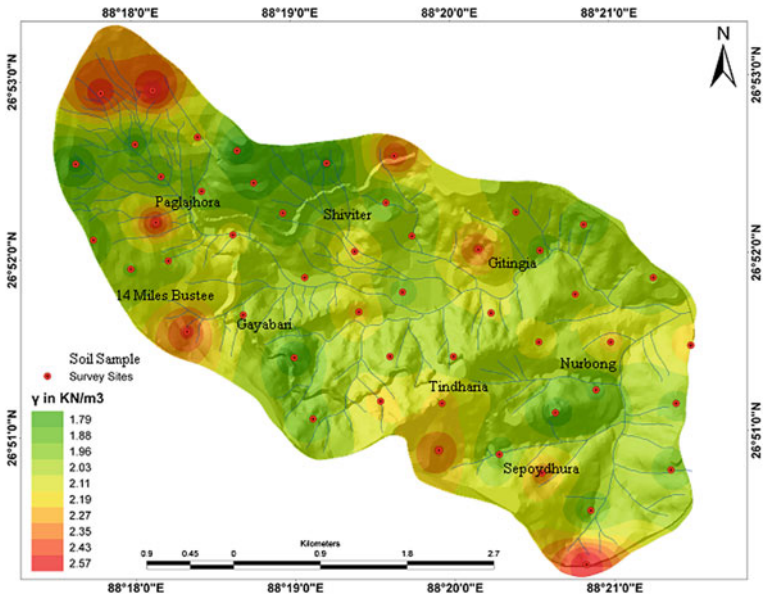

Fig. 2.16 Spatial distribution of wet soil density

Table 2.17 Wet soil density and landslide potentiality index (LPIV)

Classes	Number of pixels (F_1)	No. of landslide affected pixels (F_2)	Landslide potentiality index (LPI) = ($F_2/F_1 \times 100$)
<1.79	3,303	180	5.45
1.79–1.88	3,138	212	6.76
1.88–1.96	3,687	201	5.45
1.96–2.03	2,495	211	8.45
2.03–2.11	3,505	321	9.15
2.11–2.19	2,726	319	11.70
2.19–2.27	3,954	423	10.69
2.27–2.35	3,176	417	13.13
2.35–2.43	3,657	553	15.12
2.43–2.57	3,490	636	18.22

2.4 Conclusion

The study area Shivkhola watershed possesses a wide range of elevation between 300 m in the south-east and 2,040 m in the north. A large part of the watershed is lying between the altitude of 400 and 600 m. The steepness of the slope varies significantly from place to place and its characteristics mostly depend on the drainage density. The left hand side of the river Shivkhola is less steep in

comparison to right hand side. The analysis of hypsometric curve reveals that the potential dissection is more at Tindharia and for the stretch along the Hill Cart Road between Gayabari to Mahanadi including Paglajhora. The northeastern part of the basin near the water divide is extensively dissected and shows absolute instability. The study area is composed mainly of the Darjiling Gneiss, Daling formation composed of Chungtung formation, Lingtse Granite, Garubathan formation and Ryang formation. Gondwana formation, the most fragile one due to the presence of carboniferous rocks is located along a narrow belt being sandwiched between Daling to the north and Siwalik to the south. The structural-cum stratigraphic succession can be observed as a traverse across Tindharia-Kurseong region. The concerned study area is structurally instable as most of the unconformities are lying across the drainage lines and so subsidence zones are developed at the junctions of the drainage lines with the structural discontinuities and lineaments. The Paglajhora, the biggest subsidence zone of the study area, is situated along the Darjiling-Daling boundary. The mica schist in the Daling series is also a factor of instability as most of the slides are located on the mica schist due to its less resistance. The slope is maximum near Paglajhora area and the Hill Cart Road and North Eastern Frontier Rail line (0.61 m gauge) cross the entire river system twice through this steeper and unstable zone. The slope is least at the central part where the river develops a cut and fill terrace. The study shows that the LPI for the slope categories are increasing at a steady rate as the steepness increases and it is the indicator of the direct control of slope on the slope failure. All the cells having steepness of 19°–23° and above are affected by landslide. The positive curvature is more common indicating the tendency of immediate drainage of surface water which is detrimental to the stability of both soil and slope. Paglajhora, Gayabari, Tindharia, and Shiviter are dominated by the moderate to high levels of positive and negative surface curvature with moderate levels of slope surface dissection. Landslide prone north, south, east, north east and south east facets are closely associated with maximum slope and relief which is found at upper and lower Paglajhora, Shiviter T.E., Gayabari Lower slope and Tindharia where landslide potentiality is high. Sub-surface soil over the steep slope at the places of Tindharia T.E. and Lower Paglajhora is dominated by humus which is very loose, crumble and friable. Such humus dominated soil gets saturated very easily due to moderate amount of rain and reduces cohesion by increasing pore-water pressure and make the slope surface more vulnerable to soil slip. At marginal parts of the basin basically on the both sides of the Hill Cart Road from Tindharia to Gayabari, upslope parts from Paglajhora proper, T.E. and Shiviter upslope where the saturated soil depth is less than 1.75 m. At all these places sub-surface soil gets saturated quickly and promotes suitable condition for shallow soil slip. At the sub-surface layer of the soil percentage of pore space is high but at greater depth pore space decreases because of the existence of large percentage of finer particles. The reduction of pore space at greater depth results in the increase of water holding capacity and volumetric expansion at the sub-surface soil which increases the pore-water pressure and reduces cohesion and finally invites slope soil failure at most of the places of the Shivkhola Watershed.

References

Ahnert F (1987) Process response models of denudation at different spatial scales. Catena Suppl 10:31–50

Anabalagan R (1992) Landslide hazard evaluation and zonation mapping in mountainous terrain. Eng Geol 32:269–277

Anderson MG, Burt TP (1978) The role of topography in controlling through flow generation. Earth Surf Proc 3:331–344

Attewell PB, Farmer IW (1976) Principles of engineering geology. Chapman and Hall, London

Barton N, Choubey V (1977) The shear strength of rock joints in theory and practice. Rock Mech 10:1–54

Basu SR, Sarkar S (1985) Some consideration on recent landslides at Tindharia and their control. Indian J Power River Val Dev 1985:190–194

Beven KJ, Kirkby MJ (1979) A physically based variable contributing area model of basin hydrology. Hydrol Sci Bull 24(1):43–69

Brasher BR (1966) Use of Saran resin to coat natural solid clods for bulk-density and water retention measurement. Soil Sci 101:108

Chorley RJ, Schumm SA, Sugden DE (1985) Geomorphology. Methuen and Co Ltd, New York

Cruz O (2000) Studies on the geomorphic processes of overland flow and mass movements in the Brazilian geomorphology. Revista Brasileira de Geosciencias 30:500–503

Dapples EC (1959) Basic geology for science and engineering. Wiley, New York

Deoja et al (1991) Mountain risk engineering handbook. International Centre for Integrated Mountain Development (ICIMOD), Kathmandu, pp 875

Dhakal AS, Amada T, Aniya M (2000) Landslide hazard mapping and its evaluation using GIS: an investigations of sampling schemes for a grid-cell based quantitative method. Photogramm Eng Remote Sens 66(8):981–989

Dietrich et al (1998) SHALSTAB: a digital terrain model for mapping shallow landslide potential. National council of the paper industry for air and stream improvement. Technical report

Gao J (1993) Identification of topographic settings conducive to landsliding from DEM in Nelson County, VA, USA. Earth Surf Proc Land 18:579–591

Gilbert GK (1909) The convexity of hill tops. J Geol 17:344–350

Guimaraes RF, Montgomery DR, Greenberg HM, Gomes RAT, Fernandes NF (1999) Applicatioa of a model for the topographic control on shallow landslides to catchments near Rio de Janeiro. In: Lipard SJ, Naess A, Sinding-Larsen R (eds) IAMG99—annual conference of the international association of mathematical geology. IAMG, Trondheim, Noruega, pp 349–354

Krishnaswamy VS (1982) Geological aspects of landslides with particular reference to the Himalayan region. In: Proceedings of the international symposium on landslides, New Delhi, pp 171–185

Keen BA, Raczkowski H (1921) Relation between the clay content and certain physical properties of a soil. J Agric Sci 11:441–449

Laahiri S (1973) Some observations on structure and metamorphims of the rocks of Kurseong, Tindharia region, Darjeeling district WB. In: Jhingran AG, Valdia KS (eds) Himalayan geology, vol 3. Wadia Institute of Himalayan Geology, Delhi, pp 365–371

Lahiri S, Gangopadhway PK (1974) Structure pattern in rocks in Pankhabari—Tindharia region Darjeeling district WB with special reference its bearing on stratigraphy. In: Jhingran AG (ed) Himalayan geology, vol 4. Wadia Institute of Himalayan Geology, Delhi, pp 151–170

LSS O'Malley (1999) Darjiling district gazetteers. Logos Press, New Delhi

Mandal S, Maiti R (2012) Application of RS and GIS based semi-quantitative approach in landslide hazard risk assessment of the Shivkhola watershed, Darjiling Himalaya. Georisk Assess Manag Risk Eng Syst Geohazards 6(4):203–220

Mallet FR (1874) On the geology and mineral resources of the Darjeeling district and Western Duars. Mem Geol Surv India 2:1–72

Montgomery et al (1994) A physically based model for the topographic control on shallow landsliding. Water Resour Res 30:1153–1171

Nautiyal SP (1951) A geological report on the hill slope stability in and around Darjeeling, WB. Unpublished report of the geological survey of India

Nautiiyal SP (1966) On the stability of certain hill slopes in and around Darjeeling, WB. Bull Geol Surv India Ser B 15(1):31–48

Roy S, Sensharma SB (1967) Geological report on the stability of hill slopes in and around Darjeeling town, Darjeeling district SW. Unpublished geological survey of India report

Sarkar S (1987a) Pedogeomorphic parameters in environmental management—a case study in the upper Panchanai basin of Darjeeling Himalayas. In: Proceedings of the seminar on applied geography in the perspective of planning the environment, the urbanscape and the regional pollution. North Bengal University, pp 128–139

Sarkar S (1987b) Soil loss in the upper Mahananda basin in the Darjeeling Himalaya. Geog Rev India 49(2):47–56

Strahler AN (1952) Hypsometric (area altitude) analysis of erosional topography. Bull Geol Soc Am 63:1117–1142

US Department of the Interior, Bureau of Reclamation (1963) Earth manual. Government Printing Office, Washington, DC

Vieria et al (1998) Controles fito-morphologicos dos escorregamentos da baisa de Quintic (RJ). Revista GEOSUL 27:324–328

Zhou CH, Lee CF, Li J, Xu ZW (2002) On the spatial relationship between landslides and causative factors on Lantau Island, Hong Kong. Geomorphology 43:197–207

Chapter 3
Impact Assessment of Hydrologic Attributes and Slope Instability

Abstract Quantitative geomorphology provides a systematic approach to the analysis of a complex landscape of any size. The stability of the mountain slope depends upon the prevalence of various hydrologic variables. In the present work, the excess and deficit moisture period in a year and its role in slope instability were assessed studying rainfall and evapotranspiration. Study envisages that July and August are the most consistent rainfall months of the year where the values of co-efficient of variation are very low. The distribution of drainage and its evolution has been studied to determine the drainage concentration over the slope surface and their role in slope steepening and instability. To assume the slope saturation of materials saturation, stream confluence points/junction points were studied for individual sub-watersheds. The length of drainage per unit area and upslope contributing area were analyzed spatially in connection to the landslide potentiality. The existence of moderate drainage density may invite havoc slope failure on convex slope segment. Greater the upslope contributing area, maximum is the slope saturation and slope instability in the Shivkhola watershed. Some important drainage basin parameters such as basin shape, form factor, circularity ratio, elongation ratio, compactness factor, and elipticity index of the sub-watersheds were considered to develop the priority scale on slope instability. The sub-basin I and IV are more efficient in drainage and are more erosion and landslide prone followed by sub-watershed V, II, III and VI.

Keywords Rainfall · Drainage morphometry · Landslide potentiality · Instability rank · Watershed

3.1 Introduction

One of the most fundamental geomorphic unit is the ‘drainage basin’ in the study of geo-hydrological parameters where drainage network characteristics and its evolution strongly influences the whole hydrological parameters through initiating,

S. Mandal and R. Maiti, *Semi-quantitative Approaches for Landslide Assessment and Prediction*, Springer Natural Hazards, DOI 10.1007/978-981-287-146-6_3

encouraging and changing others sub-areal processes such as surface run-off, seepage, and sub-surface flow. But, for the development of the drainage network and for changing actual nature of the slope materials rainfall must plays an important role. The history of evolution of a drainage basin and its morphology are closely related to rainfall characteristics and geology, i.e. the type of rocks and their structure. Depending upon the susceptibility to erosion and structure of the rocks the fluvial processes operate and the landform evolution proceeds through successive stages with drainage network branching and head ward extension. Hydrological attributes mainly rainfall and drainage are the two important factors of slide and soil erosion as the material moves down slope with the help of water and it may be either surface or sub-surface flow. The water when flows on the surface with huge amount can perform remarkable erosion as the potential energy it possesses is readily transfers to kinetic energy which takes part in the mass transfer. The soil water saturates the soil and increases the pore water pressure and the weight of the mass which then becomes more prone to slide or subsidence. The occurrence of few days' continuous rainfall and their presence within the subsoil may act as the lubricating agent and which makes the down slope movement easier by reducing the friction, cohesion and increasing shearing stress in the slope material. Rainfall as a trigger has been extensively studied by number of authors i.e. Larson (1995), Polloni et al. (1996), Glade (2000), Wieczorek and Guzzetti (2000), Polemio and Petrucci (2000), Toll (2001) and Zezere (2000).

One of the most important geomorphic properties is the degree of dissection of the topography, sometimes expressed in terms of drainage density. Gradual extension of drainage network and their regular branching increase the slope steepness by increasing slope concavity and convexity. Gilbert (1909) argued that convex-concave forms reflect a gradual transition in process dominance from creep to wash with increasing distance from a drainage divide. Gilbert's model was quantified in terms of a linear stability analysis by Smith and Bretherton (1972). Drainage density and landscape structure may alternatively be controlled, by thresholds for run-off generation (Kirkby 1980; Ijjasz-Vasquez et al. 1992) or by thresholds of slope stability (Montgomery and Dietrich 1989). Drainage density in particular may be controlled to varying degrees by any of these thresholds, and each different threshold may produce a different functional relationship between drainage density and factors related to climate geology and relief. Howard (1997) represented a detachment-limited model in which the relationship between drainage density and mean erosion rates depends on (i) the dominant hill slope transport process (creep/landsliding) and (ii) the presence or absence of a threshold for run-off erosion.

The Shivkhola basin is under the humid climatic condition receiving excessive orographic monsoon rainfall, which enhances the erosion and denudation of the surface within the basin. The nature of terrain, evolution of landscape, amount of soil erosion and their removal, in the Shivkhola watershed could be well acquainted by studying various hydrological factors/attributes i.e. climatic attributes (rainfall and evaporation), drainage confluence, drainage density, upslope contributing area and others. To understand the probability or chances of landslide occurrences

phenomena to each class of all the hydrological factors responsible for slope instability, landslide potentiality index value (LPIV) is determined by means of ratio between number of landslide location to each class and total number of landslide location in the basin. So, the study of all these attributes is very much significant in analyzing the nature of slope susceptibility of the basin in term of geo-hydrology.

3.2 Climatic Attributes and Landslides

The climate of the Darjiling district is especially unique because of its position in relation to the Tibetan land mass, the wide differences in altitude, the powerful effects of the monsoon against the Himalayan barrier and the peculiar configuration of the neighboring mountains which deflects winds and affect local climate (rainfall and temperature) On account of the hilly nature of the terrain of Shivkhola watershed, there are sharp variations in rainfall even between nearby sections of the mountain ranges. The precipitation during south west monsoon constitutes about 80 % of the annual rainfall, July being the wettest month. The variation in the total rainfall from year to year is not much. On an average, there are about 120 rainy days in a year. Temperature generally touches the highest level in May. January is the coldest month of the year. Over the northern parts of the watershed the atmosphere is highly humid throughout the year. In the north-western hilly tract the relative humidity between 90 and 95 % during the rainy season. But in the low lying tracts to the east and south-east, the relative humidity is slightly less. The driest months are March and April when the relative humidity varies between 45 and 60 % (Table 3.1). The present study involves the analysis of some basic information available either from field work or some reliable secondary sources. The climatological information are collected from Tea Research Center (Kurseong), Shiviter Tea Garden and Agriculture and Soil Conservation Office (Kurseong, Darjiling).

3.2.1 Study on Rainfall

3.2.1.1 30 Years' Monthly Average Distribution of Rainfall and Assumption of Catastrophic Rainfall (mm) Year

Drainage basin is a proper spatial scale for analyzing hydrological parameters like input of rainfall and resultant output of discharge in a systematic interactive combination with other topographic and geometric attributes (Chorley 1969; Strahler 1957). Amount of rainfall is one of the triggering factors for slope instability because it affects surface run-off, infiltration, depth of the saturated soil and thus influences soil-moisture condition. Infiltration and evapotranspiration are

Table 3.1 Meteorological observation since 2001–2010 (10 years mean)

Months	Mean max temperature	Mean mini temperature	Average rainfall for 32 years in mm (P)	Mean wind speed (m/s)	Mean % of possible sunshine	Evaporation (mm/day)	Mean dew point temperature
Jan	12.83	6.16	12.57	1.00	14	0.4	9.00
Feb	13.77	7.83	16.67	1.05	31	1.3	9.00
Mar	17.22	10.89	43.76	1.26	53	2.2	9.00
Apr	21.49	14.26	94.85	1.58	54	4.7	9.00
May	21.57	15.53	302.80	1.48	27	2.6	9.00
Jun	22.34	17.27	728.35	1.52	28	4.4	9.00
Jul	22.84	17.22	995.54	1.39	07	3.9	9.00
Aug	23.05	17.60	783.92	1.26	14	4.0	9.00
Sep	21.85	16.47	587.95	1.11	15	4.1	9.00
Oct	20.89	14.41	183.29	1.11	36	1.6	9.00
Nov	18.21	11.58	12.30	1.01	63	1.3	9.00
Dec	14.57	8.55	21.90	1.19	37	0.7	9.00

considered as the important hydrological parameters that determine slope instability. The hydrologic factors like daily rainfall threshold in connection with slope angle and regolith thickness (Gabet et al. 2004), rain fall intensity, infiltration (Schumm 1956) etc. are given due importance in the analysis of slope instability. In the Shivkhola watershed the amount of rainfall increases from the month of May and it reaches peak in July then it starts decreasing and reaches minimum in January.

Analysis of monthly average rainfall since 1979–2009 also reveals that the months of June, July, August and September are experiencing rainfall of more than (between third quartile-Q_3 and first quartile-Q_1) average. On the other hand, below average rainfall is being found mostly in the months of October, November, December, January, February and March. July and August (Table 3.2) where the values of co-efficient of variation are very low (37 and 30). These monsoon months are also characterized by the catastrophic rainfall months because of the frequent occurrences of landslide events due to few days' continuous rainfall. The picturesque slope failure took place in the Shivkhola watershed due to catastrophic rainfall in the month of July of 1985, 1989, 1992, 1993, 1998, 2002, 2003, 2004, 2006 and 2007. Rainfall induced slope failure also occurred in September 1980 and 2006, August 2007 and 2010.

Table 3.2 Statistical analysis of monthly average rainfall since, 1979–2010

Months	J	F	M	A	M	J	J	A	S	O	N	D
Mean	13	17	43	95	302	728	996	784	588	183	12	23
S.D.	23	20	48	60	173	304	364	236	170	154	18	61
C.V.	176	117	111	63	57	41	37	30	28	84	150	97

3.2.1.2 Yearly Distribution of Rainfall with 3 Years Moving Average Value and Its Relation with Landslide Events

Starkel (1972) for the first time, observed the geomorphic effects of an extreme rainfall event in the eastern Himalaya (Darjiling). Froehlich et al. (1990) investigated the same area (Darjiling Himalaya) and found that shallow slides and slumps on steep slope segments occur when 24 h rainfall reaches 130–150 mm or continuous three days rainfall totals 180–200 mm Researchers (Ghosh 1950, 2009; Nautiyal 1951, 1966; Dutta et al. 1966; Basu and Sarkar 1985; Basu and Maiti 2001; Paul 1973; Sengupta 1995; Basu and De 2003; Pal 2006; Maiti 2007; Sarkar 2011) carried out a demand oriented studies in Darjiling Himalaya and identified the role of rainfall in causing landslide occurrences phenomena. The rainfall data since 1979–2009 was collected from Selim Hill Tea Estate, Tindharia Tea Estate and Shiviter Tea Estate. Analysis of yearly average rainfall since 1979–2009 (Appendix B, Table B.1) also suggests that the year 1980, 1981, 1984, 1985, 1989, 1990, 1991, 1998, 1999, 2000, 2003, 2005, 2006 and 2007 are the year of above average rainfall (317.75 mm). The devastating landslide occurrence in the 1984 and 1985, 1987, 1988, 1999, 2000, 2003, 2005, 2006, and 2009 are associated with the preceding year increasing trend average rainfall. So, the landslide phenomena in the Shivkhola watershed are related with the cumulative effects of precipitation and the changing nature of ground-water condition.

3.2.2 Evapotranspiration

Evapotranspiration, the leakage from immediate system, regulates water balance and moisture availability. To understand the water loss from the corresponding watershed monthly evapotranspiration is calculated following Jensen et al. (1990).

The equation for well-watered grass or reference ET_0 (Penman 1963) and converted to SI units (Jensen et al. 1990) is:

$$\mathbf{T_o} = \frac{\Delta}{\Delta + \gamma}(\mathbf{R_n} - \mathbf{G}) + \frac{\gamma}{\Delta + \gamma}\mathbf{6.43}(\mathbf{1.0} + \mathbf{0.53v_2})(\mathbf{e_s} - \mathbf{e_d}) \tag{3.1}$$

where,

λET_o reference ET for a well-watered grass expressed as latent heat flux density, MJ m^{-2} day^{-1},
Δ slope of the saturation vapor pressure curve in kPa/°C,
γ psychometrics constant in kPa/°C,
R_n net radiation in MJ m^{-2} day^{-1},
G heat flux density to the soil in MJ m^{-2} day^{-1},
v_2 average wind speed at a height of 2 m in m/s,
e_s saturated vapor pressure at mean air temperature in kPa,
e_d saturated vapor pressure at mean dew point temperature also e_s × mean relative humidity).

The following equations and constants were summarized from the Jensen et al. (1990)

i. Slope of the saturation vapor pressure curve:
Values for the Δ can be obtained from,

$$\Delta = 0.20(0.00738\mathrm{T} + 0.8072)^{7} - 0.000116 \tag{3.2}$$

where,
T temperature in °C.

ii. Determination of the psychrometric constant (in kPa/°C):

$$\gamma = 0.00163\, P/\lambda \tag{3.3}$$

iii. Determination of estimated atmospheric pressure:

$$\mathrm{P} = 101.3 - 0.01055\,(\mathrm{EL}) \tag{3.4}$$

iv. Determination of the latent heat of vaporization:

$$\lambda = 2.501 - 0.002361\ \mathrm{T} \tag{3.5}$$

where,
P estimated atmospheric pressure in kPa,
EL elevation in m,
λ latent heat of vaporization of water in MJ/kg.

v. The Calculation of net radiation (R_n):
The net radiation (R_n) can be calculated from,

$$\mathrm{R_n} = (1-\alpha)\mathrm{R_s} - \sigma T_a^4 \left[0.34 - 0.139(\mathrm{e_d})^{0.5}\right](0.1 + 0.9\,\mathrm{n/N}) \tag{3.6}$$

where,
R_n the solar radiation received at the earth's surface in MJ m^{-2} day^{-1},
α the radiation reflection coefficient or albedo with values near 0.25 for green crops,
σ Stefan Boltzmann Constant (4.903×10^{-9} MJ m^{-2} day^{-1} $°k^{-4}$).
T_a absolute air temperature in °k (°C +273),
n/N ratio of actual to possible hours of sunshine.

vi. Determination of the mean cloudless solar radiation:
If the solar radiation is not measured, it can be obtained from

$$R_s = (0.35 + 0.61n/N)R_{so} \tag{3.7}$$

where,
R_{so} is the mean solar radiation for cloudless skies in MJ m^{-2} day^{-1} from the table made by Jensen et al. (1990).

vii. Determination of the saturation vapor pressure:
The saturation vapor pressure is calculated from the following formula,

$$e_s = 3.38639\left[(0.00738T + 0.8072)^8 - 0.00019|1.8T + 48| + 0.001316\right] \tag{3.8}$$

where,
T the mean air temperature in °C.
The Eq. 1.8 can be used to determine the e_d by substituting the mean dew point temperature for T.

3.2.3 *Relationship Between Rainfall and Evapotranspiration and Determination of Deficit and Excess Moisture Period*

Rainfall ranging between 300 and 700 mm occurs in the month of May and September. The rainfall amounting below 150 mm is considered as deficit moisture period as evapotranspiration exceeds rainfall (Appendix B, Table B.1) that occurs in January, February, March, April (pre-monsoon) and October, November and December (post-monsoon). On the other hand in the months of May, June, July, August, September and October the precipitation exceeds the evaporation and sub-surface gets saturated. This excess moisture is spatially distributed over the basin unit. The maximum concentration is observed near the source region, where overland flow and sub-surface flow are collected to initiate surface channel following Hortons' (1932, 1945) rule. The excess moisture period (July, August, and September) experiences significant run-off (Table 3.3) from the whole basin and makes the slope surface more vulnerable. Thus soil and slope instability becomes maximum at the upper catchment near Upper Paglajhora and the rational management of the excess moisture during monsoon is earnestly needed to avoid inconvenience and loss of land and property by frequent landslide there.

Table 3.3 Monthly evapotranspiration (after Penman 1963 and Jensen et al. 1990)

Month parameters	Jan	Feb	Mar	Apr	May	Jun	Jul	Aug	Sep	Oct	Nov	Dec
T (in °C)	9.50	10.80	14.06	17.88	18.45	19.81	20.03	20.33	19.16	17.65	14.90	11.56
Δ (kPa/°C)	0.08	0.09	0.11	0.14	0.14	0.15	0.15	0.16	0.15	0.13	0.11	0.09
P (kPa)	88.22	88.22	88.22	88.22	88.22	88.22	88.22	88.22	88.22	88.22	88.22	88.22
λ (MJ/kg)	2.48	2.48	2.47	2.46	2.46	2.45	2.45	2.45	2.46	2.46	2.47	2.47
γ (kPa/°C)	0.06	0.06	0.05	0.05	0.05	0.06	0.06	0.06	0.05	0.05	0.05	0.05
e_s	1.15	1.25	1.65	2.00	2.07	2.26	2.29	2.33	2.17	1.96	1.65	1.32
e_d	1.11	1.11	1.11	1.11	1.11	1.11	1.11	1.11	1.11	1.11	1.11	1.11
$\frac{\Delta}{\Delta+\gamma}$	0.57	0.60	0.69	0.74	0.74	0.71	0.71	0.73	0.75	0.72	0.69	0.64
$\frac{\gamma}{\Delta+\gamma}s$	0.43	0.40	0.31	0.26	0.26	0.29	0.29	0.27	0.25	0.28	0.31	0.36
R_{so}(MJ m^{-2} day^{-1})	18.75	22.68	26.64	29.95	31.89	32.77	32.31	30.35	27.22	23.51	19.59	17.42
R_s (MJ m^{-2} day^{-1})	8.16	12.23	17.94	20.35	16.41	17.07	12.68	13.21	12.02	13.39	14.38	10.03
R_n	4.75	6.84	9.74	11.28	9.96	10.34	8.37	8.32	7.39	7.17	6.44	4.83
λET_o (MJ m^{-2} day^{-1})	2.88	4.66	8.52	11.08	10.23	11.21	9.76	9.61	8.25	7.59	6.10	3.88
ET (in -mm)	21.74	51.36	93.89	122.12	112.74	109.81	119.51	123.56	90.92	83.64	67.22	42.76
Rainfall (mm)	12.57	16.67	43.76	94.85	302.8	728.4	995.5	783.9	587.9	183.3	12.3	21.9
Difference	−9.17	−34.69	−50.13	−27.27	190.06	618.59	875.99	660.34	496.98	99.66	−54.92	−20.86

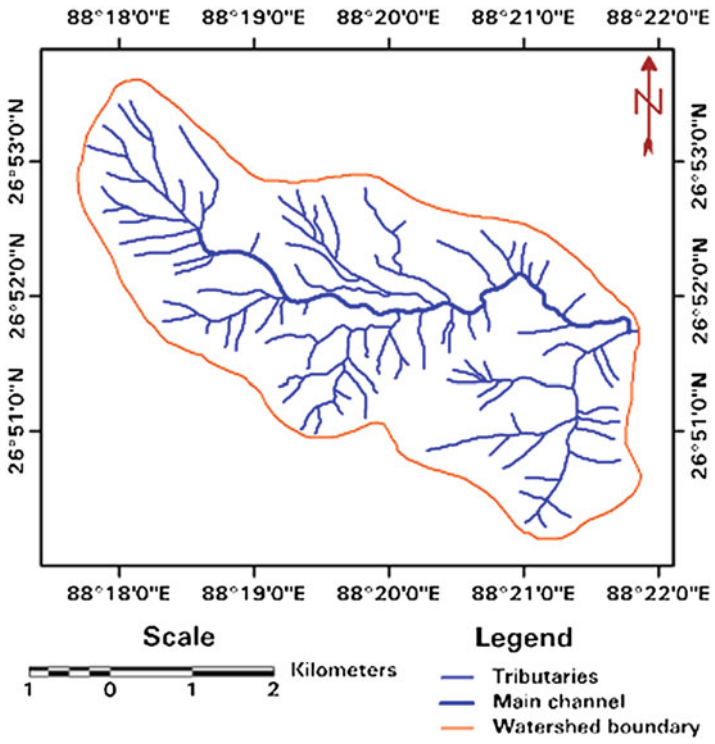

Fig. 3.1 Drainage network of 1972

3.3 Drainage Network Evolution and Landslide

3.3.1 Drainage Network Analysis of 1972

The drainage lines drawn from SOI Topographical map of 1972 reveals less drainage density and wider watershed areas of overland flow (Fig. 3.1). The possibility of head ward extension and further branching indicates potential erosion and land failure. Only few 1st order fingertip branches could reach their maximum length, allowing others to extend rapidly by head ward erosion facilitated by slope failure. This channelization is also facilitated by the human intervention along the road as the upslope drainage is concentrated on the road section and flow down slope as a collected whole. The same is true for the settlement also as the collected water from roof-top starts flowing down slope with increased energy and concentrated erosion is thus facilitated and this may initiate smaller channels and may increase gradually by either lengthening or widening.

Order wise spatial distribution of drainage network of sub-watersheds in the Shivkhola shows that maximum no. of 1st order streams (43) are found in sub-watershed 1and it also covers a large part (4.0 km^2) within this sub-watershed. Sub-

Table 3.4 Order wise spatial distribution of drainage network of sub-watersheds in Shivkhola-1972

S.no.	Order no.	No of stream segments				Total length of stream				Mean length				Area (in km^2)				Mean total area (in km^2)			
		1	2	3	4	1	2	3	4	1	2	3	4	1	2	3	4	1	2	3	4
1	4th	43	7	2	1	35.5	3.5	2.75	5.0	0.83	0.5	1.37	5.0	4.0	1.18	1.06	2.30	0.09	0.16	0.53	2.035
2	3rd	9	2	1	0	3.75	0.5	2.00	–	0.42	0.25	2.00	–	0.91	0.12	0.54	–	0.10	0.06	0.54	–
3	3rd	17	5	1	–	7.5	3.5	0.5	–	0.44	0.7	0.5	–	1.82	0.95	0.54	–	0.10	0.19	0.54	–
4	3rd	8	3	1	–	4.5	1.75	1.5	–	0.56	0.58	1.5	–	0.81	0.39	0.49	–	0.10	0.13	0.49	–
5	3rd	5	2	1	–	1.75	1.25	0.75	–	0.35	0.62	0.75	–	0.60	0.41	0.30	–	0.12	0.20	0.30	–
6	3rd	21	4	1	–	12	4.5	2	–	0.57	1.12	2.00	–	3.02	2.06	0.90	–	0.14	0.51	0.90	–

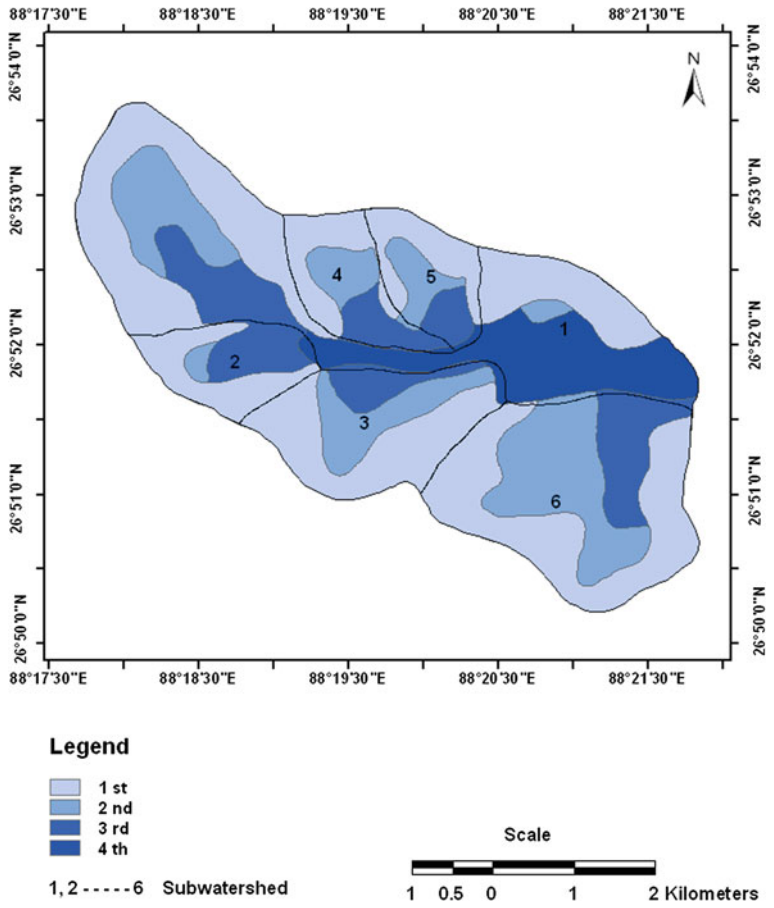

Fig. 3.2 Spatial distribution of drainage up to 4th order stream, 1972

watershed 1 ranks 2nd in terms of areal coverage. On an average most of area of sub-watershed 2, 3, 4, 5 and 6 are dominated by first order streams, followed by 2nd and 3rd orders (Table 3.4). Order wise stream network analysis of 1972 depicts that the whole basin is being mostly dominated by the impact of 1st order streams and their gradual headward extension (Fig. 3.2). The central-mid section is characterized by the cumulative effects of streams due to existence of 3rd and 4th order streams with maximum discharge.

3.3.2 Drainage Network Analysis of 1987

The drainage lines depicted in 1987 SOI (Survey of India) Topographical map, showed a further branching and extension of the channels (Fig. 3.3). The watershed

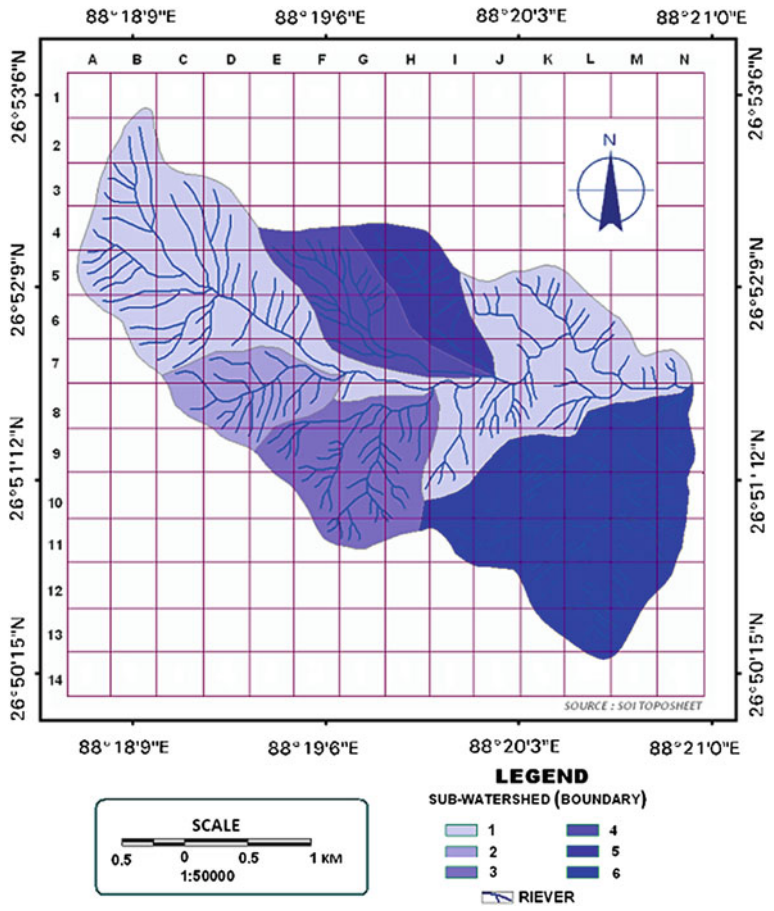

Fig. 3.3 Drainage network of 1987

areas of overland flow were reduced as the drainage was served by channelized flow and characterized by active down cutting processes over the steep slope along both sides of the main Shivkhola River. The analysis of drainage for a period during 1972–1987 revealed the extreme dynamism in the extension of the channels. The formation of numerous small channels have increased the erosion of surface and sub-surface soil as well as entraining the small soil particles and reducing the cohesive strength of the soil which could induce slope failure in near future. Because of the increased down cutting of the channels the slope surface were getting dissected and rugged gradually making some part of the region inaccessible. The interfluves are further sharpened indicating the stage of early maturity. This stage was characterized by maximum extension of slope without remarkable presence of flat surface. In such condition slope instability gets maximum attention from planners, administrators and academicians due to their frequent manifestation in slope failure.

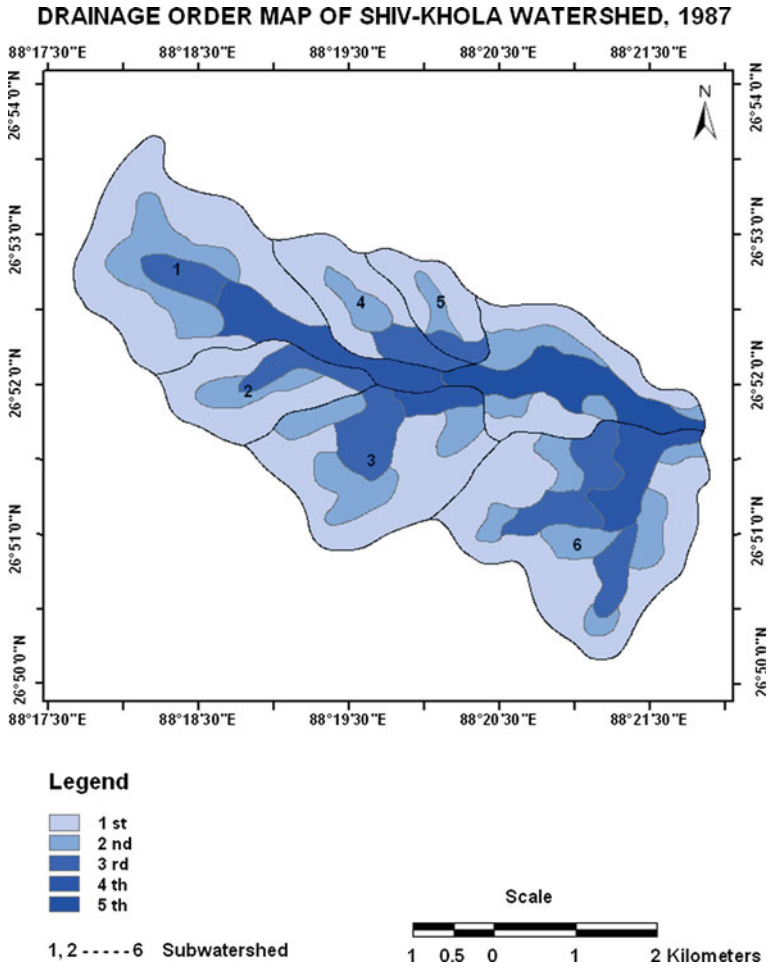

Fig. 3.4 Spatial distribution of drainage up to 5th order, 1987

Order wise spatial distribution of drainage network of sub-watersheds in the Shivkhola Watershed (1987) shows sub-watershed 6 and 1 are occupied by maximum number of 1st order streams and 4 and 5 are with minimum number of 1st order streams (Fig. 3.4). Fifth order stream is mainly found in sub-watershed 1. Sub-watershed 1 ranks 1st in terms of areal coverage which is followed by sub-watershed 6, 3, 2, 4 and 5 (Table 3.5). So, sub-watershed 1 and 6 are susceptible to soil erosion due to drainage concentration. As the drainage network of 1987 is associated with the development of first order stream over the steep marginal area and their continuous branching due to headward erosion, the first order stream

Table 3.5 Order wise spatial distribution of drainage network of sub-watersheds in Shivkhola Watershed (1987)

	Watersheds					
	1	2	3	4	5	6
No. of stream						
1st order	65	17	36	16	12	72
2nd order	18	5	7	3	2	16
3rd order	4	1	3	1	1	4
4th order	1	–	1	–	–	1
5th order	1	–	–	–	–	–
Total length of stream						
1st order	35	7.5	13	8	6	26
2nd order	8.5	1.5	4.5	2.8	1	7.3
3rd order	2.5	1.5	2.5	1.5	0.8	4.3
4th order	3.0	–	0.5	–	–	1.5
5th order	3.75	–	–	–	–	–
Mean length of stream						
1st order	0.53	0.4	0.4	0.5	0.5	0.4
2nd order	0.47	0.3	0.5	0.9	0.5	0.5
3rd order	0.63	1.5	0.8	1.5	0.8	1.1
4th order	3.00	–	0.5	–	–	1.5
5th order	3.75	–	–	–	–	–
Area in sq. km.						
1st order	3.56	0.9	1.5	1	0.7	2.4
2nd order	1.53	0.2	0.8	0.3	0.2	1.1
3rd order	0.4	0.3	0.5	0.4	0.2	1
4th order	0.94	–	0.2	–	–	0.7
5th order	1.30	–	–	–	–	–
Mean area in sq. km.						
1st order	0.06	0,05	0.04	0.06	0.06	0.03
2nd order	0.09	0.04	0.11	0.1	0.1	0.07
3rd order	0.10	0.3	0.17	0.4	0.2	0.25
4th order	0.94	–	0.2	–	–	0.7
5th order	1.30	–	–	–	–	–

covers the large part of all the sub-watershed in Shivkhola. Generally mid-section of sub-watersheds are attributed with the 2nd and 3rd order streams where the drainage concentration and maximum number of stream confluence points promotes the channel to flow with high discharge and so high rate of erosion is found in this section.

3.3.3 Drainage Concentration and Stream Confluence Point

The number of confluence points/junction points per unit area is an important index in a river basin analysis. Confluence point is a place of union of two or more streams over space which depends on the others geomorphic and geo-hydrologic attributes of the basin. It is assumed that greater number of confluence points indicate greater amount of erosion and drainage accumulation within the basin. The sub-watershed 1, 2, 3, 4, 5 and 6 are experienced with 67, 15, 32, 14, 11 and 69 confluence points respectively. On the basis of these distributed confluence point in each sub-watershed, it is inferred that the topography of sub-watershed 1 and 6 are heavily dissected followed by sub-watershed 3, 2, 4 and 5. The southern part or the right hand part of the main Shivkhola watershed (sub-watersheds-2, 3, and 6) is attributed with large number of confluence points in comparison to northern part of the basin (Fig. 3.5) mainly due to topographic configuration. The southern part is registered with dominant erosion and changing slope surface by frequent and gradual drainage convergence. It is also assumed from the drainage confluence map

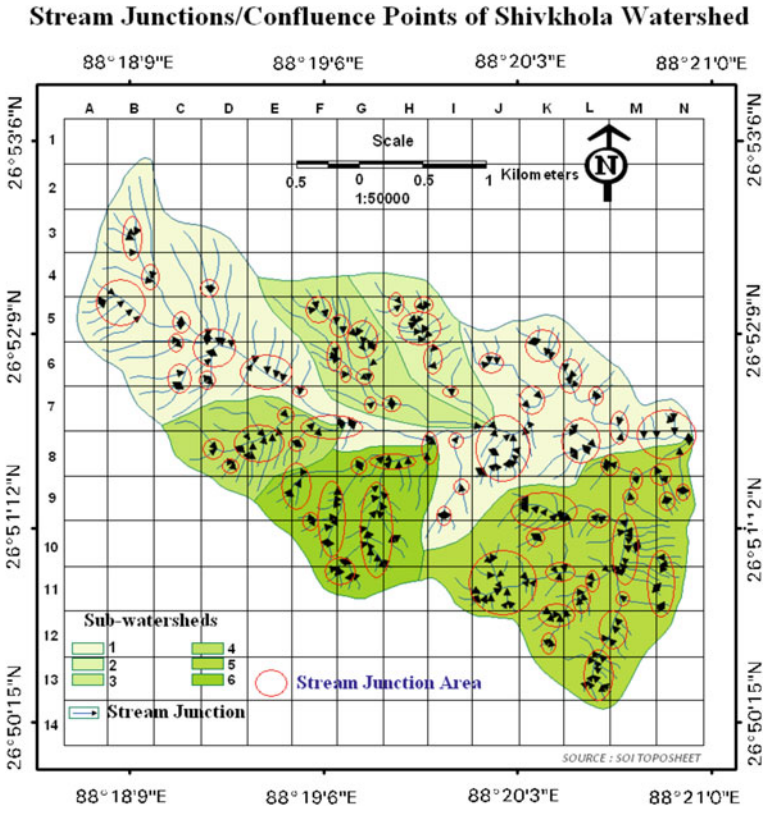

Fig. 3.5 Stream junctions points of the Shivkhola watershed

that the main stream of all the individual watersheds (sub-basins) is experiencing large no. of stream union where the valley deepening as well as valley lengthening is quite common. Such processes steepen the valley side slope and make the slope material to move downward under the influence of gravity.

3.3.4 Drainage Network Orientation

Drainage orientation is the key to understanding the way in which a drainage network fills the space that is available to it (Jarvis 1976). Drainage orientation is related to the strike and dip slopes of the underlying rocks and is very sensitive to fold axes and rock jointing. Basically, the regional slope surface and the underlying rock structure play a dominant role in changing the drainage network orientation in the Shivkhola Watershed. The interior and exterior links, length, and frequency of streams are related with the azimuth of flow direction. The main drainage line of the Shivkhola is oriented towards the south-east up to lower Paglajhora, and then it has got its course in easterly direction with sinuosity within the sub-watershed-1. The left hand two main tributaries are oriented in south-east direction through sub-watershed-4 and 5 respectively. Sub-watershed 2, 3 and 6 consist of the tributaries which are oriented in north-east direction. It is to be assumed that large part of the sub-watershed-1; 2, 3 and 6; 4 and 5 are characterized by south-east and east; north-east and south-east slope facets according to orientation of main drainage lines where the landslide potentiality is high. The study depicts that the drainage orientation plays an important role for promoting landslip as the availability of moisture content depends on it which helps to reduce cohesion and increase pore-water pressure in the soil and induces landslip.

3.3.5 Drainage Density and Landslide Potentiality

According to Horton (1945) 'Drainage density in an important indicator of the linear scale landform elements in a drainage basin'. The views of Horton (1945) and Strahler (1964) and others on drainage density are almost identical. The latter states, "in order to find out drainage density the length of the streams of all hierarchical orders should be measured, totaled up and divided by the geographical area of the drainage basin". Dury (1969) has used 'the expression of texture' and says 'in order to express the texture of dissection, we must use not the water course but the valley bottom (the thalweg), whether wet or dry'. The thalweg length divided by area is equivalent to drainage density as suggested by Horton and others.

This may be taken as the index of dissection of a drainage basin. Two areas may have identical drainage density but while one of them may have higher dissection index because of the presence of a large number of streams, the other may have lower dissection index because of the presence of small number of streams.

Drainage density is an effective indicator of slope failure as the drainage efficiency from a rainfall is determined by the drainage length in an area. The length of drainage per unit area is thus an indicator of surface flow and potential instability. The source of the drainage channels are the slide prone areas and the valley sides are also the zones of slope failure. So the potential slope failure zones are extended along the drainage lines and are concentrated at the source points. The greater drainage density is thus an indicator of potential instability. At mid-central areas, near Paglajhora, numbers of drainage channels from the upper marginal watershed region meet the main stream, and so drainage density is maximum indicating the excess surface water (Fig. 3.6). This is the main cause of slope instability at Paglajhora.

3.3.6 Upslope Contributing Area and Landslide Potentiality

Upslope Contributing Area (UCA) is an effective indicator of drainage concentration over space. The surface water accumulates in a cumulative rate away from the water divide as more Upslope Contributing Area helps in accumulation of more water and so indicates more surplus moisture and instability of slope and soil. The calculation of contributing area (Fig. 3.7) has to be made considering multiple flow direction where the cumulative flow at a point (surrogated by the upslope area) should be distributed among more than one neighboring down slope pixel (Borga et al. 1998).The topographic irregularities at concave and convex slope are responsible for the convergence and divergence of flow and thus necessitate the implication of topographic index by Quinn et al. (1991). Another concept of specific contributing area (total contributing area divided by the contour length) is computed by distributing flow from a pixel among its entire lower elevation neighbour pixel (Borga et al. 1998).

Quinn et al. (1991) proposed that Fraction of Flow (F_i) allocated to each lower neighbour is to be determined by:

$$F_i = \frac{S_i L_i}{\Sigma\, S_j L_i} \tag{3.9}$$

where the summation is for the entire lower neighbour; S is the directional slope, and L is an effective contour length that acts as the weighting factor. The value of L used here is 10 m of the pixel size of the cardinal neighbour and 14.14 m of the pixel diagonal for diagonal neighbour.

The study on Landslide Potential Index (LPI) of Upslope Contributing Area depict that the percentage of occurrence of landslides and its distribution among the different groups of contributing area shows the increasing Landslide Potential Index (LPI) with increasing value of upslope contributing area (Table 3.6). The regions of contributing area of less than 5 Km^2 experiences the LPI of 76.56 and that of 10 Km^2 experiences the LPI of 100 (Table 3.7). Figure 3.7 shows the grid wise value

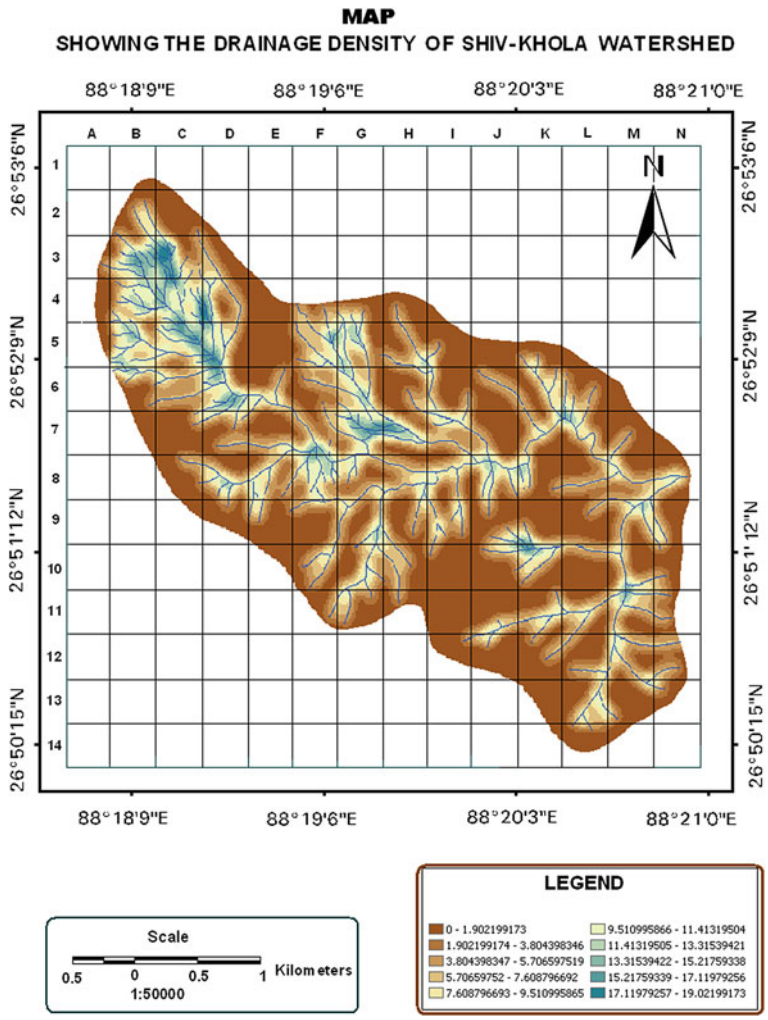

Fig. 3.6 Drainage density (km/km^2) map of the Shivkhola Watershed

of Upslope Contributing Area which gradually increases away from the water divide and the maximum of 20.98 km^2 is registered at the lower most portion of every sub-watershed. The more contributing areas are registered along the main river which experience maximum flow. Sub-watershed-I and VI are experiencing maximum upslope contributing area and maximum overland flow in the area of study. It is to be assumed that the maximum amount of soil erosion is expected in sub-watershed-I due to maximum overland flow.

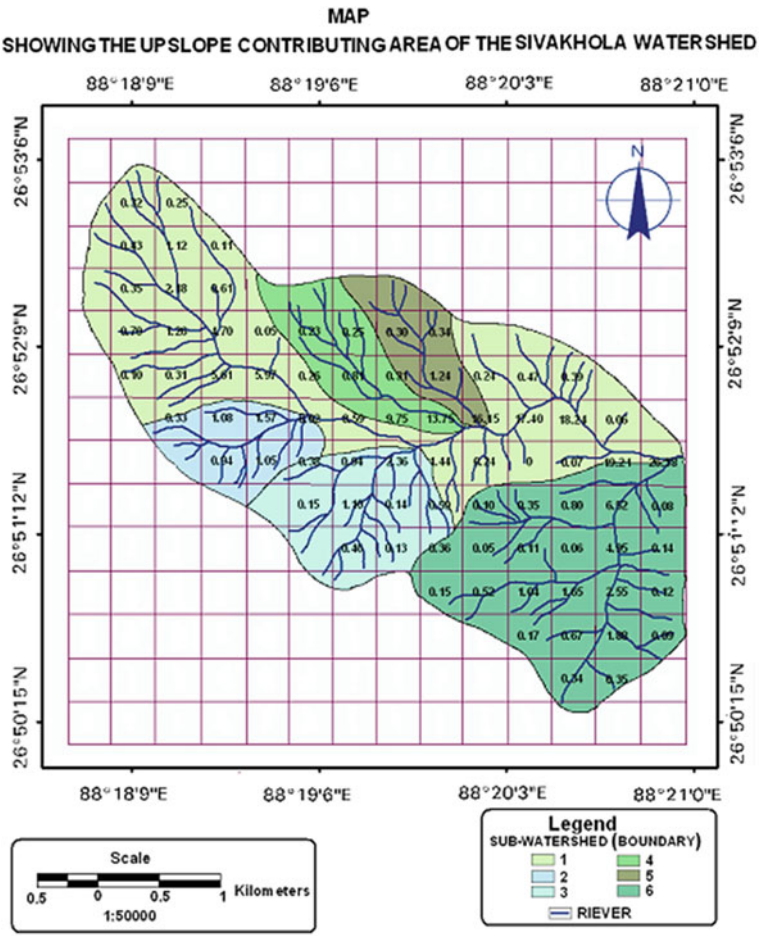

Fig. 3.7 Upslope contributing area map of Shivkhola Watershed

Table 3.6 Drainage density and landslide potentiality

Classes	Number of pixels (F1) ($N_{pix\ (Ni)}$)	% of $N_{pix\ (Ni)}$	Landslide pixels (F2) ($N_{pix(Si)}$)	% of ($N_{pix(Si)}$)	FR
0–1.90	5,560	16.78	90	2.67	0.16
1.90–3.80	5,453	16.46	109	3.23	0.20
3.80–5.71	3,289	9.93	158	4.68	0.47
5.71–7.61	5,049	15.24	137	4.06	0.27
7.61–9.51	3,477	10.49	159	4.71	0.45
9.51–11.41	2,728	8.23	465	13.78	1.67
11.41–13.31	1,875	5.66	544	16.13	2.85
13.31–15.21	2,191	6.61	542	16.07	2.43
15.21–17.12	1,942	5.86	697	20.66	3.52
17.12–19.02	1,567	4.73	572	16.96	3.58

Table 3.7 Frequency distribution and Landslide Potential Index (LPI) of upslope contributing area

Upslope contributing area (Km^2)	Number of pixels in %	Number of landslide occurrences pixels in %	Landslide occurrence ratio	Landslide potential index (LPI) = $F_2/F_1 \times 100$
<5.00	85.33	84.48	0.76	76.56
5.00–10.00	8.00	6.90	0.66	66.67
10.00–15.00	1.33	1.72	1.00	100
15.00–20.00	4.00	5.17	1.00	100
>20.00	1.33	1.72	1.00	100

3.4 Drainage Morphometry and Slope Instability

Geo-hydrologic and geometric parameters of the drainage play a significant role in changing the quality of soil and water of a small hilly sub-watershed and make the hill slope more vulnerable to slope instability. The morphometric study on river basin was first introduced by Horton (1932). Later on, this idea was developed by Miller (1953), Schumm (1956), Coates (1958), Melton (1958), Maxell (1960), Strahler (1957), Chorley (1969), and Mulder and Syvitsky (1996). During 1950s and 1960s the morphometric proposals made by Horton again were developed in the studies of drainage basin morphometry, which aimed to analyse regularities of stream networks and subsequently led to the variation in network characteristics and to investigation of statistical or topological properties of network. The hierarchical ranking of the stream in a river basin was studied by Strahler (1964). Significant contribution in various aspects of morphometric parameters have been studied by host of scientists from time to time e.g. Morisawa (1962), Gregory and Wallings (1968, 1973), Singh (1978a, b, 1981), Singh et al. (1986), and Richards (1981). Recently Chandra et al. (1984) studied watershed with the help of remote sensing method using simulation model. Quantitative geomorphology provides a systematic approach to the analysis of a complex landscape of any size and origin of the drainage basin. Some important parameters i.e. Basin Shape, Stream Length, Length of Overland Flow, Form Factor, Circularity Ratio, Elongation Ratio, Compactness Factor, Elipticity Index, Bifurcation Ratio, Relative Relief, Drainage Density, Stream Frequency, Constant of Channel Maintenance, Ruggedness Index, Dissection Index, Slope Inclination, and Upslope contributing area of the sub-watersheds have been considered to develop the priority scale.

Basin shape is referred to the shape of the outline of the drainage basin that is determined as shape of projected surface on the horizontal plane of the basin map. Mulder and Syvitsky (1996) have indicated that a majority of the rivers have elongated basins. Generally, the shape of the basin affects the flow pattern and consequently affects the surface run-off and erosional mechanism within the catchment. The basin shape may be expressed through Form Factor, proposed by Horton in 1932. The cumulative length of channel segments increases with the

channel order, it being the lowest for the first- order channels. The *law of stream length* applied in the present study revealed that the mean length of the channel segments of each of the successive orders of the shiv-khola watershed formed approximately a direct geometric series. A plot of logarithms of mean stream lengths against their respective order showed the positive exponential form of relationship between stream order and mean stream length of the different sub-basin of the siva-khola watershed. The *length of the overland flow* is the length of no channel flow from the basin perimeter to the nearest channel. It is an important independent variable affecting the quantity of water required to exceed a certain threshold of erosion. Horton (1945) and Schumm (1956) noted that the length of overland flow approximately equals half the reciprocal of drainage density. When the rainfall intensity exceeds soil infiltration capacity, the excess water flows over the land surface as overland flow.

According to Gregory and Wallings (1973) the *form factor* is the governing factor of the water courses which enter the main streams. Form factor has been introduced by Horton (1932) that shows the shape of the basin.

Form Factor defined as the ratio of the basin area to the square of the basin length using the following equation:

$$\mathrm{Rf} = \frac{\mathrm{Au}}{\mathrm{L}^2\mathrm{b}} \tag{3.10}$$

where,

A_u Basin area (km^2)
L_b Basin length (km).

If the basin is wider, the form factor will be comparatively higher, and consequently much narrower basins have low form factor values (Gregory and Wallings 1973). The calculated values of form factor of the six sub-basin for the shiv-khola watershed are 0.12, 0.40, 0.45, 0.36, 0.25 and 0.52 respectively which reveals the sub-basin-I and sub-basin-V are more elongated than other basins and that is why the erosional activities become prominent within the two sub-basin. The *circularity index*, (Rc) is expressed as the shape of the basin that was used by Miller (1953). The circularity ratio is dimensionless, whose values vary from 0 to 1. The circularity ratio obtained from the ratio of the basin area (Au) to the area of a circle (Ac) having equal perimeter as the perimeter of the drainage basin.

$$\mathrm{Rc} = \frac{\mathrm{Au}}{\mathrm{Ac}} \tag{3.11}$$

where,

Au Area of the basin
Ac Area of the circle with same perimeter as the basin.

The deviation of the values of circularity ratio from 1 shows the irregularity of the catchment. Here in case of sub-basin-I, the values of the circularity index deviates more and showing most irregularity and elongation within the whole drainage basin. Besides, sub-basin-II and IV are also indicating the lower values of circularity index and consequently revealing another two irregular segments of the Siva-khola watershed. The sub-basin III, V and VI are more regular in respect of the values of the index (values which are closer to 1). A circular basin is more likely to have a shorter lag time and a higher peak flow than an elongated basin. *Elongation Ratio* indicates how the shape of the basin deviates from a circle (Schumm 1956). It is an index to mark the shape of the drainage basin. The value of R varies from 0 (highly elongated shape to the unity (1.00) circular shape. So, the higher values of R mean more circular shape of the basin and vice versa.

Elongation ratio is defined as the ratio of the diameter of a circle which has same area as the basin to the maximum basin length.

$$R = \frac{Dc}{Lbm} \tag{3.12}$$

where,

Dc Diameter of the circle having same area as the given drainage basin
Lbm Maximum length (km).

Compactness factor of the basin is used to express the basin shape, which is indicated by the deviation of the basin area from a circle of an equal area. Compactness factor is expressed as the shape of the basin that was used by Horton and was devised by Gravelius (Gupta 1999). The compactness factor was obtained from the ratio of the perimeter of the watershed to the circumference of a circle whose area is equal to that of the drainage basin.

$$Cc = \frac{P}{\sqrt{[2]\pi A}} \tag{3.13}$$

where,

P Perimeter of the basin (km)
A Area of basin (km^2).

3.4.1 Determination of Composite Ranking Coefficient Value and Instability Rank

The form factor reveals that the sub-basin 1 and sub-basin 5 are more elongated than other basins and that is why erosional activities become prominent within these two sub-basins. The value of the circularity index for sub-watershed 1 deviates

Table 3.8 Basin geometry and composite ranking co-efficient value and instability analysis

Sub-basin	Form factor (F)	Rank	Elon-gation ratio®	Rank	Circularity index (C)	Rank	Elipticity index (E)	Rank	Compactness co-efficient (C_c)	Rank	Length of overland flow (km)	Rank	Composite rank	Instability rank
1	0.12	6	0.39	1	0.3	1	6.76	1	0.62	5	0.15	3	17	5
2	0.4	3	0.71	4	0.55	3	1.97	4	1.06	2	0.13	5.5	21.5	3
3	0.45	2	0.76	5	0.77	6	1.72	5	0.63	4	0.13	5.5	27.5	1
4	0.36	4	0.68	3	0.54	2	2.17	3	1	3	0.15	3	18	4
5	0.25	5	0.56	2	0.68	4	3.09	2	1.09	1	0.15	3	17	6
6	0.52	1	0.81	6	0.69	5	1.5	6	0.51	6	0.16	1	25	2

more from 1, showing most irregularity in shape. Besides, sub-basin 2 and 4 are also indicating the lower values of circularity index and consequently revealing another two irregular segments of the siva-khola watershed. The sub-basin 3, 5 and 6 are more regular.

The ranks were assigned to the sub-watersheds according to their forms and relative shapes in ascending order of magnitude favouring easy drainage. Sub-basin 6 was thus ranked V for maximum form factor. All the ranks for Form Factor, Elongation ratio, Circularity Ratio, Elipticity Index, Compactness Coefficient and length of overland flow were assigned accordingly and finally cumulative value were assigned as the composite ranking for drainage efficiency. Thus sub-basin 5 and 1 are more efficient in drainage followed by sub-basin 4 (Table 3.8).

3.5 Conclusion

Rainfall is the significant landslide triggering factor in the Shivkhola Watershed as most of the landslides are rain-induced. Not only that, all the recorded landslides occurred during the excess moisture period. The analysis of drainage network of 1972 and 1987 depicts that there is continuous branching of channels and these are developed through headward erosion and sharpening of interfluves between two sub-watersheds. Sub-watershed 1 and 6 are attributed with maximum number of stream, stream length, and mean area at each orders which are the indicators of more surface run-off and potential erosion and slope failure. Maximum number of stream confluence points is found in sub-watershed 1 and 6 which is followed by 3, 2, 4 and 5. The potential slope failure zones are extended along the drainage lines and concentrated at the source points. The greater drainage density is an indicator of potential instability. At the zones near Paglajhora, mid-central areas, numbers of drainage channels from the upper marginal watershed region meet the main stream. Here drainage density is maximum indicating the excess surface water. The maximum LPI is recorded within the range between 5.00 and 6.50 km/km^2 and is followed by 3.50–5.00 km/km^2 showing the effects of intensity of drainage density on slope instability. In the saucer shaped basin, the concentration of flow at the central lower portion caused the maximum density but due to gentle slope, the landslide occurrences are less. The moderate density on steeper slope caused havoc on slope instability due to cumulative effects of other triggering factors. The surface water accumulates in a cumulative rate away from the water divide as more Upslope Contributing Area (UCA) helps in accumulation of more water that indicates more surplus moisture and instability of slope and soil. Upslope Contributing Area of 20.98 km^2 is registered at the lower most portion of every sub-watershed. The more contributing areas are registered along the main river which experience maximum length and thus maximum flow. The percentage of occurrence of landslides and its distribution among the different groups of contributing area shows increasing Landslide Potentiality Index (LPI) with increasing value of upslope contributing area. The regions of upslope contributing area of less than 5 Km^2 experiences the

LPI of 76.56 and that of 10 Km^2 and more experiences the LPI of 100. The study on basin geometry states that sub-basin 1 and 5 are more efficient in drainage and more susceptible to soil erosion and slope instability.

References

Basu SR, Sarkar S (1985) Some consideration on recent landslides at Tindharia and their control. Indian J Power River Val Dev 190–194

Basu SR, Maiti RK (2001) Unscientific mining and degradation of slopes in the Darjeeling Himalayas. Chang Env Scenerio Indian Subcont (Bd) 390–399

Basu SR, De SK (2003) Causes and consequences of landslides in Darjiling-Sikkim Himalayas. India Geograph Pol 76(2):37–52

Borga M, Dalla Fontana G, Da Ros D, Marchi L (1998) Shallow landslide hazard assessment using a physically based model and digital elevation data. J Environ Geol 35(2–30):81–88

Chandra S, Sharma KP, Kashyap O (1984) Application of remote sensing methods to hydrology: watershed studies using simulation model for Upper Yamuna catchments' School of Hydrology. University of Roorkee, Roorkee

Chorley RJ (1969) The drainage basin as a fundamental geomorphic unit. In: Chorley RJ (ed) Water, earth and man. Methuen, London, pp 77–100

Coates DR (1958) Quantitative geomorphology of small drainage basins of Southern Indiana, Office of Naval Research, Geography Branch, Project NR 389-042. Technical report 10

Dury GH (1969) Hydraulic geometry. In: Chorley RJ (ed) Water, earth and man. Methuen and Co Ltd, London, pp 319–330

Dutta DE et al (1966) Landslides and erosion in Kalimpong subdivision, Darjeeling district and their bearing on North Bengal floods. Bull Geol Surv India Ser B 15(1):61–78

Froehlich W, Gil E, Kasza I, Starkel L (1990) Thresholds in the transformation of slopes and river channels in the Darjeeling Himalaya, India. Mt Res Dev 10(4):301–312

Gabet JE, Burbank WD, Putkohen KJ, Pratsituala AB, Ojha T (2004) Rainfall threshold for landsliding in the Himalayas of Nepal. Geomorphology 63(1–4):131–143

Ghosh AMN (1950) Observation of the landslides of the 11th and 12th June, 1950 in the Darjeeling Himalaya. Unpublished geological survey of India report

Ghosh S, Van Westen CJ, Carranza E, Jetten V (2009) Generation of event- based landslide inventory maps in a data-scarce environment; case study around Kurseong, Darjiling District, West Bengal, India. In: Malet JP, Remaitre A, Bogaard T (eds) Landslide processes: from geomorphologic mapping to dynamic modeling: proceedings of the landslide processes. European Centre on Geomorphological Hazards (CERG), Strasbourg, pp 37–44

Gilbert GK (1909) The convexity of hilltops. J Geol 17:344–350

Glade T (2000) Modelling landslide triggering rainfall thresholds at a range of complexities. In: Bromhead E, Dixon N, Ibsen ML (eds) Landslide in research, theory and practice. Thomas Telford, Cardiff, pp 633–640

Gregory KJ, Walling DE (1968) The variation of drainage density within a catchment. Bull Int Assoc Sci Hydrol 13:16–68

Gregory KJ, Walling DE (1973) Drainage basin form and process: a geomorphological approach. Eward Arnold, London 45 pp

Gupta SNP (1999) Morphological character of hillside slope in the Damodar baisn in Bihar. Indian Geog Stud 13:16–21. Geography Research Centre, Patna

Horton RE (1932) Drainage basin characteristics. Trans Am Geophys Union 14:350–361

Horton RK (1945) Erosional devepolment of streams and their drainage basins, hydrological approach to quantitative morphology. Geol Soc Am Bull 56:275–370

Howard AD (1997) Badland morphology and evolution: interpretation using a simulation model. Earth Surf Process Landf 22:211–227

Ijjasz-Vasquez EJ et al (1992) Sensitivity of a basin evolution model to the nature of run-off production and to initial conditions. Water Resour Res 28:2733–2741

Jarvis RS (1976) Stream orientation structures in drainage networks. J Geol 84:563–582

Jensen ME, Burman RD, Allen AG (eds) (1990) Evapotranspiration and irrigation water requirements. ASCE, New York

Kirkby MJ (1980) The stream head as a significant geomorphic threshold. In: Coates DR, Vitek JD (eds) Threshold in geomorphology. Allen and Unwin, Winchester, pp 53–73

Larson RA (1995) Slope failure in southern California: rainfall threshold, prediction and human causes. Environ Eng Geosci 1:3930401

Maiti R (2007) Identification of potential slope failure zones of shiv-khola watershed; Darjiling Himalaya, through critical analysis of slope instability—a step towards rational and scientific management of land, soil and water. UGC sponsored minor research project [F.31-210/2005 (31.03.2007)]

Maxell JC (1960) Quantitative geomorphology of the San Dimas experiment forest, California. Technical report 19, Office of Naval Research Project 389-042

Melton MA (1958) Geometric properties of mature drainage basin systems and their controlling agents. J Geol 66:442–460

Miller VC (1953) A quantitative geomorphic study of drainage basin characteristics in the Clinch mountain area, Virginia and Tenneses. Department of Geology, Columbia University, Contract N60NR271-30. Technical report 3, pp 1–30

Montgomery DR, Dietrich WE (1989) Source areas, drainage density and channel initiation. Water Resour Res 25:1907–1918

Morisawa ME (1962) Relation of quantitative geomorphology to streams flow in representative watersheds of the Appalaihian Plateau province, Department of Geology, Columbia University, ONR project technical report, vol 2, pp 389–442

Mulder T, Syvitsky JPM (1996) Climate and morphologic relationships of river implications on river loads. J Geol 104:509–523

Nautiyal SP (1951) A geological report on the hill slope stability in and around Darjeeling, WB. Unpublished report of the geological survey of India

Nautiiyal SP (1966) On the Stability of certain hill slopes in and around Darjeeling, WB. Bull Geol Surv India Ser B 15(1):31–48

Pal C (2006) Unpublished report of the investigation on the slope instability along NH-55 between Tindharia to Mahanadi. Geological Survey of India

Paul DK (1973) Evolutionary ecology. Harper and Row Publications Inc., New York, pp 1–65

Penmann HL (1963) Vegetation and hydrology. Technical communication No. 53. Commonwealth Bureau of Soils, Harpenden

Polemio M, Petrucci O (2000) Rainfall as a landslide triggering factor: an overview of recent international research. In: Bromhead E, Dixon N, Ibsen ML (eds) Landslide in research, theory and practice, proceeding of the 8th international symposium on landslides. Thomas Telford, Cardiff, pp 1219–1226

Polloni G et al (1996) Heavy rain triggered landslides in the Alba area during November 1994 flooding event in the Piemonte Region (Italy). In: Senneset K (ed) Landslide—Glissements de Terrain, vol 3. A.A. Balkema, Rotterdam, pp 1955–1960

Quinn P et al (1991) The prediction of hillslope flow paths for distributed hydrological modeling using digital terrain models. Hydrol Process 5:59–79

Richards KS (1981) General problems in morphometry. In: Goudie A (ed) Geomorphological technique. George Allen and Unwin, London, pp 26–30

Sarkar S (2011) Evolution of the Paglajhora slump valley in the Shivkhola basin, the Darjiling Himalaya, India. Geogr Pol 84(Special Issue, Part-2):117–126

Schumm SA (1956) Evolution of a drainage system and slope in badland at Perth Amboy, New Jersey. Geol Soc Am Bull 66:597–646

Sengupta CK (1995) Detailed study of geofactors in selected hazard prone stretches along the surface communication routes in parts of Darjiling and Sikkim Himalaya, Phase-I, Part-I (Rongtong-Kurseong Road Section). In: GSI (ed) Annual progress report (F.S. 1993–1994)

Singh S (1978a) Physiographic regions, landforms and erosion surfaces of Ranchi plateau. Natl Geogr 13(1):43–65

Singh S (1978b) A quantitative analysis of drainage texture of small drainage basins of the Ranchi plateau, in morphology and evolution of landforms. Geology Department, Delhi University, New Delhi

Singh S (1981) Estimation of drainage density. Natl Geogr 16(2):81–89

Singh S, Gardiner V, Ojha SS (1986) Spatial variation of drainage density in the Palamau upland. India Natl Geogr 21(1):83–99

Smith TR, Bretherton FP (1972) Stability and conservation of mass in drainage basin evolution. Water Resour Res 8:1506–1529

Starkel L (1972) The role of catastrophic rainfall in the shaping of the relief of the Lower Himalaya (Darjeeling Hills). Geogr Pol 21:103–147

Strahler AN (1957) Quantitative analysis of watershed geomorphology. Trans Am Geophys Union 38:913–920

Strahler AN (1964) Quantitative geomorphology of drainage basins and channel network. In: Chow VT (ed) Handbook of applied hydrology. McGraw Hill, New York, pp 439–476

Toll DG (2001) Rainfall induced landslides in Singapore. Proc Inst Civil Eng Geotech Eng 149:211–216

Wieczorek GK, Guzzetti F (2000) A review of rainfall thresholds for triggering landslides. Mediterranean Storms, proceedings of the EGS plinius conference, Maratea, Italy, Oct 1999, pp 407–414

Zezere JL (2000) Rainfall triggering of landslides in the area north of Lisbon (Portugal). In: Bromhead E, Dixon N, Ibsen ML (eds) Landslide in research, theory and practice, proceeding of the 8th international symposium on landslides. Thomas Telford, Cardiff, pp 1629–1634

Chapter 4
Surface Run-off, Soil Erosion and Slope Instability

Abstract The dynamic nature of a landscape results from the interaction of surface run-off with rocks and soil being guided by geo-hydrologic variables. The estimation of surface run-off and its better understanding reveals a clear idea about the degree and amount of surface erosion and slope vulnerability over the space. In this chapter Soil Conservation Service (SCS) Run-off Curve Number (CN) model proposed by United State Department of Agriculture (USDA 1972) is used to determine the surface run-off from six individual sub-watersheds for predicting the periodical spatial distribution of slope instability and soil erosion. The determined Curve Number (CN) under antecedent moisture condition-III (AMC-III) for sub-watershed I, II, III, IV, V and VI are 85.02, 73.52, 87.36, 87.76, 85.57 and 89.85 respectively. Sub-watershed I contributes maximum run-off from a rainfall of 90.5 mm (4,52,359.4 m^3) which is followed by VI, III, IV, V and II. Landslide Potentiality Index Value (LPIV) is derived for each watershed which reveals that Sub-watershed I and VI is the significant landslide prone unit of the study area. Finally, considering both run-off and LPIV an instability scale has been made which reveals that Sub-watershed VI, I and III have to be paid more attention for a proper management of land, water and soil during the months of July, August and September. All the necessary constructions, plantation and related preparedness through raising awareness and making task forces during pre-monsoon dry period are of utmost importance for managing landslip and soil erosion at Shivkhola Watershed.

4.1 Introduction

Runoff, being the most important hydrologic variable, draws the attention of hydrologists, water resource planners, local govt. etc. for water resource planning and applications. The objective mostly sought by hydrologists is the accurate and timely prediction of runoff of a given point in a drainage basin by either using a range of equation and models or direct measurement at gauging station. The stream measuring stations are more common in large river system and reservoirs where

S. Mandal and R. Maiti, *Semi-quantitative Approaches for Landslide Assessment and Prediction*, Springer Natural Hazards, DOI 10.1007/978-981-287-146-6_4

continuous monitoring generates a database of temporal variation in run-off. The gauge station at all target points are not possible to set and so, inspite of having some limitations models are to be used for estimating run-off. Run-off from a drainage basin is influenced by various climatic (type of precipitation, intensity of rainfall, duration of rainfall, areal distribution of rainfall, direction of storm movement, antecedent precipitation, evaporation and transpiration) as well as physiographic factors (land use, type of soil, area of the basin, shape of the basin, elevation, slope, orientation, type of drainage network, indirect drainage and artificial drainage). The geology or soil materials contribute to a large degree of the infiltration rate, and thus affect run-off, vegetation and the practices incident to agriculture and forestry (Schwab et al. 2002). But, it is difficult to quantify the amount of surface run-off from a drainage basin on the basis of these factors. Run-off is estimated by various methods such as (i) Empirical formula and tables (Binnie's run-off coefficients, Barlow's percentage run-off coefficients-K, Strange's Tables, Inglis and De Souza's formulae, Lacey's formula, A.N. Khosla's formula, U.P. Irrigation Department's formula, Indian Council of Agricultural Research's formulae-1971, Parker's formulae, C.C. Vermuel's formulae, I.G. Justin's formulae. J. Rodier's Coefficients-1967 and F.V. Zaleskkii U.S.S.R'S formula-1967); (ii) Estimating Losses (A.N. Khosla's relation, U.S. formula and David Lloyd's formula); (iii) Infiltration Method; (iv) Rational Methods (R.L. Gregory and C.E. Arnold's modification-1932, M. Bernard's Coefficient-1938, American Society of Civil Engineering Coefficients, W.S. Kerby formula-1959, C.F. Izzard Formula-1944 and Ben Chie Yen, Yung Yuan Shen and Ven Te Chow-USA); and (v) Unit hydrograph method and systematic unit graph method. U.P. Irrigation Research Institute Roorke (1960) developed a statistical correlation between run-off (R) and precipitation (P) in cms for Himalayan and Bundelkhand Region Rivers in Uttar Pradesh. Soil Conservation Research Demonstration and Training Centre Dehradun of ICAR (1971) analysed run-off and rainfall from 17 sub-watersheds in the Nilgiri hills and also a reliable regression equations have been reported for the estimation of nine important physiographic characters i.e. catchment perimeters in km-Lp, main stream length in km-Ls, compactness co-efficient Ce, rotundity factor $R_{F,}$ form factor $F_{F,}$ shape index $S_{I,}$ total watershed relief in m-$R_{T,}$ drainage density (km/km^2)-$D_{D,}$ and time of concentration in minutes T_C for the catchments. A rainfall-runoff modeling is developed by Singh (1988). Chow et al. (1988) also estimated surface runoff. A geomorphology based artificial neural networks (GANNs) was put forward for the estimation direct runoff over watersheds by Zhang and Govindaraju (2003). Mishra et al. (2003) presented a modified SCS-CN Method. Saragni et al. (2007) evaluated three unit hydrograph models to predict the surface runoff from a Canadian watershed. Recently, an integrated approach for estimating surface run-off using Remote Sensing and GIS in the field of hydrological research is applied by Durbude et al. (2001), Jasrotia and Singh (2006), Tripathi et al. (2002) and Zade et al. (2005).

In the present approach Remote Sensing data is used as the basic information input for computing runoff using the Soil Conservation Service (SCS) Run-off Curve Number (RCN) model proposed by United State Department of Agriculture (USDA-1972). The SCS models are mostly used in hydrology and water resource

planning of agricultural areas in the United States and other countries as well. In India an empirical model for estimation of flood discharge in Ramganga basin using Remote Sensing data was derived by Chandra and Sharma (1978). This model of SCS Curve Number is used for estimation of runoff by correlating generalized land cover with hydrologic soil groups and data is derived from the SCS table (Ragan and Jackson 1980; Tiwari et al. 1991 etc.). The SCS model is attractive because the major input parameters are defined in terms of land use and soil type. The advantage of a model having parameters defined in terms of land use or land cover is that the user can experiment with alternate forms of land development and assess the impact of that changes might have (Ragan and Jackson 1980). These models are originally developed for predicting runoff volumes from agricultural fields and small watersheds (Horn and Schwab 1963; Harrold 1957). In the present study, the evaluation of surface run-off and landslide potentiality in the basin hierarchy of the Shivkhola watershed (Fig. 4.1) will

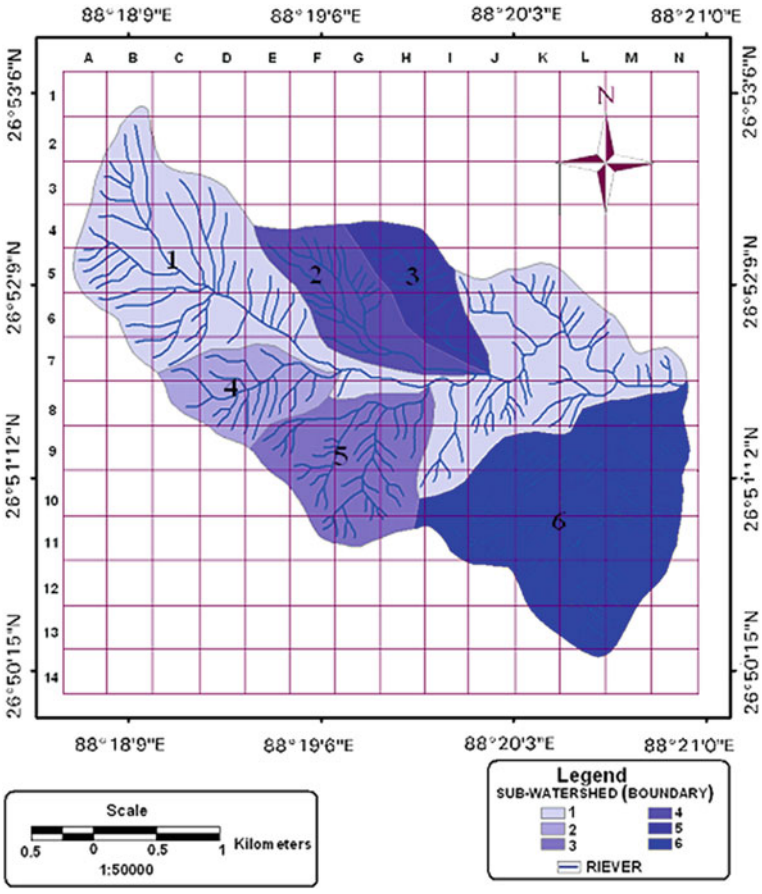

Fig. 4.1 Six sub-watersheds with drainage

help to predict the periodic slope susceptibility to soil saturation, soil erosion, and soil slip and on the basis of which we can infer a rational management procedure to reduce slope vulnerability.

4.2 Run-off Estimation

The runoff equation for small mountain watershed can be written as:

$$\mathrm{Qt} = \mathrm{f}\ (\mathrm{Pt},\ \mathrm{S},\ \mathrm{Ia}) \tag{4.1}$$

(Hand book of hydrology 1972).

Qt is the depth of runoff over the catchment during selective time period "t"
Pt is the depth of rainfall over the catchment during time period "t"
S is the potential maximum retention of water by the soil in equivalent depth over the catchment
Ia is the initial abstraction during the period between the beginnings of rainfall Pt and runoff Qt in equivalent depth over the catchment.

The relation between **S** and **Ia** is very important to understand as a part of S is retained in the soil in the form of interception, infiltration, depression storage and absorption initially in the form of Ia. Ia varies according to soil condition and Antecedent Moisture Condition (AMC) which is the existing moisture condition of soil and land and expressed as the amount of rainfall received in past 5 days.

$$Q = \frac{(P - 0.2S)^2}{(P + 0.8S)^2} \tag{4.2}$$

(Equation applicable to small hilly watershed. For a given storm 20 % (0.2S) of the potential maximum retention is the initial abstraction before runoff begins) where,

$$S = \frac{25400}{CN} - 254 \tag{4.3}$$

Q Actual direct runoff (in mm)
P Total Rainfall (in mm)
S Potential maximum retention (in mm)
CN SCS Runoff Curve Number.

4.2.1 Determination of Runoff Curve Number (RCN)

The Runoff Curve Number (RCN) is a quantitative descriptor of the land and soil complex and is commonly assigned based on information acquired from field surveys and interpretation of Aerial photograph or Satellite Imageries. The RCN of a Soil—Vegetation—Land (SVL) complex in a specific antecedent moisture condition (AMC) takes on values from 0 to 100. This number is derived from the character of the soil, vegetation, including crops and the land use of that soil as well as intensity of use. When **CN** equals to 100, **S** becomes zero (In water-logged areas or in wet paddy field). This leads to Q (Runoff) = **P** (Precipitation). In other cases, when $S \rightarrow \infty$, $\mathbf{CN} \rightarrow 0$, this gives $\mathbf{Q} = 0$.

The CN value is derived on the basis of Soil—Vegetation—Land (SVL) and Antecedent Moisture Condition complex. The soils are grouped into four types according to their hydrologic character. The land use, with respect to their hydrologic i.e. draining condition is to be analyzed with due importance. The determination of CN value requires the following data input

1. Land use—Land cover class.
2. Hydrologic Soil groups.
3. Hydrologic (Draining) condition.
4. Antecedent Moisture Condition (AMC).

4.2.1.1 Land Use and Land Treatment

Land use is the watershed cover and it includes every kind of vegetation, litter and mulch and fallow as well as non agricultural uses such as water surfaces (lakes, swamps etc.) and impervious surfaces (roads, roofs etc.). **Forest** area includes all lands classed as forest under any legal enactment dealing with forest or administered as forest whether state owned or private. **Tree crops** include woody perennial plants that reach a mature height of at least 8 ft and have well defined stems and a definite crown shape. **Plantation** is an important land use of the study area. Tea is the single plantation crop of this region and occupies a considerable section of land, and exerts a great influence on the economy and culture of the concerned society. **Open space** includes the parks, golf course, cemeteries, lawns etc. where the grass or trees cover ranges from greater than 50 % to less than 75 %. **Urban district** category reflects the commercial, business and industrial sectors of the study area where 70–85 % areas is impervious in nature. **Residential district** means the urban residential houses, either reflects the compact settlement area or the scattered houses of tea gardens, forest etc. and here 65 to 12 % area is impervious in nature. Land use and land cover map of the Shivkhola watershed is prepared with the help of LISS-III Satellite Image, Google Earth Image in consultation with Survey of India (SOI Topo-sheet. Later on, with proper ground truth verification with GPS a land use and land cover map is developed. In the present study broadly the Shivkhola

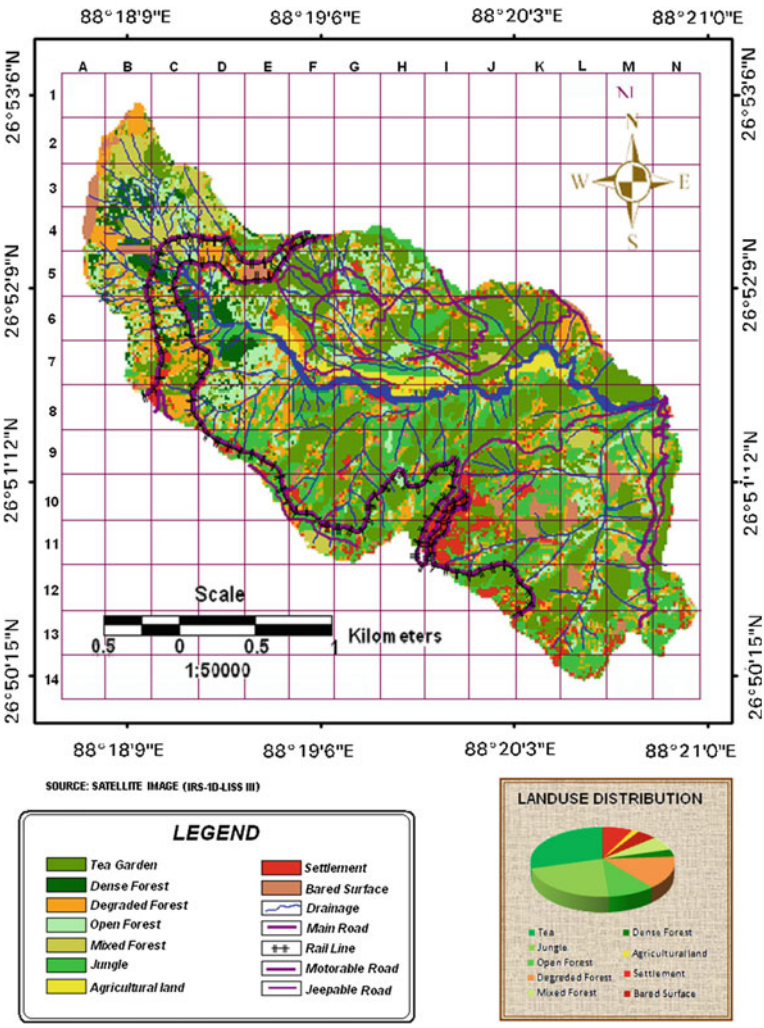

Fig. 4.2 Land use and land cover map of the Shivkhola watershed

Watershed is classified into ten individual land use pattern such as i. Bare Surface, ii. Agricultural land, iii. Jungle, iv. Roads, v. Settlement, vi. Tea garden, vii. Open forest, viii. Degraded forest, ix. Mixed forest and x. Dense forest. (Fig. 4.2). Again, hydrological soil group wise land use and land cover is attributed (Table 4.1) to extract Curve Number following Empirical Curve Number Table under different hydrological condition for each of the six sub-watersheds which the entire study area is divided into.

Table 4.1 Land use/land cover and their hydrologic conditions

Land use/land cover		Intensity and characters	Hydrologic conditions
Bared surface	Steep slope	Without any residue cover	Poor
	Gentle slope	Without any residue cover	Poor
Agricultural land		Contoured and terrace	Poor
Jungle	Upslope	50–70 % ground is covered by plant	Fair
	Down slope	<50 % ground is covered by plant	Poor
Roads	Concrete	Average 65 % area is impervious area	Poor
	Metal	Average 25 % area is impervious	Fair
Settlement	Compact	65 % average impervious area	Poor
	Disperse	25 % average impervious area	Fair
Tea garden	Upslope	More than 75 % area is covered by tea plantation	Poor
	Down slope	More than 75 % area is covered by tea plantation	Good
Open forest	Upslope	Grazed but not burned	Fair
	Down slope	Grazed but not burned	Fair
Degraded forest	Upslope	Forest and tree crops heavily grazed or burned	Poor
	Down slope	Forest and tree crops heavily grazed or burned	Poor
Mixed forest	Upslope	Wood and grass combination 50 and 50 %	Fair
	Down slope	Wood and grass combination 50 and 50 %	Good
Dense forest		>90 % ground is covered by plant	Good

4.2.1.2 Hydrologic Soil Groups

Soils are originally assigned to hydrologic soil groups based on measured rainfall, run-off, and infiltrometer data (Musgrave 1955). Most of the soil groupings are based on the premise that soils found within a climatic region that are similar in depth to a restrictive layer or water table, transmission rate of water, texture, structure, and degree of swelling when saturated, will have the similar run-off responses (National Engineering Handbook, USDA 1993). The given four hydrological soil groups are used in determining hydrologic soil cover complexes, which are used in the method for estimating runoff from rainfall. The soil properties play an important role in the estimation of runoff from the rainfall. In this concern the properties can be represented by hydrologic parameters that influence the minimum rate of infiltration obtained from a bare soil after prolonged wetting. *Hydrologic soil group-A,* having high infiltration rates and low run-off potential even when thoroughly wetted and consisting chiefly of deep, well to excessively drained sands or gravels, having high rate of water transmission (Tables 4.2 and 4.3). The USDA

Table 4.2 Infiltration rates used in hydrologic soil groupings

Class	Hydrologic soil group	Rate/hour		Remarks
		Inches	Millimeters	
Very low	D	Less than 0.1	Less than 2.5	High clayey soil
Low	C	0.1–0.5	2.5–12.5	Shallow soils, clay soils, soils low in organic matter
Medium	B	0.5–1.0	12.5–25.0	Sandy loams, silt loams
High	A	Greater than 1.0	Greater than 25.0	Deep sands well aggregated soils

Table 4.3 Permeability ratings used in hydrologic soil groupings

Group	Hydrologic soil group	Rate/hour	
		Inches	Millimeters
Very slow	D	Less than 0.05	Less than 1.30
Slow	C	0.05–0.20	1.31–5.00
Moderately slow	B and C	0.20–0.80	5.01–20.00
Moderate	B	0.80–2.50	20.01–50.00
Moderately rapid	B	2.50–5.00	50.01–130.00
Rapid	A	5.00–10.00	130.01–250.00
Very rapid	A	Greater than 10.00	Greater than 250.0

soil texture normally included in this group is sand, loamy and loamy-sand and sandy-loam. These soils have a transmission rater greater than 0.76 cm/h. Soils having moderate infiltration rates and moderately low run-off potential characterized by *Hydrologic soil group-B,* when thoroughly wetted and consisting chiefly of moderately deep to deep and moderately well to well drained soils with moderately coarse textures (Tables 4.2 and 4.3). These soils have a moderate rate of water transmission.

The USDA soil textures normally included in this group are silt-loam and loam. These soils have a transmission rate between 0.38 and 0.76 cm/h. Soils having slow infiltration rates when thoroughly wetted and consisting chiefly of moderately deep to deep and moderately well to well drained soils with moderately fine to moderately coarse textures includes *Hydrologic soil group-C* having moderately high run-off potential (Tables 4.2 and 4.3). These soils have a moderate rate of water transmission. The USDA soil textures normally included in this group is sandy clay loam. These soils have a transmission rate between 0.13 and 0.38 cm/h. Soils having very slow infiltration rates and high run-off potential when thoroughly wetted and consisting chiefly of clay soils with a high swelling potential with a permanent high water table comprising *Hydrologic soil group-D* (Tables 4.2 and 4.3). These soils have a clay pan or clay layer at or near the surface with shallow soils cover of nearly impervious material.

The USDA soil textures normally included in this group are clay loam, silt clay loam, sandy clay, silt clay and clay. These soils have a very low rate of water transmission between 0.0 and 0.13 cm/h. Some soils are classified in group D because of a high water table that creates a drainage problem; however, once these soils are effectively drained, they are placed into another group. The following parameters were used to assess run-off curve number and all these parameters are related with hydrologic soil group.

(i) **Infiltration rate**: See Table 4.2.

(ii) **Soil permeability**: These are tentatively suggested rates through saturated undisturbed areas under about 0.5 in. (12.7 mm) head of water.

(iii) **Draining parameter of the soil**: In *well drained condition* water is removed from the soil readily but not rapidly. Well drained soils are commonly intermediate in texture and moderate to rapid infiltration and permeability rate with hydrologic soil group A and B, although soils of other textural classes may also be well drained (Tables 4.2 and 4.3). In *moderately well drained situation* water is removed from the soil somewhat slowly so that the profile is wet for a small but significant part of the time. Moderately well drained soils commonly have a slowly permeable layer within or immediately beneath the solum or some combination of these conditions consisting hydrologic soil group of B and C (Table 4.3). The soil remains wet for a large part of the time in *poor drained condition*. The water table is commonly at or near the surface during a considerable part of the year.

(iv) **Effective depth of the soil**: This refers to depth of soil material that is readily penetrated by plant roots, and is important to the moisture regime of the soils. The effective depth figures are those observed during field profile examination. In case of those soils which are lying over disintegrated and weathered rock material (murrum), the total depth of such a layer has been converted into effective soil layer by assuming percent soil material in the layer. The total depth is then calculated by adding this assumed depth to overlaying thickness of soil layers.

(v) **Average clay content within the soil at various depths**: This pertains to the average clay content in the whole profile depth (Table 4.4). To derive this figure clay content of each horizon is multiplied by thickness of the horizon. Sum of all the horizons is then divided by total thickness of the profiles. Example—*Hydrologic soil group-A* have less than 10 % clay and

Table 4.4 Average clay contain according to thickness

Horizon	Thickness (cm)	Clay (%)	Avg. clay contain	
1	15	20	300	1845/75 = 24.4 %
2	20	23	460	
3	25	29	725	
4	15	24	360	
Total	75		1,845	

Hand book of Hydrology (1972)

more than 90 % sand or gravel. The saturated hydraulic conductivity of all soil layers exceeds 40.00 μm/s. The depth to water table is greater than 60 cm. *Soil group B* possesses between 10 and 20 % clay and 50–90 % sand. *Soil group C* is characterized by 20–40 % clay and less than 50 % sand. *Soil group D* consists greater than 40 % clay and less than 50 % sand.

4.2.1.3 Hydrologic Condition

Hydrologic condition indicates the effects of cover type and treatment on infiltration and runoff and is generally estimated from density of plant and residue cover on sample areas or refers to the state of vegetation growth. A poor hydrologic condition refers to pasture heavily grazed with sparse vegetation. A fair condition is for pasture moderately grazed with between half and 3/4th of the basin under plant cover i.e. the basin has 50 to 25 % plant cover. A good hydrologic condition indicates that the soil usually has a low runoff potential for the given hydrologic soil group, land cover type and treatment. Some factors to consider in estimating the effects of cover on infiltration and runoff are—i. Canopy or density of lawns, crops or other vegetation areas; ii. Amount of year-round cover; iii. Amount of grass or close seeded legumes in rotations; iv. Percent of residue cover; and v. Degree of surface roughness (Maidment 1972).

4.2.1.4 Antecedent Moisture Condition

Antecedent Moisture Condition (AMC) refers to the water content present in the soil at a given time. The AMC value is intended to reflect the effect of infiltration on both the volume and rate of runoff according to the infiltration curve (Sing 1975). The amount of rainfall in past few days reflects the condition of Antecedent Moisture and is as essential indicator of amount of initial abstraction (Ia) and percentage runoff (Table 4.5).

The Soil Conservation Service (SCS) developed three antecedent soil moisture conditions and labeled them as I, II, III. These AMCs correspond to the following soil condition:

Table 4.5 Relation between initial abstraction (Ia) and potential retention (S)

Relation between initial abstraction (Ia) and potential retention (S)	Region/soil type	Antecedent moisture condition (AMC)
Ia = 0.1S	Used in black soil region	AMC II and AMC III
Ia = 0.2S	Small hilly watershed	AMC I
Ia = 0.3S	All other regions	–

Table 4.6 Seasonal rainfall limits for the antecedent soil moisture conditions (AMC)

Condition	General description	5 days' antecedent rainfall (mm)	
		Dormant season	Growing season
I	Optimum soil condition from about lower plastic limit to wilting point	13	36
II	Average value for annual flood	13–28	36–53
III	Heavy rainfall to light rainfall and low temperature within 5 days prior to the given storm	28	53

Source Soil Conservation Service (1972)

AMC I: Soils are dry but not to the wilting point; satisfactory cultivation has taken place.
AMC II: Average condition.
AMC III: Heavy rainfall to light rainfall and low temperature have occurred within the last 5 days; Saturated soil (Table 4.6).

Initial Abstraction (**Ia**) consists mainly of interception, infiltration and surface storage, all of which occur before runoff begins. An exact determination of **Ia** is very difficult. However, for practical purpose, **Ia** can be related to S. Based on analysis of data from a large number of small watersheds, the Soil Conservation Service (1969) found **Ia** to be roughly equal to 0.2S (Table 4.4). It can also be estimated by relating to the antecedent soil-moisture index. *Potential maximum retention* (**S**) includes Ia and the infiltration occurring after runoff begins. This later infiltration is controlled by the rate of infiltration at the soil surface or by the rate of transmission in the soil profile (Hand Book of Hydrology 1972). The magnitude of '**S**' will be reduced during a successive period of storm (such as one day per week). The maximum limit of '**S**' depends on the character of soil and soil cover complex. The 'S' factor is also related with antecedent moisture condition (AMC) determined by the total rainfall in the 5 days period preceding a storm.

4.2.2 Calculation for Antecedent Moisture Condition or Cumulative Effects of Rainfall in Last Storm of the Year

4.2.2.1 Antecedent Rainfall Conditions and Curve Numbers (for Ia = 0.2S)

The rain water does not completely drains down slope as an immediate effect, but has an effect for next 5 days, on an average. So for any hydrological calculation

5 days' antecedent rainfall is considered as important to calculate its cumulative effects (Schwab et al. 2002).

The hydrological condition for the first day of a long duration storm is different to that of 5th day, even if the rainfall in each day remains same. The long time for accumulation of water to the channel is also an important factor of consideration (Handbook of Hydrology 1972). The authors studied 6 years' catastrophic average rainfall for the month of May, June, July, August. It revealed that last storm occurred in the month of September and October. July is the maximum catastrophic rainfall month for all the years. But, 5 days' antecedent average rainfall of 90.5 mm (Table 4.7) for the month of Sept' 2013 is taken into account and on the basis of which weighted curve number is converted from AMC-II to AMC-III following Schwab et al. (2002) conversion table (Table 4.8) to calculate surface run-off from the Shivkhola Watershed.

4.2.3 Estimation of Discharge (in m^3) from Individual Sub-watershed

The effectiveness of Remote sensing Data using sophisticated technique of SCS Curve Number for determining runoff and discharge of watersheds arising out of a certain rainfall is studied by Tiwari et al. (1991) and Schwab et al. (2002). In the present study the possibilities for conservation and treatment of surface water draining down the six sub watersheds are analyzed. The calculation of surface run-off from the individual sub-watersheds is associated with the following steps.

Step-I The identification and marking up of the sub-watersheds draining the water from its upslope contributing area up to the point of junction with main stream.

Step-II The division of the main basin into 6 sub-watersheds according to convenience of further calculation.

Step-III Analysis of SOI Topographical map (1987), LISS III Satellite Imagery-2002, Google Earth Image and intensive field investigation for sub-watershed wise land use classification (Tables 4.1 and 4.9).

Step-IV Determination of Curve Number under different hydrological condition for different hydrological soil group and for individual land use in AMC-II following empirical curve number table.

Step-V The Curve Number in AMC II condition for each land use category is then applied in order to estimate Weighted Curve Number (Ragan et al. 1980) for each sub watershed applying the following formula.

$$Weighted\ CN = \frac{CN_1 * A_1 + CN_2 * A_2 \ldots\ldots\ldots CN_n * A_n}{A_1 + A_2 \ldots\ldots\ldots\ldots\ldots A_n} \tag{4.4}$$

Table 4.7 Significant rainfall in post-monsoon

2007	Rain (mm)	2008	Rain (mm)	2009	Rain (mm)	2011	Rain (mm)	2012	Rain (mm)	2013	Rain (mm)
20th June	95.5	23rd May	103.5	10th June	222.72	7th June	125	3rd June	146.5	24th May	88.9
26th June	183.5	28th July	150	28th June	93.5	9th June	100	19th June	133	28th May	101.6
31st July	134.5	29th July	160	29th June	120.5	23rd June	203	7th July	175	27th June	111.7
3rd Oct	100	30th July	112.5	20th July	120	26th June	179	12th July	200.5	14th July	103.6
4th Oct	90	19th Aug	150	21st July	124.5	29th June	196.5	9th Sep	98.7	18th July	102
		31st Aug	120.5	23rd July	100	7th July	273.5	27th Sep	95.5	25th July	92.4
		17th Sep	89.5	27th July	120.5	8th July	162.5			5th Aug	114.3
		3rd Oct	130	18th Aug	145.5	21st July	146.5			25th Aug	89.4
				23rd Sep	106.2	28th July	148.5			28th Aug	102.6
						30th July	100			16th Sep	115.5
						10th Aug	191.5			25th Sep	116.3
						31st Aug	107.5			26th Sep	90.5
Days	5		8		9		12		6		12
Total	603.5		1,016		1153.42		1933.5		849.2		1228.8
Avg.	120.7		127		128.15		161.12		141.53		102.4

Table 4.8 Conversion factors from different AMC antecedent moisture condition condition

Curve number for condition II	Factor to convert curve number for condition II to	
	Condition I	Condition III
10	0.40	2.22
20	0.45	1.85
30	0.50	1.67
40	0.55	1.50
50	0.62	1.40
60	0.67	1.30
70	0.73	1.21
80	0.79	1.14
90	0.87	1.07
100	1.00	1.00

Source Schwab et al. (2002)

1, 2, …, n; Land use of different category
CN_1 Curve Number of respective land use (1)
A_1 % area under respective land use.

Step-VI The Weighted C.N. are then converted to AMC III condition (as the antecedent average rainfall corresponds to the AMC III condition) following the conversion Table No. 4.8 proposed by Schwab et al. (2002).

Step-VII The Potential Maximum Retention (S) in mm is then calculated applying the formula 4.2 (Table 4.11).

Step-VIII The estimation of actual direct run-off (Q-mm) for each sub-watershed applying the formula-2 (Table 4.11).

Step-IX The runoff is then transferred to discharge in m^3 by multiplying with sub-watershed area (Schwab 2002) (Table 4.11).

Step-X Month wise surface run-off from each sub-watershed was calculated considering 30 years' monthly average rainfall (since 1979–2009).

4.3 Relationship Between Land Use and Land Cover, Hydrological Soil Group, Curve Number (Under Average-AMC), Expected Run-off (m^3)

The analysis of land use/land covers of all sub-watersheds states that the large part of the Shivkhola watershed is covered with tea garden (4.69 km^2), open forest (3.05 km^2), jungle (3.09 km^2) settlement (2.26 km^2) and degraded forest (2.26 km^2). Dense forest, agricultural land, roads account for about 1.2, 0.36,

Table 4.9 Hydrological soil group wise land use and land cover and determined curve number (CN) under different hydrological condition for individual watersheds

Land use/land cover		Hydrological soil group	Hydrological condition	Curve number (CN)	Distribution of land uses in individual watersheds (area in km^2)					
					I	II	III	IV	V	VI
Agricultural land		B	Poor	74	0.19	0.00	0.00	0.12	0.00	0.00
Settlement	Compact	D	Poor	92	0.07	0.02	0.05	0.00	0.00	0.75
	Disperse	C	Fair	80	0.55	0.02	0.10	0.06	0.06	0.25
Concrete road	Concrete	D	Poor	92	0.48	0.11	0.18	0.12	0.00	0.32
	Metalled	C	Fair	80	0.26	0.00	0.05	0.18	0.13	0.12
Dense forest		A	Good	30	0.80	0.14	0.00	0.00	0.00	0.00
Bared Surface	Steep slope	C	Poor	91	0.15	0.00	0.02	0.03	0.03	0.23
	Gentle slope	B	Poor	85	0.04	0.00	0.00	0.00	0.00	0.18
Tea garden	Up slope	B	Poor	74	0.98	0.05	0.31	0.41	0.15	0.87
	Down slope	A	Good	62	0.37	0.07	0.30	0.08	0.30	0.24
Mixed forest	Up slope	B	Fair	76	0.62	0.01	0.06	0.03	0.05	0.06
	Down slope	A	Good	58	0.06	0.02	0.00	0.00	0.00	0.12
Degraded forest	Up slope	C	Poor	77	0.40	0.12	0.16	0.14	0.14	0.52
	Down slope	B	Poor	66	0.16	0.08	0.00	0.00	0.00	0.18
Open forest	Up slope	C	Fair	73	0.75	0.14	0.09	0.31	0.23	0.37
	Down slope	B	Fair	60	0.28	0.09	0.10	0.06	0.06	0.14
Jungle	Up slope	C	Fair	70	0.73	0.16	0.45	0.04	0.23	0.77
	Down slope	B	Poor	67	0.20	0.21	0.26	0.16	0.13	0.24

1.93 km^2 respectively and mixed forest covers 1.73 km^2. Concrete road, compact settlement, bare surface (upslope), degraded forest, tea garden (upslope), agricultural land, and down slope jungle depict the poor hydrological condition with less retention and high surface run-off. Fair and good hydrological condition is experienced in settlement, metal road, dense forest, down slope tea garden, mixed forest, open forest and jungle which encompass the hydrological soil group of C, A and B. The sub-watershed I and VI contribute maximum area of hydrological soil group C and D with poor hydrological condition. Curve Number (CN) is a descriptor of surface moisture retention and run-off which is also an expression of land use/land cover and soil characteristics. The poor hydrological condition is attributed with higher Curve Number (CN) values and maximum surface run-off. Settlement, road, bare surface, upslope degraded forest are attributed with the Curve Number (CN) of more than 76 which is an indicator of minimum retention. Dense forest, down slope jungle, mixed forest, tea garden and open forest are characterized by fair to good hydrological condition with the Curve Number (CN) value of less than 75. Dense forest, down slope tea garden, and down slope mixed forest experience good hydrological condition and minimum Curve Number (CN <65) value under hydrological soil group of A where retention is very high and run-off is very low. Curve Number (CN) value of compact settlement, concrete road, up slope bared surface are 92, 92 and 91 respectively with poor hydrological condition and provide maximum run-off (Table 4.9). The sub-watershed I and VI contribute maximum area of hydrological soil group C and D with poor hydrological condition.

Settlement, roads, bare surface, and degraded forest largely distributed in sub-watershed VI which is followed by sub-watershed III, IV, II and V. Only sub-watershed I (0.19 km^2) and IV (0.12 km^2) are experiencing agricultural land with CN value of 74. Dense forest is distributed in the sub-watershed I and II covering the area of about 0.84 and 0.14 km^2. Steep slope of the sub-watershed I and VI is dominated by tea garden that covers the area of about 0.98 and 0.87 km^2 respectively with poor hydrological condition characterized by CN value of 74. Dense forest is distributed in the Sub-watershed I and II covering the area of about 0.84 and 0.14 km^2. Steep slope of the Sub-watershed 1 and VI is mainly covered by tea gardens and that shows poor hydrological condition.

The sub-watershed I rank 1st in terms of average areal coverage of mixed forest, open forest and jungle which is followed by sub-watershed VI, III, II, V and IV. It is to be assumed that as the sub-watershed I and VI covers large upslope contributing area and are attributed with the maximum CN value, these two are the significant run-off producing units of the Shivkhola watershed (Table 4.9). Sub-watershed VI is considered as the watershed of poorest hydrological condition followed by IV, III, and V. Watershed II shows favourable hydrological condition.

4.4 Sub-watershed Wise Analysis of Curve Number (AMC-III), Potential Retention (S) and Run-off

The determined Curve Number (CN) under antecedent moisture condition-III (AMC-III) for sub-watershed I, II, III, IV, V and VI are 85.02, 73.52, 87.36, 87.76, 85.57 and 89.85 respectively. The potential retentions (Table 4.10) are very low for the sub-watershed VI (28.69 mm), IV (35.46 mm) and III (36.75 mm) which indicates that these 3 sub-watersheds are significant run-off contributors irrespective of areal coverage. In terms of surface run-off, sub-watershed-I contribute 4,52,349.40 m^3, sub-watershed-II 50,641.50 m^3, sub-watershed-III 1,90,278.00 m^3, sub-watershed-IV 1,07,109.00 m^3, sub-watershed-V 66,174.00 m^3 and sub-watershed-VI 3,48,948.30 m^3. Estimated LPIV is very high for Sub-watershed I and VI (Table 4.10). On the basis of the estimated potentialities of run-off and landslide potentiality index value (LPIV) an instability scale is made which reveals that sub-watershed I is very much prone to soil erosion and slope instability, followed by VI, IV and III. Considering the greater contributing area, sub-watershed I not only became the most contributor of the run-off of the entire Shivkhola Watershed but also became a spatial unit of high magnitude landslide potentiality. Running water on steep slope in the form of turbulent, concentrated flow or sheet wash dislodge materials from slope surface and thus deserves due importance.

4.5 Periodic (Monthly) Relationship Between Surface Run-off and Slope Susceptibility

The month wise estimated surface run-off (Table 4.11) states that the month of July experiences the higher amount of runoff and which is followed by August, June and September mainly during the rainy season. The potentiality to soil erosion, soil saturation and landslip of the sub-basin I and VI are greater because these two contribute considerable surface run-off to the Shivkhola watershed. The time span between October and March is attributed with lower amount of surface runoff throughout the watershed. This time span is called as 'the dry period' during which the potentiality to soil erosion, soil saturation and soil slip are very low, whereas that are more frequent during the wet period (July, August and September). On the basis of the surface runoff from the whole Shivkhola watershed, a year is divided into two distinct periods:—(i) less susceptible period (October–April) and (ii) more susceptible period (June–September). Thus all the required constructions and other preparedness are to be completed during less susceptible period.

Table 4.10 Calculated CN (AMC-III), retention (S) and run-off and the determination of instability rank

Sub-watershed	Weighted curve number (WCN)	Converted WCN from condition AMC-II to AMC-III	Maximum potential retention (S-mm)	Actual direct run-off (Q-mm)	Run-off (m^3)	Landslide potentiality index value (LPIV)	Instability rank
I	69.69	85.02	44.75	52.66	4,52,349.40	14.01	1
II	54.06	73.52	91.48	31.85	50,641.50	5.09	6
III	72.80	87.36	36.75	57.66	1,90,278.00	9.41	3
IV	74.69	87.76	35.46	58.53	1,07,109.00	7.36	4
V	71.13	85.57	42.83	53.80	66,174.00	6.52	5
VI	76.93	89.85	28.69	63.33	3,48,948.30	11.86	2

Table 4.11 Month wise surface run-off distribution from individual watersheds

Watershed	Parameters	Jan	Feb	Mar	Apl	May	Jun	July	Aug	Sept	Oct	Nov	Dec
I	Rainfall	12.57	16.67	43.76	94.85	302.8	728.4	995.5	783.9	587.9	183.3	12.3	21.9
	CN	85.02	85.02	85.02	85.02	85.02	85.02	85.02	85.02	85.02	85.02	85.02	85.02
	S	44.75	44.75	44.75	44.75	44.75	44.75	44.75	44.75	44.75	44.75	44.75	44.75
	Q	**0.27**	**1.14**	**15.23**	**56.48**	**255.01**	**677.32**	**943.74**	**732.64**	***537.41***	**138.74**	**0.23**	**2.91**
	Run-off	**2139**	**9793**	**130826**	**485163**	**2190535**	**5818179**	**8106727**	**6,293,378**	***4,616,352***	**1,191,777**	**1,978**	**24,997**
II	Rainfall	12.57	16.67	43.76	94.85	302.8	728.4	995.5	783.9	587.9	183.3	12.3	21.9
	CN	73.52	73.52	73.52	73.52	73.52	73.52	73.52	73.52	73.52	73.52	73.52	73.52
	S	91.48	91.48	91.48	91.48	91.48	91.48	91.48	91.48	91.48	91.48	91.48	91.48
	Q	**0.38**	**0.03**	**5.55**	**34.88**	**215.28**	**629.06**	**893.6**	**683.89**	***490.78***	**106.15**	**0.42**	**0.14**
	Run-off	**604**	**48**	**8,825**	**55,459**	**342,295**	**1,000,205**	**1,420,824**	**1,087,401**	***780,340***	**168,779**	**668**	**223**
III	Rainfall	12.57	16.67	43.76	94.85	302.8	728.4	995.5	783.9	587.9	183.3	12.3	21.9
	CN	87.36	87.36	87.36	87.36	87.36	87.36	87.36	87.36	87.36	87.36	87.36	87.36
	S	36.75	36.75	36.75	36.75	36.75	36.75	36.75	36.75	36.75	36.75	36.75	36.75
	Q	**0.65**	**1.89**	**18.12**	**61.62**	**262.77**	**668.08**	**952.72**	**741.76**	***545.99***	**145.55**	**0.59**	**4.13**
	Run-off	**2,145**	**6,237**	**59,796**	**203,346**	**867,147**	**2,204,664**	**3,143,976**	**2,447,808**	**1,801,767**	**480,315**	**1,947**	**13,629**
IV	Rainfall	12.57	16.67	43.76	94.85	302.8	728.4	995.5	783.9	587.9	183.3	12.3	21.9
	CN	87.76	87.76	87.76	87.76	87.76	87.76	87.76	87.76	87.76	87.76	87.76	87.76
	S	35.43	35.43	35.43	35.43	35.43	35.43	35.43	35.43	35.43	35.43	35.43	35.43
	Q	**0.74**	**2.04**	**18.65**	**62.52**	**264.08**	**687.54**	**954.21**	**742.93**	**547.42**	**146.72**	**0.67**	**4.37**
	Run-off	**1,354**	**3,733**	**34,129**	**114,412**	**483,266**	**1,258,198**	**1,746,204**	**1,359,562**	**1,001,779**	**268,498**	**1,226**	**7,997**
V	Rainfall	12.57	16.67	43.76	94.85	302.8	728.4	995.5	783.9	587.9	183.3	12.3	21.9
	CN	85.57	85.57	85.57	85.57	85.57	85.57	85.57	85.57	85.57	85.57	85.57	85.57
	S	42.83	42.83	42.83	42.83	42.83	42.83	42.83	42.83	42.83	42.83	42.83	42.83
	Q	**0.34**	**1.29**	**15.87**	**57.66**	**256.84**	**679.41**	**945.88**	**734.74**	**539.45**	**140.33**	**0.30**	**3.16**
	Run-off	**418**	**1,587**	**29,042**	**70,922**	**315,913**	**835,674**	**1,163,432**	**903,730**	**663,524**	**172,606**	**369**	**3886.8**

(continued)

Table 4.11 (continued)

Watershed	Parameters	Jan	Feb	Mar	Apl	May	Jun	July	Aug	Sept	Oct	Nov	Dec
VI	Rainfall	12.57	16.67	43.76	94.85	302.8	728.4	995.5	783.9	587.9	183.3	12.3	21.9
	CN	89.85	89.85	89.85	89.85	89.85	89.85	89.85	89.85	89.85	89.85	89.85	89.85
	S	28.69	28.69	28.69	28.69	28.69	28.69	28.69	28.69	28.69	28.69	28.69	28.69
	Q	**1.31**	**3.02**	**21.67**	**67.4**	**270.9**	**695.07**	**961.88**	**750.49**	**554.82**	**152.86**	**1.22**	**5.82**
	Run-off	**7,218**	**16,640**	**119,401**	**371,374**	**1,492,659**	**3,829,836**	**5,299,959**	**4,135,200**	**3,057,058**	**842,259**	**6,722**	**32,068**

CN Curve Number, *S* Potential Maximum Retention (mm), *Q* Actual direct run-off (mm), (Rainfall in mm and Run-off in m^3)

4.6 Conclusion

The Shivkhola watershed contributes significant amount of surface run-off during the catastrophic rainfall months of a year when slope surface gets saturated due to minimum retention. Area under the hydrological soil group of D and C (mainly sub-watersheds VI, I and IV) provide maximum run-off where Curve Number (CN) value is very high. The settlement areas of sub-watershed VI, concrete as well as metal roads and bare surface of sub-watershed VI and I are to be given proper attention for arresting run-off through constructing catch-water drains, proper plantation and diversion of run-off. Proper drainage from settlement area through concrete drains is to be made to protect the slope of highest priority. Upslope degraded forest of all the sub-watersheds are to be brought under thorough plantation and proper management. July and August experience pronounced run-off from all the sub-watersheds. The people should be made aware about the possible consequences of the excessive run-off during monsoon that results from either deforestation or construction. All the preparation to manage landslide through necessary constructions, plantations, preparation of task force, and detailed plan for monitoring of slope conditions are to be made during pre-monsoon period.

Immediate attention is to be paid for sub-watershed I and VI as these two are the great contributors of surface run-off and experience maximum landslide occurrences in the whole Shivkhola watershed. Some remedial measures such as plantation of first growing and rapid water holding capacity grasses over the exposed surface, construction of horizontal as well as vertical drains over large upslope contributing area which can reduce length of overland flow and can minimize the effects of maximum overland flow, and plantation along first order stream to reduce the amount of discharge are to be followed to reduce surface run-off and also to reduce soil erosion. As a whole, deforestation should be checked immediately by providing primary needs to all the poor income family those who collect forest wood for fulfilling domestic as well as commercial demand.

References

Chandra S, Sharma KP (1978) Application of remote sensing to hydrology. In: Proceedings of symposium on hydrology of rivers with small and medium catchments, Roorkee, India, vol II, pp 1–13

Chow VT, Maidment DR, Mays LW (1988) Applied hydrology. McGraw Hill, New York

Durbede DG, Purandara BK, Sharma A (2001) Estimation of surface run-off potential of a watershed in semi-arid environment-a case study. J Indian Soc Remote Sens 29(1 and 2):48–58

Handbook of Hydrology (1972) Soil conservation department. Ministry of Agriculture, New Delhi

Harrold LL (1957) Minimum water yield from small agricultural watershed. Am Geophys Union Trans 38:201–208

Horn DL, Schwab GO (1963) Evaluation of rational run-off co-efficients for small agricultural watershed. ASAE Trans 6(3):195–198, 201

Jasritia AS, Singh R (2006) Modelling un-off and soil erosion in a catchment area, using the GIS, in the Himalayan region, India. Environ Geol 51:29–37

Kerby WS (1959) Time of concentration of overland flow. Civil Eng 29:60

Maidment DR (1972) Handbook of hydrology. McGraw-Hill, New York, pp 1–75

Musgrave GW (1955) How much of the rain enters the soil? Water: U.S. Department of Agriculture Yearbook, Washington, DC, pp 151–159

Ragan MR, Jackson JT (1980) Run-off synthesis using LANDSAT and SCS models. J Hydraul Div 106:667–678

Sarangi A, Madramootoo CA, Enright P, Prasher SO (2007) Evaluation of three unit hydrograph models to predict the surface run-off from a Canadian watershed. Water Resour Manage 21:1127–1143

Schwab GO, Fangmeier DD, Elliot WJ, Frevert RK (2002) Soil and water conservation engineering, 4th edn. Wiley, New York, pp 34–35

Singh VP (1988) Hydrologic systems: rainfall-run-off modelling, vol 1. Prentice Hall, Englewood Cliffs

Tiwari KN, Pal DN (1991) Establishing SCS run-off curve number from IRS digital data base. J Indian Soc Remote Sens 19(4):24–251

Tripathi MP, Panda RK, Pradhan S, Sudhakar S (2002) Run-off modeling for small watershed using satellite data and GIS. J Indian Soc Remote Sens 30(1 and 2):39–52

U.S. Department of Agriculture, Natural Resources Conseration Service (1993) National engineering handbook, title 210-VI. Part 630, chapters 9 and 10. Washington, DC. http://directives.sc.egov.usda.gov/

U.S. Soil Conservation Service (SCS) (1972) Hydrology. Natural engineering handbook, Sect. 4. GPO, Washington, DC

Zade M, Ray SS, Dutta S, Panigrahy S (2005) Analysis of run-off pattern for all major basins of India drived using mote sensing data. Curr Sci 88(8):1301–1305

Zhang B, Govindaraju R (2003) Geomorphology based artificial neural networks (GANNs) for estimating of direct run-off over watersheds. J Hydrol 273:18–34

Chapter 5
Geomorphic Threshold and Landslide

Abstract The present study established the link between critical rainfall (c_r), critical slope angle (c_s), critical height (c_h) and landslide. The *critical rainfall* was estimated incorporating geo-technical parameters such as angle of internal friction (φ), slope angle ($\ominus$), upslope contributing area (UCA), transmissivity (T), wet soil density (p_s), and density of water (p_w). Cohesion (c), angle of internal friction (φ), unit weight of the materials (γ), and slope angle ($\ominus$) were taken into account to estimate critical slope height. The thickness of total soil (h), thickness of saturated soil (z), wet soil density (Ps), density of water (Pw), friction angle (φ) and slope steepness ($\ominus$) were considered to derive critical slope angle. Study attempted to calculate critical rain to slope failure and its return period. The temporal probability of the landslide events were estimated applying *Binomial* and *Poisson Probability Distribution Mode*l based on past landslide occurrences. The probability model suggests that occurrences of major landslides with more than 90 % certainty could be expected in every 7.5 years.

Keywords Critical slope · Critical height · Critical rainfall · Return period · Probability model

5.1 Introduction

Geomorphic threshold is significant parameters in analyzing the stability condition of particular spatial unit in a quantitative way. According to White et al. (1996) 'the minimum or maximum level of some quantity needed for a process to take place or a state to change is generally defined as threshold'. Varnes (1978) studied the role of minimum intensity and duration of rainfall to cause a landslide of shallow soil slips, debris flows, debris slides or slumps. Crozier (1997) opined a maximum threshold, beyond which there is 100 % chances of occurrences of the process at any time when the threshold value is exceeded. The most commonly investigated threshold parameters such as critical slope, critical slope height and critical rainfall

S. Mandal and R. Maiti, *Semi-quantitative Approaches for Landslide Assessment and Prediction*, Springer Natural Hazards, DOI 10.1007/978-981-287-146-6_5

(cumulative rainfall, antecedent rainfall, intensity and duration of rainfall) in relation to landslide phenomena has been attempted to identify in the present study. Starkel (1972) for the first time, observed the geomorphic effects of an extreme rainfall event in the eastern Himalaya (mainly Darjiling), India. Froehlich et al. (1990), investigated the same area and found that shallow slides and slumps on steep slope segments occured when 24 h rainfall reaches 130–150 mm or continuous 3 days rainfall totals 180–200 mm. Campbell (1975), Cotecchia (1978), Caine (1980), Innes (1983), Pomeroy (1984), Cannon and Ellen (1985), Neary and Swift (1987) Keefer et al. (1987), Cannon (1988), Kim et al. (1991), Li and Wang (1992), Ceriani et al. (1992), Larsen and Simon (1993), Wilson and Wieczoreck (1995), Wieczorek (1987, 1996), Wieczorek et al. (2000), Terlien (1997, 1998), Crosta (1998), Crozier (1999), Glade et al. (2000), Crosta and Frattini (2001), Aleotti (2004), Guzzetti et al. (2004), Gabet et al. (2004), Giannecchini (2006), Glade (1998), Zezere et al. (2005), Cardinali et al. (2006) and Dahal et al. (2006b) tried to establish rainfall-intensity thresholds for predicting the slope failure accurately. Caine (1980) first established worldwide rainfall threshold values for landslides. Montgomery and Dietrich (1994) introduced a physically based model for the topographic control on shallow landsliding in terms of geomorphic threshold. Recently Guzzetti et al. (2007) reviewed rainfall thresholds for the initiation of landslides worldwide and proposed new empirical thresholds based on the statistical analysis of the relationship between rainfall and landslide occurrences. They defined intensity-duration threshold as:

$$I = 73.90D^{-0.79} \tag{5.1}$$

where, I is the hourly rainfall intensity in millimeters (mm hr-1) and D is duration in hours.

Brunsden et al. (1981), Manandhar and Khanal (1988), Dhital et al. (1993), Upreti and Dhital (1996), Gerrard and Gardner (2000), Dhital (2003), Dahal et al. (2006a), and Dahal (2006) while other works, such as Caine and Mool (1982), Dhakal et al. (1999), De Vleeschauwer and De Smedt (2002), De Smedt (2005) focused mainly on landslide risk assessment in Himalayan terrains by analyzing physical properties of landslides and debris flows, effects of regional and local geological settings, and recommendations for environmental-friendly preventive measures.

In the Shivkhola watershed of Darjiling Himalaya, the physical processes and human actions (formation of road-cut benches and concentration of human settlement) are active on the slope in a systematic interactive combination which make the slope steeper than repose angle and thus the instability is introduced into the system. The present study attempts to identify the critical values of rainfall, slope height and slope angle beyond which there is a greater probability of slope instability. The formation of road-cut benches to develop communication network lengthens the steep slope, removes the lateral and basal support, and disturbs the soil, favours infiltration and through-flow, helping in the increase of wet soil depth. All those changes and their combined manifold after-effects help to generate

geomorphic threshold and the shear stress to increase over shear strength. Sometimes, moderate levels of rainfall for few days in the basin become more critical because of weak lithological composition. Moreover, the concentration of human settlement in Tindharia, Gayabari and Shiviter generates enormous pressure on slope materials and favours threshold values by reducing the shearing strength. The study shows that only 105.88 and 88.928 mm daily rainfall is the critical rain for initiation of slide at Tindharia and Lower Paglajhora respectively. So there is every possibility for the generation of geomorphic threshold and initiation of slide due to hydrologic factor. In this way, there is a frequent occurrence of debris slide which reduces the slope angle on landslide scar face to that of repose angle to attain temporary stability through internal feed back in a process of homeostatic adjustment.

Study involves the measurement of upslope contributing area, contour length, slope angle, transmissivity, depth of soil, depth of the saturated soil, density of water, wet soil density, unit weight of the materials, pore-water pressure, cohesion, and angle of repose for the determination of 'intrinsic threshold' (Schumm 1977a, b) condition such as critical slope angle, rainfall and slope height beyond which slope materials may undergo chemical decomposition and thereby lose its former strength and the slope may collapse without an extrinsic type of threshold being crossed. The response to threshold crossing may induce dramatic erosion and striking changes of the concerned landforms which is shaped primarily by the disturbances rather than by normal events. The recoveries of such disturbances are often a long and slow process which is mainly accomplished through Self-organized Feed Back Mechanism in the geomorphic system.

5.2 Materials and Methods

5.2.1 Angle of Internal Friction/Angle of Repose and Cohesion

The angle of repose is the angle at which the debris attains temporary stability on slope is very essential to estimate as the debris slope attains instability. The geo-technical factor like angle of repose of the debris is measured after Bloom (1991). The tangent of angle of repose of dry granular materials is slightly greater than, but approximately equals to the co-efficient of sliding friction of the material or its mass friction (φ) (Van Burkalow 1945; Bloom 1991). The cohesion and angle of internal friction is measured by tri-axial compression test (Fig. 5.1) following Mohr Stress Diagram (Fig. 5.2).

The saturated conductivity of the sail varies from 10^{-2} m s^{-1} for the soil depth less than 0.5 m–10^{-5} m s^{-1} for soil depth between 1 and 2 m (Fenti 1992). Based on these and other data (Metteotti 1996) estimated the transmissivity (T) of saturated soil to lie between 5 and 30 m^{-2} day^{-1}, with a mean value of 15 m^{-2} day^{-1}.

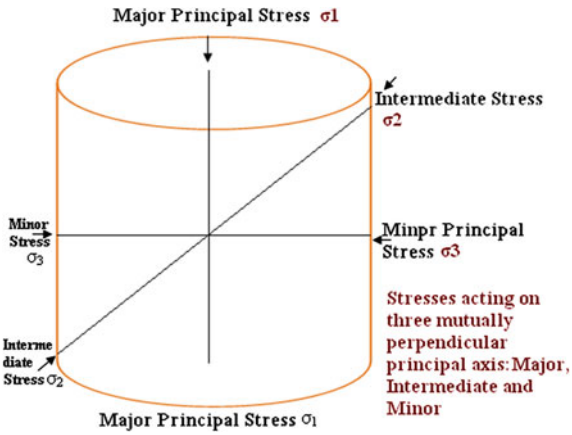

Fig. 5.1 Tri-axial soil testing mechanism

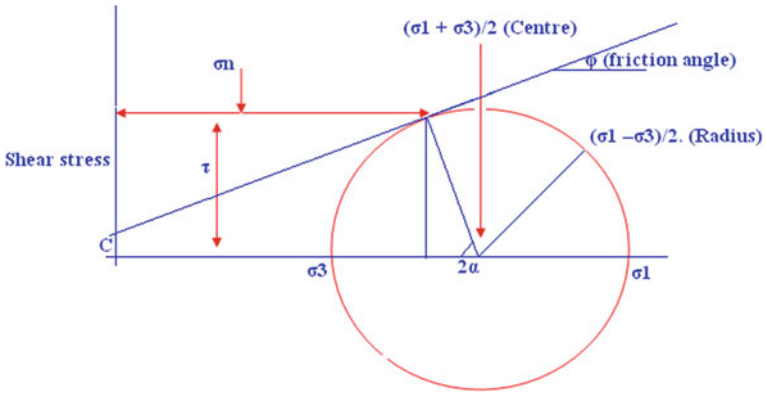

Fig. 5.2 Mohr stress diagram

The upslope contributing area (b) was estimated considering multiple flow direction where the cumulative flow at a point (surrogated by the upslope area) should be distributed among more than one neighboring down slope pixel (Borga et al. 1998).

5.2.2 *Determination of Threshold Slope Angle for Initiation of Slide*

The formation of road-cut benches introduces the steep back slope and the slope on the landslide scar is greater than the angle of repose. This situation is mainly responsible for instability. The stability equation for a mass of loose, friable cohesion less debris after (Melnikov and Chensokov 1969) is as following.

$$Safety\ Factor = \frac{Shear\ Stress}{Shear\ Strength} = \frac{W.cos\,\theta\ tan\,\varphi}{W.sin\,\theta} \geq 1 \tag{5.2}$$

tan φ	Co-efficient of friction
φ	Angle of repose
W	Weight of soil
θ	Slope on scar face.

$$or, \frac{tan\,\varphi}{tan\,\theta} \geq 1 \tag{5.3}$$

$$or, tan\,\varphi\ \geq\ tan\,\theta \tag{5.4}$$

i.e. (Angle of repose/Angle of internal friction) ≥ (Slope on scar face).

In the present study the slope angle of Tindharia and Lower Paglajhora area is 53°20′ and 48°20′ which always outweighs the angle of repose. The other indefinite slope stability model for cohesion less material and slope parallel seepage after (Borga et al. 1998) also supports the Eq. (5.5).

$$\frac{h}{z} = \frac{P_s}{P_w}\left(1 - \frac{tan\,\theta}{tan\,\varphi}\right) \geq 1 \tag{5.5}$$

H	Thickness of total soil
Z	Thickness of saturated soil
Ps	Wet soil density
Pw	Density of water
φ	Angle of repose
θ	Slope on scar face.

For maintaining the stability 'h' is needed to be greater than 'z' and $\left(1 - \frac{tan\,\theta}{tan\,\varphi}\right)$ should be positive (Table 5.1).

$$\text{So}\left(1 - \frac{tan\,\theta}{tan\,\varphi}\right) \tag{5.6}$$

$$or, \left(1 \geq \frac{tan\,\theta}{tan\,\varphi}\right) \tag{5.7}$$

$$or,\ tan\,\varphi\ \geq\ tan\,\theta \tag{5.8}$$

$$or,\ \varphi\ \geq\ \theta \tag{5.9}$$

(Angle of repose) ≥ (Slope on scar face)

Table 5.1 Calculation of threshold angle

Melnikov and Chensokov (1969)	Borga et al. (1998)	Carson (1977a, b, c)
(W cos θ tan φ)/W sin θ > 1 or, $\varphi \geq \theta$ (Dry condition) tan φ = Co-efficient of friction φ = Angle of repose W = Weight of soil θ = Slope on scar face	$\frac{h}{z} = \frac{P_s}{P_w}\left(1 - \frac{\tan\theta}{\tan\varphi}\right) \geq 1$ (Dry condition) h—Thickness of total soil z—Thickness of saturated soil Ps—Wet soil density Pw—density of water φ—Angle of repose θ—Slope on scar face	tan α = (1-u/γz $\cos^2$ α) tan φ) (Introducing pore water pressure in saturated condition) α = Threshold angle of failure u = Pore water pressure on potential sliding surface z = Depth of potential shear plane γ = Bulk unit weight of the sliding materials u = γ_w z $\cos^2$ α) (γ_w = Unit weight of soil water) Cohesion is ignored in the long term due to weathering and unloading processes u = 133.75 g/cm^2

5.2.3 Determination of Threshold Rainfall to Initiate Slide

Campbell (1975), Caine (1980), Larsen and Simon (1993) established that the empirical threshold condition to initiate landslide refers to relational value based on statistical analysis of the relationship between rainfall and landslide occurrences where as the physical thresholds are usually determined with the help of hydrologic and stability models that take into consideration of various attributes such as slope (b), upslope contributing area (a), transmissivity (T), wet soil density (p_s), density of water (p_w), slope angle (θ), angle of internal friction (φ), relation between rainfall and pore-water pressure etc. In the absolutely unstable condition the role of rainwater to initiate the threshold for sliding could be determined. If the hydrological factors like rain fall and seepage flow are considered the threshold condition for absolute instability can be predicted. The critical rainfall was derived (cr) after Borga et al. (1998) (Eq. 5.10).

$$r_{cr} = T.sin\,\theta \frac{b.p_s}{ap_w}\left(1 - \frac{tan\,\theta}{tan\,\varphi}\right) \tag{5.10}$$

5.2.3.1 Estimation of Average Catastrophic Rainfall to Obtain Return Period and Probabilistic Recurrence Interval of the Critical Rain

The Selim Hill Tea Estate situated 250 m North West of Tindharia registered 52 days having more than the critical rain fall to initiate threshold condition during the years 2005–2010 (Table E.1, Appendix E). Average day wise rainfall for catastrophic days in 2005, 2006, 2007, 2008, 2009, and 2010, are 120.7, 127, 128.5, 161.12, 141.53

and 102.4 mm respectively which are greater than the estimated threshold rainfall for initiating slide at Tindharia and Lower Paglajhora. This indicates high possibility of frequent slide in those places.

5.2.4 Threshold Slope Height to Initiate Slide

(Skempton and Hutchinson 1969) in their experience in the development of steep slope and its evolution through slides in the glacial till of County Durham found a critical slope height of 45 m at 30–35° steepness. Terzaghi (1962) calculated the critical slope height of the cliff at which failure occurs. In the present study critical height for slope failure is determined after Culmann (1866) and Carson (1977a, b, c).

$$Critical\ slope\ height\ (h_c) = \frac{4c}{\gamma} * \frac{sin\,\theta.cos\,\varphi}{1 - cos(\theta - \varphi)} \tag{5.11}$$

(Culmann 1866; Carson 1977a, b, c)

h_c Critical (threshold) slope height
$c^{/}$ Cohesion
φ Angle of internal friction
γ Unit weight of materials
θ Slope angle.

$$Critical\ slope\ height\ (h_c) = \frac{Sc}{W} \tag{5.12}$$

(Terzaghi 1962)

Hc slope height of the cliff at which failure occurs
Sc Compressive strength of the rocks
W Unit weight of the rocks.

5.2.5 Application of the 'Poisson' and 'Binomial' Probability Distribution Models to Estimate the Temporal Probability of Landslide Events

The frequent occurrence of landslides in the unstable terrain of Skivkhola watershed and their continuous monitoring through intensive field investigation and in consultation with others research works made by Starkel (1972), Basu and Sarkar (1985, 1988), Basu and Maiti (2001), Maiti (2007a, b), Ghosh et al. (2009), Sarkar (2011) and author himself have provided most reliable earlier landslide frequency

data since 1968 (Table D.1, See Appendix D). To determine the temporal probability of rain-induced landslide events the exceedance probability of one or more landslides were attempted by considering the landslide as random point events. Two major discrete probability distribution models such as the 'Poisson distribution' and the 'Binomial distribution' were mostly applied to calculate the exceedance probability of landslide (Coe et al. 2004; Crovelli 2000). According to *'Poisson distribution model'* the occurrences of landslide events that is experiencing 'n' landslides during the time 't' could be expressed by:

$$\mathrm{P}[\mathbf{N_L}(t) > = n] = e^{(-\lambda t)} * \frac{(\lambda \mathrm{t})^n}{n!} \tag{5.13}$$

where, λ = average rate of landslide occurrence.

n = 0, 1, 2, 3, … n.

So, the exceedance probability or the probability of experiencing landslide events during the time 't' could be expressed as

$$\mathbf{P}[\mathbf{N}_L(t) > = 1] = 1 - P[N_L(t) = 0] = 1 - e^{-\lambda t} = 1 - e^{\frac{t}{\mu}} \tag{5.14}$$

where, $\mu = \frac{1}{\lambda}$ and μ = mean recurrence interval between successive landslide events.

In the same way, the exceedance probability could be assessed by using the *binomial probability distribution model* with the help of following expression.

$$\mathbf{P}[\mathbf{N}_L(t) > = 1] = \mathbf{1} - P[NL(t) = 0] = 1 - (1 - P)^t = 1 - \left(1 - \frac{1}{\mu}\right)^t \tag{5.15}$$

To estimate the temporal probability of the landslide events in the Shivkhola watershed, the mean recurrence interval of known landslide event years was deduced that is 2.75 (16 known events year in 44 years). In the same way, mean recurrence interval of known major landslide events was also deduced that is 3.66 (12 major events year in 44 years). Then, both Poisson and Binomial distribution models were being applied to determine the *exceedance probability*.

5.3 Result and Discussion

5.3.1 Geo-technical Properties and Critical Slope Angle

The investigation with the temporal change in the slide scar reveals that the slope evolution is subjected to a complex interaction between physical and anthropogenic processes. The human actions in various developmental activities lead to the development of geomorphic threshold in the form of slope steepness, slope height and threshold rainfall.

Table 5.2 Calculated geotechnical parameters of two major landslide locations

Sl.No.	Parameters	Lower paglajhora	Tindharia
1	Major principal stress (kg/cm^2)	1.83	2.553
2	Minor principal stress (kg/cm^2)	0.76	0.92
3	Normal stress (kg/cm^2)	1.10	1.4044
4	Angle of rupture (Degree)	35°30′	33°
5	Angle of internal friction (Degree)	21°	24°
6	Cohesion (kg/cm^2)	0.06	0.06
7	Shear strength (kg/cm^2)	0.5	0.73

The derived geo-technical parameters of two major landslide locations show more or less identical results (Table 5.2). The thickness of the soil and that of the saturated soil during monsoon are measured to be 4.5 m (Tindharia T.E.) and 7.25 m (Lower Paglajhora). The wet soil buck density is measured to be 1.96 g/cc and density of water is 1.07 g/cc. The angle of internal friction varies from 21° to 26° with an average of 24°.

In the present study the angle of repose in sun dry condition for the concerned material varies from 21–26°. The basic requirement for the short term stability of the slope at marginal escarpment of Tindharia and Lower Paglajhora are to maintain the slope angle to be nearer or less than 21° (Table 5.3). A steep slope will decline by slope failure to an angle of repose slope to attain short term stability. This concept leads to the concept of limiting or Threshold slope angle. It is clearly observed from the Fig. 5.3 that middle section, extreme lower most part, Sepoydhura and some northern marginal parts are registering the slope angle of less than 24°. Large parts of Tindharia, Gayabari, 14 Miles Bustee, Lower Paglajhora and Shiviter are facing the slope angle of more than 24° and also are considered as the most vulnerable part of the Shivkhola Watershed. Hill Cart Road is passing through the escarpment slope which is greater than threshold slope (55–67°) and also exhibiting as very high landslide prone section of the watershed. Analysis also reveals that more than 60 % area of the Shivkhola watershed experiences above threshold slope angle of 24° (Figs. 5.3 and 5.4). In the Shivkhola Watershed high to very high landslide hazard risk is being found at the place with slope angle between 24° and 40°. Low to moderate level of risk is observed in the area pertaining to the slope angle of less than 24°. It could be demonstrated that 50 % area of the Shivkhola basin is dominated by the high intensity of landslide with a slope more than 24°.

Table 5.3 Threshold slope angle

Methods	Melnikov and Chensokov (1969)	Borga et al. (1998)	Carson (1977a, b, c)
Threshold slope angle	θ = 21–26°	θ = 21–26°	α = 9°51′ (Considering pore water pressure)

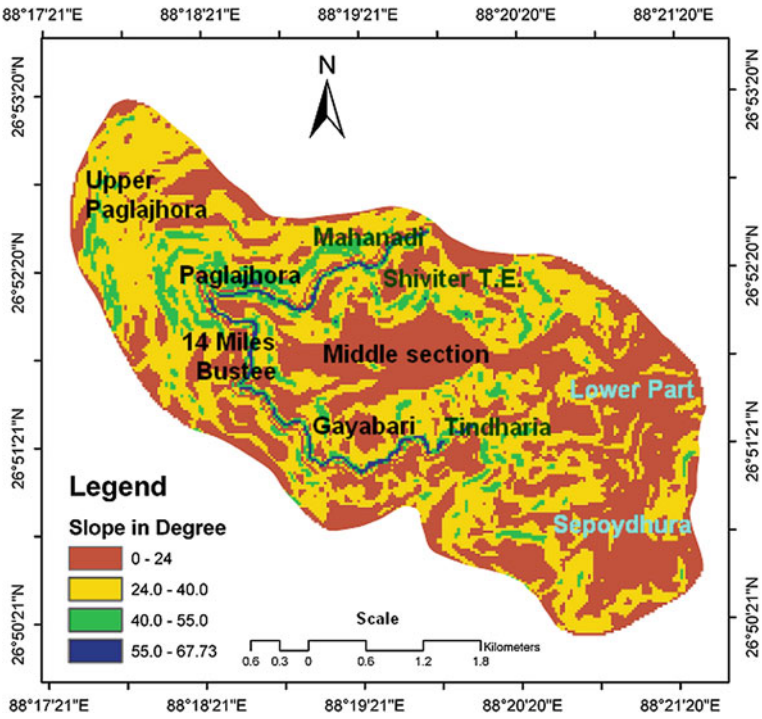

Fig. 5.3 Areal coverage of below and above of threshold slope angle (24°)

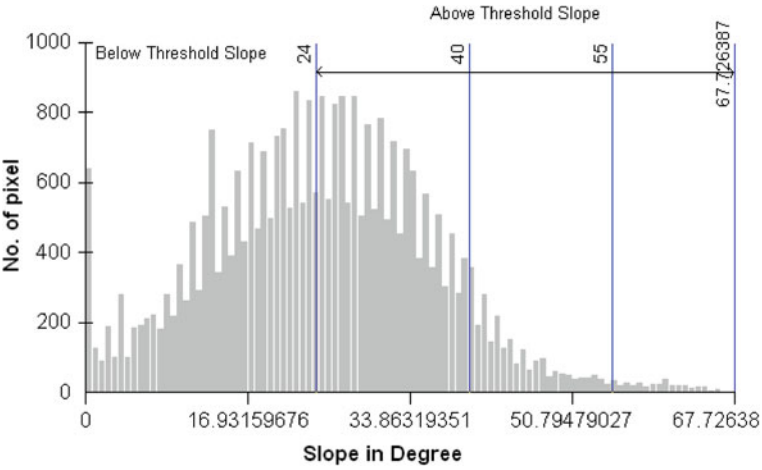

Fig. 5.4 Pixel wise distribution of slope angle

5.3.2 Calculated Critical Rainfall to Initiate Debris Slide

The calculated critical rainfall (Table 5.4) of two major landslide prone parts of the Shivkhola watershed is 105.88 mm/day (Tindharia T.E.) and 88.93 mm/day (Lower Paglajhora).

5.3.2.1 Return Period of Rainfall

The return period of the total of the catastrophic rainfall and average daily rain of catastrophic days was calculated on the basis of the rainfall data during 2001–2006 following Gumbel (1954) (Table 5.5).

$$T = (N + 1)/m \tag{5.16}$$

T Return period
N No of years
m Rank in ascending order

(Gumbel 1954)

5.3.2.2 Probabilistic Recurrence Interval of Rainfall

The calculation of recurrence interval of the total of the catastrophic rainfall and average daily catastrophic rain of days recording more than the calculated threshold rain is done by log probability law following Chow (1951), (1954) and Schwab et al. (2002).

$$Xc = x\ (1 + CvK) \tag{5.17}$$

Xc Calculated rainfall
X mean value
Cv Coefficient of variation
K Log probability Frequency Factor (calculated from the table of Chow 1954).

The daily average catastrophic rain (more than the calculated threshold) that can be experienced at a recurrence interval of 20 years (with 5 % probability) is 164.97 mm and that at a recurrence interval of 5 years (with 20 % probability) is 131.793 mm (Table 5.6).

The calculation shows that 105.88 and 88.928 mm daily rainfall is the threshold rain for Tindharia and Paglajhora respectively and the analysis of return period shows that 120.7 mm daily rainfall can occur at a recurrence interval of 1.4 years

Table 5.4 Critical rainfall (mm/day) for setting instability (Borga et al. 1998)

Location	Transmissivity (T) (m^{-2} day^{-1})	Slope (θ)	Contour length (m)	Run-off area	Wet soil density (g/cc)	Density of water (g/cc)	Friction angle (°)	Critical rainfall
Lower Paglajhora	15	48°20′	22.00	968	1.96	1.96	21	88.928
Tindharia T.E.	15	53°20′	27.00	1404	1.96	1.96	21	105.88

Table 5.5 Return period of catastrophic rainfalls after Gumbel (1954)

Year	No of days of catastrophic rainfall	Total of the catastrophic rainfall	Arranged in descending order	Rank	T = (N + 1)/m (Gumbel (1954))	Average daily rain	Arranged in descending order	Rank	T = (N + 1)/m (Gumbel (1954))
2001	5	603.5	1933.5	1	7	120.7	161.12	1	7
2002	8	1016	1228.8	2	3.5	127	141.53	2	3.5
2003	9	1153.42	1153.42	3	2.33	128.15	128.15	3	2.33
2004	12	1933.5	1016	4	1.75	161.12	127	4	1.75
2005	6	849.2	849.2	5	1.4	141.53	120.7	5	1.4
2006	12	1228.8	603.5	6	1.16	102.4	102.4	6	1.16
Mean			1130.7367			130.1500			
[a]S.D.			452.7617			19.8087			
[b]C. V.			0.4000415			0.152199			

[a] *S.D.* Standard Deviation
[b] *C.V.* Coefficient of Variation

Table 5.6 Amount of rain fall at certain probability and with specific return period (after Chow 1951, 1954)

P %	T (Years)	K	Xc (mm)
99	1.01	−2.001	90.539
50	2	−0.083	128.507
20	5	0.083	131.793
5	20	1.759	164.971
1	100	2.669	182.985

following Gumbel (1954) and 128.507 mm daily rain has a recurrence interval of 2 years with 50 % probability following Chow (1951), (1954). That means there is every possibility for the generation of geomorphic threshold for initiation of slide due to hydrologic factor. At Paglajhora the critical rainfall is 88.93 mm which is less than the estimated rainfall of 90.54 mm at the recurrence interval of 1.01 year with 99 % probability. So it can be inferred that Paglajhora is a place of higher probability of rainfall triggering landslide phenomena in every rainy season (Maiti 2007a, b).

5.3.2.3 Relationship Between Major Landslide Events and Triggering Antecedent Rainfall in the Shivkhola Watershed (Based on July Rainfall)

A relationship between antecedent cumulative rainfall and landslide events of 1993, 1998, 2003, 2007 and 2010 was established on the basis of the data recorded from earlier research works done by Ghosh et al. (2009b) and the collection of rainfall data from nearby Selim Hill Tea Estate by author himself. Only two days antecedent cumulative rainfall of 211.3 mm invited the slope failure at several places of Tindharia and Gayabari and Mahanadi (Table 5.7) in 1993. The 1998 landslide event took place due to 300–600 mm cumulative rainfall in the past 2/3 days. The 2 days' antecedent cumulative rainfall of 390 mm was responsible for 1998 landslide events. The major event of 2003 happened due to incessant rainfall of 500 mm in 2 days. 17 and 18th July, 2007 received rainfall of 124.5 and 100 mm respectively. These 2 days' antecedent cumulative rainfall of 224.5 mm caused havoc slope failure at Tindharia and Upper and Lower Paglajhora. Again 2007 faced landslide events on 8th September when 6, 7 and 8th September's antecedent cumulative rainfall amount was 275 mm.

In 2010, major and prominent landslide events happened as a result of 5 days' rainfall of 345 mm at 14 Mile near lower Paglajhora, Nurbong, Gitingia, and Shiviter. Antecedent Cumulative rainfall induced landslide analysis shows that the continuous and uniform rate of minimum amount of rainfall (approx. less than 80 mm/day) for few consecutive days can cross the geomorphic threshold and can introduce slope instability condition.

Table 5.7 Major landslide events and antecedent cumulative rainfall

Landslide events location	1 day	2 day	3 day	4 day	5 day
Tindharia and gayabari and mahanadi	110 mm	211.3 mm	265 mm	305 mm	340 mm
	2nd July, 1993	3rd July, 1993 (Landslide)			
Chunabhati, tidharia, paglajhora, mahanadi (along NH-55), jogmaya	150	390	450	485	520
	6th July, 1998	7th July (Landslide)	8th July (Landslide)		
Gayabari T.E., Along NH-55, tindharia and shiviter. paglajhora	197 mm	500 mm	527	565	590
	8th July, 2003	9th July, 2003 (Landslide)			
Tindharia and upper and lower paglajhora	124.5	224.5	255.5	300	315
	17th July, 2007	18th July, 2007 (Landslide)			
Tindharia, lower paglajhora and shiviter	91 mm	187 mm	275 mm		
	6th September 2007	7th September 2007	8th September 2007 (Landslide)		
14 Mile near lower paglajhora, nurbong, gitingia, shiviter	111.7 mm 15th June, 2010	345 mm 16th June, 2010 (Landslide)	245	295	365

5.3.3 Calculated Critical Height to Initiate Slide

The determined critical slope height after Culmann (1866) at Tindharia and Lower Paglajhora are 5.89 and 7.80 m respectively. The height of the vertical back wall along the road should be restricted to almost 5.89 m at both the places (Table 5.8) in Tindharia. The landslide affected area with more than 5.89 m height corresponding to the average threshold slope angle of 24° must be identified and shaped to that of safe height (below 5.89 m.). At Paglajhora, the critical height for slope failure is 7.80 m.

5.3.4 Temporal Probability of Landslide Events

The occurrences of major landslide events with more than 90 % certainty could be expected in every 7.5 years in case of Poisson distribution model. If we consider landslide event, then we can say that it can be expected in every 13 years with

Table 5.8 Critical height for initiation of slide

Sl. No.	Slope parameters	Tindharia	Lower paglajhora
1	Upslope contributing area (a)	1404 m^2	968 m^2
2	Contour length (b)	27 m	22 m
3	Slope angle (⊖)	53°20′	48°20′
4	Angle of internal friction (φ)	21°	21°
5	Transmissivity (T)	15 m^{-2} day^{-1} (Borga et al. 1998)	15 m^{-2} day^{-1} (Borga et al. 1998)
6	Wet soil buck density (P_s)	1.96 g/cc	1.96 g/cc
7	Density of water (P_W)	1.07 g/cc	1.07 g/cc
8	Cohesion (kg/cm^2)	0.06	0.06
9	Critical height for initiation of slide Culmann (1866) $h_c = \frac{4C\prime \sin\theta \cos\phi}{\gamma 1-\cos(\theta-\phi)}$	5.89 m	7.80 m
10	Critical height for initiation of slide Terzaghi (1962) $Hc = \frac{Sc}{W}$	9.30 m	9.30 m

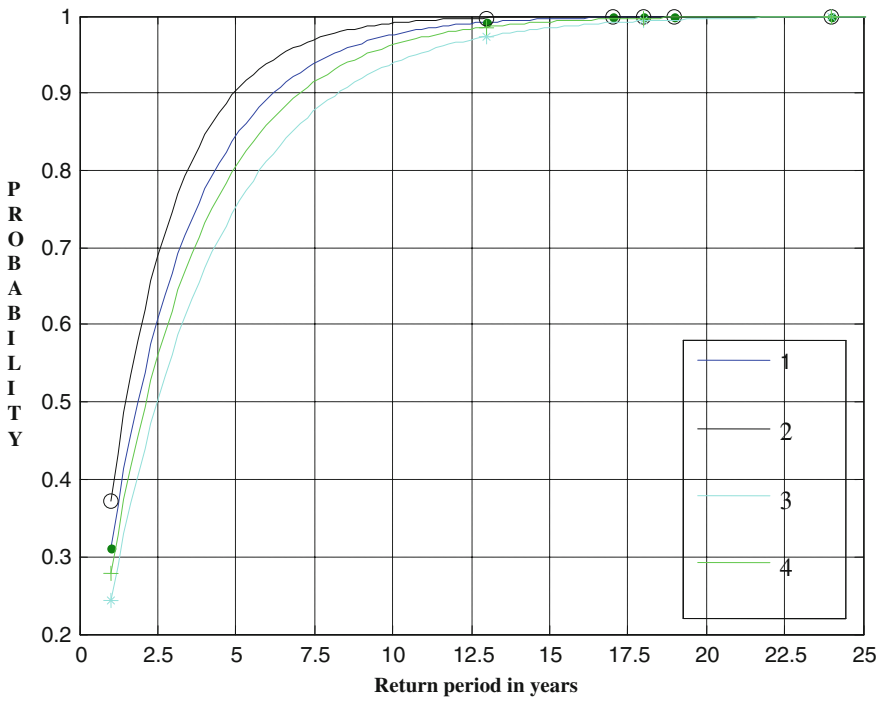

Fig. 5.5 Landslide probability and its return period

100 % certainty. In case of Binomial distribution the 100 % certainty of the major landslide events are to be expected at the return period of 19 years (Fig. 5.5). In the mountain region physical and anthropogenic processes are active on slope in an interactive combination. Construction of settlement, road and associated deforestation destabilize soil and slope. Slope is steepened, soil becomes loose and friable, lateral support is removed, soil becomes saturated by hydrological intervention. All these together lead to instability and threshold condition are achieved. Ultimately slope failure occurs and that helps to achieve temporary stability (Fig. 5.6).

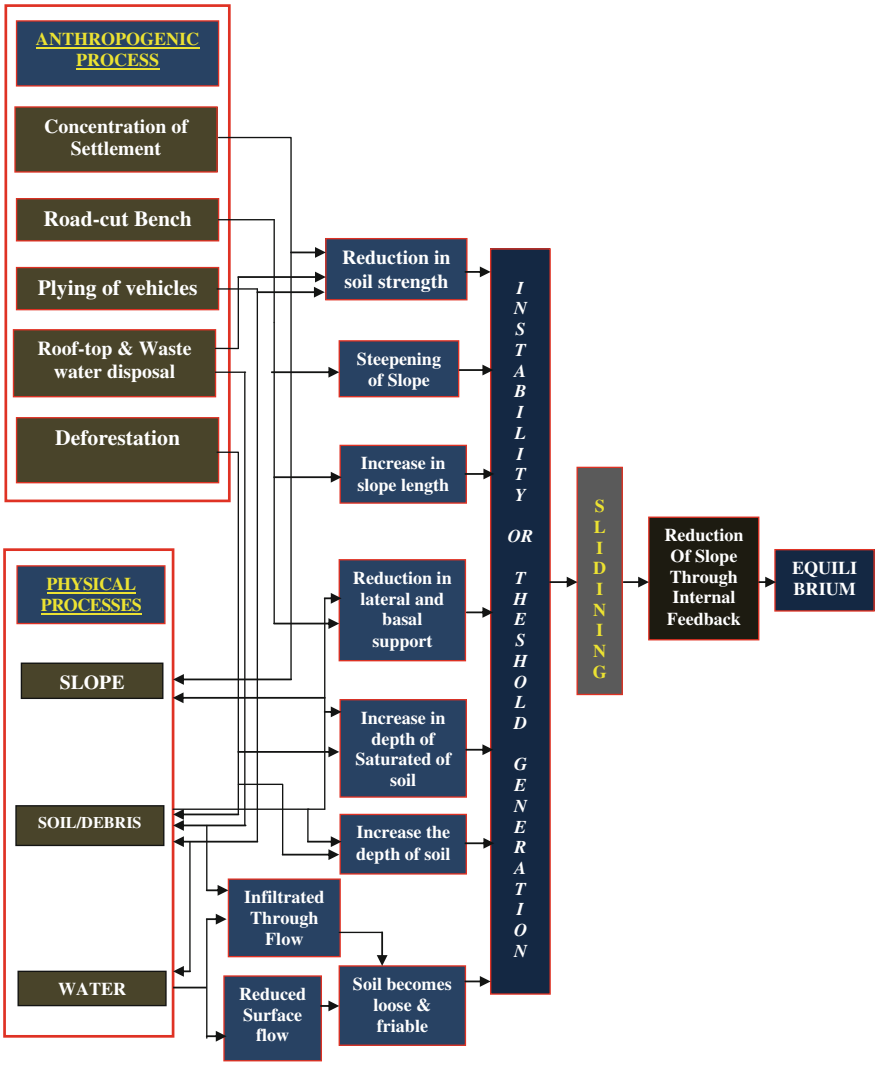

Fig. 5.6 Homeostatic adjustment through self-organized internal feedback in a complex system of interaction among physical and anthropogenic process

5.4 Conclusion

Threshold slope angle for two major landslide locations i.e. Tindharia and Paglajhora varies from 21° to 26°. Large parts of Tindharia, Gayabari, 14 Miles Bustee, Lower Paglajhora and Shiviter are facing the slope angle of more than average threshold slope angle and shows absolute instability. It is also examined that more than 60 % area of the Shivkhola Waterhsed is beyond the threshold slope angle. The calculated critical rainfall at Tindharia and Lower Paglajhora are 105.88 and 88.93 mm/day respectively. 120.7 mm daily rainfall can occur at a recurrence interval of 1.4 years following Gumbel (1954) and 128.507 mm daily rain has a recurrence interval of 2 years with 50 % probability following Chow (1951, 1954). That means there is every possibility for the generation of geomorphic threshold for initiation of slide due to hydrologic factor in Shivkhola watershed. Antecedent Cumulative rainfall induced landslide analysis shows that the continuous and uniform rate of minimum amount of rainfall (approx. less than 80 mm/day) for few consecutive days can cross the geomorphic threshold and can introduce slope instability condition. On the other hand, one or two day's heavy showers that are more than 200 mm/day rain may cause devastating slope failure in the Shivkhola Watershed. Critical slope height with 48–53° steepness may range from 5.89 to 7.80 m. Special care should be taken to reduce the height of back wall along the main road to that of 6.00 m of less. The Interaction between physical and anthropogenic processes leads to the initiation of geomorphic threshold that leads to slope failure reducing the slope through internal feedback mechanism and may proceed towards the new state of equilibrium (Fig. 5.6).

References

Aleotti P (2004) A warning system of rainfall-induced shallow failure. Eng Geol 73:247–265

Basu SR, Sarkar S (1985) Some consideration on recent landslides at Tindharia and their control. Indian J Power River Valley Dev 190–194

Basu SR, Sarkar S (1988) Ecosystem vis–a–vis Landslides, a case study in Darjeeling Himalayas. Impact of Development on Environment (Ed). The Geog Soc India, Cal II:45–53

Basu SR, Maiti RK (2001) Unscientific mining and degradation of slopes in the Darjeeling Himalayas. Chang Env Scenerio Indian Subcont (Bd) 390–399

Bloom AL (1991) Geomorphology, a systematic analysis of the Cenozoic Landforms. Prentice Hall of India Pvt. Ltd., New Delhi, pp 76–177

Borga et al (1998) Shallow Landslide hazard assessment using a physically based model and digital elevation data. J Environ Geol 35(2–30):81–88

Brunsden D, Jones DKC, Martin RP, Doornkamp JC (1981) The geomorphological character of part of the Low Himalaya of Eastern Nepal. Z Geomorph NF Suppl-Bd 37:25–72

Caine N (1980) The rainfall intensity–duration control of shallow landslides and debris flows. Geogr Ann 62A:23–27

Caine N, Mool PK (1982) Landslides in the kolpu khola drainage, middle mountain nepal. Mt Res Dev 2:157–173

Campbell RH (1975) Soil slips, debris flows, and rainstorms in the santa monica mountains and vicinity, Southern California. US Geol Surv Prof Paper 851:1–20
Cannon SH, Ellen SD (1985) Rainfall conditions for abundant debris avalanches, San Francisco Bay region. Calif Geol 38(12):267–272
Cannon SH (1988) Regional rainfall-threshold conditions for abundant debris-flow activity. In: Ellen SD, Wieczorek GF (eds) Landslides, floods, and marine effects of the storm of January 3–5, 1982, in the San Francisco Bay Region, California. US Geol Surv Prof Paper 1434:27–34
Cardinali M, Galli M, Guzzetti F, Ardizzone F, Reichenbach P, Bartoccini P (2006) Rainfall induced landslides in December 2004 in Southwestern Umbria, Central Italy. Nat Hazards Earth Syst Sci 6:237–260
Carson MA (1977a) Application of the concepts of Threshold slopes to the laramie mountains, Wyoming. Inst Br Geogr Spec Publ 3:31–48
Carson MA (1977b) Threshold and characteristic angles of straight slopes. In: Proceedings of the 4th Guelph symposium on geomorphology, Norwich Geo Books, pp 19–34
Carson MA (1977c) Angle of repose, angles of shearing resistance at angle of talus slopes. Earth Surf Process 2:263–380
Ceriani M, Lauzi S, Padovan N (1992) Rainfall and landslides in the Alpine area of Lombardia Region, central Alps, Italy. In: Interpraevent international symposium, Bern, vol. 2, pp. 9–20
Chow VT (1951) General formula for hydrologic frequency analysis. Am Geophys Union Trans 32:231–237
Chow VT (1954) The long-probability law and its engineering applications. ASCE 80 (Separate No. 536)
Cotecchia V (1978) Systematic reconnaissance mapping and registration of slope movements. Bull Int Ass Eng Geol 17:5–37
Coe JA, Michael JA, Crovelli RA, Savage WZ, Laprade WT, Nashem WD (2004) Probabilistic assessment of precipitation-triggered landslide using historical records of landslide occurrence, Seattle Washington. Environ Eng Geosci X 2:103–122
Crosta G (1998) Regionalization of rainfall threshold: an aid to landslide hazard evaluation. Environ Geol 35(2–3):131–145
Crosta G, Frattini P (2001) Rainfall thresholds for triggering soil slips and debris flow. In: Proceeding of the EGS 2nd plinius conference 2000, mediterranean storms, Siena, pp 463–488
Crovelli RA (2000) Probability models for estimation of number of coasts of landslides. USGS, Denver, Colorado
Crozier MJ (1997) The climate-landslide couple: a southern hemisphere perspective. In: Matthews JA, Brunsden D, Frenzel B, Glaeser B, Weiss MM (eds) Rapid mass movement as a source of climatic evidence for the Holocene. Gustav Fischer Verlag, Stuttgart, pp 333–354
Crozier MJ (1999) Prediction of rainfall-triggered landslides: a test of the antecedent water status model. Earth Surf Proc Land 24:825–833
Culmann C (1866) Graphische Statik, Zurich
Dahal RK, Hasegawa S, Masuda T, Yamanaka M (2006a) Roadside slope failures in Nepal during torrential rainfall and their mitigation. In: Marui H, Marutani T, Watanabe N, Kawabe H, Gonda Y, Kimura M, Ochiai H, Ogawa K, Fiebiger G, Heumader J, Rudolf-Miklau F, Kienholz H, Mikos M (eds) Proceeding of the Interpraevent international symposium, niigata 2006, Disaster mitigation of debris flow, slope failures and landslides, vol 2. Universal Academy Press, Tokyo, pp 503–514
Dahal RK, Hasegawa S, Yamanaka M, Nishino K (2006b) Rainfall triggered flow-like landslides: understanding from southern hills of Kathmandu, Nepal and northern Shikoku, Japan. In: Proceedings of the 10th international congress of IAEG, The geological society of London, IAEG2006 Paper number, vol 819 pp 1–14 (CD-ROM)
Dahal RK (2006) Geology for technical students—a textbook for bachelor level students. Brikuti Academic Publication, Exhibition Road, Kathmandu, Nepal 756 pp
De Vleeschauwer C, De Smedt F (2002) Modeling slope stability using GIS on a regional scale. In: Proceedings of the first geological belgica international meeting, vol 12. Aardkundige Mededelingen, leuven, 11–15 Sept 2002, pp 253–256

De Smedt F (2005) Slope Instability analysis using GIS on a regional scale: a case study of Narayanghat-Mungling highway section, Nepal, a dissertation report presented at Universiteit Gent. Vrije Universiteit Brusssel, Belgium

Dhakal AS, Amada TK, Aniya M (1999) Landslide hazard mapping and application of GIS in the Kulekhani watershed. Nepal, Mt Res Dev 19(1):3–16

Dhital MR, Khanal N, Thapa KB (1993) The role of extreme weather events, mass movements, and land use changes in increasing natural hazards, A Report of the preliminary field assessment and workshop on causes of recent damage incurred in southcentral Nepal, ICIMOD, Kathmandu, 19–20 July 1993, 123 pp

Dhital MR (2003) Causes and consequences of the 1993 debris flows and landslides in the Kulekhani watershed, central Nepal. In: Rickenmann D, Chen C-L (eds) Proceedings of the 3rd International conference debris-flow hazards mitigation: mechanics, prediction and assessment, vol 2. Millpress, Rotterdam, Netherlands, pp 931–942

Fenti V (1992) Indagini geologic-techniche sull' area del dispositivo di misura (in Italian). In: Marchi L (ed) II Basino attrezzato del Rio Cordon, Quadevni di Ricerca, n. 13, Ragione Veneto. Dipartimento Foreste, Venezia Mestre: (pp 109–122)

Froehlich W, Gil E, Kasza I, Starkel L (1990) Thresholds in the transformation of slopes and river channels in the Darjeeling Himalaya. India Mt Res Dev 10(4):301–312

Gabet EJ, Burbank DW, Putkonen JK, Pratt-Sitaula BA, Oiha T (2004) Rainfall thresholds for landsliding in the Himalayas of Nepal. Geomorphology 63:131–143

Gerrard J, Gardner RAM (2000) Relationships between rainfall and landsliding in the Middle Hills, Nepal. Norsk Geogr Tidsskr 54:74–81

Ghosh S, Van Westen CJ, Carranza E, Jetten V (2009) Generation of event- based landslide inventory maps in a data-scarce environment; case study around Kurseong, Darjiling District, West Bengal, India. In: Malet P, Remaitre A, Bogaard T (eds) Landslide processes: from geomorphologic mapping to dynamic modeling: proceedings of the landslide processes. European centre on geomorphological hazards (CERG), Strasbourg, France, pp 37–44

Giannecchini R (2006) Relationship between rainfall and shallow landslides in the southern Apuan Alps (Italy). Nat Hazards Earth Syst Sci 6:357–364

Glade T (1998) Establishing the frequency and magnitude of landslide-triggering rainstorm events in New Zealand. Environ Geol 35:160–174

Glade T, Crozier M, Smith P (2000) Applying probability determination to refine landslidetriggering rainfall thresholds using an empirical Antecedent Daily Rainfall Model. Pure Appl Geophys 157:1059–1079

Gumbel EJ (1954) Statistical theory of extreme values and some practical applications. Applied mathematics series 33. US bureau of standards, Washington, DC

Guzzetti F, Cardinali M, Reichenbach P, Cipolla F, Sebastiani C, Galli M, Salvati P (2004) Landslides triggered by the 23 November 2000 rainfall event in the Imperia Province, Western Liguria, Italy. Eng Geol 73:229–245

Guzzetti F, Peruccacci S, Rossi M, Stark CP (2007) Rainfall thresholds for the initiation of landslides in central and southern Europe. Meteorol Atmos Phys. doi10.1007/s00703-007-0262-7. Accessed 7 Aug 2007

Innes JL (1983) Debris flows. Prog Phys Geog 7:469–501

Keefer DK, Wilson RC, Mark RK, Brabb EE, Brown WM, Ellen SD, Harp EL, Wieczorek GF, Alger CS, Zatkin RS (1987) Real-time warning during heavy rainfall. Science 238 (4829):921–925

Kim SK, Hong WP, Kim YM (1991) Prediction of rainfall triggered landslides in Korea. In: Bell DH (ed.) Landslides, vol 2. A.A. Balkema, Rotterdam, pp 989–994

Larsen MC, Simon A (1993) A rainfall intensity-duration threshold for landslides in a humidtropical environment. P R Geogr Ann 75(1–2):13–23

Li T, Wang S (1992) Landslide hazards and their mitigation in China. Science Press, Beijing 84 pp

Maiti RK (2007a) Irrational resource extraction introducing instability in slope and hydrodynamics- a case study at lish-chunkhola basin, Darjiling Indian. J Geograph Environ 8, 9:41–51 Vidyasagar University

Maiti R (2007b) Identification of potential slope failure zones of shiv-khola watershed; Darjiling Himalaya, through critical analysis of slope instability- a step towards rational and scientific management of land, soil and water, UGC Sponsored Minor Research Project [F.31-210/2005 (31.03.2007)]

Manandhar IN, Khanal NR (1988) Study on landscape process with special reference to landslides in Lele watershed, central Nepal. Report submitted to Research Division, Tribhuvan University, unpublished, 53 pp

Metteotti G (1996) Valutazione del rischio di franosita per unbacino di tipo alpino (in Italian), Ph. D. Dissertation, University of Padova, Italy

Melnikov M, Chensokov M (1969) Safety in open cast mining. Mir Publications, Moscow

Montgomery DR, Dietrich WE (1994) A physically based model for the topographic control on shallow landsliding. Water Resour Res 30(4):1153–1171

Neary DG, Swift Jr LW (1987) Rainfall thresholds for triggering a debris avalanching event in the southern Appalachian Mountains. In: Costa JE, Wieczorek GF (eds) Debris flows/avalanches: process, recognition and mitigation. Geol Soc Am Rev Eng Geol 7:81–92

Pomeroy JS (1984) Storm-induced slope movements at East Brady, northwestern Pennsylvania. US Geol Surv Bull 1618:16 pp

Sarkar S (2011) Evolution of Paglajhora slump valley in the shivkhola basin, The Darjiling Himalaya, India. Geogr Pol, 84(Special Issue Part-2):117–126

Schumm SA (1977a) The fluvial system. Willy, New York

Schumm SA (1977b) Drainage basin morphology, bechmark papers in geology, 4. Hutchinsons and Ross, Pennsylvannia, Dowden

Schwab et al. (2002) Soil and water conservation Engineering. Wiley, New York, pp 18–47

Skempton AW, Hutchinson JN (1969) Stability of natural slope and embankment section. In: Proceedings of the 7th international congress soil mechanics engineering mexicom, pp 291–340

Starkel L (1972) The role of catastrophic rainfall in the shaping of the relief of the lower Himalaya (Darjeeling Hills). Geogr Pol 21:103–147

Terlien MTJ (1997) Hydrological landslide triggering in ash covered slopes of Manizales (Columbia). Geomorphology 20:165–175

Terlien MTJ (1998) The determination of statistical and deterministic hydrological landslide triggering thresholds. Environ Geol 35(2–3):124–130

Terzaghi K (1962) Stability of steep slopes on hard unweathered rock, Geothnique 12:251–270

Upreti BN, Dhital MR (1996) Landslide studies and management in Nepal. ICIMOD, Nepal 87 pp

Van Burkalow A (1945) Angle of repose and angle of sliding friction; an experimental study. Geol Soc Am Bull 56:669–707

Varnes DJ (1978) Slope movement types and process. In Schuster RL, Krizek RJ (eds) Landslides analysis and control. Special Report 176, Transportation Research Board, National Academy of Sciences, Washington DC, pp 12–33

White ID, Mottershead DN, Harrison JJ (1996) Environmental systems, 2nd edn. Chapman and Hall, London 616 pp

Wieczorek GF (1987) Effect of rainfall intensity and duration on debris flows in central Santa Cruz Mountains, California. In: Crosta G, Wieczorek GF (eds) Debris flows/avalanches: processes, recognition and mitigation. Reviews in Engineering Geology, vol 7. Geological Society of America, pp 23–104

Wieczorek GF (1996) Landslide triggering mechanisms. In: Turner AK, Schuster RL (eds) Landslides: investigation and mitigation, Transportation Research Board, Special Report 247. National Research Council, Washington, pp 76–79

Wieczorek GF, Morgan BA, Campbell RH (2000) Debris flow hazards in the blue ridge of central Virginia. Environ Eng Geosci 6(1):3–23

Wilson RC, Wieczorek GF (1995) Rainfall threshold for the initiation of debris flow at La Honda, California. Environ Eng Geosci 1(1):11–27

Zezere JL, Trigo RM, Trigo IF (2005) Shallow and deep landslides induced by rainfall in the Lisbon region (Portugal): assessment of relationships with the North Atlantic Oscillation. Nat Hazards Earth Sys Sci 5:331–344

Chapter 6
Slope Stability Model and Landslide Susceptibility Using Geo-technical Properties of Soil

Abstract The present study deals with the assessment of geo-technical parameters i.e. surface inclination (⊖), soil depth (z), cohesion (c), angle of internal friction (φ), soil saturation index (m), soil density (γ_s) and density of water (γ_w) and to construct 1D (one dimensional) Slope stability model for preparing the slope instability map under dry, semi-saturated and saturated condition of the landslide prone small hilly Shivkhola Watershed of Darjeeling Himalaya. To determine the spatial distribution of slope instability in the watershed, safety factor value for 50 different locations were being estimated and with the help of GIS tools. The probability or the chances of landslide phenomena in each class of slope instability maps were extracted by means of *frequency ratio* (FR) which shows that the probability/chances of landslide events could be expected as very high in the high to very high landslide susceptibility area and vice versa in all three conditions. The analysis of slope instability under three conditions also suggested that there was an aerial expansion of very high landslide susceptibility in saturated condition in comparison to dry and semi-saturated condition. This aerial expansion was the outcome of complete saturation and reduction of shearing strength of the slope materials above the failure plane surface. Finally, an accuracy assessment was made by ground truth verification of the existing landslide locations where the classification accuracy for dry, semi-saturated and saturated conditions was 93.86, 94.58 and 85.44 % respectively.

Keywords Slope stability model · RS and GIS · Landslide susceptibility · Safety factor (FS) · Frequency ratio (FR) · Accuracy assessment

6.1 Introduction

Slope instability resulted from complex geological setting combined with various geomorphological, hydrological and geo-technical factors such as slope, relief, aspect, rainfall, drainage, upslope contributing area, cohesion, angle of internal friction, wet soil density, depth of the soil, shear stress, shear strength etc. But, the

S. Mandal and R. Maiti, *Semi-quantitative Approaches for Landslide Assessment and Prediction*, Springer Natural Hazards, DOI 10.1007/978-981-287-146-6_6

factors conducive to slope instability, can be recognized at various levels of abstraction from the slope itself. The cohesion and pore-water pressure both directly control the magnitude of stress of the slope materials. These direct factors can be influenced by other factors recognized at successively more remote levels of abstraction. For example, pore-water pressure may be related to the rate of infiltration through the ground surface, which in turn, may be related to the density of vegetation cover which is again subject to change as a result of climatic conditions or land use activity. These chains of relationships may be critical in reducing the slope stability condition over time to a point where the triggering of movement may occur. Landslide susceptibility is thus a function of the degree of the inherent stability of the slope together with the intensity of causative factors capable of reducing the excess strength. So, the identification of the causative factors is the basis of many methods of landslide susceptibility assessment. In most of the case the landslide is the critical mechanism of erosional processes and in such condition landslide is inevitable and necessary part of the natural landscape process system. Although the occurrences of landslide hazards and its impact on human society cannot be prevented fully by analyzing the slope stability condition, but the better understanding of geo-technical attributes of the soil can contribute to greater knowledge and understanding about the spatial distribution of slope instability which are very much essential for land use planning. Many approaches to assess slope stability and landslide hazards were put forward by Montgomery and Dietrich (1989, 1994), Carrara et al. (1991), Hammond et al. (1992) combined a contour based steady state hydrologic model with the infinite slope stability model (simplified for cohesion less soils) to define slope stability classes based upon slope and specific catchment area. Numerous models in connection to the slope stability, shallow and deep seated landslides were introduced and verified by Varnes (1958), Young (1963), Vanmarcke (1977), Burton and Bathrust (1998), Bradinoni and Church (2004), Smedt (2005) and Bhattarai and Aoyama (2001). The geotectonic factors of slope instability were studied in details by Brudsen (1979), Windisch (1991), Carson (1975, 1977) and Borga et al. (1998). A comprehensive list of stability factors commonly employed in the factors mapping approach was given by Crozier (1986), Guzzetti et al. (1999a, b, 2003) and Tiwari and Marui (2001, 2002, 2003, 2004).

A more sophisticated approach represents the terrain in terms of differences of inherent stability based on the Safety Factor (FS). Simply, the value FS is assumed to be 1.00 at the moment of failure and the values successively greater than 1.00 represents the increasing stability and hence low susceptibility to slope failure. Determination of FS permits limiting equilibrium analysis of a slope and is particularly helpful in designing the type and magnitude of remedial measures required to achieve an acceptable FS. A considerable amount of information such as the geometry of the slope, pore-water of the slope materials, angle of internal friction and cohesion are required to assess the stress parameters of the slope materials (Glade 1998) and Safety Factor value.

The present study encompasses the assessment of geo-technical parameters of the collected soil samples from 50 landslide locations selected through stratified random sampling with representatives of different landuse and slope classes. The

geo-technical attributes include surface inclination (β), soil depth (z), cohesion (c), angle of internal friction (φ), soil saturation index (m), soil density (γ_s) and density of water (γ_w). Before planning any land use, the better understanding and investigation of geo-tectonic parameters and the preparation of a stability distribution map by applying GIS tools are very much popular and accepted approach in the present time. The major objective of the present study is to study geo-technical parameters and to identify the potential stability sites in the Shivkhola Watershed through estimating the strength parameters and the application of *1D slope Stability model* to prepare *landslide susceptibility maps.* The validity of the prepared landslide susceptibility maps under dry, semi-saturated and saturated condition were evaluated by means of a *frequency ratio* (FR). Finally, an accuracy assessment was made by ground truth verification of the existing landslide locations where the classification accuracy for dry, semi-saturated and saturated condition was 93.86, 94.58 and 85.44 % respectively.

6.2 Materials and Method

6.2.1 Slope Stability Model Concept

Two forces are responsible to determine the stability condition i.e. driving force (shear stress) and resisting force (shear strength). Shear stress is given as, $\tau = \gamma D \sin \ominus \cos \ominus$ (where γ, soil density; D, depth of the soil; ⊖, slope angle) and shear strength of Mohr and Columb defined as, $S = c + \tau \tan \varphi$ (where c: cohesion; φ: friction angle; τ: shear stress). Saturated slope material increases instability with increasing pore water pressure. The pore water pressure depends on unit weight of water (γ_w) and the height of water (D_w) above the failure plane surface. The height of the water shows the ground water condition in the soil. In this case the shear resistance of the soil is given by the following:

$$S = c + (\gamma - \gamma_w m)\, D \cos^2 \ominus \tan \varphi \tag{6.1}$$

where, m is saturation index which shows the saturation condition of the soil.

If the value of m equals to 1, the soil is completely saturated and the value of 0 indicates complete dry condition.

In many investigations of natural slope stability, infinite slope analysis had frequently been used because of its relative simplicity where the thickness of the soil is smaller than the length of the slope.

For realistic modeling 3D failure mechanism should be considered which includes different depth of sliding surface throughout the slope failure mass. Soeters and Westen (1996) recommended using infinite slope stability analysis in order to conduct deterministic analysis of the large area and due to complication in establishing vertical depth of failure plane in 3D mechanism. Monte Carlo Method, a simplified approach was considered by them reducing 3D depth to 2D equivalent

depth based on equal factor of safety. However, it is not simple to analyze 2D rotational slide due to variation in depth of sliding surface. Hence, 2D depth of rotational slide (Eq. 6.2) was then converted to equivalent translational depth without the impact of ground water (Eq. 6.3) keeping the same factor of safety.

$$\text{FS (Rotational)} = \frac{c + \gamma \cdot \tan \varnothing \sum_{i-1}^{X} z_i \times \cos^2 \beta}{\gamma \sum_{i-1}^{X} z_i \cdot \sin \beta \times \cos \beta} \tag{6.2}$$

$$\text{FS (Translational)} = \frac{c + \gamma \cdot z \cdot \cos^2 \beta \times \tan \varphi}{\gamma \cdot z \cdot \sin \beta \times \cos \beta} \tag{6.3}$$

where, γ = unit weight of the soil; z = depth of the failure surface below the terrain surface; β = the terrain surface inclination; φ = angle of internal friction; c = cohesion.

The safety factor (FS) under the influence of ground water (semi-saturated and saturated condition) of cohesive soil could also be calculated by applying the revised *1D slope stability model* with the help Eq. 6.4.

$$FS = \frac{c + (\gamma - m \times \gamma_w) \times \cos^2 \beta \times \tan \varphi}{\gamma \times z \times \sin \beta \times \cos \beta} \tag{6.4}$$

where, γ = unit weight of soil; m = soil saturation index; Z_w = height of water table above failure surface; Z = depth of failure surface below the terrain surface; γ_w = unit weight of water; β = the terrain surface inclination; φ = angle of internal friction and c = cohesion.

In completely dry condition, cohesion (c) and wetness index value (m) become zero (0) and in case of cohesion less soil, safety factor could be determined with the help of following equation.

$$Fs = \frac{\gamma D \cos^2 \theta \tan \varphi}{\gamma D \sin \theta \cos \theta} \tag{6.5}$$

$$\text{Or,} \qquad FS = \frac{\tan \varphi}{\tan \ominus} \tag{6.6}$$

The safety factor for cohesion less soil with the influence of ground water can be estimated by:

$$FS = \frac{(\gamma - m\gamma_w) D \cos^2 \ominus \tan \varphi}{\gamma D \sin \ominus \cos \ominus} \tag{6.7}$$

When the value of wetness index (m) becomes 0, the safety factor is determined by:

$$FS = \frac{(\gamma - m\gamma_w)\, D \cos^2 \ominus \tan \varphi}{\gamma \tan \ominus} \tag{6.8}$$

6.2.2 Cohesion (c) and Friction Angle (φ)

The shear strength of the soil was described as the function of normal stress on the slip surface, cohesion, and angle of internal friction. The angle of internal friction (φ) and cohesion are the two important physical properties of the soil which determines angle of rupture, shearing strength, safety factor as well as stability condition of the slope materials by developing '*stress circle*'. The relationship within all these properties to other characteristics of the soil was introduced by Terzaghi (1950) and Wu and Siddle (1995). The geo-technical factors like angle of repose of the debris were measured after Bloom (1991). The tangent of angle of repose of dry granular materials is slightly greater than, but approximately equals to the co-efficient of sliding friction of the material or its mass friction (φ) (Van Burkalow 1945; Bloom 1991). The range of cohesion and friction angle of different soil was also adopted from Foundation of Engineering Geology (Tony Waltham 2002) for the analysis of slope stability. All the tests were carried out under drained condition using 100 mm diameter and 25 mm thick specimen in Geotechnical Laboratory, GSI, Kolkata.

The major stress (σ_1), minor stress (σ_3) and cohesion (c) were estimated through tri-axial soil testing mechanism (Fig. 5.1) from Geo-technical Laboratory of GSI, Kolkata (22/com/soil/GTL/ER/O6-07). On the basis of these three major attributes a Mohr stress circle was developed to obtain angle of internal friction and angle of rupture. At first, a circle was drawn through σ_3 and σ_1 with the centre on the horizontal axis; the centre of the circle was obviously $(\sigma_1 + \sigma_3)/2$ and the radius was $(\sigma_1 - \sigma_3)/2$ (Fig. 5.2).

The values of confining pressure, σ_3, and compressive stress, σ_1 were plotted on horizontal axis where stress difference was $\sigma_1 - \sigma_3$. On a plane parallel to the greatest principal stress axis ($2\alpha = 0$) the normal stress across the plane was σ_3 and the shearing stress was 0. If the plane makes an angle of 45° with the greatest principal stress axis ($2\alpha = 90$), the shearing stress is at a maximum and the normal stress is $(\sigma_1 + \sigma_3)/2$. If the plane makes an angle of 90° with the greatest principal stress axis ($2\sigma = 180°$), the shearing stress is 0 and the normal stress is σ_1 (Billings 1987).

$$\sigma_n\,(normal\ stress) = \frac{\sigma_1 + \sigma_3}{2} - \frac{\sigma_1 - \sigma_3}{2} \cos 2\alpha \tag{6.9}$$

$$C\,(cohesion) = \frac{\sigma 1 - \sigma 3 \tan^2 (45 + \frac{\varphi}{2})}{2 + \tan (45 + \frac{\varphi}{2})} \tag{6.10}$$

For the determination of the cohesive strength and the angle of internal friction a series of experiments were done with different values of confining pressure (σ_3). The Mohr Circle shows that as the confining pressure is increased, the stress as well as the stress difference must be increased to produce rapture. A line which is the tangent of the *'Mohr Circle'* is called as the *'Mohr Envelope'*. The angle that this line makes with the horizontal axis of the diagram is the angle of internal friction, ϕ (Fig. 5.2). Along any potential plane of rupture within a rock:

$$\mu = \tau/n = \tan\phi \tag{6.11}$$

where μ is the coefficient of internal friction,
τ = shearing stress along plane,
n = normal stress along the lane,
ϕ = the angle of internal friction.

The τ is at a maximum when $\alpha = 45°$; whereas n is at a minimum when $\alpha = 0$ and at a maximum when $\alpha = 90°$. Shear fracture develops when n and τ combine to make the shear stress most effective. Actual shear fracture makes an angle of less than 45° with the greatest principal stress axis (Billings 1987).

The intercept on the vertical axis, τ_o, is the cohesive strength of the rock. The curve for the Mohr envelope is:

$$\tau = \tau_o + \sigma_n \tan\phi \tag{6.12}$$

where, the angle that fractures should theoretically make with the greatest principal axis is

$$\alpha = \pm 45 \pm \phi/2 \tag{6.13}$$

So, if the angle of internal friction is 30°, the fractures would make the angle of 30° with the greatest principal stress axis. On the other hand the shear fracture should theoretically form at 30° (Billings 1987).

The frictional angle of a particular soil depends on various factors (Cernnica 1995) like:

- State of compaction and void ratio increasing the density. The relation is not necessarily the linear one.
- Coarseness, the shape of the particle and the angularity of the particle of the soil: Angular grains interlock more effectively than rounded ones, thereby creating a larger friction angle.
- Mineralogical content of the soil: Hard gravel particles result in higher friction angles. Soft grains which may crush more easily, thereby reducing the

interlocking or bridging effects. For sand, however, the mineralogical content seems to make little difference except if the sand contains mica. In that case the void ratio is usually larger, thereby resulting in loose interlocking and lower friction angle.

- Particle size distribution of the soil: The soil having the well-graded size will have higher frictional angle than the soil having poorly graded soil.

Cohesion (C) is the attraction of particles to each other which is not directly governed by a friction law but does provide a measure of strength of a material. Thus sands do not exhibit cohesion, while soil which contains clay show cohesion. It can be measured, as in soil mechanics, by the Mohr-Coulomb Equation (Eq. 6.10).

6.2.3 Surface Inclination/Slope (β)

Slope gradients are sometimes considered as an index of slope instability, and because of the availability of a digital elevation model (DEM), slope can be numerically evaluated and depicted spatially (O' Neill and Mark 1987; Gao 1993). Firstly, the contour map at 20 m interval was prepared and digitized from the topographical map 73B/8 (1987) at the scale of 1:50,000 and subsequently used for generating Digital Elevation Model on ARC GIS platform. Then slope gradient map (Fig. 2.6) was extracted from DEM and it was the classified after Anbalagan (1992) and Dhakal et al. (2000) into ten equal classes.

6.2.4 Soil Saturation Index/Wetness Index (m)

Simple models have been developed for estimating the soil saturation of the mountainous region as the wetness index is defined in TOPMODEL by Beven and Kirkby.

$$m = 1\mathrm{n}\frac{\mathrm{a}}{\tan\theta} \tag{6.14}$$

where a, is the contributing area per unit contour length and ⊖ is the slope of the pixel.

More acceptable soil saturation model was applied by Montgomery and Dietrich (1994), Borga et al. (1998) and Pack et al. (1998). The model envisages that the soil saturation index can be determined with the help of topography, soil type, and rainfall intensity of the area under study. But in practical sense, the soil is not completely dry or fully saturated in the area, therefore it can be imagined that the soil is half saturated. The soil saturation index is either fixed for stationary scenarios i.e. dry, semi-saturated and full saturated soils, given by m = 0, 0.5 and 1.00 or can

be calculated on the basis of available rainfall data (De Smedt 2005). On the basis of this assumption, wetness index equation can easily be derived and it is possible to see the effect of few days' consecutive rainfall in 1 day, if the soil is half saturated. In the present study wetness index (m) value of 0.00, 0.50 and 1.00 under dry, half-saturated and full-saturated conditions were taken into account.

6.2.5 Depth of Failure Surface/Depth (z) of Soil Below the Terrain Surface

Repeated and continued field studies for long duration were made for the proper cognition of the processes and their interaction. The depth of the failure surface was measured by holding a measuring tape at both the margins of scar and the other tape was allowed to hang, the reading was then taken from the base of the hanging tape. The margin of the scars was surveyed by *prismatic compass*. The intensive survey of the sliding scar for 40 different landslide locations was carried on by *Abney's level* at 0.5 m interval along radial lines originating from lower most part of the scar. The altitude of the points at 0.5 m interval along the radial lines was then estimated using Sine rule in reference to the central base point of known altitude determined by *GPS* (Basu and Maiti 2001). The total thickness of soil and that of saturated soil for 10 sites during monsoon were measured from slope cutting. After estimating the approximate depth of all known points, a soil depth map (z/D) was prepared using Arc GIS tool (see Chap. 2, Fig. 2.13).

6.2.6 Soil Density (γ_s) and Density of Water (γ_w)

Specific unit weight of water and unit weight of the soil were estimated by examining the soil samples collected from 50 landslide locations during field investigation. The density of soil and water varies from place to place due to in situ geo-hydrologic condition (Fig. 2.16). The saturated soil density was also consulted and adopted from the field experiences done by Deoja (1991).

6.2.7 Identification of Major Landslide Location/Landslide Inventory Map

To determine the frequency ratio (FR) and to assess the overall classification accuracy, the major landslide location of the Shivkhola Watershed (Chap. 2, Fig. 2.1) was detected by intensive field investigation with GPS, clinometers, and Abney's level. Besides,

LISS-III Satellite Image (2010), SRTM data (2008) and Google earth image (2010) had been incorporated with the surveyed landslide locations by thorough rectification and it was then modified and mapped accordingly (Fig. 2.1).

6.3 Application of 1 Dimension Slope Stability Model and Stability Analysis

With the help of derived geo-technical parameters i.e. cohesion, friction angle, slope angle, unit weight of the soil, unit weight of water, soil depth, and saturation index value from 50 landslide location points of the Shivkhola watershed the *safety factor values* (FS) for dry, semi-saturated and saturated condition were being estimated by applying the *1D slope Stability model* (Eq. 6.4). The safety factor values were transformed into raster value domain on ARC GIS Platform. Finally, the landslide susceptibility maps/safety factor distribution maps were prepared by 'slicing' operation and then stability classes for each condition (dry, semi and saturated condition) had been performed by studying the cumulative frequency and their abrupt change points of the safety factor values (the instability threshold boundaries). A 3 × 3 'majority filter' technique was also applied to all the prepared safety factor distribution maps as a post-classification filter to reduce the high frequency variation. Higher the value of 'FS', greater is the propensity of slope stability and vice versa. To assess the chances/probability of landslide phenomena in each class to all the prepared maps under various conditions frequency ratio (FR) was extracted by means of a ratio between landslide frequency/landslide events (%) and landslide susceptibility area (%). FR value is approaching to 1 indicates equal chances of landslide events, 0 indicates lesser chances and more than 1 shows greater probability. Finally, an accuracy assessment was made after Congalton (1991).

6.4 Shear Stress, Shear Strength and Safety Factor and Stability Analysis

Safety factor (FS) refers to the ratio between the shearing forces (simply known as stress, τ) and resistance of the materials to shearing forces (shearing strength, λ). Increase in shearing stresses produces rapture within the underlying rock beds and decrease the cohesive strength as well as the shearing strength due to which the slope materials start to move downward and make the slope most vulnerable to land slip.

$$FS = \frac{(\tau = \frac{\sigma_1 - \sigma_3}{2} \sin 2\alpha)}{(\lambda) = [\sigma_n \tan \varphi + c]} \tag{6.15}$$

If the computed factor of safety is less than unity, the slope is clearly unstable and likely to fall. If the factor of safety is greater than unity we cannot assume that the slope is stable as we may not have chosen the most critical mode of failure (i.e., failure surface) (Figs. 6.1, 6.2 and 6.3).

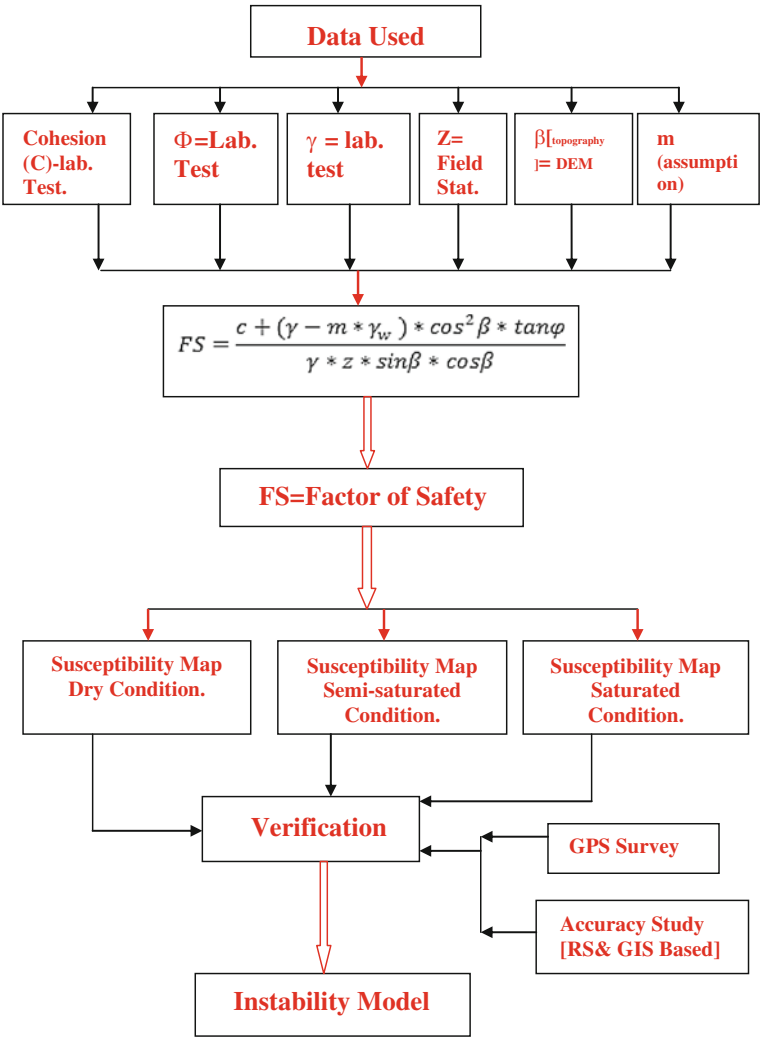

Fig. 6.1 Flow chart for landslide susceptibility maps

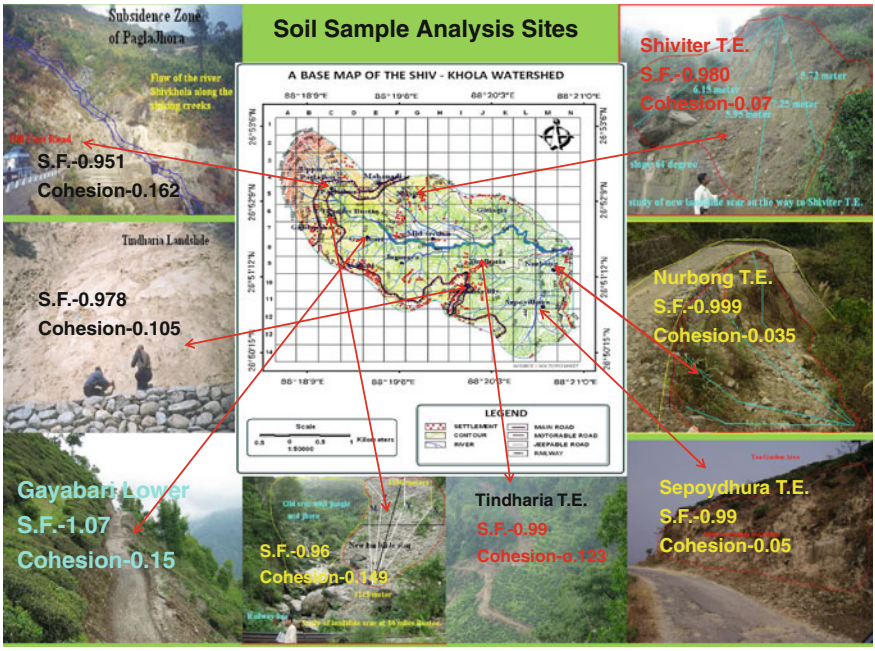

Fig. 6.2 Major landslide locations with 'FS' value in the watershed

6.4.1 Shear Stress

Shear stress is a force which deforms a mass of material by one part sliding over another along one or more failure plains. This is a force per unit area which is parallel to the surface of a body. This kind of stress is perpendicular to the normal stress. The rupture angle is obtained by developing Stress circle (Fig. 7.2). The shear stress is obtained by the following formula.

$$\tau\,(shesr\ stress) = \frac{\sigma_1 - \sigma_3}{2}\sin 2\alpha \tag{6.16}$$

where, σ_1 = major stress; σ_3 = minor stress; and α = rupture angle.

6.4.2 Shear Strength

This is a measure of the ability of a material to resist shear stress. This is an important parameter in determining the engineering and geomorphic parameters of the materials. Shear strength of the soil depends on the normal stress, angle of internal friction and cohesion which is determined applying the following formula:

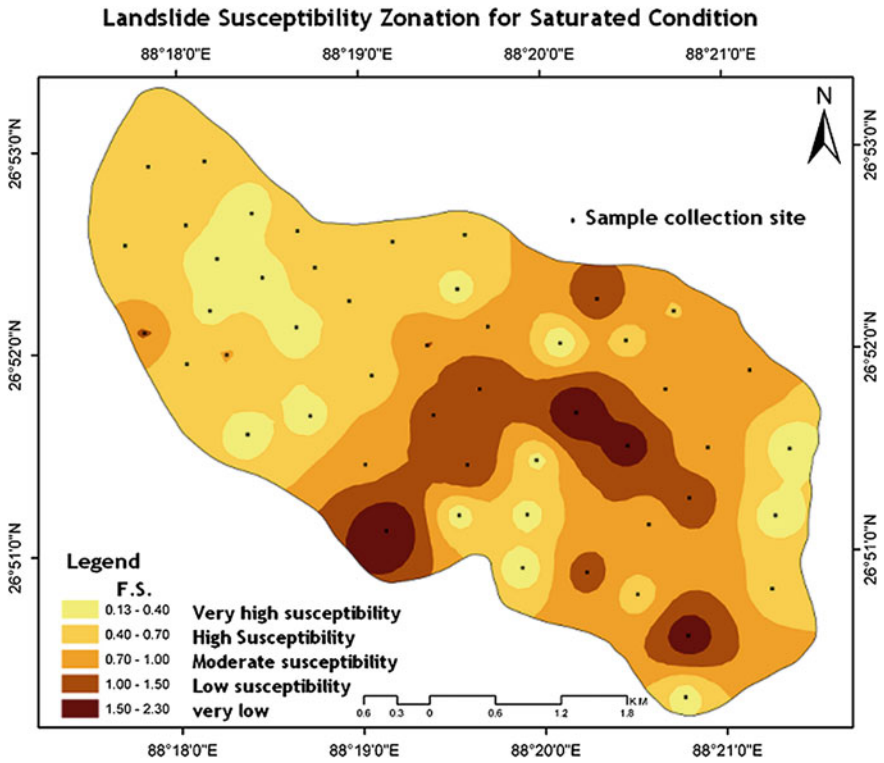

Fig. 6.3 Landslide susceptibility under saturated condition

$$\text{Shear Strength } (\lambda) = [\sigma_n \tan\phi + C] \tag{6.17}$$

where, σ_n = normal stress; ϕ = friction angle; and C = cohesion of the soil.

6.4.3 Safety Factor Based Stability Classes

See Table 6.1.

Table 6.1 The Stability Classes and Remarks

Safety factor (FS)	Slope condition	Remarks
FS < 1.5	Stable	Only major destabilizing factors lead to instability
1.25 < FS < 1.5	Moderately stable	Moderate destabilizing factor lead to instability
1 < FS < 1.25	Quasi stable	Minor destabilizing factor lead to instability
FS < 1	Unstable	Stabilizing factors are needed for stability

6.5 The Result and Discussion

6.5.1 Analysis of Strength Parameters (Shear Stress and Strength) for 10 Major Landslide Locations

The Mohr envelope is the graphical representation of geo-technical parameters which indicate the stability condition of different locations. Cohesion is low everywhere because of the entrainment of finer particles from the sub-surface layer by leaching processes, disintegration and decomposition by physical as well as chemical processes and obviously by soil saturation. In Tindharia (Fig. 6.2) and Lower Paglajhora (Fig. 6.4) the internal friction is around 19° and angle of rupture is 35°16′ and 35°30′ respectively. Mahanadi (Fig. 6.5) and Gayabari Lower Slope (Fig. 6.6) is experiencing the safety factor more than one which indicates slightly higher shear strength than shear stress. Cohesion of the soil is very low that ranges between 0.03 and 0.16. Water acts in a number of ways for removal of lateral support by toe erosion, decrease in shearing resistance, entrainment of finer matrix from the slope material and setting the coarser fraction to move, and increase in

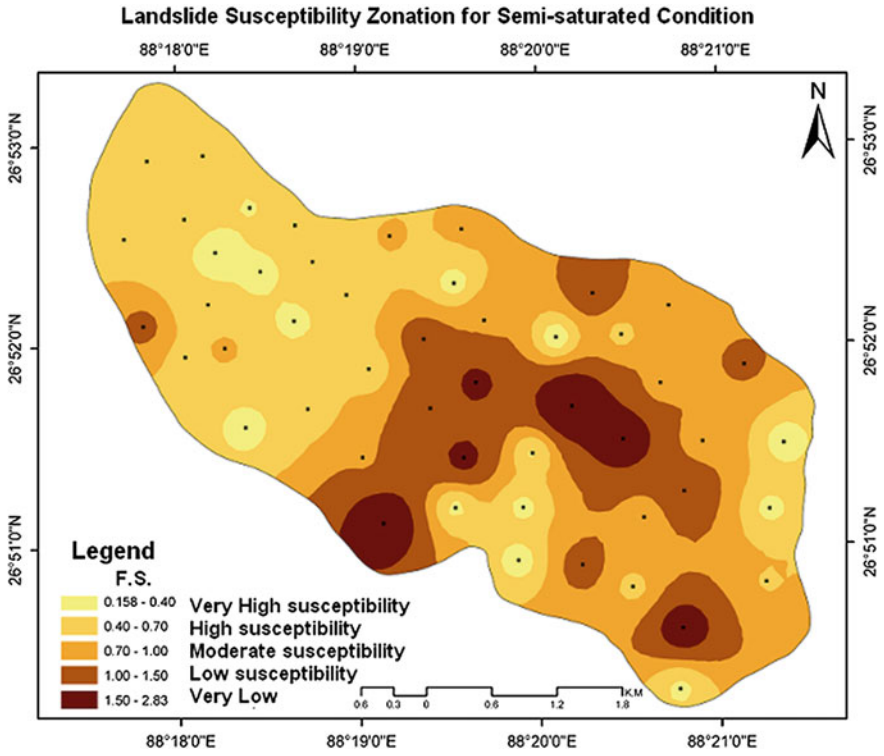

Fig. 6.4 Landslide susceptibility under semi-saturated condition

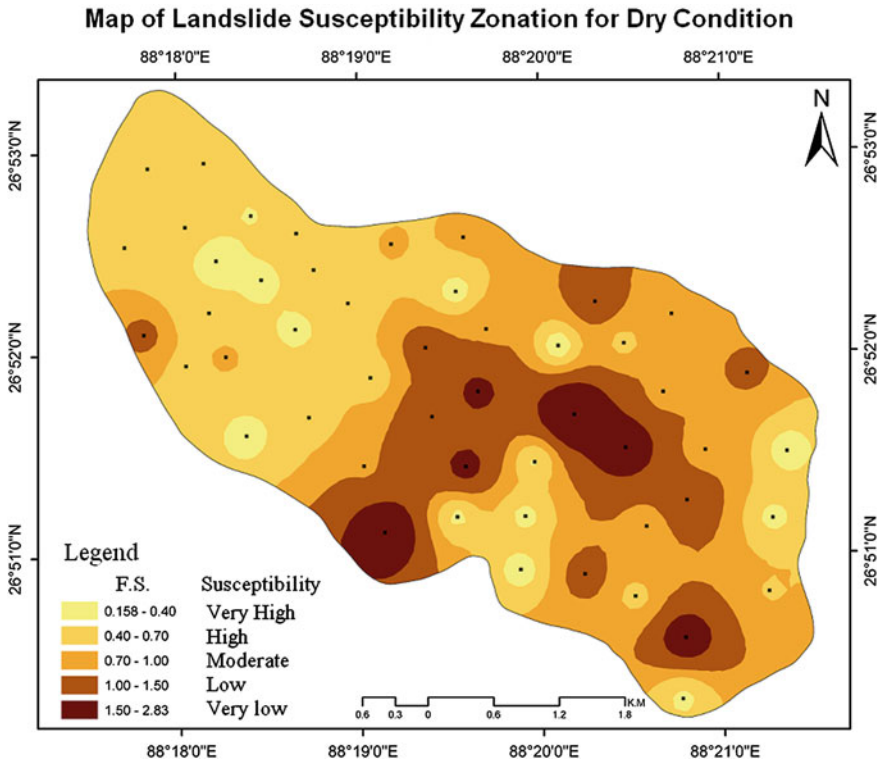

Fig. 6.5 Landslide susceptibility under dry condition

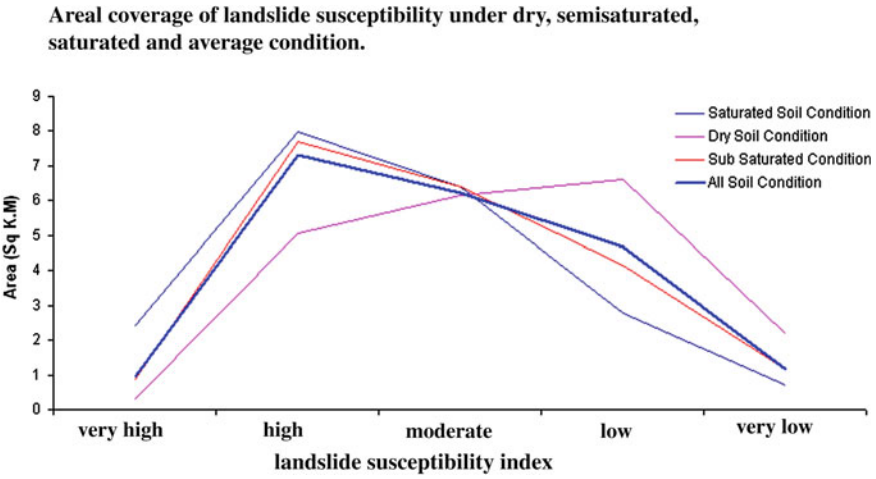

Fig. 6.6 Graphical presentation of landslide susceptibility in all conditions

pore water pressure to reduce the cohesion within the soil particles. All these as a whole, affect the slope stability. At Tindharia Proper, 14 miles Bustee, Nurbong T. E., Central part of the Basin, Shiviter T.E. the angle of rupture is 33°, 34°, 34°30° 32° and 34°15′ respectively (Table 6.2, Figs. F.1, F.2, F.3, F.4, F.5, F.6, F.7, F.8, F.9, and F.10, Appendix-G). The geotechnical parameters of the soil from different locations of the Shivkhola Watershed are represented in the following developed Mohr Stress Circles which depict the visible interpretation about the strength of slope materials (Appendix-G, Figs. F.1, F.2, F.3, F.4, F.5, F.6, F.7, F.8, F.9, and F.10).

6.5.2 *Stability Analysis Based on Safety Factor for 10 Major Landslide Locations*

A stability analysis has been made on the basis of the calculated Safety Factor's value (Table 6.3) from various sites of the Shivkhola watershed which reveals that most of the sites such as Tindharia, Lower Paglajhora (14 miles bustee), Lower Paglajhora (main slide), Tindharia Railway Station, Shiviter, Sepoydhura, Nurbong T.E. and also the mid-section of the Watershed are registered with the Safety Factors value of less than 1 and it can be assumed that the slope materials of all these places are under stress and instable in nature. Remaining soil sample analysis sites (Mahanadi and Gayabari) are attributed as Quasi Stable part.

6.5.3 *Comparative Stability Analysis Between Dry, Semi-saturated and Saturated Soil Condition Based on 1D Slope Stability Model*

The shivkhola watershed exhibits a wide range of elevation (300–2,400 m). Slope ranges between 7° and 65°. The central middle section and lower section of the watershed is attributed with very gentle slope gradient of less than 20° whereas marginal part and extreme north, south and west are characterized by very steep slope of more than 50°. Angle of internal friction varies between 18° and 33° (Table C.1, see Appendix C). Generally, slope materials having coarse grains over the steep slope shows friction friction angle than the materials with finer particles deposited along the foothills zone. At Lower and Upper Paglajhora, Tindharia Upslope, Shiviter and Nurbong the friction angle and cohesion of the soil is very low. Cohesion of the soil is high in the mid and lower part where more than 50 % particles are composed with finer particles.

The intensive field work at 50 sites in the basin reveals that depth of soil varies from 0.45 to 3.75 m in the Shivkhola Watershed. The central mid-section and lower part of the watershed are registered with maximum soil depth whereas marginal part

Table 6.2 Result of geo-technical parameters and safety factor for 10 major landslide sites

Location	σ_3	σ_n	σ_1	τ	Φ	C	λ	α	F.S.
1. Tindharia tea garden	0.90	1.31818	2.15440	0.59036	19°28′	0.123	0.588929	35°16′	0.9975760
2. Lower Paglajhora (14 Miles Bustee)	0.82	1.28942	2.3212	0.69594	22°	0.149	0.6699594	34°	0.962668
3. Lower Paglajhora	0.96	1.4583	2.43794	0.6987	19°	0.162	0.6641329	35°30′	0.950526
4. Mahanadi tea garden	0.98	1.5227	2.86	0.85192	25°	0.145	0.85504667	32°30′	1.003670
5. Gayabari lower slope (780 M)	0.89	1.27784	2.13032	0.5286	22°	0.05	0.56628	34°	1.0712826
6. Tindharia Rly. Stn.	0.92	1.4044	2.553	0.74598	24°	0.105	0.730279	33°	0.9789525
7. Shiviter T.E	0.97	1.402407	2.3351579	0.63508	21°30’	0.07	0.6224228	34°15′	0.9800699
8. Sepoydhura T.E	0.88	1.3098	2.3897	0.681316	25°30’	0.05	0.67474	32°15′	0.990349
9. Nurbong T.E. (sinking zone)	0.93	1.2965	2.0725	0.5333	21°	0.0355	0.5331	34°30′	0.99977
10. Central part of the watershed	0.87	1.403035	2.76818	0.853036	26°	0.15	0.834305	32°	0.978043

σ_1 = major principal stress; σ_3 = minor principal stress; σ_n = normal stress; τ = shear stress; Φ = angle of internal friction; C = cohesion; λ = shear strength; α = rupture angle; and F.S. = safety factor

Table 6.3 Stability analysis for 10 critical locations

Location sites	Under saturated condition		Remarks
	S.F	Stability	
1. Tindharia tea garden	0.997576	Unstable	Further concentration of settlement should be restricted, reduction of slope steepness, draining of seepage water by boreholes to reduce destabilizing factors
2. Lower Paglajhora (14 miles Bustee)	0.962668	Unstable	Surface and sub-surface drainage diversion and monitoring and draining of seepage water by boreholes, restriction on heavy loaded vehicles to reduce destabilizing factors
3. Lower Paglajhora (main slide)	0.950526	Unstable	Sub-surface drainage monitoring and draining of seepage water by boreholes, jhora training through concrete structure
4. Mahanadi tea garden	1.003670	Quasi stable	Drainage network management, plantation and afforestation, construction of retaining walls and concrete drains along the road side are to be taken into consideration in quasi stable area
5. Gayabari lower slope (780 M)	1.071282	Quasi stable	Plantation and afforestation, construction of retaining walls and concrete drains along the road side are to be taken into consideration in quasi stable area
6. Tindharia proper slide (near rly. station)	0.978952	Unstable	Human intervention should be stopped completely, application of geotextile method can bring stability over steep slope
7. Shiviter T.E	0.980069	Unstable	Establishment of horizontal drains to reduce upslope contributing area above the slide and application bio-engineering method to stabilize the slope
8. Sepoydhura T.E	0.990349	Unstable	Deforestation and haphazard concentration of human settlement and their activities should be restricted to get rid of slope failure
9. Nurbong T.E. (sinking zone)	0.99977	Unstable	Draining of seepage water by boreholes and cementing of the cracks over steep slope to reduce destabilizing factors
10. Central part of the watershed from Gayabari	0.978043	Unstable	Afforestation, plantation and other soil conservation technique must be employed. Concrete drains to monitor surface drainage and construction of retaining walls TO to duce the destabilizing factors

(north, south and western part) is attributed with minimum soil depth. Due to steep slope and active soil erosion process, the marginal area is associated with close slip plane below the slope surface due to which soil layers get saturated very easily and causes landslide. Tindharia, Gayabari Upper, Sepoydhura Upslope, Upper Paglajhora, Mahanadi, Shiviter, Gitingia are falling in the marginal minimum soil depth area of the Shivkhola watershed. On the other hand, Shivkhola R.F., and both sides of the main river is characterized by maximum soil depth with low intensity of landslide phenomena. It can be inferred that shallow seated slope instability is intimately related with minimum soil depth with steep slope.

In dry condition, around 15 sq km of the watershed is attributed by moderate to very low landslide susceptibility and only 5 sq km is characterized with high to very high landslide susceptibility with high frequency ratio. Under semi-saturated condition 0.88 sq km area is attributed with high landslide susceptibility. The area of high and very high landslide susceptibility has been increased in saturated soil condition and around 2.5 sq km area is registering high landslide susceptibility with high frequency ratio. For dry and semi-saturated condition, the area under high and very high landslide susceptibility is 5.36 and 8.5 sq km respectively and the area under low to very low landslide susceptibility is around 9 and 5 sq km Under saturated soil condition small area (3.5 %) is experienced with low landslide susceptibility having frequency ratio of 0.00. Around 14 sq km out of total area (21 sq km) of the Watershed is being characterized by moderate to very high landslide susceptibility. Under saturated condition, around 6 sq km areas show the moderate landslide susceptibility with frequency ratio value of 0.39. Upper and Lower Paglajhora, Tindharia, Shiviter and Nurbong are the places where landslide susceptibility ranges from high to very high. Lower middle section and few places of extreme south are characterized by moderate to very low landslide susceptibility (Table 6.4) under all soil saturated condition.

6.5.3.1 Stability Analysis Under Dry Condition

The slope stability map (Fig. 6.5) under dry condition reveals that only 1.58 % area of the watershed is experienced with very high landslide susceptibility where the chance of landslide phenomena is also very high according to the derived frequency ratio value (21.09). High landslide susceptibility is being found in 24.88 % area in the watershed. Maximum area of the Shivkhola watershed (30.25 %) is characterized by moderate landslide susceptibility where the frequency of landslide is 20.835. More than 40 % area of the Shivkhola watershed falls under the low to very low landslide susceptibility with frequency ratio value of 0.27 and 0.00 respectively.

6.5.3.2 Stability Analysis Under Semi-saturated Condition

Under semi-saturated condition the value of safety factor varies from 0.158 to 2.58 and 4.38 % area is under very high landslide susceptibility that is around 2.50 %

Table 6.4 Frequency ratio analysis for dry, semi-saturated and saturated soil condition

Safety factor	Landslide susceptibility	Area in sq km	Percentage of area	Landslide frequency	Frequency ratio
Frequency ratio analysis under dry condition					
0.158–0.40	Very high	0.320933	1.58	8 (33.33 %)	21.09
0.40–0.70	High	5.045979	24.88	9 (37.5 %)	1.50
0.70–1.00	Moderate	6.136645	30.25	5 (20.83 %)	0.67
1.00–1.50	Low	6.602401	30.51	2 (8.33 %)	0.27
1.50–2.83	Very low	2.188175	10.79	0 (0.00 %)	0.00
Frequency ratio analysis under semi-saturated condition					
0.158–0.40	Very high	0.88796	4.38	9 (37.5 %)	8.56
0.40–0.70	High	7.691486	37.88	10 (41.67 %)	1.10
0.70–1.00	Moderate	6.393539	31.47	4 (16.67 %)	0.53
1.00–1.50	Low	4.15209	20.44	1 (4.16 %)	0.20
1.50–2.83	Very low	1.169058	5.76	0 (0.00 %)	0.00
Frequency ratio analysis under saturated condition					
0.158–0.40	Very high	2.430299	11.97	12 (50 %)	4.17
0.40–0.70	High	7.985823	39.36	8 (33.33 %)	0.85
0.70–1.00	Moderate	6.406416	31.58	3 (12.5 %)	0.39
1.00–1.50	Low	2.763299	13.60	1 (4.17 %)	0.31
1.50–2.83	Very low	0.708297	3.50	0 (0.00 %)	0.00

greater than dry condition (Fig. 6.4). 37.88 % area of the basin is dominated by high landslide susceptibility and 31.47 % area is registered with moderate landslide susceptibility and equal chances of landslide occurrence phenomena. About 25 % of the watershed is characterised with low to very low landslide susceptibility condition. Frequency ratio value under semi-saturated condition revealed that the probability of landslide occurrence was very high in the area of very high landslide susceptibility which was followed by high, moderate and low. Under dry condition moderate, low and very low landslide susceptibility area did not have experienced major landslide events and so derived frequency ratio values tent to '0'.

6.5.3.3 Stability Analysis Under Saturated Condition

Under the complete saturated soil condition pore water pressure becomes very high and reduces the cohesive strength of the soil and mountain slope become most unstable. The values of safety factor under saturated condition ranges between 0.13 and 2.30. The area of very high landslide susceptibility had been increased in comparison to dry and semi-saturated condition. More than 50 % area of the Shivkhola watershed is attributed by high to very high landslide susceptibility. 31.585 % areas are under moderate landslide susceptibility where the probability of landslide activities is low. Under the saturated condition 11.97 % area with very

Table 6.5 Accuracy analysis

Class name	Classified total	Number correct	Producers correct	Users accuracy	Accuracy total
Accuracy study under dry condition					
Very low	0	6	0	0.00	0.00
Low	4	3	0	75	0.00
Moderate	10	9	9	90	100.00
High	17	15	14	88.23	93.33
Very high	18	17	15	94.44	88.24
Total	50	50	38		
Overall classification accuracy = 93.86 %					
Overall Kappa statistics = 0.8919					
Accuracy study under semi-saturated condition					
Very low	0	6	0	0.00	0.00
Low	0	7	0	0.00	0.00
Moderate	13	10	9	76.92	90.00
High	20	16	16	80.00	100.00
Very high	17	16	15	94.12	93.75
Total	50	50	40		
Overall classification accuracy = 94.58 %					
Overall Kappa statistics = 0.8919					
Accuracy study under saturated condition					
Very low	0	4	0	0.00	0.00
Low	0	7	5	0.00	71.43
Moderate	12	7	6	58.33	85.71
High	16	13	11	81.25	84.62
Very high	22	16	16	72.73	100
Total	50	50	38		
Overall classification accuracy = 85.44 %					
Overall Kappa statistics = 0.8919					

high landslide susceptibility shows the greater chances of landslide phenomena (Fig. 6.3). Extension of Very high landslide susceptibility under saturated condition is due to saturation of slope materials and heavy pore water pressure.

6.5.4 Accuracy Result

The comparison between assumed true data and randomly selected data from the classified image shows that the overall classification accuracy for dry, semi-saturated and saturated conditions are 93.86, 94.58 and 84.44 % respectively.

The accuracy results in different landslide susceptibility classes under dry, semi-saturated and saturated conditions are stated in Table 6.5.

6.6 Conclusion

Stability analysis on the basis of calculated safety factor values and stability classes from major landslide location shows that the places of Paglajhora, Tindharia, Shiviter T.E., Sepoydhura, and Nurbong are unstable and only Gayabari and Mahandi are quasi-stable in nature. Analysis of the geo-technical parameters reveals that the cohesion of soil ranges between 0.03 and 0.16 and angle of internal friction varies between 18° and 34°. But the major landslide location sites in the study area are registered with the friction angle from 18° to 24°. There is a tendency of an increase in areal extension of high to very high landslide susceptibility area in saturated soil condition rather than dry and semi-saturated soil. This situation indicates that soil saturation and reduction of soil cohesion is the important landslide contributing factor in the Shivkhola Watershed. Under saturated condition more that 50 % area are characterized by high to very high landslide susceptibility. More than 35 % area is dominated by high landslide susceptibility under semi-saturated condition and only 1.58 % area is experiencing very high landslide susceptibility under dry condition (Fig. 6.6). The prepared landslide susceptibility maps for all three conditions (dry, semi-saturated and saturated) express a reasonable accuracy i.e. 93.86, 94.58 and 85.44 % respectively. Moderately steep slope with low friction angle and less cohesion is very much prone to slope instability in the Shivkhola Watershed.

The prepared maps may offer useful tool for the installation and the continuous monitoring of the geotechnical attributes measuring apparatus/instruments such as field shear box for measuring the shear strength properties of the soil, permeameter, double ring infiltrometer, and piezometer to measure soil pore water pressure. The monitoring result must be served to the local Govt. Local people are to be made aware of the triggering geotechnical factors through and they are to be brought into the active monitoring and management system.

There is no any unique and generalized model available for the preparation and identification of slope instability sites as the instability condition depends upon various factors which vary from one place to others. So, one simple model could not be accepted for all landslide locations. Considering all the landslide triggering factors of the study area, one dimensional slope stability model has been adopted to conceive the spatial distribution slope instability. In the present work, our approach is to determine the potential instability location in connection to spatial distribution of geotechnical parameters. Based on the analysis priority was fixed and management options could be followed up for the Shivkhola watershed. It is observed from the study that the areal extent of potential slope instability and the chances or probability of slip under saturated condition is very high as a result of soil saturation and increased pore water pressure, less cohesion, and low friction angle. Steep slope

sites i.e. Paglajhora (lower and upper), Tindharia, Nurbong, Shiviter and Mahanadi are very much subjected to slope instability. The mid-central steep slope of the watershed must be brought under immediate attention as the propensity of areal increase in slope failure is very high as a result of drainage concentration and the percolation of water through weak lithological composition.

References

Anabalagan R (1992) Landslide hazard evaluation and zonation mapping in mountainous terrain. Eng Geol 32:269–277

Basu, S. R. and Maiti, R. K. (2001) Unscientific mining and degradation of slopes in the Darjeeling Himalayas, Changing Env. Scenerio of the Indian Subcontinent (Bd) pp 390 – 399

Bhattarai P, Aoyama K (2001) Mass movement problems along Prithwi highway Nepal. Annual Report of Research Institute for Hazards in Snowy Areas, vol 23. Niigata University, Niigata, pp 85–92

Billings MP (1987) Structural geology, 3rd edn. Prentice Hall, New Delhi

Bloom AL. (1991) Geomorphology, a systematic analysis of the Cenozoic Landforms. Prentice Hall, New Delhi, pp 76–177

Borga M et al (1998) Shallow Landslide hazard assessment using a physically based model and digital elevation data. J Environ Geol 35(2–30):81–88

Brardinoni F, Church M (2004) Representing the landslide magnitude frequency relation. In: Kirkby JM, Darby ES (eds) Earth surface processes and landforms, vol 29, no 1. Capilano river basin, British Colombia, pp 115–124

Brudsen D (1979) Mass movement. In: Embelton C, Thornes J (eds.) Process in geomorphology. Wiley, Hoboken, pp 130–186

Burton A, Bathurst JC (1998) Physically based modeling of shallow landslide erosion and sediment yield at a catchment scale. Environ Geol 35(2–3):89–99

Carrara A et al (1991) GIS technique and statistical models in evaluating landslide hazard. Earth Surf Process Land 16(5):427–445

Carson MA (1975) Threshold and characteristic angles of straight slopes. Proceedings of the 4th Guelph Symposium on Geomorphology, Norweich Geo Books, 19–34

Carson MA (1977) Angles of repose, angles of shearing resistance at angle of talus slopes. Earth Surf Process 2:363–380

Cernnica JN (1995) Geo-technical engineering: soil mechanics. Willy, Hoboken

Congalton R (1991) A review of assessing the accuracy of the classification of remotely sensed data. Remote Sens Environ 37:35–46

Crozier MJ (1986) Landslides: causes, consequences and environment. Croom Helm Australia Pty Ltd, London, p 252

Deoja BB et al (1991) Mountain risk engineering handbook. International centre for integrated mountain development (ICIMOD). Kathmandu, p 875

Dhakal AS et al (2000) Landslide hazard mapping and its evaluation using GIS: an investigation of sampling schemes for a grid-cell based quantitative method. Photogrametric Eng Remote Sens 66(8):981–989

Gao J (1993) Identification of topographic settings conducive to landsliding from DEM in Nelson County. Earth Surf Process Land 18:579–591

Glade T (1998) Establishing the frequency and magnitude of landslide-triggering rainstorm events in New Zealand. Environ Geol 35:160–174

Guzzeti F, Cardinali M, Reichenbach P, Carrara A (1999a) Comparing landslide maps: a case study in the upper Tiber River Basin, central Italy. Environ Manage 18:623–633

Guzzeti F, Cardinali M, Reichenbach P, Carrara A (1999b) Landslide hazard evaluation: an aid to a sustainable development. Geomorphology 31:181–216
Guzzeti F, Cardinali M, Reichenbach P, Ardizzone F, Galli M (2003) Impact of landslides in the Umbria region, central Italy. Nat Hazards Earth Syst Sci 5:1–17
Hammond C et al (1992) Level I stability analysis (LISA) documentation for Version 2. General Technical Report INT-285, USDA forest Service, Intermountain Research Station, p 121
Montgomery DR, Dietrich WE (1989) Source areas, drainage density and channel initiation. Water Resour Res 25(8):1907–1918
Montgomery DR, Dietrich WE (1994) A physically based model for the topographic control on shallow land sliding. Water Resour Res 30(4):1153–1171
Neill and Mark (1987) On the frequencu distribution of land slope, Earth Surface Processes and Landforms, vol.12, ISSUE-2, pp127–136
Pack RT, Tarboton DG, Goodwin CN (1998) Terrain stability mapping with SINMAP, Technical description and users guide for version 1.00, Report and software. http://www.engineering.usu.edu/dtarb/. Accessed 15 June 2007
Smedt F (2005) Slope instability analysis using GIS on a regional scale: a case study of Narayanghat-Mungling highway section, Nepal, a dissertation report presented at Universiteit Gent. Vrije Universiteit Brusssel, Belgium
Soeters R, Westen CJ (1996) Slope instability recognition, analysis and zonation. In Turner AK, Schuster RL (eds) Landslides: investigation and mitigation. Transportation Research Board Special Report 247, 129–177
Terzaghi K (1950) Mechanism of landslides, in application of geology to engineering practice. Barkley Volume, Geological Society of America, pp 83–123
Tiwari B, Marui H (2001) Shearing behaviour of landslide sliding and mining scarp soil during drained ring shear test. In: Proceedings of 15th international conference on soil mechanics and geotechnical engineering, vol 1, Istambul, pp 295–298
Tiwari B, Marui H (2002) Mechanism of shear zone formation and its effect in residual shear strength. In: Proceedings of 3rd international conference on landslides, slope stability and safety of infrastructure, pp 4–133
Tiwari B, Marui H (2003) Estimation of residualshear strength for bentonite-kaolin-Toyoura sand mixture. J Jpn Landslide Soc 40(2):124–133
Tiwari B, Marui H (2004) Objective oriented multi-stage ring shear test for the shear strength of the landslide soil. J Geotech Geoenv Eng ASCE 130(2):217–222
Van Burkalow A (1945) Angle of repose and angle of sliding friction: an experimental study. Geol Soc America Bull 56:669–707
Vanmarcke EH (1977) Reliability of earth slopes. J Geotech Eng Div ASCE 103:GT11
Varnes DJ (1958) Landslide types and processes. In: Eckel EB (ed) Landslides engineering practice: highway research board, Special Report 29, vol 544. NAS-NRC Publication, pp 20–47
Waltham, T. (2002) Foundations of Engineering Geology
Windisch EJ (1991) The hydraulics problem in slope stability analysis. Can Geotech J 28 (6):903–909
Wu W, Siddle RC (1995) A distributed slope stability model for step forested basins. Water Resour Res 31:2097–2110
Young A (1963) Deductive models of slope evolution. Rep Int Geogr Un Slopes Comm 3:45–66

Chapter 7
Application of Analytical Hierarchy Process (AHP) and Frequency Ratio (FR) Model in Assessing Landslide Susceptibility and Risk

Abstract To prepare landslide susceptibility map of the Shivkhola watershed, one of the landslide prone part of Darjiling Himalaya, RS and GIS tools were being used to integrate 10 landslide triggering parameters like lithology, slope angle, slope aspect, slope curvature, drainage density, lineament, upslope contributing area (UCA), road contributing area (RCA) settlement density, and land use and land cover (LULC). *Analytical Hierarchy Process* (AHP) was applied to quantify all the factors by estimating factors weight on MATLAB Software with reasonable consistency ratio (CR). *Frequency ratio model* (FR) was used to derive class frequency ratio or class weight incorporating both pixels with and without landslides and to determine the relative importance of individual classes. All the required data layers were prepared in consultation with SOI Topo-sheet (78B/5), LIIS-III Satellite Image (2010) by using Erdas Imagine 8.5, PCI Geomatica, and ARC GIS Software. The weighted linear combination (WLC) method was followed to combine factors weight and class weight and to determine the landslide susceptibility coefficient value (LSCV or 'M') on GIS platform. Greater the value of 'M', higher is the susceptibility of landslide. The Shivkhola watershed was classified into five landslide susceptibility zones by averaging window lengths of 3, 5, 7, and 9 and taking into account the landslide threshold boundaries value of 7.05, 9.29, 11.5, and 13.8. The overall classification accuracy rate is 92.22 % and overall Kappa statistics is 0.894. The elements like weighted LULC map, RCA (road contributing area) map and settlement density map were developed and their weighted linear combination was performed to prepare *landslide risk exposure* map. Then by integrating *landslide susceptibility map* and *landslide risk exposure map* landslide hazard risk co-efficient values were derived and a classification was incorporated on ARC GIS Platform to prepare *landslide hazard risk map* of the Shivkhola watershed. To evaluate the validity of the *landslide hazard risk map*, probability/chance of landslide hazard risk event has been estimated by means of frequency ratio (FR) between landslide hazard risk area (%) and number of risk events (%) for each landslide hazard risk class. Finally, an accuracy assessment was made through a comparative study between true GPS derived data and a set of randomly selected pixels points from the classified image corresponding to the true data from 50 locations on ERDAS Imagine (8.5) which depicts that the classification accuracy of the *landslide hazard risk map* was 92.89 with overall Kappa statistics of 0.8929.

S. Mandal and R. Maiti, *Semi-quantitative Approaches for Landslide Assessment and Prediction*, Springer Natural Hazards, DOI 10.1007/978-981-287-146-6_7

Keywords Landslide susceptibility · Landslide risk · Analytical hierarchy process (AHP) · Frequency ratio (FR) · RS and GIS · Accuracy assessment

7.1 Introduction

The identification of the causative factors is the basis of many methods of landslide susceptibility assessment. In most of the cases, the landslide is the critical mechanism of erosional processes and in such condition, landslide is inevitable and necessary part of the natural landscape process system. Although the occurrences of landslide hazards and its impact on human society cannot be prevented fully by analyzing the slope stability condition, but the better understanding of geo-technical attributes of the soil can contribute to greater knowledge and understanding about the spatial distribution of slope instability which are very much essential for land use planning. Landslides are the results of two interacting sets of forces; *the precondition factors*, naturally induced which govern the stability conditions of slopes, and *the preparatory and triggering factors,* induced either by natural factors or by human intervention. Landslide analysis is mainly done by assessing Susceptibility, Hazard and Risk (Einstein 1988). RS and GIS based landslide hazard zonation approach had been studied by Anabalangan (1992), Muthu and Petrou (2007) and Caiyan and Jianping (2009). Rowbothan and Dudycha (1998), Donati and Turrini (2002), Lee and Choi (2003), Lee et al. (2004a, b), Lee and Pradhan (2006, 2007), Pradhan and Lee (2010a, b, c), Sarkar and Kanungo (2004), Sharifikia (2007), Pande et al. (2008) and Nithya and Prasanna (2010) studied and applied the probabilistic model for landslide susceptibility and risk evaluation. Guzzetti et al. (1999a) summarized many landslide hazard evaluation studies. Jibson et al. (2000) and Zhou et al. (2002) applied the probabilistic models for landslide risk and hazard analysis. Atkinson and Massari (1998) and Vijith and Madhu (2008) introduced the logistic regression model for landslide hazard mapping. Landslide hazards were evaluated by using fuzzy logic, and artificial neural network models were used in the works of Gokceoglu et al. (2000) and Pistocchi et al. (2002). Landslide Susceptibility mapping using either multivariate or bivariate statistical approach considered the historical link between landslide controlling factors and the distribution of landslides (Guzzetti et al. 1999b, c).

The models in connection to the slope stability, shallow and deep seated landslides were introduced and verified by Varnes (1958), Young (1963), Vanmarcke (1977), Burton and Bathrust (1998), Bradinoni and Church (2004). The geotectonic factors of slope instability were studied in details by Brudsen (1979), Windisch (1991), Carson (1975, 1977) and Borga et al. (1998). Comprehensive list of stability factors commonly employed in the factors mapping approach was prepared by Crozier (1986) and Tiwari and Marui (2001, 2002, 2003, 2004). *Analytical Hierarchy Process* (AHP), a semi-quantitative method based on decomposition, comparative judgement, and synthesis of priorities are often very much useful for

regional susceptibility studies as suggested by Saaty (1980), Soeters and Van Westen (1996), Mwasi (2001), Nie et al. (2001), Yagi (2003), Komac (2006), Yalcin and Bulut (2007), Kamp et al. (2008) and Yalcin (2008). The frequency ratio (FR) model has become very popular as realistic quantitative approach in the landslide susceptibility mapping. This approach is related with the historical landslide events and their areal coverage. Lee and Pradhan (2007) argued that frequency ratio model provides a correlation between the historical slide locations and various influencing factors under consideration. Intarawichian and Dasananda (2011) applied frequency ratio model to analyze slope instability and ascribed the model as a popular quantitative method.

The present study deals with the estimation of factor's weight and class frequency ratios using 'AHP' and 'FR' model respectively. Integration between factor's weight (FW) and class frequency ratio (FR) was performed with the help of a *liner combination model.* This is done to derive pixel wise landslide susceptibility index values (LSIV) on GIS platform and to prepare landslide susceptibility map.

Landslide hazard risk analysis is the assessment of the probability of the damage of land and associated resources of different magnitudes that may occur in a region due to landslides. Earlier attempts to reduce landslide risk is largely a history of management of landslide terrain by construction of protective structures or monitoring and warning systems, or the ever-increasing sophisticated methods for mapping and delineating areas prone to landslide (Dai and Lee 2002). Risk of landslide is normally defined as the expected number of lives lost, persons injured, property damages and disrupted economic activities due to particular landslide hazard for a given area and reference period (Varnes 1984). To reduce the risk from the landslide events, the knowledge about potentiality to slope instability is crucially needed. Information of landslide events are described in the form of landslide susceptibility map of the concerned region and the preparation of this map depends largely on the complex sets of knowledge of controlling slope movement factors. Landslide analysis is mainly done by assessing susceptibility, hazard and risk (Einstein 1988). The process of creating the maps involves several qualitative or quantitative approaches (Soeters and Van Westen 1996; Guzzetti et al. 1999a; Van Westen et al. 2008). Jibson et al. (2000), Praise and Jibson (2000) and Zhou et al. (2002) have applied the probabilistic models for landslide risk and hazard analysis. *Landslide hazard risk map* was made integrating *landslide susceptibility map* and *landslide risk exposure map* on ARC GIS platform to identify the spatial distribution of potential risk prone area in a representative drainage basin, over which the attributes of land, soil and water exhibit a spatial order away from the water divide in an interacting combination with human actions.

Tectono-statigraphically, the study area, Shivkhola Watershed is located in the southern escarpment slope of Darjiling Himalaya, where high grade metamorphic rocks of the Darjiling and Chungthang groups are thrusted over low grade metamorphic rocks of the Daling Group along the *MCT* (Main Central Thrust, Mallet 1875; Sinha-Roy 1982). Main Central Thrust (*MCT*) and Main Boundary Thrust (*MBT*) are passing through the study area (Fig. 7.1). The *MCT* (a major ductile shear zone) has divided two major litho-tectonic units, the Higher Himalayan

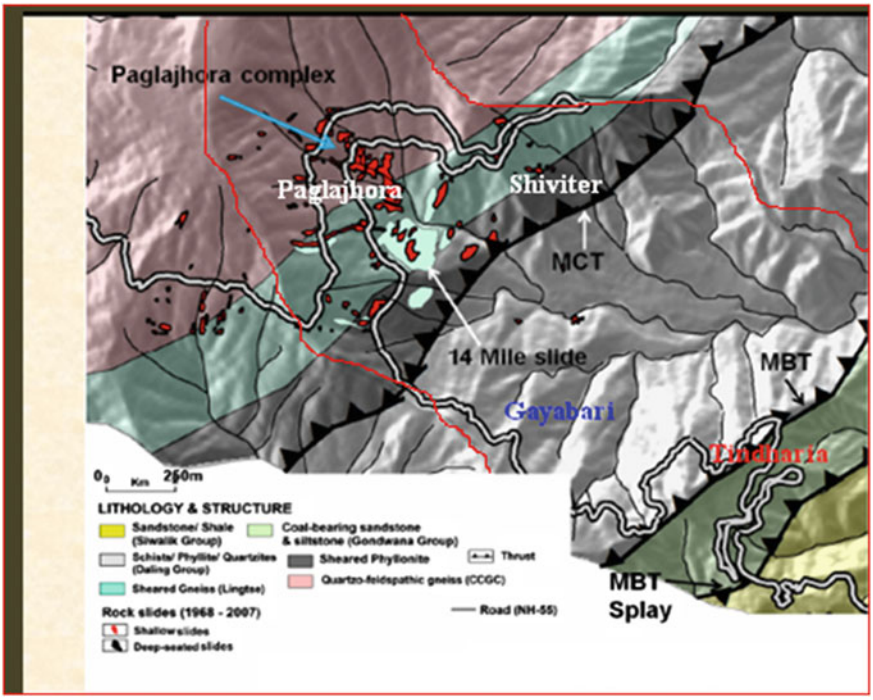

Fig. 7.1 Tectono-stratigraphy and past landslide in the Shivkhola watershed (Mandal and Maiti 2013)

Crystalline Sequence (*HHCS*) and the Lesser Himalayan Sequence (*LHS*) *in Darjiling Himalaya*. The *HHCS* comprises of quartzo-feldspathic gneisses of both igneous and sedimentary origin which suffers high grade of metamorphism (Catlos et al. 2001). The *LHS* is dominated by garnet-biotite-mica schist and chlorite schists in the upper part and slates and phyllites in the lower. The picturesque landslide affected areas are Paglajhora, Tindharia, Mahanadi, Jogmaya and Shiviter. During rainy season water percolates through the exposed rock joints and entrains the finer particles and reduces the cohesive strength of the soil.

The rapid urbanization and expansion of tourism in Darjiling Himalaya are putting unprecedented pressure on land and soil with the gradual elimination of vergin forest land after independence. Lack of land use planning coupled with vulnerable geological structure and heavy frequent rainfall have led to the formation of vicious cycle of soil erosion and landslide during and after monsoon seasons, causing devastating damage to human lives and properties. Significant studies in Darjiling Himalaya identified the causes and consequences of major landslide

occurrences phenomena (Dutta 1966). Since 1968, the Shivkhola watershed of Darjiling Himalaya faced 128 approachable landslide events, of which 76 events were identified as reactivated (not 70 m away from old slided area) and 52 as fresh events (70 m away from the old slided area) (Appendix D, Table D.1). The considered landslide events took place in 16 years and out of which 12 years were recognized as the major landslide years. All the landslide events occurred during the monsoon period being triggered by continuous and heavy showers. Rainfall on all the major landslide events date was more than the critical rainfall calculated after Borga et al. (1998). Most of the landslide events occurred in the lithological unit of Darjeeling Gneiss, Daling, Damuda and Siwalik.

In the present study of landslide hazard risk mapping in Shivkhola Watershed of Darjiling Himalaya prioritized class ranking value (PCRV) and prioritized factors rating value (PFRV) for each thematic data layers and their consistency checking was accomplished through pair-wise comparison matrix as described by Saaty (1980, 1990, 1994), and Saaty and Vargas (2001). *Landslide hazard risk map* was made integrating *landslide susceptibility map* and *landslide risk exposure map* on ARC GIS platform to identify the spatial distribution of potential risk prone area.

In the Shivkhola Watershed, Lower Paglajhora, Tindharia, Shiviter and Mahanadi are the major and prominent landslide location sites where settlement, communication lines, and tea garden area are being affected severely. Since 1968, Paglajhora alone has had 10 landslide events, all in the above mentioned landslide event years. The majority of these landslides was dangerous as in most of the events Hill Cart Road (NH-55) was affected and the communication line between Siliguri and Darjiling was completely interrupted, from days to month. Paglajhora sinking zone faced massive slope failures in 1998, 2002, 2005 and 2011 which indicates that the occurrence of landslides in the region is ongoing. This poses a tremendous threat to upslope settlement and Hill Cart Road (life line between Siliguri and Darjiling Town). The landslide events at Tindharia also used to cut-off the Hill Cart Road and brought tremendous threat to tourists, upslope settlements and tea gardens. In Shiviter, around 8 acres of land were destroyed by the destructive slope failure in the past 10 years. The physiographic configuration (arcuate) that provide a favourable condition for producing hydrostatic pressure, proximity to Main Central Thrust (MCT) and Main Boundary thrust (MBT), intensely fractured and sheared bed rock, toe cutting and headward erosion of debris covered slope by fast flowing tributaries, immense pressure over the fragile slope materials by man-made concrete structure, moderate to steep slope gradient, improper drainage and accumulation of highly anisotropic materials with a great thickness and low shearing resistance have made these landslide locations in the Shivkhola watershed most unstable in character. The main purpose of the present study is to prepare landslide susceptibility map and landslide hazard risk map applying RS and GIS semi-quantitative approach and to compare risk dominated part of Paglajhora, Tindharia, and Shiviter with the prepared risk map by incorporating landslide inventory statistics and frequency ratio (FR) analysis.

7.2 Materials and Methods

The thematic data layers of all the landslide inducing factors were integrated to prepare landslide susceptibility map using a linear combination model in GIS. The Analytical Hierarchy Process (AHP) was used to derive prioritized factor rating value (PFRV) and a FR Model was applied to obtain prioritized class rating value (PCRV) for all the landslide triggering factors considered in the study. The integration between PFRV and PCRV were made in a linear combination model on GIS platform to estimate *landslide susceptibility index value* (LSIV) for each pixel and a suitable classification technique was incorporated to prepare the landslide susceptibility map of the Shivkhola watershed. The data used in the present study are Satellite image (IIRS P6/Sensor-LISS- III, Path-107, Row-052, date-18/03/2010), modified SRTM data with scene size 1° lat. and 1° long. (date-5th April, 2008), Google Earth Image (1st September, 2010), Geological Map (Geological Survey of India, East Kolkata) and Topographical Map (78B/5, Survey of India). Data layers for landslide inducing factors were generated using ERDAS Imagine 8.5, Arc View and ARC GIS Software.

7.2.1 Landslide Susceptibility Assessment

The following section presents the methods and results of the landslide susceptibility analyses in this study.

7.2.1.1 Determination of Landslide Triggering Factors

The landslide triggering factors were identified by interviewing the local people and an investigation of the landslide sites in the watershed through intensive fieldwork. During 10 days field work in July 2011, landslide locations were identified and marked with GPS. Lithological structure, land use and land cover type around the landslide scar, slope angle, construction of human structure and their role to promote landslide, drainage network, altitude and slope aspects were investigated to determine landslide triggering factors. The landslide triggering factors including lithology, slope angle, drainage, slope aspect, slope curvature, lineament, upslope contributing area (U.C.A.), land use/land cover, road contributing area (RCA) and settlement density were taken into account to prepare landslide susceptibility map of the Shivkhola watershed and their hierarchical arrangement was made on priority basis. Shivkhola watershed is a small mountain basin where rainfall is uniformly distributed over the entire area, so rainfall intensity was not considered in the landslide susceptibility calculation (Mandal and Maiti 2011, 2012, 2013).

7.2.1.2 Generation of Landslide Inducing Factor Maps

First, the *contour map* at 20 m interval was prepared and digitized from the SOI Topo-sheet (1987, 78B/5) at the scale of 1:50,000 and subsequently employed for generating the Digital Elevation Model (DEM) using ARC GIS Software. Then *slope gradient*, *slope curvature* and *slope aspect map* were derived from DEM and classification was made to derive all these parameters in raster value domain following the earlier works of Dhakal et al. (2000). Surface curvature is a topographic attribute that describes the convexity/concavity of a terrain surface. Curvature depicts the slope gradient or slope direction (aspect), usually in a particular direction. A positive curvature indicates that the surface is upwardly convex at a grid cell and a negative curvature indicates that the surface is upwardly concave at that grid cell. A value of zero indicates that the surface is flat. The expected values of all three output raster images for a hilly area can vary from −0.5 to 0.5; for steep, rugged mountains the value can vary between −4 and 4.

The *lithological map* of the study area was collected from Geological Survey India (GSI), Kolkata (Eastern Region) and necessary modifications were incorporated after intensive field investigation. Final lithological map was prepared and transformed into raster value domain on ARC GIS Platform. Class weight value for each lithological class was assigned according to rock mass strength, described by GSI. A Drainage density map (length of drainage/m^2) was made from the topographical map (78B/5, 1987) and classified into ten equal intervals.

The *lineament* exhibits the zone of weakness surface of some linear to curvilinear features such as fracture, joint, fault etc. in the geological structure. There are no basic differences between these three features. All these linear to curvilinear features were identified as the same deformed surface where the propensity of slope instability is very high. To generate lineament map (distance from lineament in meters) of the Shiv-khola watershed, PCI-GEOMATICA was used and in the extraction process 3 SRTM bands of wavelengths were taken into account: Near Infrared (Band-I; 0.7–1.3 μm), Red (Band-II; 0.6–0.7 μm) and Green (Band-III; 0.5–0.6 μm). The '*Lineament extraction*' algorithm was used to prepare lineament map. The study area was classified into ten classes on the basis of the distance (m) from lineaments.

Upslope Contributing Area is an effective indicator of drainage concentration over space. The place with more contributing area encompasses more soil saturation that reduces soil cohesion. The specific contributing area (total contributing area divided by the contour length) is computed by distributing flow from a pixel among its entire lower elevation neighbour pixel (Borga et al. 1998). Quinn et al. (1991) proposed that the Fraction of Flow (F_i) allocated to each lower neighbour (i) is determined by using Eq. 7.1. An upslope contributing area map was prepared based on calculated contributing area value for each (0.25 km^2) grid and it was divided into 6 equal classes (Fig. 3.7, Chap. 3).

$$F_i = \frac{\text{SiLi}}{\sum \text{SiLi}} \tag{7.1}$$

where, the summation (Σ) is for the entire lower neighbour; S is the directional slope, and L is an effective contour length that acts as the weighting factor. The value of L used here is 10 m of the pixel size of the cardinal neighbour and 14.14 m of the pixel diagonal for diagonal neighbour.

The *road contributing area* (*RCA*) *map* (Fig. 7.6) was made by multiplying road contributing length (RCL) with road contributing width (RCW) with eight equal classes from the concerned topographical sheet and it was converted into raster value domain on ARC GIS Platform. The *Settlement Density Map* (Fig. 7.4) was prepared by applying 3 × 3 karnel in ARC GIS platform and the whole basin was classified into seven equal density classes. Land use and land cover (LULC, Fig. 7.5) map of the Shivkhola watershed is prepared with the help of LISS-III Satellite Image (2010) and Google Earth Image in consultation with SOI Topo-sheet (78B/5). After verifying the ground truth with GPS a land use and land cover map is developed in GIS. The Shivkhola Watershed was classified into 10 individual land use type: (i) bare surface, (ii) agricultural land, (iii) jungle, (iv) roads, (v) settlement, (vi) tea garden, (vii) open forest, (viii) degraded forest, (ix) mixed forest and (x) dense forest (Fig. 4.2, Chap. 4).

7.2.1.3 Landslide Inventory Map

A *Landslide Distribution Map/Inventory Map* (Fig. 2.1, Chap. 2) was created to determine landslide affected area (%) and frequency of landslide for each class of the landslide inducing factors/factors. Mandal and Maiti (2011) identified major and minor landslide locations during field investigation and mapped them by evaluating the SOI topographic map (78B/5), satellite image (IRS LISS-III, 2000), SRTM data (2008), and Google Earth Image (2010). Several field investigations were conducted to identify the landslide locations and to cross-check the prepared landslide map. Then, the map was digitized and converted into raster value domain in ARC GIS Software. All the landslide triggering factor maps were linked with the prepared landslide inventory map to understand the degree of importance of each factor in landsliding.

7.2.1.4 AHP and Quantification to Each Factor Map/Prioritized Factor Rating Value

AHP is a decision making and semi-quantitative value judgement approach which serve the objectives of the decision makers. This process is employed to support the decision on the instability rank of the factors by estimating prioritized factor rating value (PFRV). In the AHP, different factor preference and their conversion into

Table 7.1 Scale of preference between two parameters

Scale	Degree of preference	Explanation
1	Equally	Two activities contribute equally to the objective
3	Moderately	Experience and judgement slightly to moderately favour one activity over another
5	Strongly	Experience and judgement strongly or essentially favour one activity over another
7	Very strongly	An activity is strongly favoured over another and its dominance is showed in practice
9	Extremely	The evidence of favouring one activity over another is of the highest degree possible of an affirmation
2, 4, 6 and 8	Intermediate values	Used to represent compromises between the references in weight 1, 3, 5, 7 and 9
Reciprocals	Opposites	Used for inverse comparison

numerical value was accomplished with the help of comparative oral judgment and synthesis of priorities. A couple comparing matrix was constructed on the basis of the preference of a factor as compared with the other factor and arithmetic mean method was applied to arrange landslide triggering factors hierarchically and to determine *prioritized factor rating value/eigenvector* (*PFRV*) with reasonable consistency ratio (CR) on MATLAB software after Saaty (1980) (Table 7.2). To develop pair-wise comparison matrix, each factor/class was rated against every other factor by assigning a relative dominant value ranging between 1 and 9 on the basis of the relative importance of the factors in terms of landslide frequency. The value also varies between the reciprocals 1/2 and 1/9 for inverse comparison (Table 7.1).

Another appealing feature of the AHP is the ability to evaluate pair-wise rating inconsistency. The eigenvalues enable to quantify a consistency measure which is an indicator of the inconsistencies or intransivities in a set of pair-wise ratings. Saaty presented that for a consistent reciprocal matrix, the largest eigenvalue λ_{Max} is equal to the number of comparisons n (Table 7.2).

In AHP, an index of consistency, known as the CR (Consistency Ratio), is used to indicate the probability that the matrix judgements were randomly generated (Saaty 1994).

$$CR = CI/RI \tag{7.2}$$

where RI is the average of the resulting consistency index depending on the order of the matrix given by Saaty and CI is the consistency index that is expressed in the following equation. If the value of CR is smaller or equal to 10 %, the inconsistency is acceptable, but if the CR is greater than 10 %, the subjective valued judgement needs to be revised.

A measure of consistency, called consistency index CI, is defined as follows:

Table 7.2 Landslide triggering factors and determined prioritized factor weights

Factors	1	2	3	4	5	6	7	8	9	10	Prioritized rating
Slope	1	2	3	4	5	6	7	8	9	9	0.2944
Lithology	1/2	1	2	3	4	5	6	7	8	9	0.2150
Drainage	1/3	1/2	1	2	3	4	5	6	7	8	0.1537
Lineament	1/4	1/3	1/2	1	2	3	4	5	6	7	0.1087
Curvature	1/5	1/4	1/3	1/2	1	2	3	4	5	6	0.0764
UCA	1/6	1/5	1/4	1/3	1/2	1	2	3	4	5	0.0535
RCA	1/7	1/6	1/5	1/4	1/3	1/2	1	2	3	4	0.0375
LULC	1/8	1/7	1/6	1/5	1/4	1/3	1/2	1	2	3	0.0266
Settlement density	1/9	1/8	1/7	1/6	1/5	1/4	1/3	1/2	1	2	0.0193
Slope aspect	1/9	1/9	1/8	1/7	1/6	1/5	1/4	1/3	1/2	1	0.0149

CI = 0.0615; R.I (random index) = 1.49 and CR = 0.0413 (consistent). *RCA* road contributing area; *UCA* upslope contributing area; *LULC* land use and land cover
Source Saaty (1980)

$$\mathrm{CI} = \lambda_{\mathrm{Max}} - \mathrm{n/n} - 1 \tag{7.3}$$

Saaty and Vargas (2001) randomly produced reciprocal matrices using scales 1/9, 1/8, 1/7, …, 1, …, 8, 9 to evaluate a so called random consistency index (RI). The average RI of 500 matrices is given in Table 7.3.

7.2.1.5 Frequency Ratio Model and Prioritized Class Rating Value

Frequency ratio (FR) model is also a well accepted and popular quantitative approach for the preparation of landslide susceptibility map. Lee and Talib (2005), Pourghasemi (2007), Lee and Pradhan (2007), Jadda (2009), Avinash and Ashamanjari (2010), Intarawichian and Dasananda (2011) successfully applied 'FR' model to generate landslide susceptibility zoning map. To obtain *frequency ratio (FR)* for each class of all the data layers a combination has been established between landslide inventory map and criterion maps using following equation.

$$\mathrm{Fr_i} = \frac{\mathrm{N_{pix(S_i)}}/\mathrm{N_{pix(N_i)}}}{\sum \mathrm{N_{pix(S_i)}}/\sum \mathrm{N_{pix(N_i)}}} \tag{7.4}$$

$\mathrm{N_{pix(S_i)}}$ The number of pixels containing slide in each class (i),
$\mathrm{N_{pix(N_i)}}$ Total number of pixels having class (i) in the whole watershed,
$\sum \mathrm{N_{pix(S_i)}}$ Total number of pixels containing landslide,
$\sum \mathrm{N_{pix(N_i)}}$ Total number of pixels in the whole area of the watershed.

Table 7.3 Random index (RI)

N	1	2	3	4	5	6	7	8	9	10	11	12	13	14	15
RI	0	0	0.58	0.90	1.12	1.24	1.32	1.41	1.45	1.49	1.51	1.53	1.56	1.57	1.59

The derived *frequency ratio* (FR) value of more than '1' indicates, strong and positive relationship between landslide occurrences in each class of the data layers and high landslide susceptibility where 'FR' value of less than '1' depicts the negative and low landslide susceptibility. In this study, 'FR' values for each class were accepted as *prioritized class rating value* (PCRV) or *prioritized class weight* (PCW).

7.2.1.6 Linear Combination Model and Landslide Susceptibility Map

Avinash and Ashamanjari (2010) and Intarawichian and Dasananda (2011) used a landslide susceptibility index value (LSIV) which is the summation of class-and factor-weighted values.

'FR' values for each class (PCRV) or prioritized class rating value, (Table G.1, Appendix G) as well as *prioritized factor's weighted values* (PFRV) for each factor map was taken into account in calculating the *landslide susceptibility index value* (*LSIV*) with the following linear combination model:

$$LSIV = \sum_{i=1}^{n} (W_i * FR_i) \times \mathrm{FV} \tag{7.5}$$

where, n: total number of factors included in the study (n = 10); $W_{i:}$ Factor's weight (PFRV), FV IS factor value, and FR_i: Class Frequency Ratio/class weight.

The 'LSIV' varied from '4.81' to '16.00'. Higher the value of 'LSIV', greater was the propensity of landslide phenomena and vice versa. The LPIV based frequency curve showed many oscillations. To classify the watershed into 5 susceptibility zones moving averages with averaging window lengths of 3, 5, 7, and 9 were considered for smoothing the frequency distribution curve (Fig. 7.2). After analyzing four new curves, the Shivkhola Watershed was classified into 5 landslide susceptibility zones i.e. very low, low, moderate, high, and very high with class boundaries were demarcated at the significant changes of gradient of the curves. The abrupt change points on frequency curve (landslide threshold boundaries) were 7.05, 9.29, 11.5, and 13.8 which were recognized as class boundaries to classify the map. A 3 × 3 'majority filter' technique was applied to the map as a post-classification filter to reduce the high frequency variation.

To verify the landslide susceptibility map, *landslide density* under each susceptibility class was computed. The landslide inventory map was crossed with prepared landslide susceptibility map to derive landslide affected pixels for each susceptibility classes (zones). Research by Sarkar and Kanungo (2004) indicates that the higher the landslide density, greater is the probability and larger the area is affected by landslide in each landslide susceptibility class.

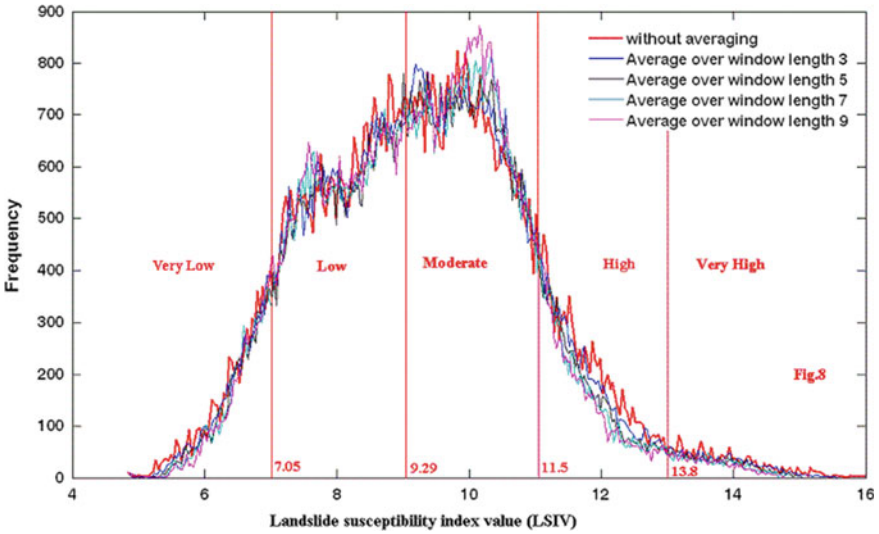

Fig. 7.2 Frequency distribution of landslide susceptibility index value of the Shiv-khola watershed in West Bengal, India

7.2.1.7 Accuracy Assessment of the Landslide Susceptibility Map with Field Data (GPS Survey)

Accuracy assessment is a general term for comparing the classification with geographical data that are assumed to be true, in order to determine the classification process that was accomplished by using Erdas Imagine (8.5). True data were derived by ground truth verification with the help of GPS from the existing 50 landslide locations. Simultaneously, a set of randomly selected 50 reference pixels points from the classified image corresponding to the true data (GPS record) were used for evaluating the validity of landslide susceptibility map after Congalton (1991).

7.2.2 Landslide Risk Assessment

In this study, landslide risk map was made with the help of following principle (Mandal and Maiti 2012).

Landslide Hazard Risk = Landslide susceptibility × Landslide Risk Exposure/ Intensity of Risk Elements.

The entire methodology to prepare the *landslide hazard risk map* of the Shiv-khola Watershed could be summarized under following heads (Fig. 7.3).

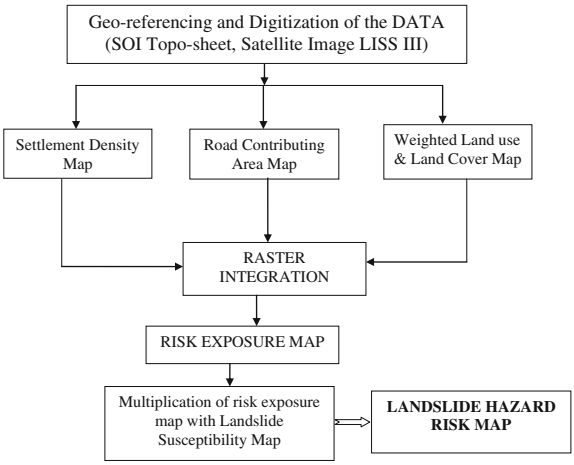

Fig. 7.3 Methodology of landslide hazard risk map

7.2.2.1 Preparation of Weighted Risk Factor/Element Maps (Weighted Land Use/Land Cover Map, Road Contributing Area Map and Settlement Density Map)

In the present study, land use and land cover, road network, and settlement were considered as important risk factors/elements because these three are worst affected by landslide events in the study area. To derive the weighted risk factor maps the developed numerical scale of 1–10 was applied to assign the scores for each class of the risk factor maps. *Weighted land use/land cover map* (Fig. 7.5) is the expression of the intensity of risk induced land use pattern in the Shivkhola watershed. A weighted land use/land cover map was developed assigning more weightage values considering the landslide contributing units to the significant landslide triggering land use pattern i.e. tea garden area, degraded forest, bare surface and agriculture. Weighted value to each class/range of the road contributing area (RCA) map was assigned considering the intensity and impact of road network on landslide and thus a *weighted road contributing area map* (Fig. 7.6) was made on GIS platform. *Settlement Density Map* was prepared by assigning more weighted values to high density class and low for low density class for raster integration and a *weighted settlement density map* (Fig. 7.4) was made accordingly. Three risk factor maps were classified into low, moderate and high intensity zones.

7.2.2.2 Integration Between Weighted Land Use and Land Cover, Road Contributing Area and Settlement Density and the Development of Risk Exposure Map

To integrate risk factor maps prioritized class rating values (PCRV) and prioritized factor rating value (PFRV) were obtained for each class and each risk factors maps developing *couple-comparing matrix* (Table 7.4) according to Saaty (1980). Then,

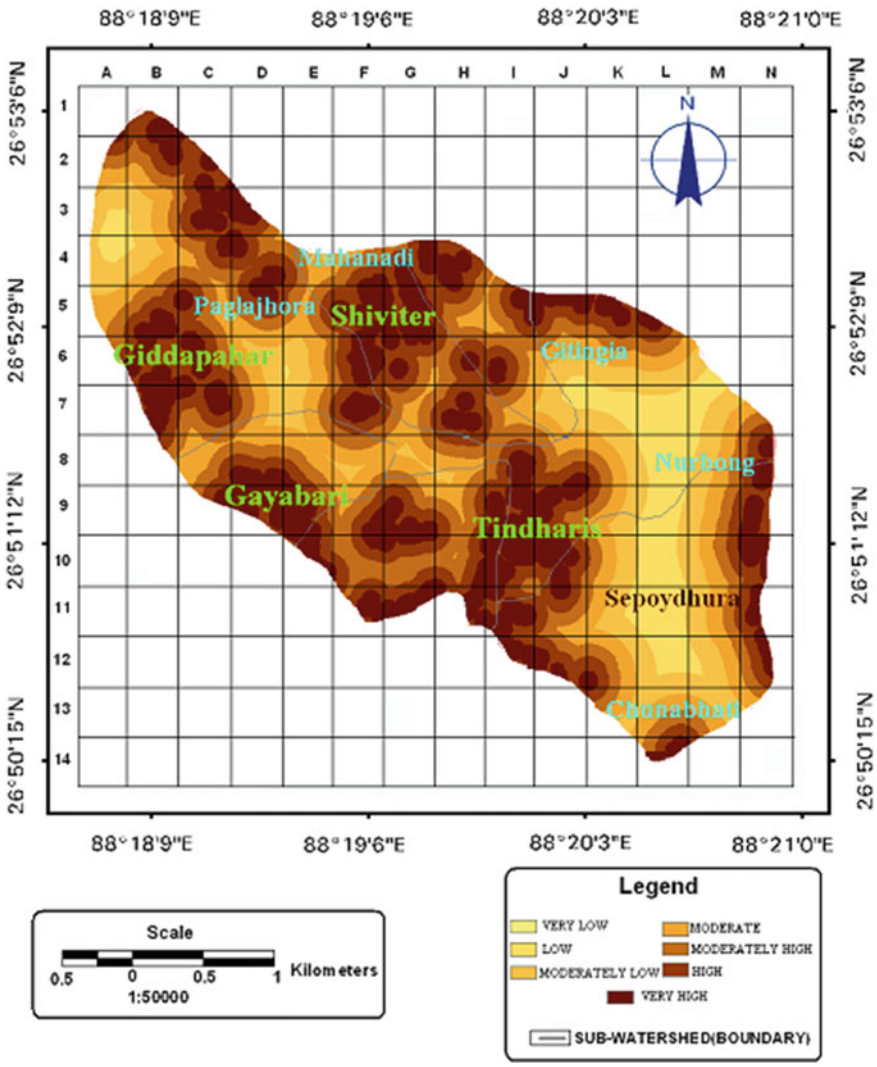

Fig. 7.4 Settlement density map

a linear combination model was performed on ARC GIS platform to derive *landslide risk exposure co-efficient value*. The derived *landslide risk exposure co-efficient value* ranges between 0.19 and 7.24 and here the values of 0.75, 1.45, 2.55, 3.85, 4.90, and 6.15 were taken into account as threshold points to classify the watershed into 7 landslide risk intensity zones. Risk exposure map (Fig. 7.7) shows the intensity of risk elements over the space which were delineated here as very low to very high ranges. The intensity of risk elements are high to very high at Tindharia Upper as well as Lower, very few parts at Gayabari upper slope, Giddapahar, Shiviter, and upper Paglajhora.

Table 7.4 Determined prioritized class rating value (PCRV) and prioritized factor rating value (PFRV) of three landslide hazard risk element maps

Weighted LULC map	Low		Moderate		High	Very high		PFRV-0.691
PCRV	0.06		0.12		0.25	0.55		
Weighted RCA map	Very low	Low	ML	M	MH	H	VH	PFRV-0.218
PCRV	0.02	0.04	0.05	0.09	0.13	0.24	0.43	
Weighted settlement density map	Very low	Low	ML	M	MH	H	VH	PFRV-0.091
PCRV	0.03	0.04	0.05	0.11	0.14	0.27	0.37	

PCRV prioritized class rating value, *PFRV* prioritized factor rating value, *LULC* land use and land cover, *RCA* road contributing area, *ML* moderately low, *M* moderate, *MH* moderately high, *H* high, *VH* very high

7.2.2.3 Preparation of Landslide Hazard Risk Map

The prioritized class rating value (PCRV) against each class of landslide susceptibility map and risk exposure map were estimated by developing couple-comparing matrices on MATLAB Software (Table 7.5) after Saaty (1980). Then, raster integration between *landslide susceptibility* and *landslide risk exposure* was performed by overlay analysis on ARC GIS platform and finally *landslide hazard risk co-efficient* (R) values were derived for each pixel. To classify 'R' value the same method was followed like the landslide susceptibility map and the Shivkhola Watershed was divided into four landslide hazard risk zones i.e. low, moderate, high and very high.

7.2.2.4 FR Study to Establish the Validity of Landslide Hazard Risk Zones

To evaluate the validity of landslide hazard risk map *frequency ratio* (FR) value was estimated for each landslide hazard risk class by means of a ratio between landslide hazard risk area (%) and landslide hazard risk events (%). The 'FR' value approaching towards '0' indicates lower landslide probability and the value approaching away from '0' or toward '1' or more than '1' denotes greater chances of landslide risk event in future. The records of the landslide hazard risk events in the unstable terrain of the Skivkhola watershed were collected from the study accomplished by Basu and Ghatowar (1988), Basu and Sarkar (1985, 1988), Basu and Ghosh (1993), Basu and Maiti (2001), Maiti (2007a, b), Ghosh et al. (2009), and author himself that were taken into account to estimate frequency ration (FR). The records depict that since 1968–2011, the Shivkhola watershed faced 128

Table 7.5 Prioritized class rating value (PCRV) of landslide susceptibility and landslide risk exposure with consistency ratio (CR)

Landslide susceptibility map	Very low (VL)	Low (L)	Moderately low (ML)	Moderate (M)	MH	H	VH	Consistency ratio (CR) = 0.02
PCRV	0.02	0.04	0.12	0.13	0.17	0.19	0.33	
Landslide risk exposure map	Very low (VL)	Low (L)	Moderately low (ML)	Moderate (M)	MH	H	VH	Consistency ratio (CR) = 0.049
PCRV	0.027	0.036	0.053	0.103	0.143	0.266	0.376	

approachable landslide events and amongst them 76 events were treated as reactivated (not 70 m away from old slided area) and 52 as fresh events (70 m away from the old slided area) (Appendix D, Table D.1). Out of 16 prominent landslide events year during the period 1968–2011, 12 years had been recognized as the major landslide hazard risk events years because in these years destructive landslide events completely cut-off communication lines, destroyed human settlements, reduced tea garden area and threatened human lives and properties severely. Considering 36 landslide hazard risk events which occurred within 12 landslide risk event years at different parts of the Shivkhola 'FR' values were derived and probable chances of future hazard risk events were estimated for each landslide hazard risk zone.

7.2.2.5 Accuracy Assessment of the Landslide Hazard Risk Map with Field Data (GPS Survey)

The accuracy assessment of the landslide hazard risk map was made by using Erdas Imagine (8.5). Accuracy assessment is a general term for comparing the classification with geographical data that are assumed to be true, in order to determine the classification process. Basically, the true data were derived for ground truth verification with the help of GPS from the existing/active 50 landslide location with risk elements (settlement, road and tea and agriculture). Simultaneously, a set of randomly selected 50 reference pixels points from the classified image corresponding to the true data (GPS record) were used for evaluating the validity of landslide hazard risk map (Congalton 1991).

7.3 Result and Discussion

7.3.1 Relationship Between Landslide Susceptibility and Landslide Triggering Factors

Landslide susceptibility map of the Shivkhola Watershed was the product of an interaction between factors and existing landslide. *Slope gradient* (Fig. 2.6, Chap. 2) of the watershed varies from very gentle gradient (around 10°) in the mid central and mid-lower part to that of high (more than 60°), towards the marginal part/water divide. Most of the landslide phenomena were found in the area of above 35° slope gradient where class weight value ranges between 5.35 and 77.56 (Appendix G, Table G.1). South, south east, north, east and north easterly facing slope (Fig. 2.7, Chap. 2) were registered with highest class weight values of 29.23, 23.63, 69.63, 53. 51, and 14.86 respectively. All these slope facets were associated with moderate to high landslide susceptibility and large number landslide events. The derived 'FR' and class weight values revealed that high to very high landslide susceptibility zones are characterized by high *positive* and *negative curvature.* Lower Paglajhora, Gayabari

(Lower), Shiviter (Lower), Tindharia T.E. were characterized by upwardly concave or negative curvature and highest class weight value ranging from 52.09 to 165.71. The marginal part of the watershed mainly Upper Paglajhora, 14 miles (upslope) bustee, Gayabari (Upper), and Tindharia (Upper) registered high positive curvature (Fig. 2.8, Chap. 2) with maximum landslide frequency and class weight of more than 40. Lithologically, Darjiling Gneiss, Gorubathan, Lingste Granite and Reyang Formation (Fig. 2.4, Chap. 2) showed the maximum number of landslide phenomena. Probability of Landslide phenomena was very high for the lithological composition of gneiss, mica-schist and granulite. Class weight values of Lingtse Granite, Gorubathan Formation and Chungtung Formation were 48.98, 50.31 and 23.10 respectively (Table G.1, Appendix G). All these lothological groups were accompanied with large number of landslide activities and greater chances of landslip probability in future. *Drainage density* (Fig. 3.6, Chap. 3) was very high at Lower Paglajhora, Gayabari and Shiviter T.E. which were attributed by high landslide susceptibility and high frequency ratio (>2.5). The value of *the drainage density* increased away from the marginal part to the central part. The area having more that 11 km length of drainage/km^2 were attribute with highest class weight (>140) and greater probability of landslide phenomena. The values of *Upslope Contributing Area* (UCA) increases away from the water divide and the maximum of 20.98 km^2 experienced the lower most portion of the watershed (Fig. 3.7, Chap. 3). The upslope contributing area having less than 5 km^2 experienced less saturation excess run-off and less intensity of landslide. The more contributing areas were registered along the main rivers that had maximum length and thus maximum flow. The study envisaged that the place with the UCA of 5.00–10.00 km^2 and 10.00–15.00 km^2 were attributed as high 'FR' value of 1.21 and 1.48 and class weight values of 20.93 and 48.39 respectively. These places were very much prone to landslide. In Shivkhola Watershed tea garden, jungle, roads and settlement (Fig. 7.5) were characterized by high 'FR' of 1.23, 1.15, 1.98 and 1.14 and highest class weight of 23.73, 15.62, 99.31 and 14.09 (Table G.1, Appendix F). The analysis showed that tea garden, road and settlement were dominated by high intensity of landslide and could be treated as maximum probable areas of landslide occurrences. Road contributing area (RCA) was high at the places of Tindharia, Paglajahora, Mahanadi and Shiviter where the landslide frequency was also very high (Fig. 7.6). At all those places the RCA ranged from 0.008 to 0.014 km^2 and the class weight value ranged between 29.84 and 169. 12. In the study area, construction of roads and slope modification caused by human intervention were responsible for slope instability. The moderate to high intensity of human settlement at Tindharia, Gayabari, Shiviter, Mahanadi and Lower Paglajhora (Fig. 7.4) depicted high 'FR' and maximum class weight as well as greater probability of landslip (Fig. 7.7).

In Shivkhola Watershed, Lower Paglajhora, Shiviter and Tindharia were very highly susceptible to landslide; Upper Paglajhora, Gayabari, 14 Miles Bustee and Nurbong T.E. were characterized by high landslide susceptibility; Mahanadi and Giddapahar were of moderate landslide potentiality; and marginal waxing slope of water divide and low-central wanning slope were registered with low landslide susceptibility (Fig. 7.8).

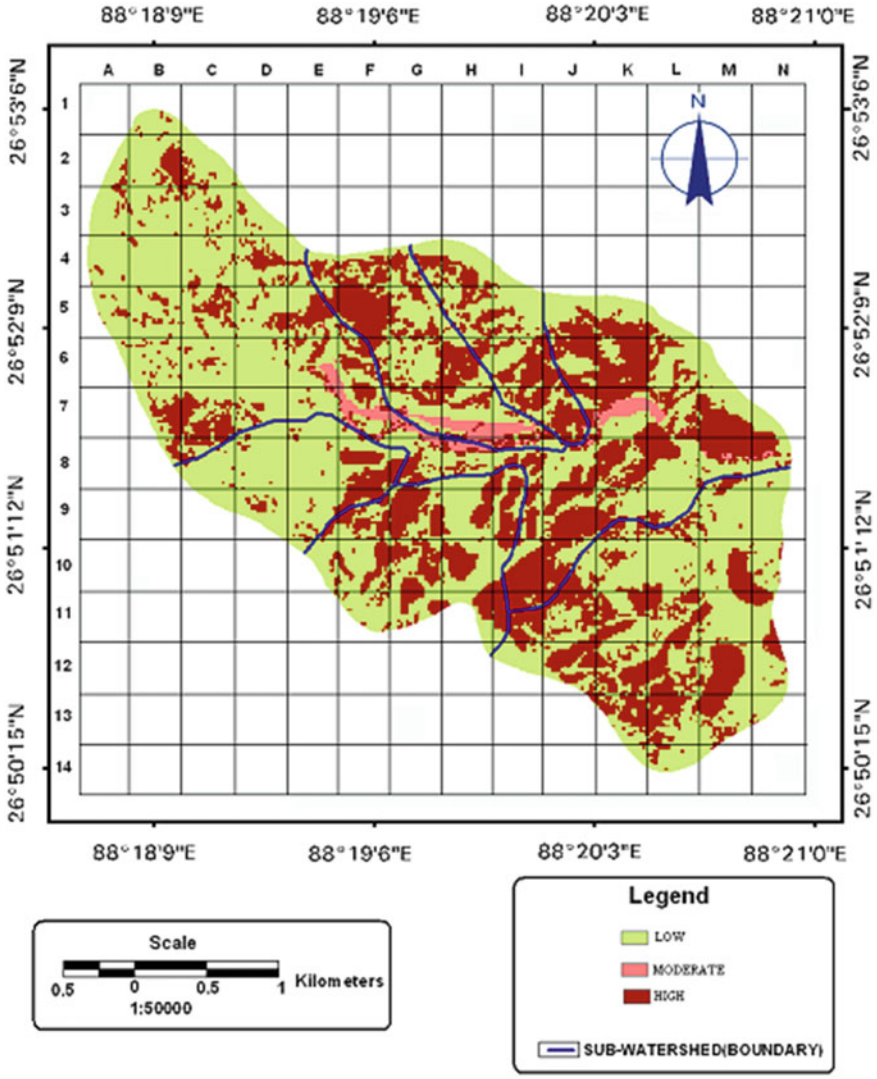

Fig. 7.5 Weighted land use and land cover map

The study revealed that around 50 % area of the Shivkhola watershed was classified as being in the moderate to very high landslide susceptibility with 71 % landslide phenomena. Low to very low susceptibility zones together accommodate 27 % of the landslide phenomena (Table 7.6). Landslide density in each susceptibility class was derived to evaluate the intensity of landslide activities. The landslide density value ranges from 0.031 to 0.25. The calculated density value of

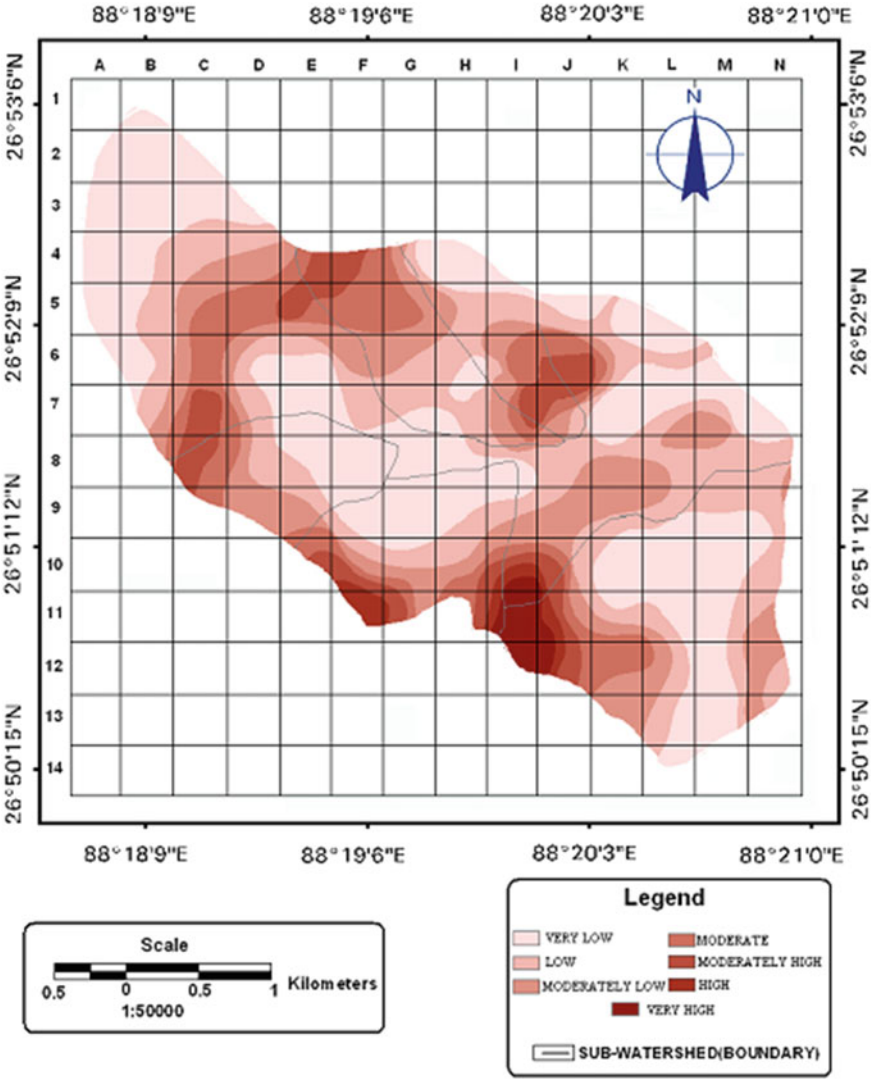

Fig. 7.6 Weighted road contributing area map

0.25 and 0.15 for very high and high landslide susceptibility zones of the watershed depicts the higher intensity of landslide activities compared to other landslide susceptibility zones. Here, frequency study shows that more than 19.58 % area is attributed with high to very high landslide probability, around 48.8 % with moderate landslide probability and remaining area with low landslide probability (Table 7.6). In landslide susceptibility classes of high and very high, the 'FR' values are 2.41 and 3.39 that indicate greater chances of landslide probability. The determined landslide density and frequency ratio reveals that the areas with high

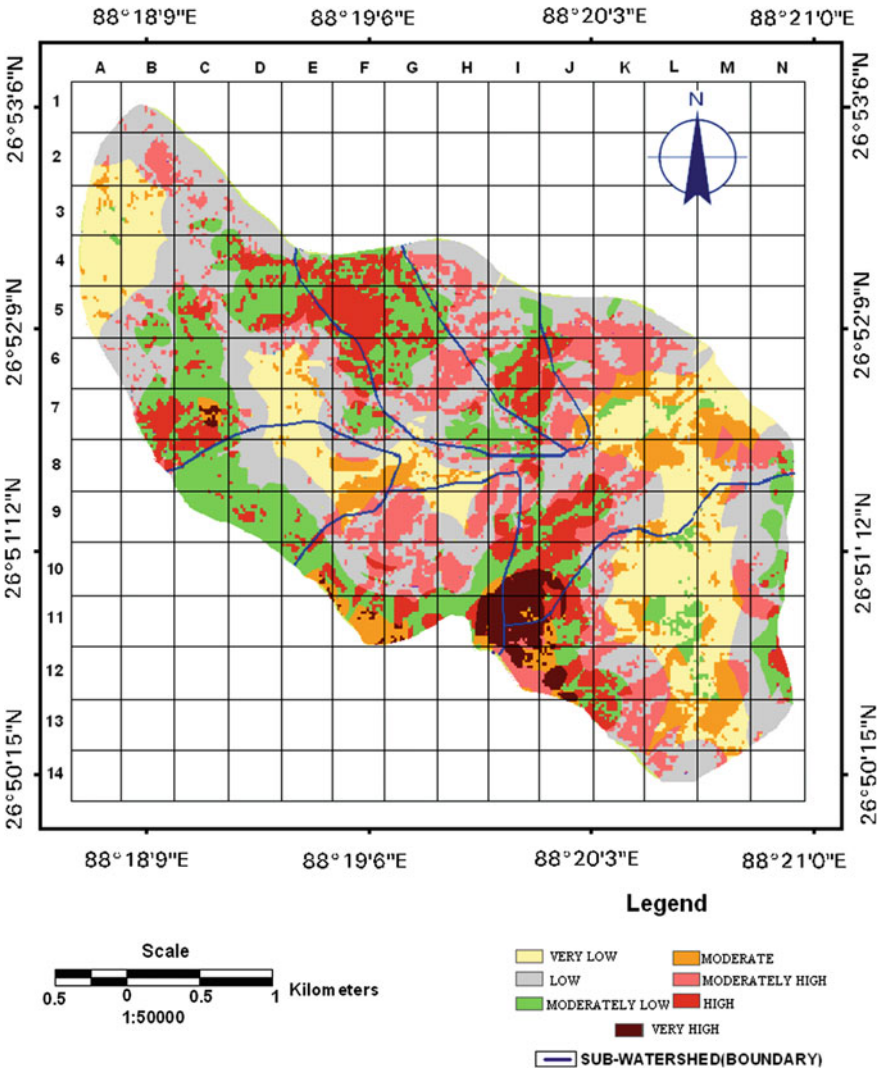

Fig. 7.7 Risk exposure/intensity map

and very landslides susceptibility are expected to have fresh landslide phenomena and here lies the validity of the present landslide susceptibility mapping approach.

A relationship was established between landslide potential index and landslide affected pixels which show that 27.22, 45, 50.03, 76.03 and 95.62 % landslide affected areas are distributed in 8.75, 28.66, 45, 78 and 92 % landslide susceptible areas. Around 35 % landslide affected pixels are distributed in 27 % of high to very high landslide potentiality zones that indicate the higher probability of landslide activities (Fig. 7.9). On the other hand 73 % landslide susceptible areas are attributed with 65 % landslide affected pixels.

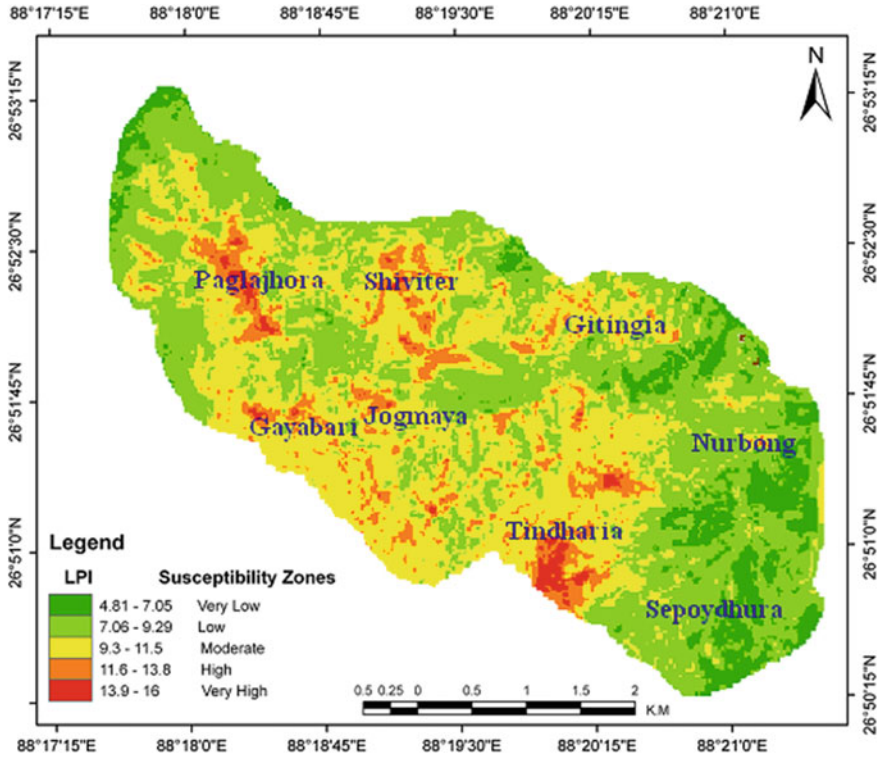

Fig. 7.8 Landslide susceptibility map

Table 7.6 Relationship between landslide susceptibility (%), landslide frequency (%) and frequency ratio (FR) and landslide density

Landslide susceptibility	Pixel (15 × 15 m) (b)	% (B)	Landslide pixel (15 × 15 m)(a)	% (A)	Frequency ratio (FR) (A/B)	Landslide density (a/b)
Very low	7,707	9.03	245	4.47	0.50	0.031789282
Low	35,386	41.46	1,247	22.74	0.54	0.035239925
Moderate	34,364	40.26	2,676	48.8	1.21	0.077872192
High	6,932	8.12	1,074	19.58	2.41	0.154933641
Very high	964	1.30	242	4.41	3.39	0.251037344

7.3.2 Accuracy Result of Landslide Susceptibility Map

The comparison between true data and randomly selected data from the classified image was made on GIS Platform that showed the overall classification accuracy of 92.22 % and overall Kappa Statistics was 0.894. The class wise accuracy result is shown in Table 7.7 that indicates acceptable results.

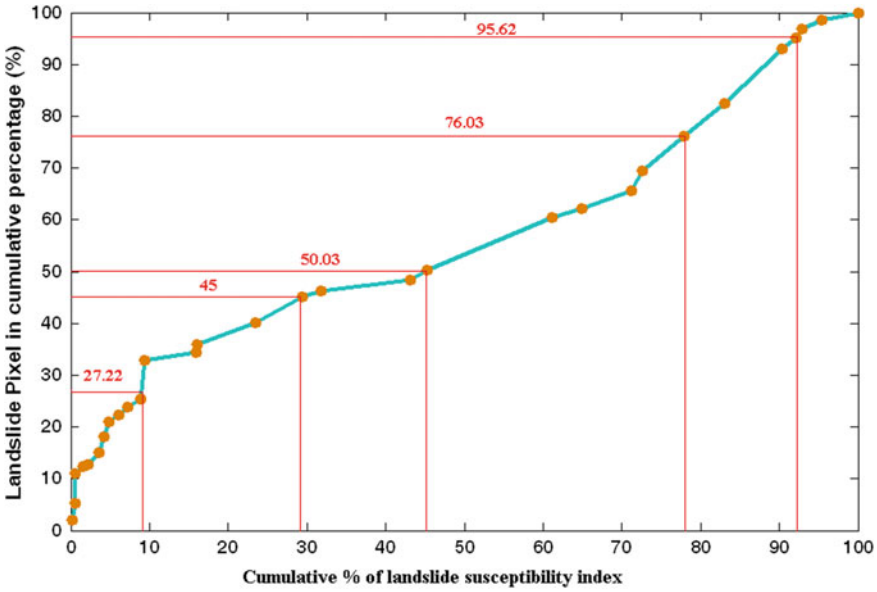

Fig. 7.9 Pixel wise distribution of landslide potentiality index

Table 7.7 Accuracy assessment/comparison of landslide susceptibility with field data

Class name	Classified total	Number correct	Producers correct	Users accuracy	Accuracy total
Very low	0	5	0	0.00	0.00
Low	4	3	0	75.00	0.00
Moderate	11	10	9	90.91	90.00
High	16	15	13	93.75	86.67
Very high	19	17	17	89.47	100.00
Total	50	50	39		
Overall classification accuracy = 92.22 %					
Overall Kappa statistics = 0.894					

7.3.3 Analysis of Landslide Hazard Risk

Study represents that the watershed is dominated by high landslide hazard risk followed by very high, moderate and low landslide hazard risk. In terms of areal coverage, 17.92, 25.37, 29.35 and 27.34 % area of the watershed is recognized by low, moderate, high and very high landslide hazard risk respectively (Fig. 7.10). Figure 7.11 shows the spatial distribution of landslide hazard risk where Lower Paglajhora, Tindharia and Shiviter are registered with high risk exposure due to

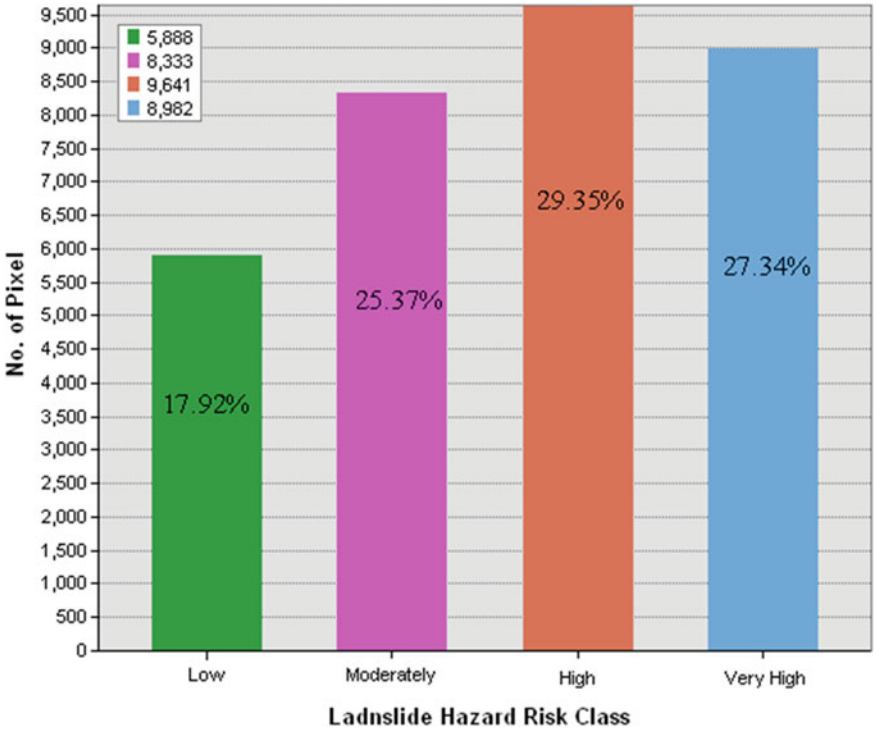

Fig. 7.10 Distribution of pixel/area (%) within landslide hazard risk classes

high intensity of risk elements (road, settlement and tea garden) that leads to high to very high landside hazard risk. The developed landslide hazard risk map of the Shivkhola Watershed exhibits a clear picture about the spatial location of vulnerability and risk of landslide hazard. The marginal parts and lower most segment of the basin experiences low intensity of risk elements and are also least affected by slope instability. Landslide hazard risk is very high at lower paglajhora, Shiviter Tea Garden Area, Tindharia etc. Lower Gyabari and Sepoydhura are the places of moderate to low probability of landslide hazard risk. Moderate level of risk is found at middle as well as lower section of the Shivkhola Watershed. It can be concluded that the watershed is dominated by the moderate to high level of landslide hazard risk. Landslide hazard risk is too high at Mahanadi, Tindharia and Shiviter because of higher intensity of the risk elements.

After thorough analysis of the intensity and magnitude of damage, 36 landslide events are marked as risky out of a total of 128 since 1968. Again the distribution of landslide among various landslide risk zone shows that very high, high and moderate risk areas experienced 62, 43 and 22 landslide events respectively and out of

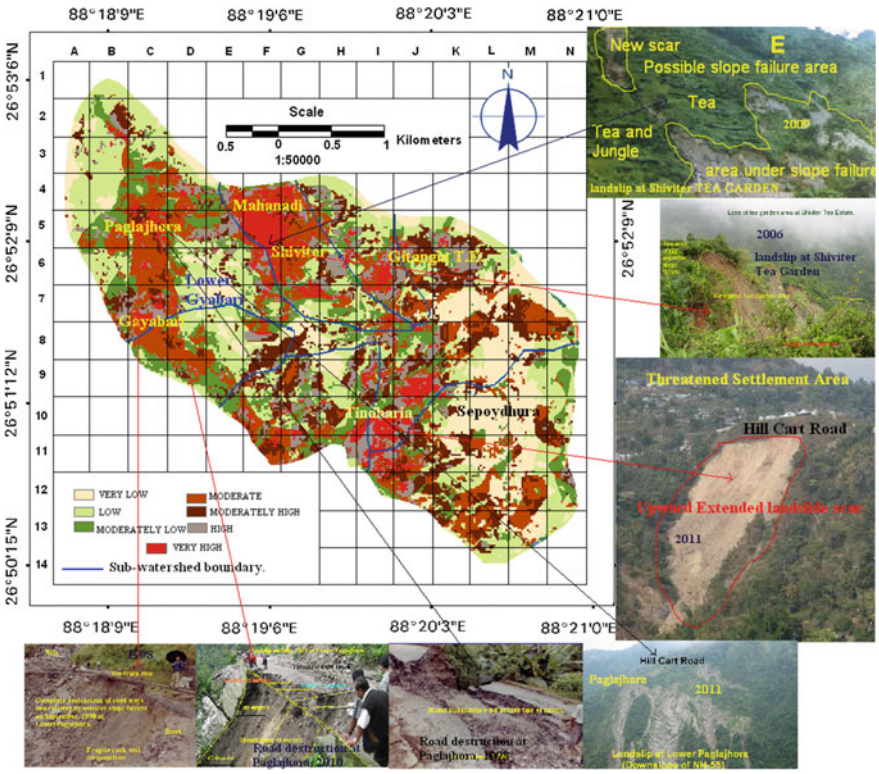

Fig. 7.11 Landslide hazard risk map with few significant risk events (field photo)

those 16, 13 and 7 are identified as riskful events. Frequency ratio for each low, moderate, high and very high landslide hazard risk zone are 0.00, 0.66, 1.42 and 2.48 respectively which also shows very low chance, tendency towards equal chance, high and very high chance of landslide hazard risk events in the respective hazard risk zones (Table 7.8). Analysis of frequency ratio conclude that there is a greater probability of future occurrence of risk events at the places of Lower Paglajhora, Tindharia and Shiviter in future and these three locations are presently existing in high to very high landslide hazard risk zone where frequency ratio is more than '1'.

The determined threshold slope angle of Paglajhora, Tindharia and Shiviter ranges from 13° to 37° and cohesion of the soil from 0.01 to 0.70 with greater percentage of sand particle. Very fragile and fragmented lithological composition helps easy percolation of rain water that generates adequate pore-water pressure for promoting downward movement of slope materials at Paglajhora and Tindharia. The existence of moderate to high intensity of risk elements and human intervention associated with all favourable geomorphic and geo-hydrologic landslide triggering

Table 7.8 Frequency ratio (FR) analysis and landslide probability for each risk zone

Landslide risk class	No. of pixels	Area (%)	Frequency landslide events	Frequency of risk event	Frequency of risk events (%)	Frequency ratio (FR)	Probability/chance of the risk event
Low (L)	8,982	27.34	1	0	0.00	0.00	Very low
Moderate (M)	9,641	29.35	22	7	19.44	0.66	Tendency towards equal
High (H)	8,333	25.37	43	13	36.11	1.42	High
Very high (VH)	5,888	17.92	62	16	44.44	2.48	Very high
Total	32,844	100	128	36	100		

factors have recognized Lower Paglajhora, Tindharia and Shiviter as high to very high landslide hazard risk zone in the Shivkhola Watershed.

The thickness of the soil and that of the saturated soil during monsoon are measured to be 4.5 m (Shiviter T.E.) and 7.25 m (Lower Paglajhora) and 1.28 m (Shiviter T.E) and 1.30 m (Lower Paglajhora) respectively at the back wall of the landslide scar though it is a bit lower further upslope on steeper section. The wet soil buck density is measured to be 1.96 g/cc and density of water is 1.07 g/cc. The angle of internal friction varies from 19° to 23° with an average of 21°. The calculated critical rainfalls of two major landslide prone parts of the Shivkhola watershed are 105.88 mm/day (Shiviter T.E.) and 88.93 mm/day (Lower Paglajhora) after Borga et al. (1998). Following Chow (1951, 1954, 1964) the calculated rainfall of 90.539 mm which is less than the critical rainfall of those two places at the recurrence interval of 1.01 year with 99 % probability.

The determined safety factor (FS) of all three locations are less than '1' which is measured considering the stress parameters such as major principal stress ($\boldsymbol{\sigma}_1$), minor principal stress ($\boldsymbol{\sigma}_3$), normal stress ($\boldsymbol{\sigma}_\mathbf{n}$), shear stress ($\tau$), angle of internal friction (Φ), cohesion (C), shear strength (λ), and rupture angle (α) applying Direct Shear Test Mechanism and developing Mohr's Stress Circle (Table 7.9). All the above mentioned parameters have recognized Paglajhora, Tindharia and Shiviter as significant unstable sections in the Shivkhola watershed. Not only that the slope steepening developed by road-cut benches and toe erosion, plying of heavy loaded vehicles and its enormous pressure on more fragile slope materials, depletion of forest cover in a rapid pace, continuous and regular orographic rainfall in rainy season, easy percolation of water through fragmented rock-soil composition and increase pore water pressure have caused destructive slope failure and damaged human structure and disrupted normal life by cutting-off the communication lines at all these three locations and have treated them as most significant landslide hazard risk prone sectors of the Shivkhola Watershed.

A comparative study has been made here to establish the interrelationship between all the landslide triggering factors (slope angle, slope curvature, slope aspect, lithology, drainage density, upslope contributing area, settlement density, road contributing area and land use and land cover.) considered in the present study as well as to figure out the different levels of abstraction of all the parameters in landslide hazard risk zones (Table 7.8). Study revealed that high and very high landslide hazard risk zones covering the places of Pahlajhora sinking zone, Tindharia, Shiviter, and 14 Miles Bustee are closely associated with 35–45° slope angle; north-east, south-east, north, east and south slope aspect; high posivite and high negative curvature; drainage density of 3.5–6.5 km/km^2; upslope area of more than 5 km^2; high settlement density; moderate to high road contributing area; and land use/land cover of settlement, road, degraded forest and open forest (Table 7.10).

Table 7.9 Measured geo-technical parameters for Tindharia, Shiviter and Paglajhora

Location	σ_3	σ_n	σ_1	τ	Φ	C	λ	α	F.S.
1. Tindharia Tea Garden	0.90	1.31818	2.15440	0.59036	19°28′	0.123	0.588929	35°16′	0.9975760
2. Lower Paglajhora (14 Miles Bustee)	0.82	1.28942	2.3212	0.69594	22°	0.149	0.6699594	34°	0.962668
3. Lower Paglajhora	0.96	1.4583	2.43794	0.6987	19°	0.162	0.6641329	35°30′	0.950526
4. Tindharia Rly. Stn.	0.92	1.4044	2.553	0.74598	24°	0.10 5	0.730279	33°	0.9789525
5. Shiviter T.E.	0.97	1.402407	2.3351579	0.63508	21°30′	0.07	0.6224228	34°15′	0.9800699

σ_1 = major principal stress; σ_3 = minor principal stress; σ_n = normal stress; τ = shear stress; Φ = angle of internal friction; C = cohesion; λ = shear strength; α = rupture angle; and F.S. = safety factor

Table 7.10 Comparative study between landslide triggering factors and landslide hazard risk zones

Hazard risk class	Lithology	Slope	Aspect	Curvature	Drainage density (km/km^2)	U.C.A (km^2)	Settlement density	R.C.A.	Land use/ land cover	Location
Very high	Gneiss/mica-schist	45°–70°	North/ east/ south	High Positive/ high negative	5–6.5	>10	>1.25	High	Degraded forest and settlement (20.11 and 12.55)	Lower pag-lajhora /shi-viter / Tindharia
High	Quatzite schist, phyllite	30°–45°	NE/SE	Moderate positive/ negative	3.5–5.5 and more than 8	5–10	0.5–1.25	Moderate to high	Road/mixed and open forest	/Gayabari/ 14 miles bu-stee/Nur-bong T.E Mahanadi/
Moderate	Soft sand-stone, shale	20°–30°	Flat	Low	2.00–3.50	<5	0.25–0.50	Low	Jungle	Giddapahar/ upper paglajhora
Low	Conglomerate/ shale/ sandstone	<20°	NW	Around (0)	<2.00	<5	<0.25	Low	Dense forest	Marginal/ mid-central part

UCA Upslope contributing area; *RCA* Road contributing area

Table 7.11 Accuracy assessment/comparison of landslide susceptibility with field data

Landslide hazard risk class	Classified total	Number correct	Producers correct	Users accuracy (%)	Accuracy total (%)
Very low	0.00	1	0	–	–
Low	0.00	1	0	–	–
Moderately low	0.00	3	0	–	–
Moderate	19	17	15	78.95	88.24
Moderately high	8	6	5	62.50	83.33
High	17	16	16	94.12	100.00
Very high	6	6	6	100.00	100.00
Total	50	50	42		
Overall classification accuracy = 92.89 %					
Overall Kappa statistics = 0.8929					

7.3.4 Accuracy Result of Landslide Hazard Risk Map

The comparison between assumed true data and randomly selected data from the classified image has been made on GIS Platform that shows the overall classification accuracy is 92.89 % and overall Kappa Statistics is 0.8929 %. The class wise accuracy result is shown in Table 7.11 that indicates acceptable results.

7.4 Conclusion

Very fragile and fragmented lithological composition helped easy percolation of rain water that generated adequate pore-water pressure for promoting downward movement of slope materials at Paglajhora and Tindharia. The combinations of moderate to high intensity of risk elements and human intervention associated with all favourable geomorphic and geo-hydrologic landslide triggering factors have recognized Lower Paglajhora, Tindharia and Shiviter as high to very high landslide hazard risk zone in the Shivkhola Watershed. The calculated critical rainfalls of two major landslide prone parts of the Shivkhola watershed are 105.88 mm/day (Shiviter T.E.) and 88.93 mm/day (Lower Paglajhora) after Borga et al. (1998). Log probability analysis after Chow (1951, 1954, 1964) shows that the rainfall of 90.539 mm is expected at the recurrence interval of 1.01 year with 99 % probability. This revealed high-potentiality of slide at these locations. Not only that, the slope steepening caused by road-cut benches and toe erosion, plying of heavy loaded vehicles, depletion of forest cover in a rapid pace, continuous and regular orographic rainfall in rainy season, easy percolation of water through fragmented rock-soil composition and increase pore water pressure have caused destructive slope failure at all these three locations.

The derived prioritized factor rating values (PFRV) were high for Slope steepness (0.2944), lithology (0.2150), drainage (0.1537), and lineaments (0.1087) indicating as the significant contributing factors for landsliding in the Shivkhola watershed. The slope aspect, settlement density and LULC were registered with minimum prioritized factor rating values of 0.0149, 0.0193 and 0.0266 that proved these factors as less significant to promote landslide activities. Road contributing area (RCA), slope curvature and upslope contributing area were proved to be moderately important in the present context. Analytical hierarchy process is proved to be important to efficiently identify the landslide triggering factors of most importance. It may again be helpful as a support in decision making process for efficient management. The study revealed that lithological composition with steep slope and drainage network orientation are to be given more priority in the decision of structural construction, specially the construction of roads.

References

Anabalagan R (1992) Landslide hazard evaluation and zonation mapping in mountainous terrain. Eng Geol 32:269–277

Atkinson PM, Massari R (1998) Generalized linear modeling of susceptibility to landsliding in the central Apennines, Italy. Comput Geosci 24:373–385

Avinash KG, Ashamanjari KG (2010) A GIS and frequency ratio based landslide susceptibility mapping: Aghnashini river catchment, Uttara Kannada, India. Int J Geomat Geosci 1 (3):343–354

Basu SR, Sarkar S (1985) Some consideration on recent landslides at Tindharia and their control, Indian. J Power River Valley Dev 1985:190–194

Basu SR, Sarkar S (ed) (1988) Ecosystem visavis Landslides, a case study in Darjeeling Himalayas. Impact of development on environment. Geog Soc India Cal II:45–53

Basu SR, Ghatowar L (1988) Landslides and soil erosion in the gish drainage basin of the Darjeeling Himalaya and their bearing on North Bengal floods. Studia Geomorph Carpatho Bale 22:105–22

Basu SR, Ghosh L (1993) A comprehensive study of landslides and floods in the lish basin of the Darjeeling Himalaya, Indian J Power River Valley Dev 43:196–203

Basu SR, Maiti RK (2001) Unscientific mining and degradation of slopes in the Darjeeling Himalayas. Chang Env Scenerio Indian Subcont (Bd) 390–399

Borga M et al (1998) Shallow landslide hazard assessment using a physically based model and digital elevation data. J Environ Geol 35(2–30):81–88

Brardinoni F, Church M (2004) Representing the landslide Magnitude Frequency relation; Capilano river basin, British Colombia. Kirkby JM, Darby ES (eds) Earth surface processes and landforms, vol 29, issue 1, pp 115–124

Brudsen D (1979) Mass movement. In: Embelton C, Thornes J (eds) Process in geomorphology. Wiley, New York, pp 130–186

Burton A, Bathurst JC (1998) Physically based modeling of shallow landslide erosion and sediment yield at a catchment scale. Environ Geol 35(2–3):89–99

Caiyan WU, Jianping Q (2009) Relationship between landslides and lithology in the three Gorges reservoir area based on GIS and information value model, vol 42, issue 2. Higher Education Press and Springer, pp 165–170

Carson MA (1975) Threshold and characteristic angles of straight slopes. In: Proceedings of the 4th Guelph symposium on geomorphology, Norweich Geo Books, pp 19–34

Carson MA (1977) Angles of repose, angles of shearing resistance at angle of talus slopes. Earth Surf Processes 2:363–380
Catlos EJ, Harrison TM, Kohn MJ, Grove M, Ryerson FJ, Manning CE, Upreti BN (2001) Geochronologic and thermobarometric constraints on the evolution on the main central thrust, central Nepal Himalaya. J Geophys Res 106:16177–16204
Chow VT (1951) General formula for hydrologic frequency analysis. Am Geophys Union Trans 32:231–237
Chow VT (1954) The long-probability law and its engineering applications. ASCE 80:1–25 (Separate No. 536)
Chow VT (ed) (1964) Handbook of applied hydrology. Mc Grow-Hill Book Company, New York
Congalton R (1991) A review of assessing the accuracy of classification of remotely sensed data. Remote Sens Environ 37:35–46
Crozier MJ (1986) Landslides: causes, consequences and environment. Croom Helm Australia Pty Ltd., London, 252p
Dai FC, Lee CF (2002) Landslide characteristics and slope instability modeling using GIS; Lantau Island, Hong Kong. Geomorphology 42:213–228
Dhakal AS, Amada T, Aniya M (2000) Landslide hazard mapping and its evaluation using GIS: an investigations of sampling schemes for a grid-cell based quantitative method. Photogram Eng Remote Sens 66(8):981–989
Donati L, Turrini MC (2002) An objective and method to rank the importance of the factors predisposing to landslides with the GIS methodology, application to an area of the Apennines (Valnerina; Perugia, Italy). Eng Geol 63:277–289
Dutta KK (1966) Landslips in Darjeeling and neighbouring hills slopes in June 1950. Bulletin of the geological survey of India. Ser B 15(1):7–30
Einstein HH (1988) Landslide risk assessment procedure. In: Proceedings of the fifth international symposium on landslides, pp 1075–1090
Ghosh S, Van Westen CJ, Carranza E, Jetten V (2009) Generation of event- based landslide inventory maps in a data-scarce environment; case study around Kurseong, Darjiling district, West Bengal, India. In: Malet JP, Remaitre A, Bogaard T (eds) Landslide processes: from geomorphologic mapping to dynamic modeling: proceedings of the landslide processes. European centre on geomorphological hazards (CERG), Strasbourg, pp 37–44
Gokceoglu C, Sonmez H, Ercanoglu M (2000) Discontinuity controlled probabilistic slope failure risk map of the Altindag (settlement) region in Turkey. Eng Geol 55:277–296
Guzzetti F, Carrara A, Cardinali M, Reichenbach P (1999a) Landslide hazard evaluation: a review of current techniques and their application in a multi-scale study, Central Italy. J Geomorphol 31:181–216 (Elsevier, London)
Guzzetti F, Cardinali M, Reichenbach P, Carrara A (1999b) Comparing landslide maps; a case study in the upper Tiber River basin, central Italy. Environ Manage 18:623–633
Guzzetti F, Cardinali M, Reichenbach P, Carrara A (1999c) Landslide hazard evaluation: an aid to a sustainable development. Geomorphology 31:181–216
Intarawichian N, Dasananda S (2011) Frequency Ratio model based landslide susceptibility mapping in lower Mae Chaem watershed, Northern Thailand. Environ Earth Sci 64:2271–2285
Jadda M (2009) Landslide susceptibility evaluation and factor analysis. Eur J Sci Res 1450-216X33(4):654–668
Jibson WR, Edwin LH, John AM (2000) A method for producing digital probabilistic seismic landslide hazard maps. Eng Geol 58:271–289
Kamp U, Growley BJ, Khattak GA, Owen LA (2008) GIS based landslide susceptibility mapping for the 2005 Kashmir earthquake region. Geomorphology 101:631–642
Komac M (2006) A landslide susceptibility model using the analytical hierarchy process method and multivariate statistics in perialpine Slovenia. Geomorphology 74:17–28
Lee S, Choi U (2003) Development of GIS based geological hazard information system and its application for landslide analysis in Korea. Geosci J 7:243–252

Lee S, Ryu JH, Won JS, Park HJ (2004a) Determination and publication of the weights for landslide susceptibility mapping using an artificial neural network. Eng Geol 71:289–302

Lee S, Choi J, Min K (2004b) Probabilistic landslide hazard mapping using GIS and remote sensing data at Boun, Korea. Int J Remote Sens 25:2037–2052

Lee S, Pradhan B (2006) Landslide hazard assessment at Cameron highland Malaysia using frequency ratio and logistic regression models. Geophys Res Abs 8. SRef-ID: 1607-7962/gra/EGU06-A-03241

Lee S, Pradhan B (2007) Landslide hazard mapping at Selangor, Malaysia using frequency ratio and logistic regression models. Landslides 4(1):33–41

Lee S, Talib JA (2005) Probabilistic landslide susceptibility and factor effect analysis. Environ Geol 47:982–990

Maiti RK (2007a) Irrational resource extraction introducing instability in slope and hydrodynamics- a case study at Lish-Chunkhola basin, Darjiling, Indian. J Geogr Environ 8&9:41–51 Vidyasagar University

Maiti RK (2007b) Critical analysis of slope instability on mining scars at Tindharia Cricket Colony, Darjiling, West Bengal. In: Proceedings of eighteenth convention and national seminar on "quarternary" climatic changes and landforms, organized at Manonmaniam Sundaranar University, Tirunelveli, Tamilnadu, pp 189–205

Mallet FR (1875) On the geology and mineral resources of the Darjeeling district and Western Duars. Mem Geol Surv India 2:1–72

Mandal S, Maiti R (2011) Landslide susceptibility analysis of Shivkhola watershed, Darjiling: a remote sensing and GIS based analytical hierarchy process (AHP). J Indian Soc Remote Sens. doi:10.10007/s12524-011-0160-9

Mandal S, Maiti R (2012) Application of RS and GIS based semi-quantitative approach in landslide hazard risk assessment of the Shivkhola watershed, Darjiling Himalaya. Geo Risk Assess Manag Risk Eng Syst Geohazards 6(4):203–220

Mandal S, Maiti R (2013) Integrating the analytical hierarchy process (AHP) and the frequency ratio (FR) model in landslide susceptibility mapping of Shiv-khola watershed, Darjeeling Himalaya. Int J Disaster Risk Sci 4(4):200–212

Muthu K, Petrou M (2007) Landslide hazard mapping using an expert system and a GIS. IEEE Trans Geosci Remote Sens 45(2):522–531

Mwasi B (2001) Land use conflicts resolution in a fragile ecosystem using multi criteria evaluation (MCE) and a GIS based Decision Support System (DSS)

Nie et al (2001) The application of remote sensing technique and AHP-fuzzy method in comprehensive analysis and assessment for regional stability of Chongqing City, China. In: Proceedings of the 22nd international Asian conference on remote sensing, vol 1. University of Singapore, Singapore, pp 660–665, 5–9 Nov 2001

Nithya ES, Prasanna RP (2010) An integrated approach with GIS and remote sensing technique for landslide zonation. Int J Geomatics Geosci 1(1):66–75

Pandey A, Dabral PP, Chowdhary VM, Yadav NK (2008) Landslide hazard zonation using remote sensing and GIS: a case study of Dikrong river basin, Arunachal Pradesh, India. Environ Geol 54:1517–1529

Pistocchi A, Luzi L, Napolitano P (2002) The use of predictive modeling techniques for optimal exploitation of spatial databases: a case study in landslide hazard mapping with expert system-like methods. Environ Geol 41:765–775

Porghasem H (2007) Landslide hazard zoning statistical frequency ratio method in the basin Safarood. M.Sc thesis, Tarbiat Modarres University, Noor, pp 1386

Pradhan B, Lee S (2010a) Delineation of landslide hazard areas on Penang Island, Malaysia, by using frequency ratio, logistic regression, and artificial neural network models. Environ Earth Sci 60:1037–1054

Pradhan B, Lee S (2010b) Landslide susceptibility assessment and factor effect analysis: backpropagation artificial neural networks and their comparison with frequency ratio and bivariate logistic regression modeling. Environ Models Softw 25(6):747–759
Pradhan B, Lee S (2010c) Regional landslide susceptibility analysis using back-propagation neural network model at Cameron highland, Malaysis. Landslides 7(1):13–30
Parise M, Jibson WR (2000) A seismic landslide susceptibility rating of geologic units based on analysis of characteristics of landslides triggered by the 17 January, 1994 Northridge, California earthquake. Eng Geol 58:251–270
Quinn et al (1991) The prediction of hillslope flow paths for distributed hydrological modeling using digital terrain models. Hydro Processes 5:59–79
Rowbotham D, Dudycha DN (1998) GIS modelling of slope stability in Phewa Tal watershed, Nepal. Geomorphology 26:151–170
Saaty TL (1980) The analytical hierarchy process. McGraw Hill, New York, 350p
Saaty TL (1990) The analytical hierarchy process: planning, priority setting, resource allocation, 1st edn. RWS Publication, Pittsburgh, 502p
Saaty TL (1994) Fundamentals of decision making and priority theory with analytic hierarchy process, 1st edn. RWS Publication, Pittsburgh, 527p
Saaty TL, Vargas LG (2001) Models, methods, concepts and applications of the analytic hierarchy process, 1st edn. Kluwer Academic, Boston, 333p
Sarkar S, Kanungo DP (2004) An integrated approach for landslide susceptibility mapping using remote sensing and GIS. Photogram Eng Remote Sens 70(5):617–625
Sharifikia M (2007) RS and GIS application in Geo-hazard- A case study part of central Alborz-Iran. Ph.D. thesis submitted in Geology Department, University of Delhi, India
Sinha-Roy S (1982) Himalayan main central thrust and its implication for Himalayan inverted metamorphism. Tectonophysics 84:197–224
Soeters R, Westen CJ (1996) Slope instability recognition, analysis and zonation. In: Turner AK and Schuster RL (eds) Landslides: investigation and mitigation. transportation research board special report 247. National Academy Press, Washington, DC, pp 129–177
Tiwari B, Marui H (2001) Shearing behaviour of landslide sliding and mining scarp soil during drained ring shear test. In: Proceedings of XVth international conference on soil mechanics and geotechnical engineering, vol 1, Istambul, pp 295–298
Tiwari B, Marui H (2002) Mechanism of shear zone formation and its effect in residual shear strength. In: Proceedings of 3rd international conference on landslides, slope stability and safety of infrastructure, vol 1, pp 4–133
Tiwari B, Marui H (2003) Estimation of residualshear strength for bentonite-kaolin-Toyoura sand mixture. J Japn Landslide Soc 40(2):124–133
Tiwari B, Marui H (2004) Objective oriented multi-stage ring shear test for the shear strength of the landslide soil. J Geotech Geoenviron Eng ASCE 130(2):217–222
Van Westen CJ, Castellanos Abella E, Sekhar LK (2008) Spatial data for landslide susceptibility, hazards and vulnerability assessment: an overview. Eng Geol 102(3–4):112–131
Varnes DJ (1958) Landslide types and processes. In: Eckel EB (ed) Landslides engineering practice: highway research board, special report 29, vol 544. NAS-NRC Publication, Washington, DC, pp 20–47
Vanmarcke EH (1977) Reliability of earth slopes. J Geotechl Eng Div ASCE 103 (GT11):1247–126
Varnes DJ (1984) Landslide hazard zonation review of principle and practice. Natural hazards, UNESCO, Paris
Vijith H, Madhu G (2008) Estimating potential landslide sites of an upland sub-watershed in Western Ghat's of Kerala (India) through frequency ratio and GIS. Environ Geol 55:1397–1405
Windisch EJ (1991) The hydraulics problem in slope stability analysis. Can Geotech J 28 (6):903–909

Yagi H (2003) Development of assessment method for landslide hazardness by analytical hierarchy process (AHP). Abstract volume of the 42nd annual meeting of the Japan Landslide Society, pp 209–212

Yalcin A, Bulut F (2007) Landslide susceptibility mapping using GIS and digital photogrammetric techniques: a case study from Ardesen (NE Turkey). Nat Hazard 41(1):201–226

Yalcin A (2008) GIS based landslide susceptibility mapping using analytical hierarchy process and bivariate statistics in Ardesen (Turkey): comparisons of results and confirmations. Catena 72:1–12

Young A (1963) Deductive models of slope evolution. Rep Int Geogr Un Slopes Comm 3:45–66

Zhou CH, Lee CF, Li J, Xu ZW (2002) On the spatial relationship between landslide and causative factors on Lantau Island, Hong Kong. Geomorphology 43:197–207

Chapter 8
Landslide Mitigation

Abstract The fundamental impetus of any kind of natural hazard and risk management is an awareness of threat, a notion of responsibility and a brief that human action might reduce the risk. Various components such as susceptibility analysis, hazard and risk identification, consequence analysis, hazard analysis, and risk evaluation are included in the landslide management framework. In the present study of the Shivkhola Watershed for slope stabilization, some mitigation measures have been proposed on the basis of community wisdom assessed through perception study on people living in four landslide prone villages such as Paglajhora, Tindharia, Gayabari and Giddapahar. The value of experience depicts that Catchwater drain along the junction between road and the hill slope, jhora training, retaining wall, catchment water drainage, introduction of vegetation etc. may bring stability of slope. Besides, author's intensive field investigation suggested that the construction and maintenance of buildings, introduction of landslide warning system, and improvement of soil strength would be taken into account as landslide mitigation measures. Here, some *control works* and *restraint works* have been taken into account to reduce landslide hazard and risk.

Keywords Shivkhola watershed · Control work · Restraint work · Value experience · Slope stability

8.1 Introduction

Natural hazard and risk management includes of the threat, a notion of responsibility. Various components such as scope definition, hazard and risk identification, consequence analysis, hazard analysis, risk calculation, and evaluation are included in the landslide management framework. No hazard modification method should be treated as absolute safe. Most methods developed to address the physical hazard are best described as control measure, reduction measures or mitigation measures-not preventive measures. 'Prevention' is the ultimate form of event modification.

S. Mandal and R. Maiti, *Semi-quantitative Approaches for Landslide Assessment and Prediction*, Springer Natural Hazards, DOI 10.1007/978-981-287-146-6_8

Whereas, mitigation is the desired result of risk reduction measures. Various methods that can be selected as the risk reduction measures in the landslide prone area are summarized in Table 11.1. Howell et al. (2006) contend that the geological community has a crucial role to play in educating local planners and engineers about the types of hazards facing their communities, the extent, place and economic consequences of these hazards and how to reduce exposure to them.

A successful landslide mitigation measures in the Shivkhola watershed needs some fundamental requirements and on the basis of these the basic goals and objectives of management options can be achieved. The following capabilities, resources and philosophies were suggested to provide better and effective landslide hazard and risk management after Crozier (2004).

- A technical and scientific information base.
- An informed and capable local and regional Government.
- An appropriate statutory and legal infrastructure.
- An informed and capable professional and technical community to manage and execute a risk reduction programme.
- A philosophical basis for determining the acceptability of risk.
- A risk reduction programme with the methods, policies, goals and objectives.
- An effective practice and experience.
- An effective system of communication and education.

Schuster and Kockelman (1996) identifies four approaches to reducing landslide risk.

- Restricting development in the landslide prone-areas;
- Developing and implementing excavation, grading, landscaping and construction codes;
- Implementing physical measures to prevent or control landslides, such as drainage, slope geometry modifications and structures; and
- Developing monitoring and warning system (Table 8.1).

Landslide of different types occurs frequently in geotechnically active domains in Himalaya, North East India and in stable domains in Westerns Ghats and Nilgiri Hills in South India. Landslides have had disastrous consequences and in 2005, over 500 lives were lost due to landslide. As a part of management of this significant natural hazard, National Core Group for Landslide Hazard Mitigation was formed. This core group comprising key national ministers and institutions for drawing a strategy for monitoring the impact of landslides, devising landslide hazard mitigation, monitoring the activities related to landslide hazard mitigation including hazard zonation, evolving an early warning system and protocols for landslide hazard/risk reduction. The Geological Survey of India (GSI) was declared as the Nodal Agency for Landside Hazard mitigation studies. The responsibility of the GSI in accordance with landslide mitigation includes:

Table 8.1 Landslide hazard reduction measures options (Crozier 2004)

Methods for landslide mitigation	Applied activities relating to the methods
1. Physical methods	• Toe buttressing
	• Slope reinforcement: bolts, anchors, pins, piles
	• Grouting fissures and joints
	• Chemical reinforcement of the soils
	• Chunam plastering
	• Bioengineering
2. Hydrological methods	• Surface water diversion
	• Geotextile covers
	• Development of artificial drains
	• Draining of water from slope debris by horizontal drains
3. Site grooming	• Removal of heavily weathered debris from the susceptible slope surface
	• Lowering the steepness of upslope in the landslide prone area
	• Contouring the land surface to divert the flow of water
	• Bioengineering
4. Regulations	• Imposition of laws against waste water disposal, construction of concrete and multi-storied building and slope clearance in and around landslide affected area
	• Building codes
	• Earth work/foundation and drainage standards
5. Land use planning schemes	• Restriction on the landslide induced activities
	• Rules on the changing the slope coverage
6. Education	• Awareness programme and peoples participation
	• Radio and T.V. broadcasting about cause and effect of landslide of the region
	• Development of the communication system
7. Warning systems	• Periodic survey of the landslide area and continuous monitoring
	• Warning system based on the triggering agent i.e. accumulated rainfall
8. Loss-sharing scheme	• Insurance

- Coordinating and undertaking the geological studies for landslide hazard mitigation.
- Carrying out landslide hazard zonation for different scales as per prescribed parameters.
- Studying the factors responsible for landsliding.
- Monitoring landslide.
- Suggesting precautionary and preventive measures.
- Developing a quick response mechanism to investigate the incidences on emergency basis.
- Evolving an early warning system.

- Developing an inventory/database on landslide hazard.
- Development of awareness strategy and awareness programmes in the hazard prone areas.

With the establishment of National Disaster Management Act (NDMA) in 2005 some more responsibilities were entrusted to GSI as Nodal Agency which includes assisting NDMA in drawing up the policies, plans, and guidelines in case of landslide hazards and advise NDMA in technical matters.

Landslide mitigation works are to be conducted in order to stop or reduce the landslide movement so that the resulting damages can be minimized. With a clear understanding of the causes and mechanics of the landslide, the landslide control works can be implemented in the Shivkhola Watershed. Basically, landslide mitigation works are broadly classified into two categories such as *control works* and *restraint works*. The control works involve modifications of the natural conditions of landslides such as topography, geology, ground water, and other conditions that indirectly control portions of the entire landslide movement. The restraint works rely directly on the construction of structural elements. Landslide control works involves surface drainage control works, sub-surface drainage control works, soil removal works, buttress fill works, and the development of river structure. The *surface drainage control works* can be accomplished with the introduction of drainage collection work and drainage channel works. The drainage collection works are to be designed to collect upslope water by introducing corrugated half pipes horizontally at regular interval to reduce the length of over length flow and to minimize the seepage. The drainage channel works are to be designed to remove the collected water out of the landslide affected areas.

The *sub-surface drainage control works* are to be incorporated to remove the ground water within the landslide mass and to prevent the inflow of ground water into the landslide mass from the surrounding areas. This type of works are to be achieved with the development of intercept under drains and trench drains, horizontal gravity drains, drainage wells, and drainage tunnels investigating the landslide prone area properly. *Soil removal works* are to be applied for small to medium size landslides. The *buttress fill* is placed at the lower portions of the landslide in order to counterweight the landslide mass. It is most effective if the soils generated by the soil removal works are used.

Retaining walls are also to be constructed to prevent smaller sized and secondary landslides that often occur along the toe portion of the larger landslides. Because of the large-scale earth-movement and numerous springs that are expected in landslide terrain, crib walls are common instead of conventional reinforced concrete retaining walls. The *anchor works* utilize the tensile force of anchor bodies embedded through the slide mass and into stable earth, and are connected to thrust blocks located on the ground surface. The thrust blocks are anchored with a tendon that counteracts the driving forces of the landslide to restrain the slide movement.

The protection measures which could be adopted to reduce the risk of landslide may broadly be grouped into following heads (Selby 2005):

- Avoidance, removal or diversion of the problem.
- Reduction of the forces tending to cause materials movement.
- Increasing the forces which can resist the downward movement of the materials.
- Provision of the landslide warning system.

Various landslide mitigation practices are present in the work of Zaruba and Mencl (1976), Schuster and Krizek (1978), and Veder (1981). Keefer et al. (1987) introduced a landslide warning system based on the duration, amount and intensity of rainfall in urban area. Gray and Leiser (1982) propounded biotechnical method for landslide mitigation.

8.2 Problem Perception Over the Major Landslides Prone Areas of the Shivkhola Watershed, Darjiling Himalaya

Before going to take a suitable management option for the landslide prone area, Shivkhola Watershed, a perception study has been made about the problems facing by the people living in the concerned study area. Not only that, a priority was given on the suggestions put forwarded by them and accordingly a rational management proposal has been established. The slope instability is the most important problem almost everywhere in the surveyed settlements except at Gayabari. The main settlement area is situated on relatively stable part but the settlement at tea gardens are still prone to landslips and thus affected badly. Considering the 1st rank problems only, almost all of the respondents of Pagla jhora, Tindharia and Giddapahar are equivocal of this problem. Both of these two settlements are extremely affected by slope failure. The rational management of this problem is of utmost importance for the safety of lives, property and landmass. The survey on the migration into these areas shows that since last 70 or more years, fresh population are migrated to add concentrated pressure on slope in spite of being marked as highly landslide prone (Maiti 2007).

Considering the value of experiences of interacting with such a problem, an opinion survey is made to realize the best possible suggestions for ameliorating the problem. The opinion survey shows that maximum of the respondents are in favour of plantation on bare slope and restriction of slope clearing and thus the slope should be brought under vegetation coverage. Some of them think about proper drainage system which should take care of the waste water as well as the roof top water to be guided to the nearest jhora with utmost care so that no water can percolate down during the journey to the jhora. Out of a total of 163 1st rank opinions, 32.5 % are equivocal of plantation on bare slope and 13.5 % are of restriction on slope clearing. Nearly 14 % of 1st rank suggestion is for proper development of drainage system.

8.3 Recommended Landslide Mitigation Practices

After discussing the problems perceived by the people living in the landslide affected areas in the Shivkhola watershed, the applicability of various landslide mitigation measures that could be incorporated in this connection to reduce the degree and frequency of landslide phenomena for the concerned study area were analyzed in detail. It is true that the suggestions for landslide mitigation measures can only minimize/reduce the rate of harmful effect of slope failure to the communities but cannot check the landslide activities in the area absolutely. The following recommendations must be introduced immediately in the suitable places of very high landslide susceptible and risk prone areas in the Shivkhola, such as Paglajhola, Tindharia, Shiviter Gayabari, Nurbong, Giddapahar and Mahanadi. Others area should also be brought under the scheme of landslide mitigation measures for reducing or checking the future landslide phenomena.

8.3.1 Armouring the Catch-Water Drain Along the Junction Between Road and the Hill Slope

The landslides along the Hill Cart Road especially at Tindharia, Paglajhora, and Mahanadi and Giddapahar section are due to the concentration of the upland drainage, along the drain at the base of back slope along the Hill Cart Road and the Narrow Gauge Rail. A huge run-off from a large upslope area pass through the drain along the junction between road and the hill slope (Fig. 8.1). This junction should be completely cemented so that no significant water can pass through it causing harm to the road. Maximum of the damage from outer margin of the road is made

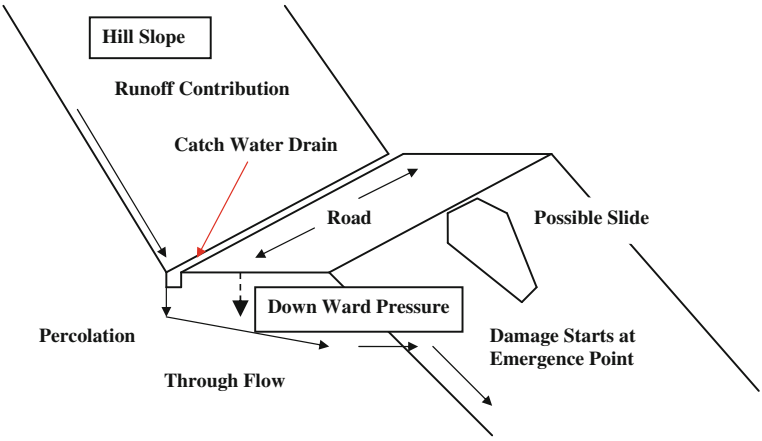

Fig. 8.1 Schematic diagram showing the damage by Percolation along the drain at the junction of Hill side and Road

due to this factor. The fore most step for managing the slope, soil and water is the plastering of the drain for not to allow easy percolation along the hill side. The runoff from the hill sides is easily concentrated along the drain at the junction with road and makes its journey as through flow under the road saturating the underlying materials. The water when emerges out at the outer margin may develop a channel and thus in due course, by head ward extension, starts damaging the road. Once created such landslide scars keep on increasing at a faster rate until the road is completely wiped out.

8.3.2 Jhora Training

Considering huge discharge, laden with high amount of abrasive tools and consequent basal scour and erosion during monsoon the *Jhora Training* seems to be important to save the slope from failure. The technique of *jhora training* includes the construction of Guide Walls along the side banks in descending steps, *gabion drops* and *guide structures*. Slope along the jhora bed is to be broken into gabion drops like small steps (Fig. 8.2).

The torrential water which flows down slope with huge velocity is interrupted with breaks of slope and water is allowed to fall from restricted height (over fall) and thus the erosive power of flowing water can be restricted (Figs. 8.3, 8.4 and 8.5). The cemented course will not allow water to infiltrate inside in the sinking areas mainly. All the jhoras along the Hill Cart Road has to be managed at the junction point with hill Cart Road and Narrow Gauge Rail Line. The length of the riser and height of the heads are to be fixed by analyzing the gradient along the long profile of the concerned jhora and the stability of the materials in response to the

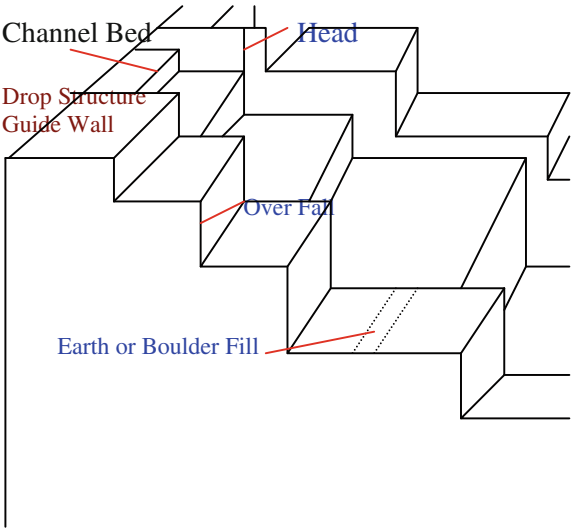

Fig. 8.2 A design of jhora training

Fig. 8.3 Jhora training at lower Paglajhora

Fig. 8.4 Jhora training at 14 Miles Bustee

velocity and discharge of the flow during storm. Though in some cases *jhora training* is practiced and proved to be successful, the training of all the jhoras is yet to be achieved. After the massive destruction in May, 2011 at Lower Paglajhora, along the main nala which was passing through the slided area was trained with concrete small steps to arrest the percolation or seepage of channel water (Fig. 8.3).

Fig. 8.5 Jhora training at Paglajhora

The main problem in the *Jhora Training* is the clearance of seepage water from the interior mass. The conduits or the holes made for the clearance of seepage water is mainly clogged with clay and thus water cannot be allowed to drain due to lack of proper maintenance. The subsidence and sinking of the materials are facilitated due to storage of seepage water at the back of the concrete structure being facilitated by the weight of the overlying materials.

8.3.3 Retaining Wall

Retaining walls are made to resist the pressure of dislodged materials or to resist the pressure of earth filling deposited behind it after its formation. The retaining wall should conform to the repose angle of the constituent slope materials. The repose angle in dry condition can be easily measured by pouring the sun-dry materials from vertical position on a near horizontal surface. At the time of the construction of the retaining walls, the possible pressure from the backfill, the nature of basement, angle of repose and hydraulic character of the slope forming materials are to be studied for the fixation of depth of foundation, width and height of the berms (steps) of the wall.

The further refined concept of angle of internal friction may be introduced which is approximately equal to angle of repose (Van Burkalow 1945) but not exactly same as it includes the inter-granular friction as well as interlocking. The steep, high

wall should be avoided and may be inserted with few berms. The foundation base of the walls should be 1/10th of the height +30 cm and the wider base should have a back slope towards the backfill. Such type of *retaining wall* should be a well accepted management technique along the Hill Cart Road.

Sometimes unnecessary huge overburden is imposed on the unstable slope due to concentration of materials by constructing huge *retaining wall* with large boulder and thus fresh slide occurs. To avoid the unnecessary overburden of the concrete retaining wall at the places of weak lithology of Lower Paglajhora boulder made *retaining wall* (Figs. 8.6, 8.7 and 8.8) with wire net could have been the best procedure. Such method not only reduce the pressure but also helps for easy coming

Fig. 8.6 Retaining wall at lower Paglajhora

Fig. 8.7 Boulder made retaining wall at Shiviter

Fig. 8.8 Retaining wall at lower Paglajhora

out of the seepage water from the slope materials which can reduce the pore-water pressure and can check the landslide.

Interruption of drainage from the *back fill* is the main cause of failure of *retaining wall* and which is generally observed at Shiviter (Fig. 8.7), Paglajhora and Tindharia. The loose clay and silt are generally drained with water and helps in clogging the weep holes. Only the retaining wall could not be able to manage such slope failure. Here, *Shotcrete technique*, a soil-cement mixture that can be sprayed above the retaining wall (open surface) to prevent erosion from weathering and percolation of rain water. The steep slope of the massive slope failure section of 14 Miles Bustee would be shaped and reduced and then retaining wall may be constructed with full care.

For the shallow debris slide (Fig. 8.7) on the way to Shiviter Tea Garden Gabion Mattresses, a rectangular basket made up of wire mesh that are filled with small rocks built by hands, can be laid end to end and side to side on the slided scar with a fairly solid foundation. Several gabion mattress can be joined together to prevent soil erosion and slope materials failure. Before the placement of the gabion mattress the slope has to be well prepared and a filter layer is placed beneath it to resist the movement of finer particles entrainment from the sub-surface soil that can improve the soil strength. Sometimes the weight of the retaining wall is so high so that additional stress cannot be resisted by the slope and thus entire slope moves down slope. The bamboos net are fixed at regular interval to restrict the down slope movement of dislodged materials. The thrust from the backfill is so high so that these bamboo structures are damaged (Fig. 8.9). The introduction of vegetation on the slide scar at the back fill of each bamboo structure in a process of developing total green cover may be an effective management on suitable slope.

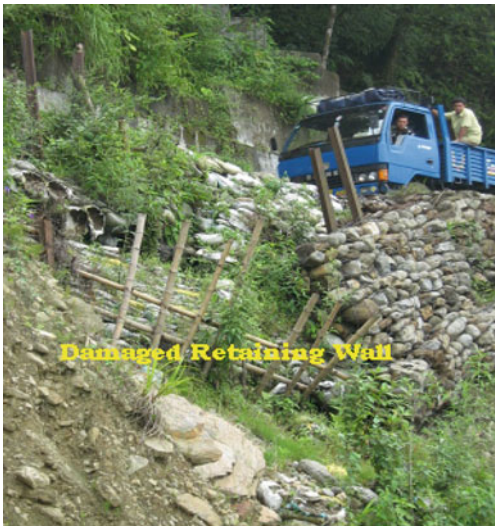

Fig. 8.9 Damaged retaining wall, 14 Miles Bustee

8.3.4 Breast Wall

Breast walls are the construction close to the slope base built to protect freshly cut slope from slope failure. Along the roads, the breast wall is constructed along the inward side of the slope. It is one of the popular soil and slope conservation measures and is frequently observed along the road cuts. Slopes need to be trimmed and flattened before construction. More stable concave slopes are not often formed due to the construction of breast wall at the base by further cutting and steepening. As already mentioned the back fills are prone to more slide due to lack of easy drainage of the seepage water. The weep holes are often clogged with clay and silt and need to be monitored regularly and other options of immediate and easy drainage should be open. The new road cuts are very much prone to down slope movement of soil and slope materials and the necessity of *breast wall* and *retaining wall* is urgently felt to restore the stability of the vulnerable slopes mainly at Tindharia (Figs. 8.10 and 8.11), Sepoydhura and Shiviter. At Paglajhora *breast wall* with jhora training has been established to check seepage pressure as well as landslip (Fig. 8.10).

8.3.5 Catchment Water Drainage

Drainage may be used to prevent surface or sub-surface water reaching the slide area or to remove it from the slide area (Bianco and Bruce 1991). Water in the slide area may be the result of steady seepage flows, or it may be released from the soil or rock mass by stress changes or chemical activity, for example loading or the

Fig. 8.10 Breast wall at Paglajhora

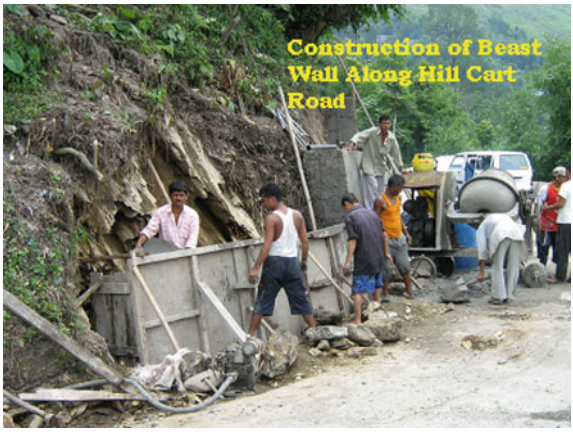

Fig. 8.11 Breast wall at Tindharia

decomposition of refuse (Bromhead et al. 1996) respectively. The diversion of water from the potential slope failure zone is mainly done through *Catch Water Drain*. The diversion is made from more damage prone areas to that of less. The natural drainage after being interfered with, they attempt to redesign themselves which may be detrimental to the slope. Sometimes natural processes of weathering due to lithological characters may develop brittle and fragile slope forming materials which through interaction with surface and sub surface water may become susceptible to down slope movement. Thus the slope has to be completely excluded from both surface and sub surface water and for this purpose, *Catch Water Drain* is the best option. The gully (Channels or streams) heads are prone to landslide where the runoff enters into the channel head helping it to progress further uphill. The slide scars extend uphill and the scarps along the sides also extend upslope increasing the area of the slide scar and bringing more and more area under the

destruction with the help of accumulated surface and sub surface water. The through flows are highly active in these regions and a high rate of 5–12 m/hr of the subsurface flow even during spring has been observed in eastern Himalayan slope. Water entering into the soil few meters upslope is released on the scar faces making the slope instable. Generally a series of near parallel drains are to be constructed above the gully head to collect the water to restrict it to take part in destruction. These should have a non-eroding graded gradient with a cemented mortar and should be drained into a non-erosive channel. In a sinking zone and on highly permeable rocks, closure spacing of the drains are necessary. At Pagla Jhora region such *Catch Water Drains* are to be constructed for arresting the surface water from the large upper catchment and may be diverted to either 2nd or 4th sub-watershed.

8.3.6 Continuous Monitoring of Sub-surface Water

For efficient and effective planning for drainage arrangement in this distress area, knowledge on the pore water pressure is needed. Thus, installation of *Piezometer* on slopes at different levels in Paglajhora sinking zone is necessary. To assess the slope instability condition, a network of monitoring instruments could be installed in order to provide, together with others climatic data, the piezometric response deep inside the landslide and to measure the rate of deformation at several points in the interests of public safety (Angeli et al. 1994a, b). The installation of high-strength steel anchors and sub-horizontal drains are to be drilled into the slope to assist in removal of ground water in accordance with an engineering design just in the sinking area of Lower Paglajhora, Shiviter tea garden and Nurbong Tea Estate.

Basically, the sub-surface drainage network can be managed by the following good engineering practice.

- Introduction of sub-surface drain in the sinking zone and provision of filter around subsurface drain.
- Provision of drain behind retaining walls.
- Use of flexible pipelines with access for maintenance.
- Prevention of inflow of surface water.

8.3.7 Landslide Mitigation by Improving Soil Strength

Usually, a simple method for increasing the shear strength of soil is to reduce the pore water pressure and that can be accomplished by reducing the sub-surface horizontal and downward flow of water through applying the following methods.

- *Grouting* or *void filling* by cementing materials or chemical and development of concrete step like structure along first order drainage in Paglajora sinking zone and Nurbong sinking area that may reduce the seepage and permeability and also can reduce the pore water pressure within the soil.
- Development of artificial drainage upslope may act to prevent the ingress of water into the slided area and that can be introduced in Lower Paglajhora, Gayabari, Tindharia and Shiviter.
- A certain type of first growing vegetation can minimize pore space within the soil and moderates infiltration characteristics, controls run-off and reduce soil moisture condition through transpiration. This type of process is to be ensured in Shiviter, 14 Miles Bustee, Mahanadi and Sepoydhura landslide area.
- Unstable Slope coverage by *plastic/synthetic* cloths in small landside scar can be more effective mechanism for reducing rain water percolation and pore water pressure at Paglajhora, Shiviter Landslide (on the way to Shiviter T.E.), Tindharia Railway. Station. Landslide, Sepoydhura T.E. landslide etc.
- *Chunam Plaster* mechanism could be applied at some places i.e., Chunabhati, Mahanadi, Tindharia and Paglajhora where slope surface is exposed to surface run-off and rainfall. This technique can prevent slope from erosion and water infiltration and restrict pore water pressure and also enhance slope stability condition by increasing the soil strength. It covers the slope surface with a hard water proof shell (Fig. 8.12).
- In Paglajhora and Tindharia care should be taken in the construction of drainage measures to ensure that pore water pressure is not increased.

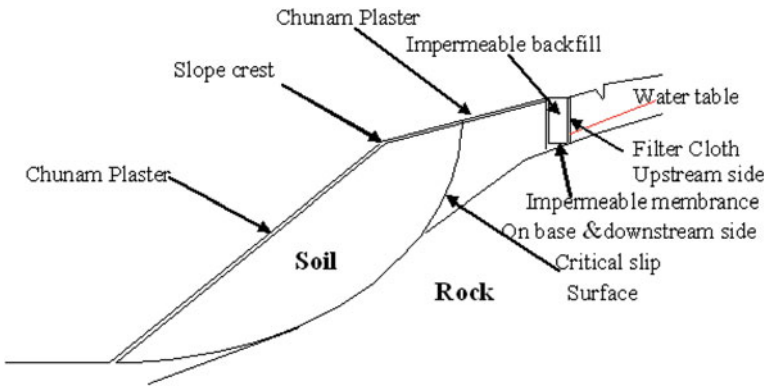

Fig. 8.12 Mechanism of Chunam Plaster to protect a soil slope

8.3.8 *Geo-textile Method for Landslide Mitigation (A Bio-engineering Approach)*

Among many other methods applied for soil erosion control and slope stabilization, bio-engineering approach is one of the best choices. Gray and Leiser (1982) and Howell et al. (2006) established bio-engineering methods to protect soil erosion and slope instability. Collison (1993) assessed the role of vegetation cover on slope stability. *Bio-engineering* is the utilization of vegetation may be alone or in combination with geotechnical structure, for the protection of slopes by reducing and controlling factors that cause instability. In the Shivkhola watershed, massive landslide area with steep slope at Lower Paglajhora (not approachable, below the Hill Cart Road, Fig. 8.13) should be brought immediately under the *geo-textiles method* (mainly the jute nets) with an integrated scheme of introduction and maintenance of the grass and fern seedlings at the opening of the net at regular interval so that at maturity the entire slope becomes covered with vegetation thatch. Another section of Paglajhora (Fig. 8.14) that faced massive landslide phenomena on May, 2011 should also be brought under this *geo-textile mechanism.* The introduced vegetation will get the nutrient from the decomposed jute net and grow to its maximum soon to offer optimum protection of slope. *Jute geotextiles* are the most effective among all types of geotextiles-both natural and man-made (Thomson and Ingold 1986). Additionally, hygroscopic nature of jute yarns in the *Jute geotextile* cause them to swell by around 20 % when wet. This situation will promote to reduce the velocity of sub-surface water as well as entrapment of soil particles. Before netting the slope, a fertilizer is to be spread on the slope in order to

Fig. 8.13 Landslip at Paglajhora

Fig. 8.14 Massive landslip at Paglajhora

promote faster growth of vegetation and soil on the surface of slope is first graded to remove the unevenness present, where possible. The area may be seeded with very limited quantity of Pennisetum species/Vetiveria species grasses known for quick and easy growth and have root depth nearly equaling the existing soil cover, i.e. around 40–50 cm. The netting of slopes generally will stop the downward movement of slope materials as it reduces the impact of direct rain drops and acts as a barrier to surface flow and even holds together slope material. Such method could be very much applicable in Shivkhola Watershed mainly at the places of Lower Paglajhora (Fig. 8.14), marginal North East part of Shiviter Tea Garden, and Tindharaia where structural measures are not possible enough due to very steep slope gradient and very fragile rock-soil composition. Proper care for recurring growth of the vegetations on the specified and managed surface has to be taken for year long protection of the slope from landslip.

8.3.9 Introduction of Vegetation and Slope Stability

The role of vegetation in improving slope stability is well recognized and comprehensive reviews may be found in several publications of Greenway (1987), Phillips and Watson (1994), Gray and Sotir (1996). In general, vegetation influence slope stability through both hydrological and mechanical mechanisms (Table 8.2). Hydrological mechanism that lead to lower pore water pressure and soil moisture

Table 8.2 Effects of vegetation on slope stability (After Greenway 1987)

Hydrological mechanisms	Mechanical mechanisms
1. Foliage intercepts the rainfall, causing absorptive and evaporative losses that reduce rainfall available for infiltration	1. Roots reinforce the soil, increasing soil shearing strength
2. Roots and stems increase the roughness of the ground surface and the permeability of the soil, leading to increased infiltration capacity	2. Tree roots may anchor into film strata, providing support to the upslope soil mantle through buttressing and arching
3. Root extracts soil moisture from the soil, which is lost to the atmosphere via transpiration, leading to lower pore water pressures	3. Vegetation exposed to the wind transmits dynamic forces into the slope
4. Depletion of soil moisture may accentuate cracking in the soil, resulting in higher infiltration capacity	4. Roots bind soil particles at the ground surface, reducing their susceptibility to soil erosion

are beneficial, while those that yield higher soil water are adverse. Mechanical mechanisms that increase shear resistance in the slope are beneficial, while those that increase shear stress are adverse. Simply, vegetation covered surface generally reduce the ability of rainfall to cause slope failure through the process of interception and evaporation and consequently, increases the shear strength in underground soil by the network of roots. For the interception by trees, the structure of the canopy is to be analysed by the free throughfall co-efficient, the stemflow partitioning coefficient, the canopy storage capacity and the trunk storage capacity. In the present study of Shivkhola watershed, suitable vegetation cover is of great importance at Paglajhora up and down slope, Tindharia T.E., 14 Miles Bustee and Nurbong Tea Garden area as it affects the slope hydrology and slope stability and determines throughfall, stem flow, root water uptake, permeability, root reinforcement, vegetation surcharge and interception loss from input rainfall that is described here in an integrated *vegetation-slope model* (Greenway 1987; Fig. 8.15). The connection between forest cover and deep-seated landslide initiation is less clear than with shallow landslide; however, any land use or management practice that alters hydrological pathways and timing could potentially influence deep-seated mass movement activity (Phillips et al. 1990).

Dense vegetation cover and the network of tree roots are considered to be a major contributor to soil strength and slope stability in the area where roots are present (Phillips and Watson 1994). Various studies have also used the tensile strength of tree roots as a measure of the contribution of vegetation to increasing a slope's stability and thereby reducing the incidence of landsliding (Gray and Sotir 1996; Montgomery et al. 2000). As a result of increase rate of deforestation, the Shivkhola Watershed is facing the problems of soil erosion due to direct falling of rain drops and slope failure due to sub-surface soil saturation very easily. Considering the importance of vegetation cover and to avoid such problems of erosion and slope failure, afforestation programme is to be introduced in the landslide affeceted area such as Paglajhora (Fig. 8.16), Tindharia, Mahanadi, Sepoydhura, Shiviter and Nurbong immediately where most of the slope surface area is exposed

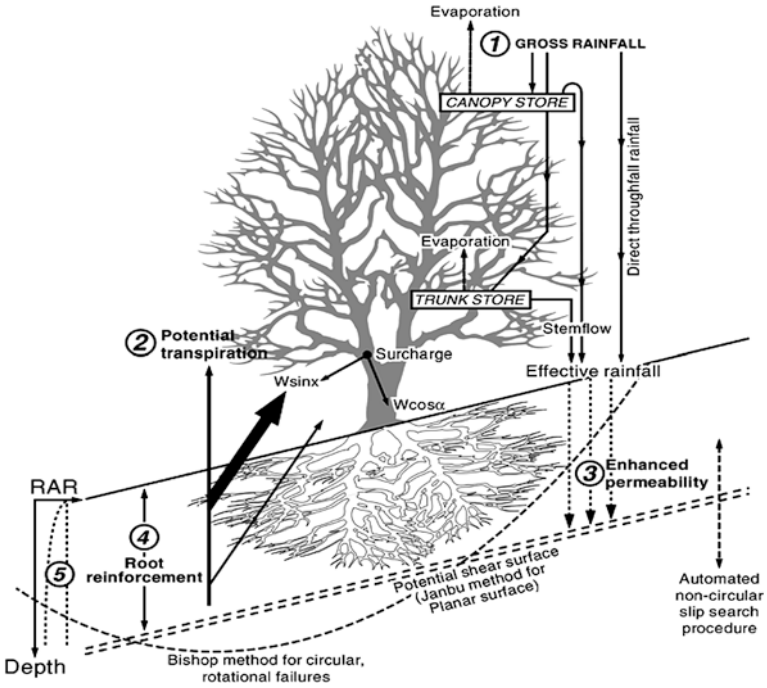

Fig. 8.15 Integrated slope-vegetation model, Greenway (1987)

Fig. 8.16 Afforestation at Paglajhora

Fig. 8.17 Plantation along first order channel

to sub-aerial processes. The on-site benefit of afforestation include a marked reduction in shallow landsliding (Pearce et al. 1987; Phillips et al. 1990), substantially reduced rates of earth flow movement (Phillips et al. 1990), and cessation of gullying processes (Bayfield and Meister 1998; Phillips et al. 2000). Development of first order stream and its flow through sub-surface soil over steep mountain slope is the major cause of soil erosion and slope instability at several places in the Shivkhola Watershed. For freshly-exposed slope surface created by road cutting which is basically found on the way to Shiviter T.E. and Tindhariea T.E. and of course aside the Hill Cart Road, the *vegetative turfing* (introduction of fast growing grasses, bushes, trees and bamboos) can be most effective mitigation measures in the vulnerable areas of Shivkhola Watershed. Sometimes sprays has to be provided to the exposed slope surface to improve the moisture condition of the soil and to facilitate *vegetal turfing*.

A preventive measure of soil erosion has been taken by saplings plantation along first order channel at Gayabari Lower slope (Fig. 8.17). In the slope failure prone areas of the Shivkhola watershed, wild fern are to be grown profusely and can be used for slope protection due to some unique taxonomic characters. The compound leaves are 0.5–1 m long and convex upward and are arranged in successive vertical layers. The rain drops falling on the convex leaves having a down slope trend are conveyed down slope through the tips of the leaves and thus seldom get opportunity to reach slope surface (Fig. 8.18). Thus the thick fern cover is an essential slope protector which restricts soil from being saturated and thus pore water pressure can be controlled to restore slope stability (Maiti 2007). The fern may be introduced to the upper catchments of Paglajhora, 14 Mile landslide area etc.

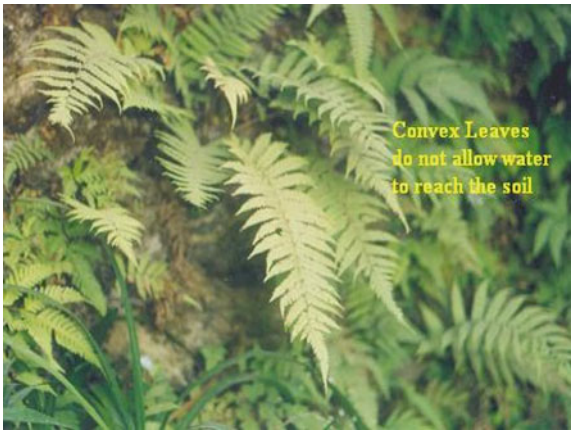

Fig. 8.18 Introduction of Fern Vegetation

8.3.10 Maintenance and Continuous Monitoring of NH-55, Hill Cart Road

Landslide Monitoring is an important and integral part of landslide investigation as well as landslide management. The major objectives of landslide monitoring system are:

- To provide information that can assist landslide investigation and analysis.
- To determine the rate of change of the areal extent of the major landslide location in the watershed.
- To identify the link between ground movement, rainfall and ground water that can promote slope materials to move downward.
- To provide early warning in the landslide affected areas mainly at Paglajhora, Shiviter and Tindharia where movements could affect life and property.
- To monitor the effectiveness of landslide management strategies taken along the Hill Cart Road.

In a number of unstable locations, where monitoring has taken place over several years, a monitoring strategy has been established which includes the gathering of information on both meteorology and ground movements. Increasingly taking into account the cost of manual data gathering, electronic systems are being used, allowing easier data acquisition, interpretation and storage (Fort et al. 2000). It is generally observed from the previous experience that after the destruction of slope by landslide, emergency attention is given to the affected areas and huge amount is spent for the restoration and rehabilitation. It can be suggested strongly for regular monitoring of the potential failure area and a little precautionary measure may save the slope as well as huge property from destruction.

The records of subsidence (Table 8.3) of Hill Cart Road at Lower Paglajhora are a significant landmark of slope instability in the Shivkhola Watershed. Near about

Table 8.3 Records of the rate of road subsidence from lower Paglajhora sinking zone (By author himself)

Years	Rate of subsidence of Hill Cart Road from Rail Bench	Result of the subsidence
May' 2006	No prominent subsidence took place	Unaffected the Hill Cart Road
July' 2007	0.75 m	Affected the Hill Cart Road
September' 2008	1.03 m	Affected the Hill Cart Road during continuous rainfall
August' 2009	1.50 m	Road blockage due to lowering of road bench by heavy monsoon rainfall
June' 2010	5.00 m	Failure washed away the marginal subsided part and damaged the transport network completely

2 km length of the Hill Cart Road which is stretching along the steep north, east and south facing slope with fragile lithological composition is heavily affected by the down slope movement of slope materials and the subsidence of road and rail-cut benches (Fig. 8.19).

Fig. 8.19 Road subsidence at Paglajhora

8.3.11 Road Diversion to Avoid the Paglajhora-Sinking Zone

The problem of the road subsidence and sinking in the Paglajhora region (Gayabari-Mahanadi-Giddapahar Sector) has been a severe bottleneck since long along the N.H.-55. The N.H.-55 (Hill Cart Road) has been constructed in the British regime with a very low gradient up to the fabulous hill city Darjeeling. To take advantage of this low gradient (around 1:50) road bench, the Himalayan toy train tract was also planned and aligned by them along the hill cart road. With time it has become the busiest route to transport heavy traffic to the remote areas of Darjeeling district, W.B. Till date, the journey path of the Himalayan queen (Darjeeling Himalayan toy train) has somehow been maintained to attract the tourist from all over the world. Recently, this toy train has become christened as World Heritage Site by UNESCO, and the maintenance procedure has become more active as well. As most of the land slide occurs along Hill Cart Road (NH-55), and a huge amount is spent for the Post-Slide Management, an attempt for pre-slide management of the susceptible areas has to be introduced with immediate effects with less efforts and investment. A sector wise job assignment has to be made for regular supervision of the slope stability and a serious drive for pre-slide management of potential slope failure zones are to be introduced and it should be considered as emergency as that in post slide condition. For all monitoring programme, it is essential that accurate records are kept about various landslide inducing parameters and rate of change of the landslide affected areas by thorough inspections. Not only will monitoring systems allow the implementation of an emergency response if required; they can cite baseline of information and can increase the knowledge about the landslide prone area, the Shivkhola Watershed.

As new alignment of the rail bench from other route at such a low gradient to avoid the 2 km long problematic stretch of Paglajhora Sinking Zone (Fig. 8.20) is perhaps not a pragmatic proposition. Though, an alternative route of heavy traffic can be possible in the area. Already a by-pass route has been developed which is joining Giddapahar with Gayabari avoiding Paglajhora. The said road is aligned along a ridge line, baring steep gradient with numerous zigs and is suitable for only small/light vehicle. An alternative road from Rohini T.E. to Kurseong has been implemented and the upslope vehicles are passing along this road and thus the stress has been reduced a bit on NH-55 as well as on affected sites of Paglajhora, Gayabari, and Tindharia etc. But the imposition and strict implementation of restriction on heavy vehicle can only assure relief on these instable areas along the Hill Cart Road (NH-55).

8.3.12 Construction and Maintenance of Buildings

Landslide in the Shivkhola Watershed is a common problem as it damages roads, buildings and other infrastructure but much can be done to mitigate such damages

Fig. 8.20 Reconstruction of the Hill Cart Road near Paglajhora

but the lack of maintenance generally makes all the constructions more susceptible to slope failure and that is why the regular maintenance is more important to mitigate landslide. In the field of landslide mitigation, the local authority, the developer, the architect and the contractor and in due course the building owner have to play an important role in terms of ensuring landslide management activities in the most suitable manner by taking into account the steepness of slope, geotechnical properties of the slope materials and the relative weight of the concrete structure for further construction in the landslide prone area of Shivkhola Watershed.

In terms of construction techniques, there are a number of techniques for minimizing the impacts of ground movement through appropriate design. In this cases, the foundation of the building and location sites are more important. Traditional strip foundation can easily fracture, causing significant structural damage at Tindharia, Mahanadi and Gayabari Tea Garden. Rafts can accommodate slight movements and span minor fissures and voids that may form beneath the raft over the lifetime of the building. Beside light-weight framed buildings, which may be of timber with brick or concrete infill or sheet construction materials, are likely to be least problematic in future. At Giddapahar, Tindharia Upslope and Shiviter Tea Garden area, construction of the houses should have raft foundation with jacking points. Light weight, low rise buildings composed of materials that will not be prone to visible cracking and damage may be effective. Human activities such as slope cut and fill operation over the steep slope in the surrounding of dense settlement area (Tindharia, Mahanadi and Sepoydhura) and lack of maintenance of waste water and roof-top water disposal adversely affect the ground stability condition. Residents both in groups or individual, can work together to ensure the

management of roof-top water and household used water through pipes and its channelization to concrete drains. Last of all, specific rules should be imposed for the establishment of concrete houses in the landslide prone area of the Shivkhola Watershed and that can ensure the slope stability.

8.3.13 Landslide Warning System

USGS introduced an inventory of landslides (debris flow) from the storm of 27th June, 1995 in Madison County by using aerial photography, field investigations, rainfall measurements from rain gauges and National Weather Service Doppler Radar Observations (Morgan et al. 1999). The inventory data are being used to ascertain the conditions that caused the debris flows and to develop methods of warning system of such events in the future (Morrissey et al. 2001). In Shivkhola Watershed, at risk prone areas of Paglajhora Sinking Zone and Tindharia slope failure is mainly triggered by heavy and continuous rainfall. So, continuous monitoring of rainfall and pore-water pressure by installing *weather station* and *piezometer* respectively is essential. Recorded parameters as well as their possible impact should be simulated and forecasted to the people living in the region through local electronic media. To execute the process, local Government in association with others non-govt organization and local people should come forward for installing weather station and piezometer in the landslide hazard risk area of Shivkhola Watershed mainly along the Hill Cart Road. At present Satellite systems are used to monitor the movement of the landslide (Hutchinson et al. 2002). In UK National Survey Authority has installed a base station from where landslide movement is obtained at a very small time interval. This type of satellite based system can be installed in the destructive landslide prone areas of Darjiling Himalaya to detect landslide movement. The rate of movement then be transmitted to the people living in the landslide risk prone area which can help to rehabilitate the people. Besides, GPS and Total Station could be utilized to assess the areal extension and direction of landslide masses at regular time interval. Such assessment of areal extension of landslide may also impart knowledge on the possible impact of landslide phenomena.

For combating the problem of slope failure the following remedial measures should be adopted immediately in the Shivkhola Watershed, Darjiling Himalaya.

- Lined catch water drains at every 20 m intervals above the nala on the downslope and upslope should be constructed for the collection of surface run-off.
- Horizontal Perforated pipes should be placed at the slided area during the monsoon period for draining out of the sub-surface water.
- Vegetal turfing over the steep tea garden slope is to be introduced for minimizing the recharge of the ground water.
- Continuous monitoring of ground water condition with the help of necessary accessories (Peizometer).

- Replacement of human settlement from vulnerable areas.
- Afforestation of the hill slope with local shrubs to absorb the moisture content from the sub-surface soil.
- The Concentration of human settlement in and around landslide prone area should not be permitted by the local Government and a strict rule is to be regulated.
- The plying of heavy loaded vehicles through the landslide prone area should not be allowed.
- The local community is to be brought under the landslide mitigation programme and they are to be educated on landslide risk management.

8.4 Conclusion

The success of landslide hazard and risk mitigation measures depends on the continual iterative processes of information input and managerial response. There are many aspects of landslide management that are still poorly understood. It is clear from the intensive field investigation and people's perception that the communities have to be taken collective responsibility by enacting legislation to guide the landslide hazard management process. Continuous advancement in science and technology in landslide mitigation measures can be efficient tools to reduce the consequences of landslide phenomena for the unstable Shivkhola Watershed.

The Shivkhola watershed exhibits a wide range of elevation between 300 and 2,040 m with varying steepness of slope. The development and extension of the drainage network over steep mountain slope makes the topography rugged in nature. The interaction between slope, relief and drainage network associated with weak lithological composition such as structural discontinuities have made the places of Lower Paglajhora, Shiviter, Gayabari, and Tindharia most susceptible to slope failure. It is seen that most of the slided and subsidence zones are linked with more stream junction/confluence of the drainage lines, structural discontinuities and lineaments. The spatial distribution of landslide locations in different lithological unit of individual sub-watershed depicts that sub-watershed-I is lithologically unstable followed by watershed II and V. Spatial distribution of amplitude of relief reveals that sub-watershed-I, IV, II and III are dominated by landslide as there is a positive relation between relief and the landslide frequencies.

The drainage concentration along the weakness planes could be checked or reduced by reducing the upslope contributing area with the establishment of horizontal as well as vertical concrete drains just above and within the sinking zone and slide scar. The identification of structural discontinuities/weakness planes and their cementation can reduce the seepage and pore-water pressure in the soil and promote slope stability to some extent. The sub-watershed-I, II, III and western part of VI are dominated by large number of lineaments/discontinuities/weaknesses planes. Basically, the rocks of Darjiling gneiss, Daling formation, Lingtse granite,

Garubathan formation and Reyang formation are very much attributed with weaknesses planes and associated land slide phenomena which are common in the right hand side of the main Shivkhola River and are to be brought under such management technique to minimize the slope failure. The potential dissection and roughness of the topography is very high in the north, north-east, east, south and south-east facing escarpment slope of Lower Paglajhora, Mahanadi, Shiviter, Gayabari Up-slope and Tindharia through which the Hill Cart Road and Railway Line is passing. At all those places slope is attributed with high positive curvature that invites immediate drainage concentration and makes the places detrimental to slope failure. The extreme lower segment of the slope is registered with high negative curvature caused by active toe erosion of the main river that also invites drainage concentration. The places of more dissection and the roughness should be avoided for the establishment of new settlement and further construction to reduce the landslide hazard risk. Besides, the diversion of drainage lines just above the potentially active slided area and cementation by developing concrete steps along the drainage lines can reduce the concentration of both surface and sub-surface drainage water and reduce the pore-water pressure. The more convexity of the slope could also be reduced modifying the topography up to the threshold slope angle of 24° that can control more drainage concentration and make the slope more stable. The extreme middle and lower most part of the basin is characterized by cut and fill terrace where slope stability is very high due to less slope steepness. Sub-watershed-II is more susceptible for slope instability as most of it lies on steeper slope and is followed by sub-watershed-III and I.

The study envisages that the middle most part of a particular slope facet is more prone to failure due to easy and maximum drainage concentration. The extreme marginal part of the basin is registered with low landslide potentiality because of the less drainage concentration. The areas lying in the mid-central part of the slope segment in Lower Paglajhora, Tindharia, Gayabari and Shiviter are dominated by moderate level of drainage density indicating the more saturation excess surface water which is an indicator of potential erosion and instability. All the first order tributaries are characterized by head-ward extension and branching which produces sharpened interfluves and make the slope steeper beyond threshold slope angle. The central part of the watershed shows the maximum concentration of drainage but due to gentle slope gradient the propensity to slope failure is less. Watershed-III is more prone to slope instability as it possesses higher drainage and deserves more attention for management. In watershed-III nearly 92 % of the basin area posses the lower value of Constant of Channel Maintenance and it means higher drainage density and is thus detrimental to the slope and soil stability.

The upslope contributing area increases toward the main tributaries where the concentration of channels and accumulation of water promotes more excess moisture and instability of slope and soil. The large numbers of drainage concentration at Lower Paglajhora, Shiviter, 14 Miles Bustee and Gayabari have made the places more susceptible to soil erosion and slope failure. The places of landslip induced by drainage concentration should be brought under the measures of catch water concrete drains and installations of horizontal pipe with filters to extract

sub-surface water that can resist seepage and reduce pore-water pressure and bring stability to the slope and soil.

Land use and land cover plays a significant role in the Shivkhola Watershed as it influences surface run-off, slope material saturation, potential retention of rainfall and pore-water pressure. Since 1950, rapid rate of deforestation and clearing of forest cover in connection to the expansion of settlement, establishment of communication lines and fulfillment of the socio-economic demand of the local people have aggravated the problems of soil loss and slope failure. The establishment of settlement and communication lines and transformation to flat surface invites the concentration of drainage water and make steep back wall very much critical to slope failure. In Shivkhola Watershed, degraded forest rank first in terms of triggering land use factor of slope instability and that is followed by settlement, road, open forest, tea garden, mixed forest, jungle, dense forest, bare surface and agricultural land. The major landslide sites Lower Paglajhora is associated with degraded forest and road contributing area (RCA); Tindharia with communication lines and settlement concentration; 14 Miles Bustee with RCA; and Shiviter with haphazard concentration of settlement, degraded forest and open forest. Spatially, the sub-watershed-I, III, IV and VI are dominated by degraded forest, settlement and road and tea garden. To keep the slope safe from slope failure, the human intervention over steep escarpment slope should be stopped at any cost. Not only that the places characterized by degraded forest, open forest and bare surface will have to be brought under effective afforestation and plantation programme and that would be monitored by the local inhabitants. A strict Government rules against the illegal modification of slope and clearance of forest cover must be imposed for the healthy growth of vegetation that can maintain the stability of soil and slope.

The dense forest, down slope jungle, mixed forest, tea garden, and open forest area are characterized by fair to good hydrological condition with the curve number (CN) value of 75 that shows maximum retention and minimum run-off as well as lower rate of soil loss. On the other hand settlement, road, bare surface, upslope degraded forest are attributed with the Curve Number (CN) of more than 76 which is an indicator of minimum retention and maximum run-off and soil erosion. The derived instability rank based on CN, retention, run-off, and landslide potentiality suggests that Sub-watershed VI, I and III have to be paid more attention for a proper management of land, water and soil as these three are characterized by maximum run-off and high susceptibility to slope failure. To manage the land, water and soil in all these three sub-watersheds a well accepted land use planning should be launched immediately by introducing several afforestations programme with active community participation. The people of landslide prone area should also be restricted from constructional works during the moisture period i.e. June-September.

The most landslide prone area, the Shivkhola watershed of Kurseong Sub-division of Darjiling Himalaya registers the continuous growth of household and population. This continuously adds huge population pressure on the existing land and soil resources. The growth rate of household during the period of 1981–1991 and 1991–2001 are 75 and 169 % respectively where as the growth rate of

population during the same periods are 28.83 and 253 %. Such unprecedented growth of household and population as a result of migration from surrounding depressed rural areas is recorded at the places of Tindharia, Giddapahar, Gayabari, Paglajhora, South Shivkhola Tea Garden, Jogmaya Tea Garden, Selim Hill Tea Garden etc. Everyday functioning of such huge population for livelihood collection put tremendous pressure on the land resources damaging slope and vegetation cover leads to soil loss and slope failure. Most of the houses are made up of concrete floors which exert immense pressure on fragile slope materials. On the other hand tin/asbestos roofed houses release maximum concentrated flow of water on land and erode the slope materials easily. Except Paglajhora, most of the houses are one storied and a considerable percentage is two storied which puts excess weight on weak lithology. Nearly 50 % houses of all the villages do not have roof top and waste water disposal system and this situation favours the water to enter into the soil and thus destabilize the slope materials and ultimately threatens the entire settlement area. To resist the problems of slope failure caused due to human intervention on unstable slope in the Shivkhola Watershed, the landslide prone areas should not be allowed for further concentration of settlement. The steep slopes must be avoided for the construction of roads. The restriction on the plying of heavy loaded vehicles and on the construction of two or three storied buildings and the imposition of wooden structured houses, the restriction on the illegal deforestation are to be made. Introduction of afforestation and plantation programme for the unstable sections, and the provision of appropriate roof top water and waste water disposal system to release the water through pipes and concrete drains are to be regularized effectively. Finally, the people should be made aware about the unscientific interaction between man and land or soil and that can minimize the harmful impact of population pressure on land and bring the stability to the slope material.

The analysis of critical slope angle, rainfall and height suggests that the Shivkhola Watershed is a most unstable section of Darjiling Himalaya. In the existing weak lithological composition threshold slope of the unstable sections range from 21° to 26° with an average value of 24°. The large parts of Tindharia, Paglajhora, Gayabari, and Shiviter possess the slope angle of more than 24° that indicates absolute instability. Around 100 mm/day rain may become critical to the landslide prone sections in the watershed. The slope height ranging from 5.89 to 7.80 m. is very much critical and beyond this there is a great chance of slope failure at the places of Tindharia and Paglajhora. The special care must be taken to reduce the height of back wall along the main road as well as the marginal part of the slided scar to that of 5.00 m of less with respect to the below threshold slope angle of 24°. As the rain water is the main triggering factor for reducing cohesion, angle of internal friction and increasing the pore-water pressure which altogether increase the driving force to the slope materials, the most suitable way would be the application of synthetic plastic for covering the extreme unstable section mainly along the Hill Cart Road not to percolate the rain water through soil and slope in the rainy season. The installations of rain gauge stations at all the major landslide locations for the continuous monitoring of rainfall and the relevance of cumulative

rain in landsliding should be transmitted to the people through electronic media which can aware the people to avoid the negative impact of slope failure.

In the Shivkhola Watershed, Tindharia Tea Garden, Lower Paglajhora (14 Miles Bustee), Proper Paglajhora, Tindharia Proper (Rly. Stn.), Shiviter Tea Garden, Sepoydhura T.E., Nurbong T.E., and Lower Gayabari are unstable under saturated condition where safety factor values are lying below '1'. At all those places cohesion and angle of internal friction is very low. Friction angle ranges between 19° and 26° and cohesion varies from 0.0355 to 0.162. One dimensional (1D) slope stability model based landslide susceptibility maps for dry, semi-saturated and saturated condition indicates that here is a tendency of an increase in areal extension of high to very high landslide susceptibility area in saturated soil condition. Under saturated condition more than 50 % area are characterized by high to very high landslide susceptibility whereas under semi-saturated condition more than 35 % area is dominated by high landslide susceptibility. This situation demonstrates that soil saturation and reduction of soil cohesion is the important landslide contributing factor in the Shivkhola Watershed. To monitor the soil saturation and cohesion, sub-surface drainage monitoring and draining of seepage water by boreholes could be the best stabilizing factors in the existing weak lithological composition. The application of geotextile method and introduction of first growing grasses over fragile lithology can bring stability over steep unstable slope. Besides the construction retaining walls and breast wall, jhora training through concrete structure and cementation of cracks and weaknesses planes can bring the stability to the soil and land.

The spatial distribution of slope instability of six individual sub-watersheds in the Shivkhola Basin could be well explained by means of the interaction between morphometric, geometric and hydrologic factors. The synthesis of basin geometry such as Form Factor, Elongation ratio, Circularity Ratio, Elipticity Index, Compactness Coefficient and Length of Overland Flow reveals the composite ranking in terms drainage efficiency. On the basis of total composite index values (CIV), first priority should be given for rational management of land, water and soil in sub-watershed-I and II, which is followed by IV, III, VI and V. It is also seen that the sub-watershed-I and II are most vulnerable due to steep slope, high drainage efficiency, friable lithological composition and more anthropogenic pressure.

Landslide susceptibility analysis based on the landslide hazard evaluation factor rating approach (LHEF) shows that PaglaJhora, Gayabari, Tindharia, Northern and central part of Shivitar T.E., Tindharia T.E., and Gitingia T.E. are the places of very much susceptible to catastrophic slope failure with positive relationship between landslide triggering factors and landslide susceptibility values. On the other hand Analytical Hierarchy Process (AHP) based prepared landslide susceptibility map reveals that Paglajhora, 14 Miles Bustee, Tindharia, Nurbong and Shiviter are experiencing high to very high landslide susceptibility. But no danger of landslide exists at the places of Gitingia, Sepoydhura, lower Gayabari, extreme mid, lower and marginal section of the watershed and lower slope of Tindharia. The traffic, property, and life are under threat at the places of Lower Paglajhora, Tindharia (near railway station), Shiviter tea estate and Tindharia Tea Garden where the slope

failure causes great damages to all those properties. Study shows that the places with moderate level of landslide susceptibility and high intensity of risk elements are registered as high to very high landslide hazard risk areas. AHP based developed couple-comparing matrix and derived prioritized factor rating value (PFRV) reveals that lithology, concentration of human settlement, drainage and slope are the most significant landslide triggering factors in the Shivkhola Watershed. In the Shivkhola Watershed landslide susceptibility and hazard risk is very much associated with moderate to steep slope (>40°); north, north-east; east, south-east and south facing slope; degraded forest, high settlement and road contributing area, tea garden, and bare surface; high positive and high negative slope curvature; moderate level of drainage density over steep escarpment slope; and weak lithology-foliated gneiss, phyllite, mica-chlorite-schist and quartz-schist. In Lower Paglajhora and 14 Miles Bustee, except along the Hill Cart Road the landslide hazard risk is moderate, yet there exists very high level of landslide susceptibility. On the other hand, because of the existence of high intensity of risk elements, the moderate level of landslide susceptibility areas of Mahanadi, Gayabari and Jogmaya are experienced with high to very high landslide hazard risk.

Before going to introduce any management actions for the landslide prone mountain basin, the Shivkhola, the identification and analysis of landslide triggering factors and prepared landslide susceptibility and landslide hazard risk map should be used as an effective tool to the local administration, planners and policy makers. The priority must be given to high to very high risk prone areas as these areas are dominated by risk elements such as road, settlement, tea garden and other resources and experience frequent landslide phenomena.

The utilitarian and environmental concept about the resource utilization advocate the harnessing of optimum utility for long in a sustainable manner and thus rational utilization of resource becomes inevitable. The land and associated soil and water are the basic resources available on the earth. In such a highly instable region, the protection of slope and soil is a great challenge through rational use of these resources for harnessing greater utility over long time. Management of already destroyed slope is a great concern today where the danger of instability is crudely exposed. The present work reveals that rational management of potential slope failure zones, where the danger is not exposed yet, is of most important and to be considered as emergency as that in case of immediate response to a fresh landslide. Pre-slide management of slope requires the identification of susceptible zones. The present work identifies such vulnerable zones of varied priority applying functional, systematic and metastable approach of slope evolution where the stability is expressed as a function of a numbers of factors. The site specific management of slope is necessary along with the general treatment recommended above and timely response to this instability problem only can save the region from potential destruction and the proper execution of the suggestion made may save the resources and ultimately the society and thus the present work will find social relevance.

References

Angeli et al (1994a) A system of monitoring and warning in a complex landslide in Northeastern Italy. Landslide News 8:12–14

Angeli et al (1994b) Longterm monitoring and remedial measures in a coastal landslide (Italy). In: Proceedings of the VIIth ISL, Trondheim, Norway, Balkema, Rotterdam

Bayfield MA, Meister AD (1998) East coast forestry project review. Report of Ministry of Agriculture and Forestry

Bianco B, Bruce DA (1991) Large landslide stabilization by deep drainage wells. In: Slope stability engineering-application and development. Thomas Telford, London, pp 319–326

Bromhead EN et al (1996) Stabilisation of an urban refuse dump and its planned extension near Ancona, Marche, Italy, engineering geology of waste disposal. Geol Soc Eng Geol 11:87–92

Collison AJC (1993) Assessing the influence of vegetation on slope stability in the tropics. Ph.D. thesis, University of Bristol

Crozier MJ (2004) Management frameworks for landslide hazard and risk:issues and options. In: Glade T (ed) Landslide hazard and risk. Wiley, Chichester, pp 331–350

Fort DS et al (2000) Instrumentation and monitoring of the coastal landslides at Lyme Regis, Dorset, UK. In: Bromhead E et al (eds) Landslides in research, theory and practice. Thomas Telford, London

Gray DH, Sotir RB (1996) Biotechnical and soil bioengineering slope stabilisation. Wiley, New York

Gray DH, Leiser AJ (1982) Biotechnical slope protection and erosion control. Van Nostrand Reinhold, New York

Greenway DR (1987) Vegetation and slope stability. In Anderson MG, Richards KS (eds) Slope stability. Wiley, Chichester, pp 187–230

Howell JH, Sandhu SC, Vyas N, Sheikh R, Rana SS (2006) Introducing bio-engineering to the road network of Himachal Pradesh. J Indian Road Congr 67–3

Hutchinson JN et al (2002) Landslide movement affecting the lighthouse at St Catherine's point, Isle of Wight. In: McInnes RG, Jakeways J (eds) Instability planning and management. Thomas Telford, London, pp 291–298

Keefer DK et al (1987) Real-time landslide warning during heavy rainfall. Science 238:921–925

Maiti R (2007) Identification of potential slope failure zones of Shiv-Khola watershed; Darjiling Himalaya, through critical analysis of slope instability- a step towards rational and scientific management of land, soil and water. UGC Sponsored Minor Research Project [F.31-210/2005 (31.03.2007)]

Montgomery DR, Schmidt KM, Greenberg HM, Dietrich WE (2000) Forest clearing and regional landsliding. Geology 28:311–314

Morgan B et al (1999) Historical and potential debris-flow hazard map of area affected by the June 27, 1995, storm in Madison County, Virginia. US Geological Survey Geologic Investigations Series Map I-2623B, scale 1:24000

Morrissey M et al (2001) Regional application of a transient hazard model for predicting initiation of debris flows in Madison County, Virginia. US Geological Survey Open File Report 01-481

Pearce AJ, O'Loughlin CL, Jackson RJ, Zhang XB (1987) Reforestation: on-site effects on hydrology and erosion, Eastern Raukumara range, New Zealand. Forest hydrology International Association of Hydrological Sciences, Wallingford, pp 489–497

Phillips CJ, Watson AJ (1994) Structural tree root research in New Zealand: a review. Landcare research science series 7. Manaaki Whenua Press, Lincoln

Phillips CJ, Pearce AJ, Marden M (1990) Effectiveness of reforestation in prevention and control of landsliding during large cyclonic storms. In: Proceedings, 19th IUFRO conference, Montreal, pp 358–361

Phillips CJ, Marden M, Miller D (2000) Review of plant performance for erosion control in the East Coast region. Landcare research contract report LC9900/111 prepared for Ministry of Agriculture and Forestry (Unpublished)

Schuster RL, Krizek J (eds) (1978) Landslides: analysis and control. Transportation Research Board, Washington

Schuster RL, Kockelman WJ (1996) Principles of landslide hazard reduction. In: Turner AK, Schuster RL (eds) Landslides: investigation and mitigation, transportation research board, National Research Council, Special Report 247. National Academy Press, Washington, DC, pp 91–105

Selby MJ (2005) Hillslope materials and processes. Oxford University Press, Oxford (Reprinted Volume)

Van Burkalow A (1945) Angle of repose and angle of sliding friction: an experimental study. Geol Soc Am Bull 56:669–707

Veder C (1981) Landslides and their stabilization. Springer, New York

Zaruba Q, Mencl V (1976) Engineering geology. Elsevier, Amsterdam

Appendix A

To assess size class distribution of the soil particles Keen-Box Method was applied. The soil samples were collected from 50 different locations of the Shivkhola Watershed (Appendix A). On the basis of analyzed soil samples, spatial zonation of granule, sand, silt and clay were made and finally all the maps were incorporated with landslide inventory map to determine the potential stability of the soil particles. The depth of soil for each location was determined studying the landslide scars, slope cutting and boring the slope surface (**Appendix A**) (Table A.1).

S. Mandal and R. Maiti, *Semi-quantitative Approaches for Landslide Assessment and Prediction*, Springer Natural Hazards, DOI 10.1007/978-981-287-146-6

Table A.1 Soil texture and depth analysis of the watershed

Sample no.	Location of the collected samples	Latitude and longitude	Saturated soil depth (in m)	Granule (%)	Sand (%)	Silt (%)	Clay (%)
1.	Mahanadi T.E.	26°53′30″N/88°24′02″E	1.55	41.59	55.84	1.47	1.05
2.	Paglajhora R.F.	26°52′43″N/88°22′30″E	1.45	37.17	56.38	3.03	0.26
3.	Upper Paglajhora	26°22′20″N/88°18′00″E	1.40	8.25	88.11	1.98	1.65
4.	Giddapahar T.E.	26°02′20″N/88°17′05″E	1.25	6.36	87.47	2.98	3.18
5.	Sepoydhura T.E.	26°52′03″N/88°23′03″E	2.00	44.29	44.40	2.98	2.49
6.	Nurbong T.E.	26°49′57″N/88°23′30″E	2.55	25.68	72.51	0.75	1.05
7.	Nurbong T.E. near sinking zone	26°51′37″N/88°23′28″E	2.75	46.04	50.05	2.19	1.71
8.	Gitingia T.E.	26°52′03″N/88°22′45″E	1.15	22.26	73.47	2.31	1.95
9.	Shiviter T.E. (Upper)	26°52′38″N/88°20′40″E	0.85	30.54	69.21	0.13	0.11
10.	Lezipur T.E.	26°52′26″N/88°20′08″E	0.75	28.32	68.86	1.59	1.24
11.	Shiviter T.G. (M.B)	26°52′51″N/88°19′52″E	1.85	33.60	61.92	2.03	2.43
12.	Shiviter lower	26°50′20″N/88°19′20″E	2.95	17.52	79.34	1.42	1.71
13.	Lower Paglajhora	26°52′55″N/88°18′24″E	0.55	27.75	69.16	1.47	1.62
14.	14 miles bustee	26°52′02″N/88°18′17″E	0.65	47.10	51.49	0.64	0.75
15.	Gayabari proper	26°52′41″N/88°18′46″E	1.20	19.42	76.70	1.67	2.22
16.	Shivkhola R.F.	26°52′50″N/88°18′40″E	3.75	39.63	58.34	0.93	1.09
17.	Shivkhola Central	26°52′47″N/88°18′38″E	3.50	34.22	62.36	1.90	1.52
18.	Jogmaya T.E.(1234M)	26°52′35″N/88°18′45″E	3.25	29.08	68.30	1.14	1.47
19.	Shiviter labor line	26°52′53″N/88°18′52″E	0.95	28.24	69.22	1.05	1.40
20.	14 Mile Bustee proper	26°52′51″N/88°18′25″E	0.75	37.47	61.11	0.70	0.70
21.	Tindharia proper	26°51′28″N/88°20′17″E	1.25	38.82	60.81	0.16	0.24
22.	Tindharia Rly. Stn.	26°51′23″N/88°20′08″E	1.20	30.42	67.46	0.61	0.91
23.	Gayabari upslope	26°52′40″N/88°18′43″E	0.45	23.97	73.71	1.03	1.29
24.	Gayabari lower slope	26°52′40″N/88°18′43″E	1.55	33.50	64.81	0.81	1.12
25.	Tindharia tea garden	26°51′38″N/88°20′20″E	3.15	28.73	54.32	2.95	1.87

(continued)

Table A.1 (continued)

Sample no.	Location of the collected samples	Latitude and longitude	Saturated soil depth (in m)	Granule (%)	Sand (%)	Silt (%)	Clay (%)
26.	Tindharia managers B	26°51′25″N/88°19′19″E	2.10	36.27	49.53	2.25	1.47
27.	Chunabhati	26°51′01″N/88°20′24″E	0.65	32.58	65.98	0.94	0.35
28.	Mid-slope at the right sight of Tindharia	26°51′23″N/88°20′25″E	0.90	34.35	71.15	1.14	.64
29.	Near chunabhati railway station	26°51′00″N/88°20′227″E	1.05	34.25	62.75	1.18	0.65
30.	Extreme lower segment from Tindharia T.E.	26°51′30″N/88°19′22″E	1.76	31.72	59.35	1.99	1.48
31.	Upslope from Gitangea T.E.	26°52′20″N/88°22′35″E	1.35	29.20	63.75	2.05	1.69
32.	Right slope from Tindharia	26°51′10″N/88°19′17″E	1.19	35.50	64.20	0.92	0.75
33.	Central part of the watershed	26°51′45″N/88°19′00″E	2.05	33.25	61.50	1.65	1.53
34.	Shiviter T.E.	26°52′51″N/88°19′52″E	1.81	28.90	69.55	1.12	1.35
35.	Upslope of Shiviter T.E.	26°52′55″N/88°20′45″E	1.49	35.95	66.74	0.94	0.62
36.	Gayabari upslope	26°52′42″N/88°18′49″E	2.15	32.29	64.46	1.32	1.55
37.	Lower segment of Shivkhola R.F.	26°51′45″N/88°18′30″E	1.63	31.85	65.21	1.34	1.18
38.	Between lower Paglajhora and Mahanadi	26°52′58″N/88°18′34″E	1.32	30.68	65.48	1.41	1.23
39.	Lower slope from lower Paglajhora	26°52′55″N/88°18′28″E	0.11	30.45	65.50	1.40	1.20
40.	Few kms before 14 miles basti	26°52′49″N/88°18′27″E	1.05	31.85	67.45	1.39	1.27
41.	Extreme upslope of paglajhora	26°57′58″N/88°17′34″E	1.45	25.30	72.92	1.89	1.26
42.	Extreme upslope of paglajhora	26°57′56″N/88°17′32″E	1.39	23.35	73.95	1.98	1.39
43.	Extreme upslope of paglajhora	26°57′54″N/88°17′30″E	1.00	19.75	75.55	2.08	1.72
44.	Middle section btwn. Nurbong and Tindharia T.E.	26°51′10″N/88°19′42″E	1.73	33.84	63.39	1.46	1.22
45.	Lower slope from Tindharia	26°51′00″N/88°19′05″E	1.67	30.95	65.21	1.18	1.24
46.	Chunabhati (along road side)	26°49′00″N/88°20′26″E	1.07	34.45	64.30	1.16	0.73
47.	14 miles basti	26°52′50″N/88°18′24″E	0.75	35.90	61.25	0.74	0.59
48.	Shiviter manager's bunglaw	26°52′53″N/88°18′47″E	1.53	30.55	61.39	2.10	1.80
49.	Mahanadi (along the Hill Cart Road)	26°53′20″N/88°24′12″E	1.55	32.95	63.45	1.78	0.87
50.	Central part of the watershed	26°51′45″N/88°18′40″E	2.59	29.7	67.95	1.08	1.40

Source Laboratory analysis by author himself

Appendix B

Appendix B shows the rainfall statistics since 1979–2009. This rainfall statistics helped to assess the return period and the recurrence interval of critical rainfall for landsliding. The month of June, July and August are the consistent rainfall months of a year when the propensity of slope failure is of great. Not only that the occurrence of rainfall were incorporated with the landslide events which showed a positive relationship between consistent rainfall and landslide in the Shivkhola Watershed (Table B.1).

S. Mandal and R. Maiti, *Semi-quantitative Approaches for Landslide Assessment and Prediction*, Springer Natural Hazards, DOI 10.1007/978-981-287-146-6

Table B.1 Rainfall statistics since 1979–2009 (rainfall in mm)

Year	Jan	Feb	Mar	Apr	May	Jun	Jul	Aug	Sep	Oct	Nov	Dec
1979	12.5	62.5	00	74.00	265.5	731.75	588	989.5	386.25	122.5	00	00
1980	00	00	56.25	150	168.25	249.5	739.25	757.75	447.5	268.5	75.00	35.00
1981	2.5	16.5	97.5	35	261	883.5	870.5	620.5	725.5	725.25	12.5	12.5
1982	3.25	53	00	83.5	150	462	350	800	600	275	4.75	13.00
1983	00	00	00	12.8	203.21	830.20	701.5	1087.7	765.59	293.8	00	00
1984	31	5	63	199	490.5	611	1287	884.5	570.6	4.80	00	00
1985	00	10	80.30	187.1	161.1	1123	594.6	473.25	462.1	89.5	10	00
1986	22.5	25	5	10	288.8	685.15	1276.97	646.93	591.62	223.12	29.05	10.5
1987	44	76	00	203.25	592.59	949.5	1432.2	850.2	982.8	362.05	00	8.5
1988	00	00	27	46.12	462.34	1042.6	1641	905	1042	484.18	00	00
1989	10	12	33	120	208.9	947.4	752.5	632.5	577.5	179	00	00
1990	59.05	24.4	6.7	34.25	69.72	203	416	718.13	445.2	250.5	00	00
1991	2	00	125	51.3	35.1	113	379.7	271	299	00	00	00
1992	1.00	25.00	57.5	125	568.8	889.5	1200	982.5	520	171.5	5.6	1.5
1993	2.85	37	65.25	204.5	796.5	1025.5	999.5	785.25	457.8	85	35	2.25
1994	3.5	45	51.8	79.5	420.5	675.2	795.5	1195.5	653.5	154.5	17.25	1.5
1995	4.00	28	49.5	131	214	493.9	1161.8	752.2	484.5	110.4	00	00
1996	00	00	24.6	84.2	266.1	838	1130.8	706.6	613.8	175.4	00	32
1997	60.0	27.4	30.6	19.2	204.6	29.4	677.8	608.6	551	19	00	00
1998	10	17.6	50	45.00	405.5	675.5	978.4	795.2	735	75.6	4.95	15
1999	00	4.5	22.5	57.2	178.6	748.6	1007.3	1006.3	610.7	157.6	00	00
2000	7.2	13.5	89.5	19.6	121.3	369.7	750	890.4	748	8.2	00	251.4
2001	00	00	246	87.5	145.8	641.6	1367	1035.3	395.8	26.8	27.2	10
2002	00	00	30.6	60.2	427.1	938.6	1013.1	732.9	569.8	274.6	00	00

(continued)

Table B.1 (continued)

Year	Jan	Feb	Mar	Apr	May	Jun	Jul	Aug	Sep	Oct	Nov	Dec
2003	5.0	00	15.00	127.6	498.4	995.8	1040.2	877.3	542.6	16.2	00	00
2004	00	00	00	62.8	194.4	709.8	655.8	235.4	372.6	9.2	12.4	14
2005	8.6	11.2	2.4	65.5	175.4	1000.25	1520.31	325.56	523.05	250.5	20	25
2006	6	7.25	12.35	204	180.4	1340.7	1811.8	602	648.8	279.8	00	251.8
2007	00	00	28.8	123.6	288.2	570.2	1268	828.4	363.4	129	24	6
2008	105	25.2	45.6	145.6	375.5	657.8	1155.4	985.7	578.5	211.3	54	4.5
2009	2.5	7.25	35.75	111.5	475.8	987.25	1245	1125	724.5	157.35	34.8	3.95

Appendix C

Appendix C consisting depth of soil, slope angle, angle of internal friction, cohesion, wet soil density, specific yield of soil, and safety factor (for dry, semi-saturated and saturated conditions). With the help of all these geo-technical parameters of soil, a slope stability model (1-D Slope stability model) was applied to determine the value of safety factor and on the basis of safety factor value, spatial distribution of landslide susceptibility was assessed under dry, semi-saturated and saturated condition. To establish the model the saturation index (m) of value 0.00, 0.5 and 1.00 were taken for dry, semi-saturated and saturated conditions respectively. The cohesion (c) and friction angle (φ) of the soil were estimated using *'tri-axial soil testing mechanism'*. Slope angle was assessed studying the prepared slope map from DEM (Digital Elevation Model) (Table C.1).

S. Mandal and R. Maiti, *Semi-quantitative Approaches for Landslide Assessment and Prediction*, Springer Natural Hazards, DOI 10.1007/978-981-287-146-6

Table C.1 Result of field measurement and laboratory test of soil samples observed and collected from different location of the watershed

Sample no.	(Z in m)	(Θ)	Φ	(c) kg/cm^3	(γ in KN/m^3)	(γ_w-KN/m^3)	FS (dry condition)	FS (semi-saturated)	FS (Saturated)
1.	1.55	42°	28°	0.42	1.86	0.92	0.883	0.737	0.5916
2.	1.45	54°	23°	0.21	2.13	1.01	0.452	0.378	0.3052
3.	1.40	37°	27°30′	0.11	1.89	0.89	0.7773	0.6146	0.4519
4.	1.25	38°	31°	0.65	1.97	0.82	1.3687	1.2019	1.0351
5.	2.00	39°	26°	0.45	2.01	0.90	0.8312	0.6963	0.5615
6.	1.35	39°	19°	0.02	2.01	1.12	0.4402	0.3218	0.2033
7.	2.75	49°	19°30′	0.03	2.25	1.09	0.3176	0.2430	0.1685
8.	1.15	35°	25°15′	0.60	2.05	0.85	1.215	1.0756	0.9360
9.	0.85	66°	24°	0.04	1.95	0.76	0.2631	0.2245	0.1859
10.	0.75	64°	29°	0.71	2.04	0.79	1.448	1.3958	1.3435
11.	1.85	67°	24°	0.02	2.36	1.08	0.2017	0.1584	0.1152
12.	2.95	22°	28°	0.65	2.21	0.99	1.6033	1.3085	1.0137
13.	0.55	65°	21°15′	0.01	2.00	0.84	0.2050	0.1670	0.1289
14.	0.65	46°	22°	0.32	2.05	0.82	0.8708	0.7927	0.7147
15.	1.20	51°	23°	0.79	1.88	0.77	1.0597	0.9893	0.9189
16.	3.75	59°	28°	0.67	2.06	0.78	0.5159	0.4554	0.3949
17.	3.50	57°	29°	0.66	2.10	0.76	0.5565	0.4675	0.2569
18.	3.25	15°	22°	0.33	2.22	0.81	1.6907	1.4157	1.1406
19.	0.95	63°	25°	0.25	1.98	0.77	0.5661	0.5199	0.4737
20.	0.75	64°	22°	0.04	2.35	1.01	0.2546	0.2123	0.1699
21.	1.25	48°	21°	0.05	2.23	0.98	0.3817	0.3058	0.2298
22.	1.20	52°	20°	0.07	2.22	0.88	0.3385	0.2822	0.2352
23.	0.45	46°	26°	0.91	1.99	0.85	2.5050	2.4044	2.3038
24.	1.55	20°	29°	0.52	2.03	0.73	2.0372	1.7634	1.4895
25.	3.15	24°	25°	0.06	2.11	0.75	1.0716	0.88551	0.69937
26.	2.10	13°	24°	0.58	2.13	0.74	2.52008	2.18508	1.85008

(continued)

Table C.1 (continued)

Sample no.	(Z in m)	(Θ)	Φ	(c) kg/cm^3	(γ in KN/m^3)	(γ_w-KN/m^3)	FS (dry condition)	FS (semi-saturated)	FS (Saturated)
27.	0.65	36°	27°	0.86	1.96	0.69	2.12086	1.99742	1.87398
28.	0.90	26°	25°	0.10	1.90	0.68	1.104495	0.784422	0.7623225
29.	1.20	37°	25°	0.25	2.30	0.91	0.7041	0.6021	0.5001
30.	2.20	28°	31°	0.81	2.22	0.87	0.9137	0.8131	0.7124
31.	1.70	38°	24°	0.41	1.99	0.54	0.8197	0.7423	0.6650
32.	1.30	36°	29°	0.75	1.97	0.53	1.3788	1.2178	1.1735
33.	2.65	27°	23°	0.06	2.11	0.77	3.546	2.9152	2.2843
34.	1.75	35°	32°	0.48	2.05	0.81	1.1772	1.000	0.8246
35.	1.15	39°	27°	0.51	2.40	1.05	0.8783	0.7582	0.6382
36.	2.18	44°	21°	0.09	2.44	1.11	0.3323	0.2627	0.2874
37.	1.72	64°	22°	0.25	2.15	0.98	0.3686	0.3237	0.2788
38.	1.65	49°	33°	0.24	1.89	0.66	0.7199	0.6214	0.5228
39.	1.40	61°	24°	0.08	1.97	0.53	0.3152	0.2820	0.2488
40.	1.35	25°	19°	0.06	2.02	0.72	0.7958	0.6642	0.5326
41.	1.49	30°	21°	0.09	2.55	1.09	0.7196	0.5774	0.4353
42.	1.40	42°	31°	0.17	2.48	1.09	0.7658	0.6191	0.4725
43.	0.85	51°	20°	0.35	1.85	0.61	0.7499	0.7013	0.6527
44.	1.45	23°	30°	0.40	1.93	0.65	1.7576	1.5285	1.2995
45.	1.50	55°	20°	0.22	2.04	0.96	0.4078	0.3479	0.2879
46.	0.95	66°	27°	0.15	2.58	1.29	0.3915	0.3348	0.2781
47.	0.65	49°	25°	0.08	2.47	1.22	0.5060	0.4059	0.3057
48.	1.15	38°	18°	0.29	2.00	0.72	0.6757	0.6009	0.5260
49.	1.23	47°	27°	0.32	1.79	0.50	0.7665	0.7002	0.6338
50.	3.05	18°	26°	0.78	1.99	0.60	1.9384	1.7121	1.4858

Z = soil depth; Θ = slope angle; φ = angle of internal friction; c = cohesion; γ = specific yield of soil; γ_w = unit weight of water; and m* = wetness index with 20 year return period of rainfall intensity

Appendix D

To determine the probability of future landslide events using the probability model, major and minor landslide event in the Shivkhola Watershed since 1968–2011 (**Appendix** D) were taken into account from the work done by researchers such as Basu and Sarkar (1985, 1988) Basu Basu and Maiti (2001), Maiti (2007, 2011) Ghosh (2009b), Sarkar (2011), and Mandal and Maiti (2011, 2012 and 2013). In this study, the occurrences of reactivated and fresh landslides were considered (Table D.1).

S. Mandal and R. Maiti, *Semi-quantitative Approaches for Landslide Assessment and Prediction*, Springer Natural Hazards, DOI 10.1007/978-981-287-146-6

Table D.1 Occurrences of major and minor landslide event in the Shivkhola watershed since 1968–2011

Event date and Year	Important location	Type of the landslide events	No. of landslides	No of reactivated slides	No of new slides	Triggering factors
3rd, 4th, and 5th Oct., 1968	Giddapahar, Gayabari. Paglajhora.	Major and most deadful	13	4	9	Unprecedented continuous rainfall of 221.4 mm in 4 days
1980	Paglajhora, 14 miles Bustee, Tindharia.	Major event	6	2	4	Due to incessant rainfall of 299.2 mm in 2 days
17th Sept., 1984	Shivite T.E., Nurbong T. E., Mahanadi and Giddapahar.	Minor and local	5	3	2	Continuous rainfall
17 and 18th Oct., 1985	Maanadi, Sepoydhura, Gayabari	Major events	6	4	2	Continuous rainfall
7th Sept., 1986	Mahanadi, Tindharia, Chunabhati	Minor and local	5	2	3	Continuous rainfall triggering
10 and 11th Sept., 1991	Paglajhora and Chunabhati Area	Major event	5	3	2	Due to incessant rainfall of 462.5 mm in 2 days
1st, 2nd, and 3rd July, 1993	Tindharia and Gayabari and Mahanadi	Prominent major event	4	2	2	Due to heavy and concentrated rainfall of 211.3 mm in 2 days
1995	Paglajhora, Giddapahar, Tindharia and Gayabari	Minor and local event	7	5	2	Cumulative rainfall and formation of road-cut benches with heavy vehicles
6th, 7th, and 8th July, 1998	Chunabhati, Tidharia, Paglajhora, Mahanadi (along NH-55)	Prominent major event	10	8	2	300–600 mm cumulative rainfall in 2/3 days
2002	Giddapahar, Tindharia and Gayabari, Nurbong, Gitingia	Prominent major event	13	6	7	Cumulative rainfall and construction of road-cut benches and plying of heavy loaded vehicles

(continued)

Table D.1 (continued)

Event date and Year	Important location	Type of the landslide events	No. of landslides	No of reactivated slides	No of new slides	Triggering factors
8 and 9th July, 2003	Gayabari T.E., Along NH-55, Tindharia and Shiviter. Paglajhora,	Prominent major event	12	11	1	Due to incessant rainfall of 500 mm in 2 days
2005	Shiviter T.E. and lower Paglajhora, Jogmaya T.E.	Major event	9	3	6	Heavy and continuous rainfall and subsidence of road at Paglajhora
2006	Tindharia, 14 Miles Bustee, Gitingia, Nurbong	Major event	10	6	4	Heavy rainfall
17, 18th July and 6th, 7th, and 78th, Sept., 2007	Tindharia and upper and lower Paglajhora.	Prominent major event	6	4	2	Heavy rainfall
16th June, 2010 morning	14 Mile near lower Paglajhora, Nurbong, Gitingia, Tindharia	Prominent major event	9	6	3	Heavy rainfall of 345 mm in 2 days
10th May, 2011	Lower Paglajhora	Prominent major event	8	7	1	Heavy showers and the vibration caused by Sikkim earthquake

Total no. of landslide events year-16
No. of major landslide events year-12
Total no. of landslide events occurrences in the watershed since 1968–2011 = 128 (identified)
Total no. of reactivated landslide in the watershed-76
Total no. of fresh landslide (not associated with old slide/70 m. away from old slide) events year-52

Appendix E

Appendix E dealt with catastrophic rainfall events since 2005–2010 (Table E.1).

S. Mandal and R. Maiti, *Semi-quantitative Approaches for Landslide Assessment and Prediction*, Springer Natural Hazards, DOI 10.1007/978-981-287-146-6

Table E.1 Analysis of catastrophic rainfall event during 2005–2010

2005	Rain in mm	2006	Rain in mm	2007	Rain in mm	2008	Rain in mm	2009	Rain in mm	2010	Rain in mm
20th June	95.5	23rd May	103.5	10th June	222.72	7th June	125	3rd June	146.5	24th May	88.9
26th June	183.5	28th July	150	28th June	93.5	9th June	100	19th June	133	28th May	101.6
31st July	134.5	29th July	160	29th June	120.5	23rd June	203	7th July	175	16th June	111.7
3rd Oct	100	30th July	112.5	10th July	120	26th June	179	12th July	200.5	14th July	103.6
4th Oct	90	19th Aug	150	17th July	124.5	29th June	196.5	9th Sep	98.7	18th July	102
		31st Aug	120.5	18th July	100	7th July	273.5	27th Sep	95.5	25th July	92.4
		17th Sept.	89.5	27th July	120.5	8th July	162.5			5th Aug	114.3
		3rd Oct	130	18th Aug	145.5	21st July	146.5			25th Aug	89.4
				23rd Sept.	106.2	28th July	148.5			28th Aug	102.6
						30th July	100			16th Sept.	115.5
						10th Aug	191.5			25th Sept.	116.3
						31st Aug	107.5			26th Sept.	90.5
No of days	5		8		9		12		6		12
Total	603.5		1016		1153.42		1933.5		849.2		1228.8
Average	120.7		127		128.15		161.12		141.53		102.4

Source Selim Hill Tea Estate 2007 (1/2 km. Crow fly distance from Tindharia)

Appendix F

See Figs. F.1, F.2, F.3, F.4, F.5, F.6, F.7, F.8, F.9 and F.10.

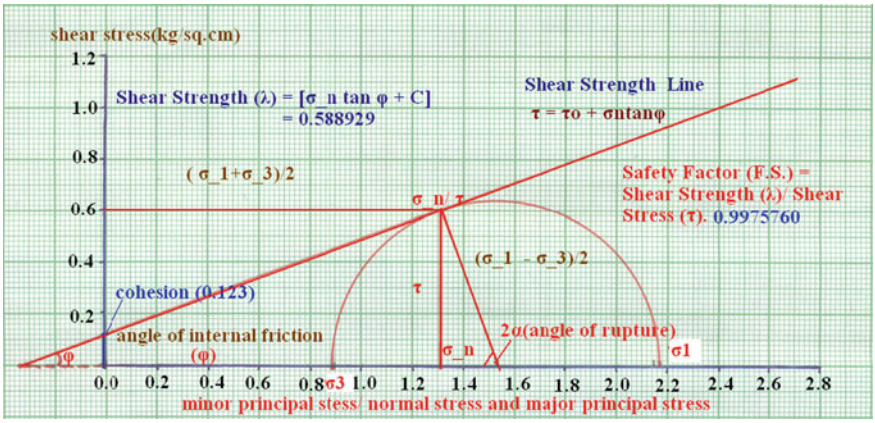

Fig. F.1 Plotting of the geotechnical attributes from Tindharia tea estate

S. Mandal and R. Maiti, *Semi-quantitative Approaches for Landslide Assessment and Prediction*, Springer Natural Hazards, DOI 10.1007/978-981-287-146-6

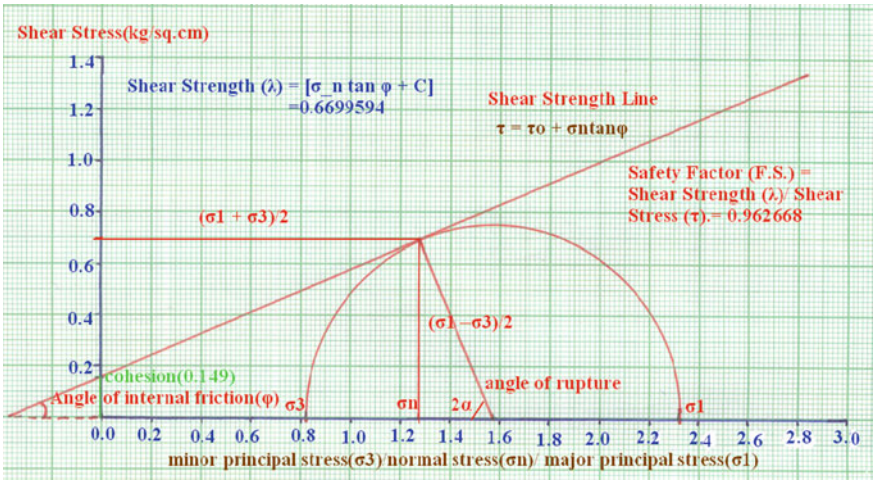

Fig. F.2 Plotting of the geotechnical attributes from 14 Mile Bustee

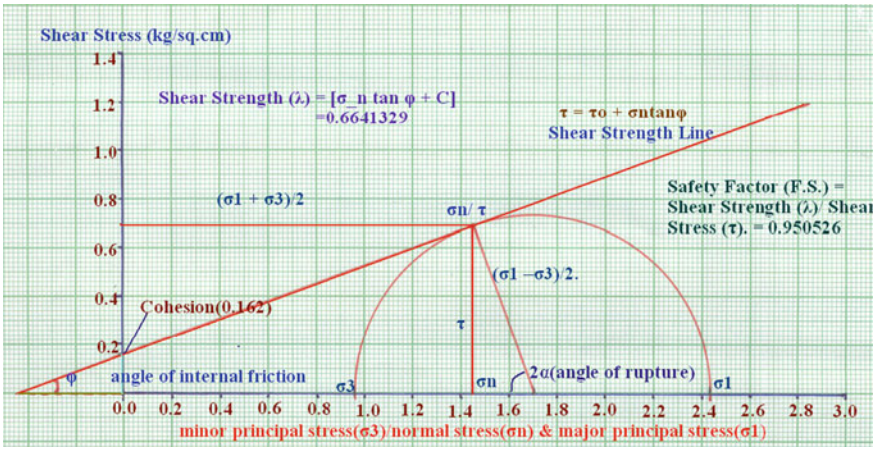

Fig. F.3 Plotting of the geotechnical attributes from Paglajhora (lower)

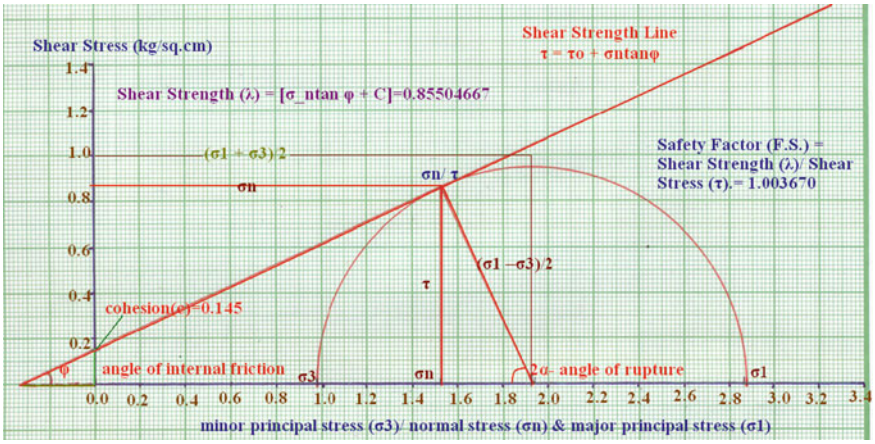

Fig. F.4 Plotting of the geotechnical attributes from Mahanadi

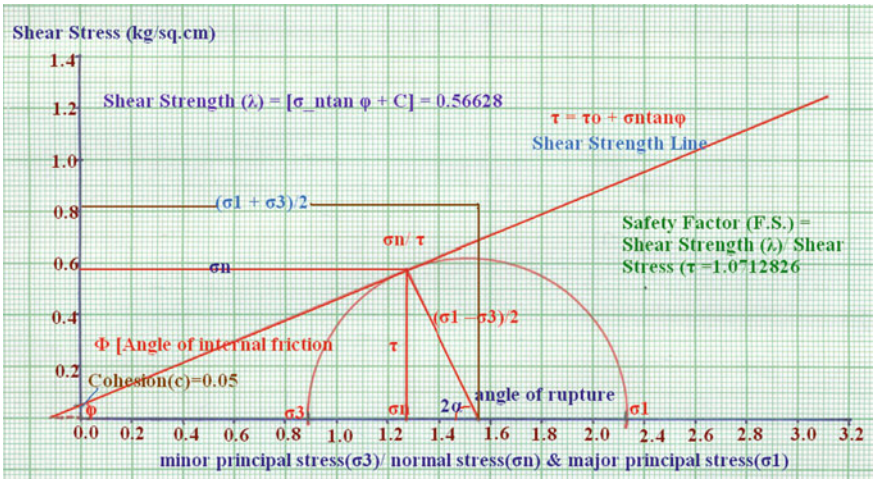

Fig. F.5 Plotting of the geotechnical attributes from Gayabari lower

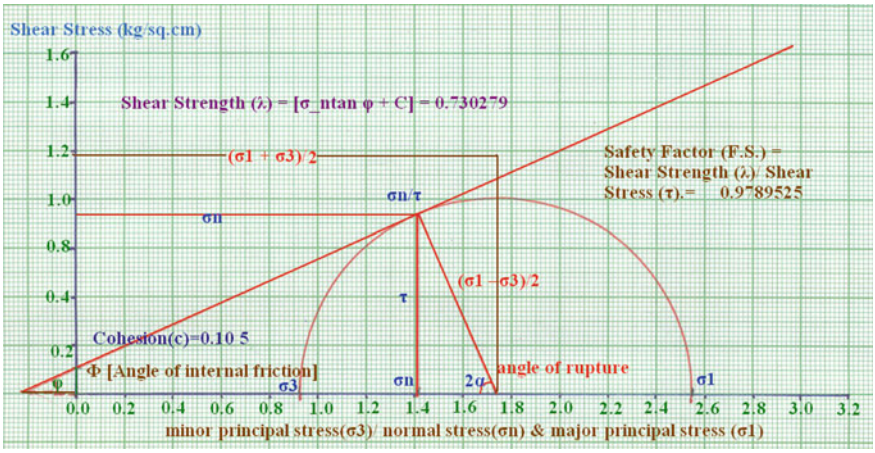

Fig. F.6 Plotting of the geotechnical attributes from Tindharia proper

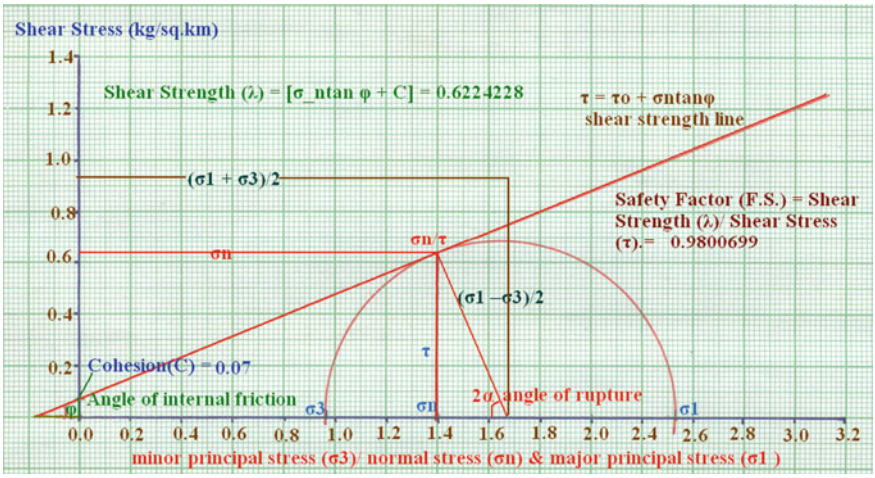

Fig. F.7 Plotting of the geotechnical attributes from Shiviter tea estate

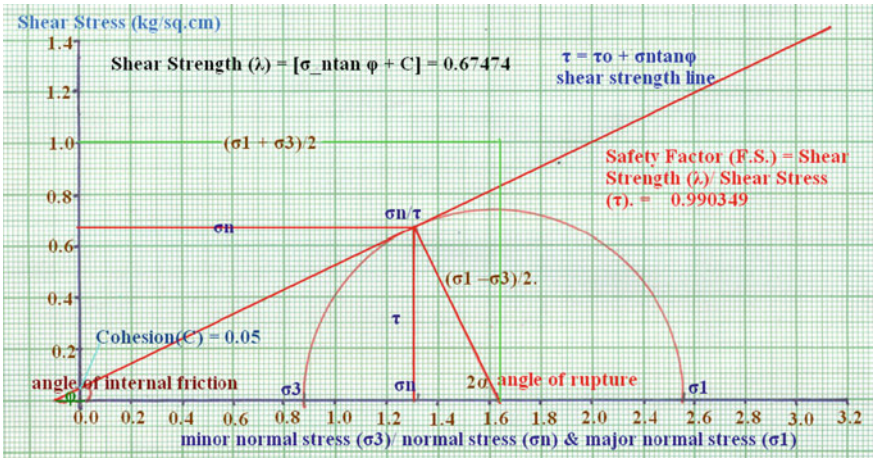

Fig. F.8 Plotting of the geotechnical attributes from Sepoydhura tea estate

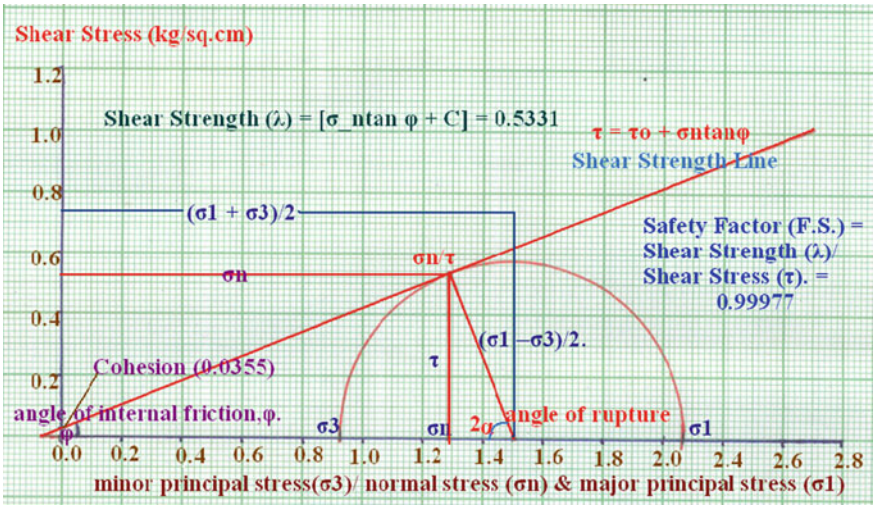

Fig. F.9 Plotting of the geotechnical attributes from Nurbong tea estate

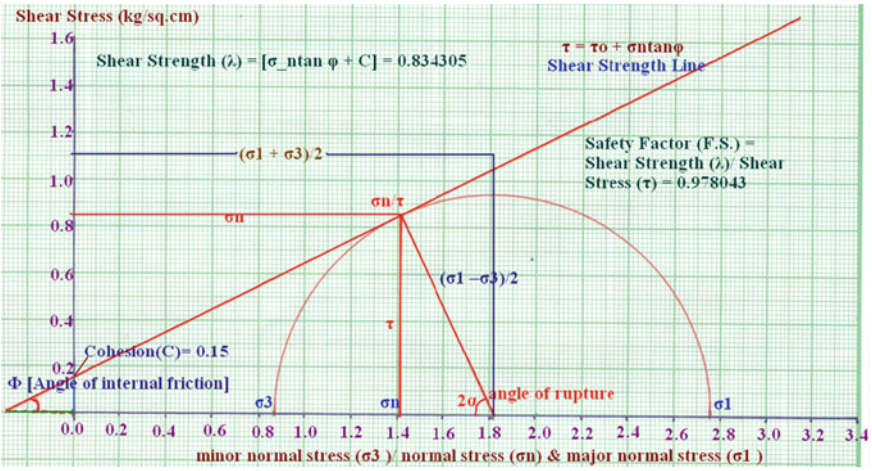

Fig. F.10 Plotting of the geotechnical attributes from mid-central part of the basin

Appendix G

This appendix describes the determination of frequency ratio and class weight for each class of the landslide triggering factors such as slope angle, slope aspect, slope curvature, lithological composition, lineaments, drainage density, land use and land cover, upslope contributing area, road contributing area, road contributing area and settlement density. The table also reveals the relative significance of each class of the landslide triggering factors in terms of landslide. The determined class weight values were used to perform the linear integration model and to prepare the landslide susceptibility map of the Shivkhola Watershed (Table G.1).

S. Mandal and R. Maiti, *Semi-quantitative Approaches for Landslide Assessment and Prediction*, Springer Natural Hazards, DOI 10.1007/978-981-287-146-6

Table G.1 Class frequency ratio/prioritized class rating value and class weight

Classes	Number of pixels (F1) ($N_{pix(Ni)}$)	% of $N_{pix(Ni)}$	landslide pixels (F2) ($N_{pix(Si)}$)	% of ($N_{pix(Si)}$)	FR	Class weight (W)
Slope angle (in degree) −1						
0–7.17	3353	10.12	190	5.63	0.53	−45.14
7.17–14.34	3238	9.77	202	5.99	0.61	−39.43
14.34–19.92	3587	10.83	211	6.26	0.58	−42.99
19.92–24.97	2445	7.38	201	5.96	0.81	−19.60
24.97–29.75	3555	10.73	311	9.22	0.86	−14.33
29.75–34.53	2776	8.38	329	9.75	1.16	16.71
34.53–39.57	3854	11.63	413	12.24	1.05	5.35
39.57–45.95	3276	9.89	427	12.65	1.28	28.53
45.95–54.71	3557	10.74	543	16.09	1.49	50.85
54.71–67.73	3490	10.53	646	19.15	1.82	83.29
Slope Aspects (direction of slope) −2						
Flat	784	2.37	24	0.711	0.3	−71.2
North	3879	11.71	665	19.72	1.68	69.63
North East	3797	11.46	443	13.13	1.15	14.86
East	4346	13.12	675	20.01	1.53	53.51
South East	6290	18.99	789	23.39	1.23	23.63
South	4556	13.75	597	17.70	1.29	29.23
South West	3332	10.06	35	0.74	0.07	−19.31
West	2870	8.66	69	2.05	0.24	−77.77
North West	3277	9.89	76	2.25	0.23	−78.62
Slope Curvature (positive, negative and zero) −3						
−25.87 to −11.41	995	3.00	221	6.55	2.18	120.3

(continued)

Table G.1 (continued)

Classes	Number of pixels (F1) ($N_{pix(Ni)}$)	% of $N_{pix(Ni)}$	landslide pixels (F2) ($N_{pix(Si)}$)	% of ($N_{pix(Si)}$)	FR	Class weight (W)
−11.41 to −5.73	785	2.37	210	6.23	2.63	165.71
−5.73 to −2.33	2111	6.37	486	14.40	2.26	128.41
−2.33 to −0.63	2431	7.34	374	11.09	1.51	52.09
−0.63–0.50	10045	30.32	388	11.50	0.38	−63.18
0.50–2.49	6302	19.02	268	7.95	0.42	−59.23
2.49–7.31	5438	16.41	464	13.76	0.84	−16.48
7.31–14.69	3343	10.09	475	14.08	1.40	40.28
14.69–24.33	895	2.70	222	6.58	2.44	146.23
24.33–46.45	786	2.37	265	7.86	3.32	325.34
Lineaments (Distance from lineament in m) −4						
0.00–57.42	3381	10.20	624	18.50	1.81	82.75
57.42–126.32	3786	11.43	668	19.80	1.73	74.63
126.32–229.68	3695	11.15	451	13.37	1.20	20.25
229.68–356.00	3252	9.82	522	15.48	1.58	58.71
356.00–528.26	4799	14.48	444	13.16	0.91	−9.29
528.26–723.45	4141	12.50	286	8.48	0.68	−32.74
723.45–964.65	3887	11.73	221	6.55	0.56	−44.95
964.65–1251.75	3921	11.83	120	3.56	0.30	−71.21
1251.75–1642.20	1419	4.29	37	1.10	0.26	−75.74
1642.20–2925.40	850	2.57	0	0.00	0.00	0.00
Drainage density (length of drainage/sq. m) −5						
0–1.90	5560	16.78	90	2.67	0.16	−85.62
1.90–3.80	5453	16.46	109	3.23	0.20	−81.82

(continued)

Table G.1 (continued)

Classes	Number of pixels (F1) ($N_{pix(Ni)}$)	% of N_{pix} $_{(Ni)}$	landslide pixels (F2) ($N_{pix(Si)}$)	% of ($N_{pix(Si)}$)	FR	Class weight (W)
3.80–5.71	3289	9.93	158	4.68	0.47	−53.77
5.71–7.61	5049	15.24	137	4.06	0.27	−74.68
7.61–9.51	3477	10.49	159	4.71	0.45	−56.08
9.51–11.41	2728	8.23	465	13.78	1.67	68.64
11.41–13.31	1875	5.66	544	16.13	2.85	188.32
13.31–15.21	2191	6.61	542	16.07	2.43	145.57
15.21–17.12	1942	5.86	697	20.66	3.52	257.10
17.12–19.02	1567	4.73	572	16.96	3.58	263.22
Geology (Lithological Composition) −6						
Darjiling gneiss	6695	20.21	692	20.52	1.02	1.55
Chungtung formation	4203	12.69	525	15.56	1.23	23.10
Lingtse granite	3150	9.51	475	14.08	1.48	48.98
Gorubathan formation	2945	8.89	448	13.28	1.49	50.31
Reyang formation	5925	17.89	621	18.41	1.03	3.00
Damuda formation (Gondwana)	3203	9.67	490	14.53	1.50	51.17
Siwalik groups	7010	21.56	122	3.62	0.17	−84.41
Land use and land cover (LULC) −7						
Tea	2310	6.97	290	8.60	1.23	23.73
Jungle	2657	8.02	312	9.25	1.15	15.62
Open forest	531	1.60	19	0.56	0.35	−66.03
Degraded forest	1522	4.59	112	3.32	0.72	−28.22
Dense forest	2114	6.38	194	5.75	0.90	−10.04
Bared surface	4758	14.36	379	11.24	0.78	−22.15

(continued)

Table G.1 (continued)

Classes	Number of pixels (F1) ($N_{pix(Ni)}$)	% of N_{pix} $_{(Ni)}$	landslide pixels (F2) ($N_{pix(Si)}$)	% of ($N_{pix(Si)}$)	FR	Class weight (W)
Road	1074	3.24	216	6.40	1.98	99.31
Settlement	3037	9.17	352	10.44	1.14	14.09
Agricultural land	6880	20.77	566	16.78	0.81	−19.54
Mixed Forest	9281	28.01	933	27.66	0.99	−1.28
Upslope contributing area (UCA in km/sq.km) −8						
<5.00	11421	34.47	1089	32.29	0.94	−6.46
5.00–10.00	7520	22.70	923	27.36	1.21	20.93
10.00–15.00	6611	19.95	993	29.44	1.48	48.39
15.00–20.00	5215	15.74	253	7.50	0.48	−53.30
>20.00	2364	7.14	113	3.35	0.47	−54.01
Road contributing area (RCA-km/sq.km) −9						
<0.002	5720	17.26	0	0.00	0.00	0.00
0.002–0.004	5307	16.02	79	2.34	0.15	−86.92
0.004–0.006	4220	12.74	440	13.04	1.02	2.46
0.006–0.008	4370	13.19	461	13.67	1.04	3.68
0.008–0.010	4003	12.08	527	15.62	1.29	29.84
0.010–0.012	3522	10.63	572	16.96	1.60	60.60
0.012–0.014	2957	8.93	608	18.03	2.02	103.80
>0.014	2532	7.64	686	30.34	3.97	169.12
Settlement density (no of settlement/sq. m) −10						
Very low	6445	19.45	235	6.97	0.36	−65.34
Low	5780	17.45	329	9.75	0.56	−44.89

(continued)

Table G.1 (continued)

Classes	Number of pixels (F1) ($N_{pix(Ni)}$)	% of $N_{pix(Ni)}$	landslide pixels (F2) ($N_{pix(Si)}$)	% of ($N_{pix(Si)}$)	FR	Class weight (W)
Moderately low	4858	14.66	374	11.09	0.76	−24.82
Moderate	4397	13.27	499	14.79	1.11	11.68
Moderately high	4265	12.87	591	17.52	1.36	37.05
High	3774	11.39	658	19.5	1.71	72.54
Very high	3612	10.90	687	20.37	1.87	88.39

Index

S. Mandal and R. Maiti, *Semi-quantitative Approaches for Landslide Assessment and Prediction*, Springer Natural Hazards, DOI 10.1007/978-981-287-146-6